

THESIS ON CIVIL ENGINEERING F68

Spatio-Temporal Changes in the Components of Extreme Water Levels on Estonian Coasts

KATRI PINDSOO



TALLINN UNIVERSITY OF TECHNOLOGY
School of Engineering
Department of Civil Engineering and Architecture
School of Science
Department of Cybernetics, Wave Engineering Laboratory

The thesis was accepted for the defence of the degree of Doctor of Philosophy in Engineering on 25 August 2017

Supervisor: Prof. Dr. Tarmo Soomere
Department of Cybernetics, School of Science and Department of Civil Engineering and Architecture, School of Engineering, Tallinn University of Technology, Estonia

Opponents: Prof. Dr. Jaak Monbaliu
Department of Civil Engineering, Faculty of Engineering Science, University of Leuven, Belgium

Prof. Dr. Magnus Larson
Water Resources Engineering, Department for Building and Environmental Technology, Faculty of Engineering, Lund University, Sweden

Defence of the thesis: 06 October 2017, Tallinn

Declaration:

Hereby I declare that this doctoral thesis, my original investigation and achievement, submitted for the doctoral degree at Tallinn University of Technology, has not been submitted for a doctoral or an equivalent academic degree.



/Katri Pindsoo/

Copyright: Katri Pindsoo, 2017
ISSN 1406-4766
ISBN 978-9949-83-150-0 (publication)
ISBN 978-9949-83-151-7 (PDF)

EHITUS F68

Ekstreemsete veetasemete komponentide ajalis-ruumiline muutlikkus Eesti rannikul

KATRI PINDSOO

Contents

List of publications constituting the thesis	6
Author's contribution to the publications	6
List of figures	7
Introduction	12
Effect of climate change on coastal flooding	12
Components of elevated water levels	14
Wave-induced addition to water level	16
The course and distribution of high water levels in the Baltic Sea	19
Increasing trends in the extreme water levels in the Baltic Sea	21
The objectives and outline of the thesis	23
Approbation of the results	25
1. Quantification of the role of waves affecting the water level in the vicinity of the city of Tallinn	27
1.1. Reconstruction of wave properties	27
1.2. The highest waves in the nearshore of Tallinn	32
1.3. Joint impact of shoaling and refraction	34
1.4. Evaluation of wave-induced set-up	38
1.5. Almost-incident waves and endangered areas	41
1.6. Evidence of the rotation of wind direction in strong storms	44
2. Contribution of wave set-up to extreme water levels.....	48
2.1. Observed water levels.....	48
2.2. Modelled water levels.....	50
2.3. Extreme value distributions	53
2.4. Projections based on block maxima	55
2.5. Projected water levels and contribution of wave set-up	57
2.6. Synchronisation of high wave set-up and offshore water level	61
3. Spatial variability in trends in extreme water levels.....	67
3.1. Trends in the annual maxima of the total water level.....	67
3.2. Maxima of storm surge heights and weekly average water levels	70
3.3. Spatial distribution of slopes of trends	72
3.4. The role of the averaging interval	75
3.5. Possible changes in the directional structure of forcing	77
Conclusions	80
Summary of the results.....	80
Main conclusions proposed to defend	82
Recommendations for further work	83
Bibliography	85
Acknowledgements	101
Abstract	102
Resümee	103
Appendix A: Curriculum Vitae	104
Appendix B: Elulookirjeldus.....	110

List of publications constituting the thesis

The thesis is based on four academic publications which are referred to in the text as Paper I, Paper II, Paper III and Paper IV. All papers are indexed by the ISI Web of Science.

- Paper I Soomere T., **Pindsoo K.**, Bishop S.R., Käär A., Valdmann A. 2013. Mapping wave set-up near a complex geometric urban coastline. *Natural Hazards and Earth System Sciences*, 13(11), 3049–3061.
- Paper II Eelsalu M., Soomere T., **Pindsoo K.**, Lagemaa P. 2013. Ensemble approach for projections of return periods of extreme water levels in Estonian waters. *Continental Shelf Research*, 91, 201–210.
- Paper III **Pindsoo K.**, Soomere T. 2015. Contribution of wave set-up into the total water level in the Tallinn area. *Proceedings of the Estonian Academy of Sciences*, 64, 338–348.
- Paper IV Soomere T., **Pindsoo K.** 2016. Spatial variability in the trends in extreme storm surges and weekly-scale high water levels in the eastern Baltic Sea. *Continental Shelf Research*, 115, 53–64.

Author's contribution to the publications

- Paper I I performed the runs of the wave model, calculations of wave-driven set-up and analysis of the results, and contributed to the writing of the relevant parts of the manuscript.
- Paper II I contributed to the analysis and visualization of the data, calculated parameters of extreme value distributions and wrote the parts of the manuscript that addressed the reasons for deviations of modelled and observed data sets.
- Paper III I performed the calculations, visualization and analysis of the results, drafted the manuscript and contributed to the creation of its final version, and acted as the corresponding author.
- Paper IV I performed the majority of calculations, created visualization and contributed to the analysis of the results and manuscript writing and polishing.

List of figures

- Figure 1.** Location scheme of the Baltic Sea, relative Fennoscandian uplift (mm/yr, data from NKG2016LU release) and historical water level maxima on the Baltic Sea coasts (cm, bold numbers; redrawn from Averkiev and Klevanny, 2010).13
- Figure 2.** Contribution of different components of high water level in Pärnu (location shown in Figure 1) during the storm Gudrun 09.01.2005.15
- Figure 3.** Computational areas of the sequence of wave models designed to evaluate the time series of wave properties in the Tallinn Bay area. Small cyan squares along the coast in the lower right panel reflect the grid points from which the wave data are used in Paper I and Paper III. The offshore water level is represented by values evaluated in 11 nearshore grid cells (grey squares) of the Rossby Centre Ocean (RCO) circulation model (Paper III). Adapted from Paper III.28
- Figure 4.** Study area in the vicinity of the city of Tallinn. The selected nearshore grid points of the wave model are numbered from west to east. Analyses in Paper I are performed for the grid cells 1–105. The study area is extended until grid cell 174 in Paper III. Reproduced from Paper III.32
- Figure 5.** Maximum wave heights, higher quantiles and median wave height in the nearshore of the study area in 1981–2012. Thin lines indicate the modelled wave heights and bold lines show values for the breaking wave heights calculated from Eq. (5). Geographical locations are indicated in Figure 4. Reproduced from Paper I.33
- Figure 6.** Propagation directions of the highest numerically simulated waves in single segments of the study area in 1981–2012. Notice that wave models traditionally indicate the direction in which waves propagate. Reproduced from Paper I.34
- Figure 7.** Six storms that caused the highest waves in different coastal sections of the study area in 1981–2014. The horizontal lines indicate the storms that produced the highest wave set-up in at least one section. Each storm is marked with a different colour. The colours vary cyclically. Note that wind records are missing in the Kalbådagrund data set during the maximum and aftermath of an extreme eastern storm on 29–30 November 2012 when the all-time highest significant wave height of 5.2 m was recorded for the second time in the Gulf of Finland (Pettersson et al., 2013). Therefore the largest waves approaching from the east may be missing in our reconstructions. See Figure 4 for the numbering of coastal sections. Adapted from Paper III.35
- Figure 8.** Wave transformation from the grid cell where wave properties were calculated until the breaking point of waves. Source for the background: Estonian Land Board WMS service, www.maaamet.ee.36

Figure 9. A typical shape of the graph of the polynomial in Eq. (3).38

Figure 10. Wave-driven variations in the average water level in the nearshore.....39

Figure 11. Maximum wave heights, higher quantiles and median wave height for waves approaching from a direction of maximally $\pm 45^\circ$ with respect to the normal to the coast. Thin lines indicate the modelled wave heights and bold lines show values for the breaking wave heights calculated from Eq. (4). Reproduced from Paper I.41

Figure 12. The highest breaking waves (coloured lines) approaching from different ranges of directions with respect to the coast normal in the study area. The bold blue line shows the all-time highest waves approaching from any direction and the bold red line shows the all-time highest almost incident waves ($\pm 10^\circ$ with respect to the coast normal). The light red bars indicate the regions with a gently sloping coast in which the maximum set-up likely exceeds 0.4 m. Reproduced from Paper I.42

Figure 13. Maximum wave set-up values and higher quantiles of set-up heights for the coastal sections where high set-up is an issue. Reproduced from Paper I.....43

Figure 14. Coastal sections potentially affected by high wave set-up (red squares) in the urban area of the city of Tallinn based on wind data from 1981–2014. The arrows indicate the directions of wave propagation associated with the highest set-up for single coastal segments. Yellow squares indicate coastal stretches where the maximum wave set-up is < 0.2 m, green squares – areas where high wave set-up is evidently not possible because of the convex shape of the shoreline and blue squares – areas containing various engineering structures. Reproduced from Paper III.....44

Figure 15. Scheme of 50 storms that caused the highest wave set-up ($\pm 15^\circ$ from the shore normal) in different segments of the study area in January 1981–October 2012. The horizontal lines indicate single storms that produced the highest wave set-up in at least one section. Each storm is marked with a different colour. The colours vary cyclically. Reproduced from Paper III.....45

Figure 16. Scheme of 58 storms that caused the highest wave set-up ($\pm 15^\circ$ from the shore normal) in different segments of the study area in January 1981–February 2014. The horizontal lines indicate single storms that produced the highest wave set-up at least in one section. Each storm is marked with a different colour. The colours vary cyclically. Reproduced from Paper III.....46

Figure 17. Location scheme of the four sites used in this study. Red circles indicate the observation sites and green rectangles – the associated points of the circulation model. Reproduced from Paper II.49

Figure 18. Frequency of occurrence of deviations of the water level from the long-term mean in the RCO simulations (6-h values in 1961–2005, upper panel) and in measurements in Tallinn Harbour (1945–15.05.1995). As the measurement site was

relocated from Tallinn Old Harbour to Muuga Harbour in 1996, the distribution of observed values does not contain the highest examples in the 2000s (1.35 m in 2001; 1.52 m in 2005). The recordings of the largest values after the turn of the millennium raised the question of whether the overall dynamics of the water level may have changed since 1996. A similar change has been registered in the statistics of wave-driven set-up in the vicinity of Tallinn for 1981–2012. All the highest waves have occurred after 1995 but the highest set-up apparently occurred in many locations before 1995 (Paper I). A probable reason is a change in the wind direction in the strongest storms, with obvious changes in the local water level dynamics. Reproduced from Paper II.....52

Figure 19. Return periods of extreme water levels at Narva-Jõesuu according to the results of the 6-h RCO data (upper panels) and the observed 1-h data set (lower panels). Note that the latter data constitute a semi-synthetic data set obtained based on actual observations and the output of HIROMB as explained above. The left panels correspond to projections based on annual maxima, the right panels – to projections based on maxima over stormy seasons. Single markers represent the set of block maxima. Reproduced from Paper II.56

Figure 20. Return periods of extreme water levels according to different projections in Narva-Jõesuu, Ristna, Tallinn and Pärnu. Block maxima: red circles – annual maxima of the RCO 6-h data, blue circles – stormy-season maxima of the RCO 6-h data; red rhombi – annual maxima of the RCO 1-h data, blue rhombi – stormy-season maxima of the RCO 1-h data; red squares – annual maxima of the observed data set; blue squares – stormy-season maxima of the observed data set. The markers showing the block maxima derived from the 1-h RCO data almost coincide with those for the RCO 6-h data set. Yellow lines: projections using the Gumbel distribution, magenta – GEV distribution; cyan – Weibull distribution. Note that the difference between the observed and hindcast block maxima corresponding to the calendar years (red) or to stormy seasons (blue) does not become evident in the scale of the image but considerably impacts the relevant projections starting from return periods of about 20 yr. Reproduced from Paper II.58

Figure 21. Left panel: Location of the water level observation peel (green circle) in Narva-Jõesuu at the left bank of the Narva River. The white line to the east of the observation site indicates the border between Estonia and Russia. The right bank of the river is blurred by the image provider. Right panel: Location of the water level observation peel (green circle) in Ristna (Kalana Harbour). Source: Estonian Land Board, www.maaamet.ee. Reproduced from Paper II.....60

Figure 22. Storms (above) and wind directions (below) that were responsible for the highest total water levels at the shoreline. See Figure 4 for the numbering of coastal sections. Reproduced from Paper III.....62

Figure 23. Scatter diagrams of the occurrence of different offshore water levels and various wave set-up values at four representative sections of the study area:

section 24 (Tiskre, a bayhead open to the north-west and partially to the west), section 85 (Pirita Beach, open only to the north-west), section 92 (western coast of the Viimsi Peninsula; open to the west) and section 124 (eastern coast of the Viimsi Peninsula; open to the north-east). The colour code corresponds to ≥ 2 occasions (otherwise the area is left white) with a particular wave set-up (with a step of 0.05 m) and water level (with a step of 0.1 m). Single cases of wave set-up > 0.45 m and water levels > 0.8 m (outside the rectangle bordered by green lines) are represented as separate circles. The situations with zero wave set-up (waves propagating offshore) and cases with offshore water levels below the long-term average are not shown. Reproduced from Paper III.63

Figure 24. The contribution of the hindcast instantaneous offshore water level and wave set-up to the all-time highest water level at the shoreline. The modelled all-time offshore water level maximum (not shown) varies insignificantly (from 1.6 to 1.7 m) along the shore. White diamonds indicate the all-time highest set-up values. Reproduced from Paper III.64

Figure 25. The proportion of wave set-up and offshore water level in the formation of annual maxima of the total water level at the shoreline at five representative sections of the study area: a) Tiskre (section 24), b) Pirita (85), c) Viimsi (92), d) Muuga (124), e) a location close to Muuga Harbour (126) where wave set-up almost does not contribute. See Figure 2 for the numbering of coastal sections. Reproduced from Paper III.65

Figure 26. Left panel: Scheme of the Baltic Sea. Right panel: Water depth at the selected RCO model grid cells in the eastern Baltic Sea (colour scale) and locations of water level gauges (yellow squares in Pärnu, Ristna, Tallinn and Narva-Jõesuu) used in the analysis. The grid cells are numbered consecutively from the western coast of Latvia to the eastern Gulf of Finland, and then counter-clockwise along the coast of the Gulf of Riga starting from Cape Kolka. Reproduced from Paper IV...68

Figure 27. Trends in stormy-season (green circles, 7.1 mm/yr, red line) and annual (cyan squares, visible if different from the stormy-season maxima, 6.4 mm/yr, black line) modelled water level maxima near Tallinn (Figure 28) in 1961–2004. The Sen’s slope for both trends is 6.4 mm/yr. The confidence intervals for the Sen’s slope of stormy-season maxima and for the annual maxima are [0.9, 11.6] mm/yr and [2.3, 9.8] mm/yr, respectively. Reproduced from Paper IV.69

Figure 28. Slope (mm/yr) of trends in the stormy-season and annual maxima of total water level in 1961–2004. Reproduced from Paper IV.70

Figure 29. Numerically simulated total water level (green circles connected with a blue line), its 198-h (8.25-day) average (red) and the positive part of the residual (the total water level minus the 8.25-day average, interpreted as the positive storm surge, blue, lower panel) near Tallinn. Reproduced from Paper IV.71

Figure 30. Trends in the maxima of water level components near Tallinn in 1961–2005. a) Trends in stormy-season (circles, 3.8 mm/yr, Sen’s slope 4.0 mm/yr, 95%

confidence interval [0.0, 7.4] mm/yr; red trendline) and annual (squares, visible only if different from the stormy-season maxima, 3.8 mm/yr, Sen's slope 3.5 mm/yr, 95% confidence interval [1.3, 6.8] mm/yr; black trendline) maxima of the weekly average water level; b) trends in stormy-season maxima (circles, 4.6 mm/yr, Sen's slope 3.7 mm/yr, 95% confidence interval [1.6, 5.8] mm/yr; red trendline) of the (relative) storm surge heights and in similar annual maxima (squares, visible only if different from the stormy-season maxima, 3.3 mm/yr, Sen's slope 2.9 mm/yr, 95% confidence interval [0.7, 5.1] mm/yr; black trendline). Reproduced from Paper IV.....72

Figure 31. Slope (mm/yr) of trends in the stormy-season and annual maxima of storm surge heights (total water level minus 8.25-day average) in 1961–2004. Reproduced from Paper IV.....73

Figure 32. Alongshore variation in the slopes of trends (mm/yr) of water level components in 1961–2004. Red and cyan: total water level, stormy seasons and calendar year, respectively; magenta and yellow: 8.25-day average, stormy seasons and calendar year, respectively; green and grey: storm surge, stormy seasons and calendar year, respectively. For the observed data sets the colours are the same, circles indicate trends for stormy-season maxima and squares – trends for annual maxima. The typical width of 95% confidence intervals for various slopes is ± 2 mm/yr. The numbering of grid cells follows Figure 4. Adapted from Paper IV.74

Figure 33. Spatial variations in the slope of the trendline of the maxima of the average water level for different averaging lengths. Dark and light grey: 18-h average, stormy-season and annual maxima, respectively; red and orange: 8.25-day (198-h) average stormy-season and annual maxima, respectively (equivalent to yellow and pink lines in Figure 32); light and dark green: 16.25-day (390-h) average stormy-season and annual maxima, respectively; blue and cyan: 24.25-day (582-h) average stormy-season and annual maxima, respectively. The lines representing slopes for stormy-season maxima are wider than their counterparts for annual maxima. The numbering of grid cells follows Figure 26. Adapted from Paper IV.....77

Figure 34. Annual average zonal and meridional air-flow components and their trendlines for 1982–2013 at Kalbådagrund in the Gulf of Finland. Reproduced from Paper IV.....78

Introduction

Effect of climate change on coastal flooding

The increasing concentration of the world's population near the ocean shores combined with gradual changes in the Earth's climate have greatly upsurged the vulnerability of coastal areas. In particular, various coastal engineering structures and especially built environments located in low-lying areas are facing large challenges. The associated problems of adaptation to the effects of climate change, management of the interaction of the (possibly adverse) synergies of various changes, regulation of different conflicts in the use of the existing land and sea resources, ensuring functioning of the necessary infrastructure and mitigation of the multitude of marine induced risks and hazards are most vivid in urban areas (e.g. Hall et al., 2010). On top of that, the complexity of coastal cities is rapidly increasing.

Coastal flooding is the classic example of marine-induced hazards for nearshore communities. According to several scenarios for future global climate changes (e.g., Cheng et al., 2013; O'Grady and McInnes, 2010; Torresan et al., 2012; Hallegatte et al., 2013), the related risks may be radically amplified.

A comprehensive analysis of the potential risks and associated damages is severely complicated by the nature of the most extreme flooding events. A devastating flooding is usually caused by the interplay of several drivers. This interplay may have various forms, from simple synchronisation in time and space of some physical drivers (e.g., low pressure and strong onshore winds) up to complicated interactions of increased water level with the geometry of the nearshore seabed and properties of beaching waves. These drivers often have fundamentally different predictability, physical, dynamical and statistical properties. A direct consequence of the behaviour of the drivers is a different level of correlations between their contributions. For example, dangerous water levels are usually produced by an unfortunate combination of high tide, low atmospheric pressure and strong wind-driven surge. The resulting high water level may be additionally enhanced by the impact of breaking waves (known as wave set-up).

It is often well known which component affecting water levels contributes most to extreme coastal flooding. This thesis largely concentrates on a complementary, but equally intriguing question: Which component (or its physical driver) of unusually high water levels is (or can be in the future) responsible for the largest contribution to the *increase* in the extreme water levels?

Even though the words "water level" and "sea level" are often used as synonyms, it is convenient to employ these terms to denote different readings. When talking about water level, I shall have in mind the water level at the immediate nearshore. The relevant reading includes all local effects, most importantly in the context of this thesis, the impact of wave set-up. The term "sea level" is reserved to the offshore (modelled, measured or observed) readings of the position of the sea surface. This reading, sometimes also called offshore water

level, includes all phenomena that are replicated by contemporary ocean models but excludes wave set-down and set-up in the nearshore.

Many authors emphasise the importance of the current gradual increase in global sea level and particularly the acceleration of this increase in most examples of projected marine climate change (Cazenave et al., 2014). This process is associated with major consequences in some regions (Hallegatte et al., 2013). The related economic damages to low-lying coastal areas may lead to a worldwide welfare loss of almost 2% by the end of the 21st century (Darwin and Tol, 2001; Pycroft et al., 2016).

The rate of sea level rise varies in different parts of the World Ocean. The Baltic Sea (Figure 1) has experienced a faster sea level rise than the adjacent regions during the last century (Stramska and Chudziak, 2013). Most of this increase is associated with the intensification of westerlies (Suursaar et al., 2006a; Stramska and Chudziak, 2013). This region has several specific features that affect the course

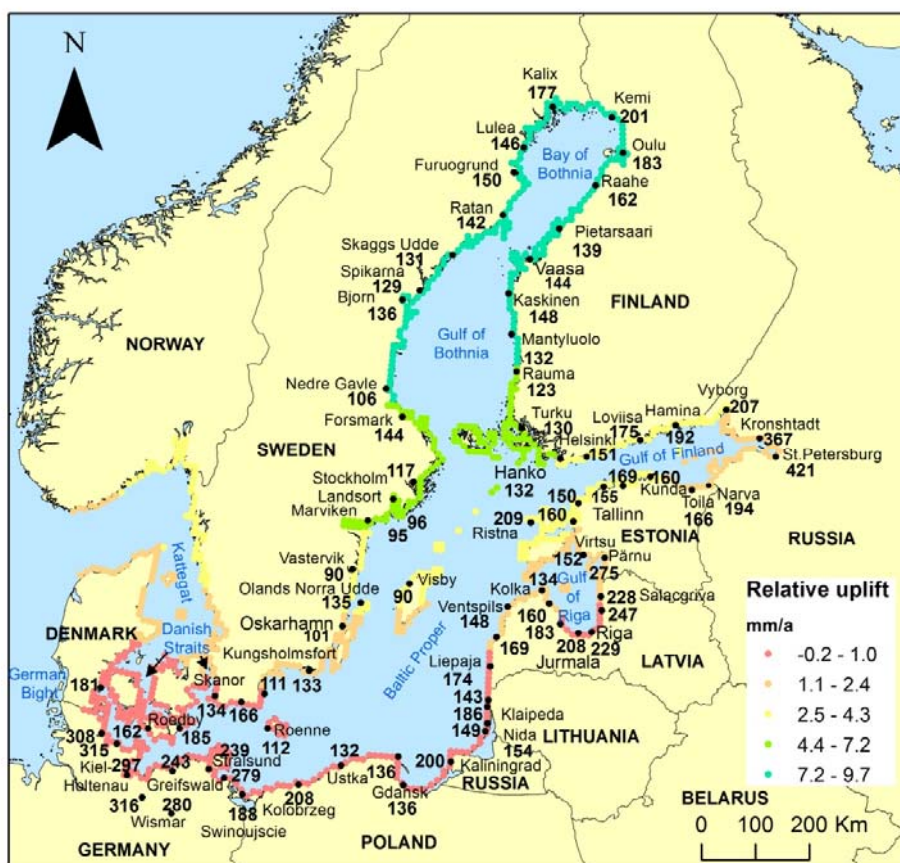


Figure 1. Location scheme of the Baltic Sea, relative Fennoscandian uplift (mm/yr, data from NKG2016LU release) and historical water level maxima on the Baltic Sea coasts (cm, bold numbers; redrawn from Averkiev and Klevanny, 2010).

of local water level. Extensive basin-wide variation in the salinity of sea water (Ekman and Mäkinen, 1996) and spatial differences in the tectonic motions, largely driven by postglacial uplift (Richter et al., 2012), lead to substantial variability in long-term properties of the observed (relative) water levels in different areas of the Baltic Sea (Scotto et al., 2009). The northern part of this basin experiences a rapid uplift (up to 10 mm/yr, Figure 1) and an associated relative sea level decrease (Johansson et al., 2001). A weak relative sea level rise is characteristic of the central part of the sea (Dailidienė et al., 2004, 2006), whereas the southern sections of the sea are affected by a gradual downlift on the order of 0.2 mm/year (Harff and Meyer, 2011) and thus a faster sea level rise than in the rest of this water body.

The increase in global sea level contributes only a fraction to the total loss due to marine-induced hazards. Devastating coastal floodings and associated phenomena are economically extremely damaging (Meyer et al., 2013). While sea level rise is a slow process and thus principally manageable, coastal floodings that develop at timescales of a few hours may lead to massive losses of lives and desertification of entire coastal communities (Dube et al., 2009).

Other contributors to unusually high water levels do not necessarily follow the course of global sea level. For example, on the German North Sea coast before the mid-1950s and from about 1990 onwards, changes in high sea levels matched mean sea level changes. However, from the mid-1950s to 1990 the course of the highest water levels significantly differs from that observed in the mean sea level (Mudersbach et al., 2013).

Components of elevated water levels

Water level and its extremes at the shores are usually driven by a multitude of contributors with greatly different predictability. Among those, tides are almost perfectly regular and caused by extra-terrestrial drivers. A reasonable forecast of the reaction of sea surface to low atmospheric pressure (so-called inverted barometric effect) and the properties of wind-driven surge requires dedicated atmospheric and ocean circulation models. The elevated water level caused jointly by a wind surge and inverted barometric effect is customarily called storm surge. The resulting high water levels may be additionally amplified by specific events and mechanisms such as tide–surge interactions (Batstone et al., 2013; Olbert et al., 2013), meteorologically driven long waves (Pattiarachi and Wijeratne, 2014; Pellikka et al., 2014; Vilibic et al., 2014) or seiches (Vilibic, 2006; Kulikov and Medvedev, 2013).

Most of the Baltic Sea basin is a micro-tidal area where the related water level variations are just a few centimetres (Leppäranta and Myrberg, 2009). Only in some locations of the eastern Gulf of Finland tide-driven fluctuations in the local water level reach about 0.1 m (Särkkä et al., 2017). The quasi-periodic seasonal fluctuations of the average water level form only about 10% of the total water level variations (Raudsepp et al., 1999; Medvedev, 2014).

Many coastal segments of the Baltic Sea are particularly vulnerable with respect to storm surge. This phenomenon creates the highest local water levels in bayheads of elongated relatively shallow sub-basins of the sea (Figure 1). The predominance of westerlies among strong winds often generates such events in the eastern regions of this water body (Suursaar et al., 2006a; Averkiev and Klevanny, 2010). Historical water levels have exceeded 4 m in the eastern Gulf of Finland. Saint Petersburg, for example, has experienced flooding heights up to 4.21 m (Averkiev and Klevanny, 2010). Water levels above 2 m often occur on the eastern coast of the Gulf of Riga. The maximum water level recorded in Pärnu is 2.75 m (Suursaar et al., 2006b; Figure 2). Easterly storms have produced water levels of over 3 m in some locations of the German coast of the sea.

A large part of these records is created by the possibility of generation of extensive subtidal-scale variations in water level in semi-sheltered basins that are connected with the open ocean via narrow and shallow straits (e.g., Chesapeake Bay, Bosley and Hess, 2001). Namely, populations of very high water levels that may persist for many weeks in such areas are naturally created by unfavourable atmospheric conditions that force large water volumes into such basins. The overall freshwater surplus usually results in the outflow of brackish water from the Baltic Sea into the Atlantic Ocean (Leppäranta and Myrberg, 2009). Even moderate westerly winds over the Danish straits with speeds of only 2–5 m/s can block the outflow (Lehmann et al., 2012), reverse the typical estuarine circulation and cause an increase in the water volume of the Baltic Sea.

A series of cyclones (Post and Kõuts, 2014) that force large amounts of the North Sea water to flow into the Baltic Sea (Stigebrandt and Gustafsson, 2003; Lehmann and Post, 2015; Lehmann et al., 2017) exert the largest impact to the Baltic Sea water volume. The water level in the entire sea may rise by 1 m above the long-term mean (Johansson et al., 2001). For many coastal segments this value is comparable to the all-time maximum storm surge height (Averkiev and Klevanny, 2010, Figure 1).

These fundamentally aperiodic extensive variations in the water volume of the entire Baltic Sea are driven by atmospheric impact. They may persist from several weeks (Feistel et al., 2008; Leppäranta and Myrberg, 2009) to a few months

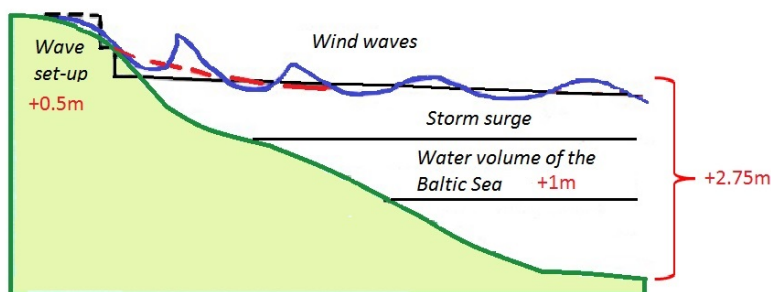


Figure 2. Contribution of different components of high water level in Pärnu (location shown in Figure 1) during the storm Gudrun 09.01.2005.

(Paper IV). Their occasional presence markedly complicates the analysis of the extreme values and return periods of local water level. The most devastating surges in many coastal segments of this sea are created by storms that approach after a series of previous storms have forced unusually large water volumes into the Baltic Sea (Johansson et al., 2001).

Several sections of the coast of the eastern Baltic Sea do not host the above-discussed extremely high water levels. The test area in several studies in this thesis is an urban area in the vicinity of the city of Tallinn at the southern coast of the Gulf of Finland (Figure 3). This area, like the entire Baltic Sea, is micro-tidal and water level is mostly governed by the atmospheric forcing. Its shores are sheltered from the most frequent storms that blow from the south-west and the all-time maximum water level has only reached 1.52 m since the end of the 19th century (Averkiev and Klevanny, 2010). The typical high water levels in this area are about 0.7–0.9 m above the long-term mean during the autumn–winter stormy season. As a result, some parts of the city of Tallinn are not protected even against a moderate water level rise. For example, several low-lying areas (such as the 1980 Olympic sailing centre) were flooded on 8–9 January 2005.

On top of these relatively large-scale phenomena, wave-induced processes contribute substantially to the total water level under certain conditions. As ocean waves are not perfectly linear, their propagation induces a mass transport with the intensity proportional to the squared wave height (Starr, 1947). The propagation of such waves into shallower water leads to a decrease in local water level. This phenomenon is called (wave-induced) set-down (Dean and Dalrymple, 1991). The lowest average water level occurs at the breaking line.

The nature of the impact of waves strongly depends on their approach angle. The waves that approach the coast under relatively large angles with respect to the shore normal mostly produce alongshore current (Dean and Bender, 2006). Further propagation of breaking waves through the surf zone towards the shore under a relatively small angle with respect to the shore normal is accompanied by the transport of water towards the coast. Differently from the generation of set-down, the transport here is owing to the release of the momentum carried by ocean waves in the process of breaking. As a result, the average water level at the shoreline can be considerably higher than beyond the surf zone. This phenomenon is called wave set-up.

Wave-induced addition to water level

Wave set-up is one of the most dangerous components of devastating floodings. In unfortunate conditions, the set-up height may reach about 1/3 of the offshore wave height (Vetter et al., 2010). Set-up events of about 2 m in height have been observed in numerous locations (Heidarzadeh et al., 2009; Hoeke et al., 2013; Melet et al., 2016). The role of set-up is relatively large at coasts with a narrow and rapidly deepening shelf (more generally, in regions where the wind surge remains moderate) and a limited tidal range. Such coasts usually host a moderate range of

variation in water level. For example, in Florida wave set-up can be 30–60% of the total 100-yr storm surge (Dean and Bender, 2006).

The quantification of the magnitude and timing of wave set-up is crucial to understanding the full scale of extreme events because it may additionally raise the already high water level. The relevant knowledge is vital for the design of coastal engineering structures and low-lying infrastructure in locations that are open to high waves. The impact of wave set-up may become evident at the entrances to shallow-water inlets or lagoons (Bertin et al., 2009; Irish and Canizares, 2009; Torres-Freyermuth et al., 2012). For example, rough seas that elevate the water level in the inlets to the Venice Lagoon may considerably contribute to the formation of the “aqua alta” in Venice even when they do not hit the shore (L. Cavaleri, personal communication, 2010).

The analysis of the potential of wave set-up is currently often included into various mapping exercises of flood hazards (e.g., Cariolet and Suanez, 2009; Harper et al., 2009; Jain et al., 2010a, b). This approach is increasingly important in the context of potential changes in the directional structure of the wind and wave climate (McInnes et al., 2009). The quantification of the contribution of wave set-up is crucial for adequate estimates of the erosion of the higher parts of the beach where unprotected sediment is often particularly vulnerable (Trenhaile, 2009). Various ways for the evaluation of wave set-up are included into forecasts performed using the classic wave models (SWAN Technical Documentation, 2007; Roland et al., 2009; Moghimi et al., 2013). However, acquiring an adequate estimate of the contribution from this phenomenon is one of the largest challenges in the modelling of storm surges and associated inundation (Dukhovskoy and Morey, 2011; Melet et al., 2016).

Even though several attempts in this direction have been made in the context of the Baltic Sea (Alari and Kõuts, 2012; Paper II), the existing flooding maps and operational water level forecasts in Estonia generally do not take this phenomenon into account (Lagemaa et al., 2013). The above-mentioned maximum water levels have been measured in the locations that are not strongly affected by wave set-up. Therefore, they basically characterise the offshore water level. The actual water level during certain storms may be much higher in some sections of the coast. For example, even a moderate wave set-up, say, about 0.5 m, may lead to serious consequences in certain segments of the city of Tallinn.

A major reason for this situation is that the relationship between the offshore or breaking wave properties and the wave set-up height is still under extensive discussion (Hsu et al., 2006; Shi and Kirby, 2008; Nayak et al., 2012). The results of the conversion of wave-driven momentum into the development of elevated water levels depend on many local factors such as the nature of the seabed of the surf zone (Apostos et al., 2007). As these factors may largely vary in time and space, and may depend on the sea level, it is natural that the relevant estimates diverge radically (Stockdon et al., 2006). The SWAN model usually hindcasts the set-up height that is in the range of 10–15% of the offshore wave height (Filipot and Cheung, 2012; Nayak et al., 2012). The set-up height may even become

negative (i.e., approaching high waves may lead to a local decrease in the average water level at the shoreline) in the presence of a specific kind of vegetation and/or very rough bottom (Dean and Bender, 2006).

High wave set-up events certainly occur only during severe storms or extreme swell events. Their magnitude often strongly varies along relatively short coastal sections. As wind and wave directions, wave periods and water levels in various heavy storms may be somewhat different, refraction-driven changes in wave properties are also different. Thus, the particular locations hosting the highest wave set-up and maximum water level elevations normally vary from one storm to another. This feature complicates the estimation of the maximum water level and associated city planning exercises along urbanised coastal stretches with complicated geometry (Valdmann et al., 2008). A natural solution to this problem is the use of a long time series of wave properties to properly resolve the gaps in data sets associated with infrequent occurrence of storms from certain directions, which may affect some vulnerable locations.

The problem of building an accurate “climatology” of set-up events is very acute in micro-tidal, semi-enclosed water bodies such as the Baltic Sea (Figure 3). These water bodies are vulnerable to the increase in the offshore water level and also to changes in the wave approach directions. Such changes have recently been identified for several regions (Räämet et al., 2010; Charles et al., 2012b). The situation is furthermore complicated in urban areas. Coastal floodings are a particular challenge to modellers and managers in such areas because of possible interactions between surface and sewer flows (Dawson et al., 2008).

The properties of wave set-up crucially depend on the approach angle of waves. Generally, this angle varies in time and space according to the nearshore bathymetry, properties of offshore waves and the instantaneous local water level. An additional problem in the Baltic Sea is that the outcome of wave modelling substantially depends on the particular wind information (Nikolkina et al., 2014). However, long-term statistical properties of wave fields are still reasonably reproduced by even relatively low-quality wind information (Räämet et al., 2009). The properties of wave set-up are customarily associated with the approach angle at the breaker line. This angle is well defined only if the nearshore is homogeneous in the alongshore direction and the wave field is monochromatic (Larson et al., 2010; Viška and Soomere, 2013; Lopez-Ruiz et al., 2014, 2015). Consequently, it is relatively easy to predict the properties of wave set-up on long, basically straight coastal sections (O’Grady et al., 2015). It is customary to use simplified schemes for the evaluation of the impact of refraction and shoaling on wave properties in the nearshore of such coastal segments (e.g., Larson et al., 2010). In many occasions it is acceptable to assume that waves propagate directly onshore (O’Grady et al., 2015). A direct generalisation of this viewpoint is the approach used in Paper I where only the properties of the highest waves that approach from a relatively narrow range of directions are taken into account.

The course and distribution of high water levels in the Baltic Sea

The traditional methods for the analysis of the course of water level and forecast of extreme situations rely on long-term water level records and numerical simulations. Along with the direct search for the worst-case scenarios (e.g., Averkiev and Klevanny, 2010), extreme water levels and related risks are often addressed using the probabilistic approach. The classic targets are extreme water levels and their return periods (e.g., Purvis et al., 2008; Haigh et al., 2010a, b; Arns et al., 2013) and various statistical parameters of water level variations (Serafin and Ruggiero, 2014; Fawcett and Walshaw, 2016). The same approach has been broadly applied to the analysis of average and extreme wave properties (e.g., Orimolade et al., 2016; Rueda et al., 2016a), and more recently towards understanding the properties of meteotsunamis and their potential contribution to marine coastal hazards (Geist et al., 2014; Bechle et al., 2015).

The empirical distribution of deviations of the water level from its long-term average resembles a normal distribution in the eastern Baltic Sea (Johansson et al., 2001; Suursaar and Sooäär, 2007). The factual distribution is slightly skewed: the elevated water levels are more probable than the equivalent low water levels. The difference from a relevant Gaussian distribution is insignificant for moderate deviations of both signs. Also, extremely large deviations from the average exclusively correspond to elevated water levels (Johansson et al., 2001), high water levels are usually short-living transient events and low water levels often persist for a much longer time. The largest discrepancy between normally distributed values and measured or modelled water levels is evident for extreme surges (Johansson et al., 2001; Suursaar and Sooäär, 2007).

A natural reason for the mismatch between the empiric distributions of different water levels and a Gaussian one is that many processes may contribute to the formation of the water level. The appearance and properties of probability distributions of various contributors to extreme water levels are fundamentally different. A typical example in this context is the Baltic Sea. As discussed above, the total water level in this sea is formed as a joint impact of two components. The first component, the empiric probability distribution of the extensive subtidal or weekly-scale variability matches well the classic quasi-Gaussian distribution. The other component that reflects the local storm surge has an exponential distribution and apparently mirrors a Poisson process (Soomere et al., 2015b). Further, the probabilities of occurrence of different single wave heights follow either a Rayleigh (Longuet-Higgins, 1952), Weibull (Forristall, 1978) or Tayfun (Socquet-Juglard et al., 2005) distribution. Similarly, the empirical probabilities of average or significant wave heights usually resemble a Rayleigh or, more generally, a Weibull distribution (Muraleedharan et al., 2007; Feng et al., 2014). In contrast, meteotsunami heights have been shown to better match Pareto-type distributions (Bechle et al., 2015).

The drivers of the most devastating coastal floodings are usually not completely independent. It is therefore necessary to consider multivariate distributions of their

properties in order to build an adequate understanding of their potential danger. It is customary to address the possibility of a simultaneous occurrence of storm surges and large waves (e.g., Hawkes et al., 2002; Wadey et al., 2015; Rueda et al., 2016b) but joint distributions of wave heights, periods and directions are less often considered in this context (Masina et al., 2015).

The above-discussed features naturally complicate the analysis of certain properties of water levels. Limited deviations of the empirical distribution of single water level recordings from a Gaussian distribution are insignificant in the analysis of commonly occurring water levels (Stramska, 2013), spatial and seasonal variations and trends of sea level (Hünicke and Zorita, 2008; Scotto et al., 2009; Hünicke, 2010; Stramska et al., 2013), or certain quantiles of water levels (Barbosa, 2008; Donner et al., 2012). The non-Gaussian properties may have a much larger impact on calculations of probabilities of rare events and projections of extreme water levels and their return periods (Suursaar and Sooäär, 2007; Johansson et al., 2011). Such projections usually extrapolate the core properties of the water level statistics far beyond the time interval covered by observations or model hindcasts. This is not always acceptable in basins like the Baltic Sea (e.g., Mudersbach and Jensen, 2009). It is therefore not surprising that different methods frequently yield significantly different predictions of extreme water levels (e.g., Sterl et al., 2009) or large spreading of the results obtained using the same technique but with slightly different options or model parameters (Arns et al., 2013). Also, even the initial de-trending of a set of water level recordings, often applied as a background procedure, may modify the results of the projections in question.

The problem is further complicated by the above-discussed skewness of the distribution of water levels that leads to a much higher increase in the annual maxima compared to the mean values (Jaagus and Suursaar, 2013). The long-term course of water levels is not necessarily linear in many locations (Donner et al., 2012). This is the case in the Baltic Sea where a shift in the water level trend occurred in the 20th century (Johansson et al., 2001, 2014; Dailidienė et al., 2006). Another hidden problem is that the generic features of extreme value statistics (see Section 2.3) are not necessarily granted when the set of water level values contains a population with completely different properties. For example, if the water level time series has a large number of outliers, its extreme values not necessarily obey any classic (Fréchet, Weibull or Gumbel; Coles, 2001) extreme-value statistics. This is also the case in the Baltic Sea where extreme water level events in some locations (e.g., Pärnu, Figure 2) cannot be adequately described by any single commonly used extreme value distribution (Suursaar and Sooäär, 2007).

A promising way to circumvent this problem is to use an ensemble approach (Christiansen et al., 2010) for the evaluation of projections of rare water level events. This alternative is a standard approach for approximately solving the problems that are highly sensitive with respect to the input data or model parameters (Araújo and New, 2006). The basic idea is that a certain average of a cluster of projections often provides a much better forecast than any single model

(Cheung, 2001). This approach is widely used in the neighbouring seas (e.g., Sterl et al., 2009; Mel et al., 2013) but has only recently been applied to the Baltic Sea conditions to project the local mean sea level rise (Johansson et al., 2014).

Increasing trends in the extreme water levels in the Baltic Sea

The contributions of various drivers of water levels can be considered as mostly independent of each other. This assertion greatly simplifies the analysis and forecast of maximum water levels because of the possibility of considering separately the course of water level variations driven by each driver (e.g., Losada et al., 2013; Howard et al., 2014; Weisse et al., 2014). Detailed analysis of the behaviour of single components of the water level is particularly relevant and convenient in situations where contributions to the elevated water levels act at largely different time scales.

For example, the classic approach in this field is to separate the total water level into components driven by fundamentally different mechanisms. Examples of such components are the long-term mean and its slow variations (e.g., driven by postglacial uplift), tides (driven by extra-terrestrial forces) and storm surges driven by local atmospheric impacts (Pugh and Vassie, 1978, 1980; Haigh et al., 2010a). Another way of separation is to split the total water level into periodic and random components (Haigh et al., 2010b). Such attempts are widely used in notably different environments, including the sites that host a substantial range of so-called subtidal (time scales from diurnal to seasonal) water level variability (Percival and Mofjeld, 1997; Wong and Moses-Hall, 1998; Guannel et al., 2001; Wilson et al., 2014).

The impact of multiple drivers on the formation of elevated water levels explains why sea level extremes usually do not follow any simple rule (Weisse et al., 2014). The situation is particularly complicated in the eastern Baltic Sea. Water level time series in certain sites of the eastern part of this sea contain a few extremely high recordings. These values are considered as statistically unpredictable outliers (Suursaar and Sooäär, 2007; Suursaar et al., 2015), but are nevertheless caused by storms of reasonable strength. It is likely that they are produced when a strong storm occurs during a time period characterised by an increased water level of the entire sea.

The distinction of the impact of different drivers on the total water level is a complicated problem. The relevant approaches range from various filtering and averaging techniques to the use of wavelet methods (Percival and Mofjeld, 1997; Bastos et al., 2013; Johansson, 2014).

A simple classic approach to the analysis of the basic features of the past behaviour of high water levels is to look at linear trends of water level maxima and at similar trends of the counterparts of these maxima. This tool has been useful for obtaining a first approximation of the magnitude of the overall sea level rise (Cazenave et al., 2014) and identifying its contribution to the increase in the local water level maxima (Mudersbach et al., 2013; Xu and Huang, 2013). The technique

of the evaluation of linear trends has highlighted an increase in the magnitude of local storm surges on the coasts of the open ocean (Sun et al., 2013; Talke et al., 2014), shelf seas (Weisse et al., 2012) and semi-enclosed basins (Ullmann et al., 2007; Wiśniewski and Wolski, 2011; Masina and Lamberti, 2013).

The use of this technique is complicated in areas where long-term trends are superposed by extensive short-term or quasi-periodic variations in the course of water level. The Baltic Sea hosts several variations of this kind in different parts of the sea. Johansson et al. (2001) demonstrated that several statistical properties of short-term sea level variability have clearly changed in the northern Baltic Sea over the 20th century. The frequency and duration of storms have increased in the German Bight but no trend is evident in the height of storm surges in this region (Gönnert, 2003). The trends in maxima of water levels systematically exceed similar trends in water level minima (Barbosa, 2008). The most interesting feature is extensive variation (from about 2 to 9 mm/yr, Suursaar and Sooäär, 2007) in the slopes of trends in the local water level maxima along the Estonian coast. Importantly, the changes in the mean and maximum water levels are almost uncorrelated.

The analysis of spatial variations in the slopes of these trends provided in this thesis was inspired by the circumstance that two components can be clearly distinguished in the total water level observed or simulated in the nearshore of the eastern Baltic Sea (Soomere et al., 2015b). One of these components (weekly-scale average water level, interpreted as a proxy for the entire Baltic Sea level) represents a quasi-Gaussian process while the other one (the total water level minus the weekly average, interpreted as the local storm surge (Haigh et al., 2010a)) reflects a Poisson process. Even though the probability distributions of these components are different, the distinction of these components makes it possible to shed more light on their role of in the decadal changes in the maximum water levels.

The objectives and outline of the thesis

Many aspects of annual and seasonal fluctuations, as well as extreme values of the water levels at the Estonian coasts have been studied during several decades. There are still many gaps in the understanding of how the total water level is created and which mechanisms play a governing role in the formation of the highest water levels.

This thesis addresses the properties of three mechanisms that most contribute to the formation of extreme water levels at the Estonian coast: the behaviour of the water volume of the Baltic Sea, the local storm surge and the wave-driven addition to the local water level. The central hypothesis, supported by a wide range of evidence, is that the contributions from these mechanisms vary strongly along the Estonian coasts and also in time. The properties of these variations, however, are largely unknown.

The main idea is to separate the contribution of each component from the measured, observed or modelled water level time series, and to complement the outcome with the results of high-resolution wave modelling in selected areas. The core assumption is that the relevant contributions to the total water level are largely independent and thus can be, to a first approximation, analysed separately. As the interplay of these mechanisms is apparently most complicated in coastal areas with complex geometry and the resulting danger is the greatest in low-lying urban areas, a large part of the research deals with the urban area of the city of Tallinn.

The main objectives of this thesis are as follows:

- to quantify the potential contribution of the wave set-up phenomenon to the nearshore water level along a low-lying urban area with complex geometry (the coastline of the city of Tallinn) affected by winds from a wide range of directions;
- to evaluate the magnitude of spatial variations in set-up height, specify long-term temporal changes in its maxima, identify the underlying changes in the “climate” of storms and distinguish its contribution to the formation of the total water level extremes;
- to develop a technique for detecting a systematic contribution of wave set-up to local water level observations or measurements;
- to establish the role of the major components contributing to the increase in the total water level maxima and associated coastal floodings on the eastern coast of the Baltic Sea.

To fulfil these objectives, Chapter 1 starts from an insight in to the importance of wave-induced set-up in the formation of the local water level. The magnitude of the set-up height is governed by parameters of the approaching waves and certain features of the nearshore. The properties of waves are found using a high-resolution triple-nested version of the spectral wave model WAM. To reach an adequate replication of nearshore wave properties, the wave model is forced with high-quality marine winds recorded in the central part of the Gulf of Finland at Kalbådagrund since 1981. This chapter mainly follows Paper I and highlights the

main feature of the “climate” of wave set-up heights, establishes a relationship between the particular storms and stretches where a remarkably high water level may occur in idealised conditions, and provides evidence showing that wind direction in a part of strong storms may have rotated over decades.

The results presented in Paper I raise the question about whether and how the contribution from wave set-up to the total water level could be detected. Chapter 2 starts with the presentation of an attempt to indirectly distinguish the contribution of wave set-up from the other components of high water levels. The main idea is to compare historically measured water level data sets at harbours with the outcome of contemporary ocean circulation models. These models adequately describe the offshore water levels that are affected by variations in the total water volume of the Baltic Sea and the local storm surges but ignore wave set-up. The impact of wave set-up most likely becomes evident from the projections of extreme values of water levels. The influence is identified using the ensemble approach of extreme value projections built based on the block maxima method (Paper II). Further on, Chapter 2 also addresses the question of whether very high offshore water levels may occur simultaneously with extreme wave set-up heights. Similarly to Chapter 1, this analysis is performed for the shores of the Tallinn area (Paper III). The simple answer is: the synchronisation of extreme offshore water levels and large set-up heights often occurs in coastal segments that are open to the predominant wind directions and never in segments that are sheltered from such winds.

The most intriguing question is: which of the two major components of the Baltic Sea water level makes the greatest contribution to the rapidly increasing extreme water levels on the Estonian coasts? This problem is only addressed from the viewpoint of offshore water levels in Chapter 3 of this thesis. The extreme offshore water levels are created here when a strong storm surge occurs during a time interval of a largely increased water volume of the entire Baltic Sea. The components are separated by a simple filtering technique (Soomere et al., 2015b). The analysis reveals not only great variations in the role of these two components in the increase in the extreme water levels at the Estonian coasts but also signals that wind direction may have changed in a part of storms (Paper IV).

Approbation of the results

The basic results described in this thesis have been presented by the author at the following international conferences:

Pindsoo K., Soomere T. 2017. Trends in the extreme water levels of the Baltic Sea. Oral presentation at the *11th Baltic Sea Science Congress* (12–16 June 2017, Rostock, Germany).

Pindsoo K., Soomere T. 2017. Wave set-up in the urban area of city of Tallinn, Estonia. Poster presentation at the *11th Baltic Sea Science Congress* (12–16 June 2017, Rostock, Germany).

Pindsoo K., Soomere T. 2016. Trends in the components of extreme water levels signal a rotation of winds in strong storms in the eastern Baltic Sea. Poster presentation at the *European Geosciences Union General Assembly 2016* (17–22 April 2016, Vienna, Austria).

Pindsoo K., Soomere T. 2015. Laineaju panus ekstreemsetesse veetasemetesse Tallinna ümbruses (The contribution of wave set-up into extreme water levels in the vicinity of the City of Tallinn). Poster presentation (in Estonian) at the *METE OBS 150, Eesti geofüüsika konverents* (2–3 December 2015, Tõravere, Estonia).

Pindsoo K., Soomere T. 2015. Spatial variability in the trends in extreme water level components in the Eastern Baltic Sea. Oral presentation at the *Baltic Earth/Gulf of Finland PhD Seminar* (19 November 2015, Tallinn, Estonia).

Pindsoo K., Soomere T. 2015. Trends in extreme water levels of the eastern Baltic Sea. Oral presentation at the *10th Baltic Sea Science Congress: Science and Innovation for Future of the Baltic and the European Regional Seas* (15–19 June 2015, Riga, Latvia).

Pindsoo K., Soomere T. 2015. Contribution of wave set-up into the total water level in the Tallinn area. Oral presentation at the *10th Baltic Sea Science Congress: Science and innovation for future of the Baltic and the European regional seas* (15–19 June 2015, Riga, Latvia).

Pindsoo K., Soomere T., Eelsalu M. 2015. Ekstreemsete veetasemete tulevikuprojektsioonid (Projections of extreme water levels). Oral presentation (in Estonian) at the conference *Eesti veeteaduse horisonid* (Horizons of water resources research in Estonia) (28 April 2015, Limnoloogiakeskus, Estonia).

Pindsoo K., Soomere T. 2015. Contribution of wave induced set-up into total water level in the urban area of Tallinn. Poster presentation at the *International Scientific Seminar on Climate Modelling and Impacts: From the Global to the Regional to the Urban Scale* (10 March 2015, Hamburg, Germany).

Pindsoo K., Soomere T. 2014. Wave set-up climatology in the city of Tallinn, Estonia. Poster presentation with 10 minutes oral introduction at the *IUTAM*

Symposium on Complexity of Nonlinear Waves (08–12 September 2014, Tallinn, Estonia).

Pindsoo K., Soomere T. 2014. Changing wave set-up climate in the urban area of Tallinn. Oral presentation at the *1st International Conference on Mathematics and Engineering in Marine and Earth Problems* (22–25 July 2014, Aveiro, Portugal).

Pindsoo K., Soomere T. 2014. Signal of wave climate change reflected by wave set-up height. Poster presentation at the *2nd International Conference Climate Change – The Environmental and Socio-economic Response in the Southern Baltic Region* (12–15 May 2014, Szczecin, Poland).

Pindsoo K., Eelsalu M., Org M., Soomere T. 2014. Trends in long-term components and rapid variations in the water level: a case study for Tallinn Bay. Poster presentation at the *Baltic Earth Workshop "Natural Hazards and Extreme Events in the Baltic Sea Region"* (30–31 January 2014, Helsinki, Finland).

Pindsoo K., Soomere T. 2013. Wave set-up in the urban area of the City of Tallinn, Estonia. Poster presentation at the *9th Baltic Sea Science Congress* (26–30 August 2013, Klaipėda, Lithuania).

Pindsoo K., Soomere T. 2012. The water level rise caused by wave set-up in the urban area of the city of Tallinn, Estonia. Oral presentation at the *6th International Student Conference "Aquatic Environmental Research"* (17–19 October 2013, Palanga, Lithuania).

1. Quantification of the role of waves affecting the water level in the vicinity of the city of Tallinn

Many sections of the Estonian coast are open to the predominant strong wind directions and therefore often host substantial wave set-up heights. The magnitude of this phenomenon is evidently highly variable along our coasts because of very complicated coastal geometry. This chapter addresses the “climate” of set-up heights along the waterfront of the city of Tallinn and its vicinity, including a large area to the east of Tallinn that is open to the north-east. This mostly urban shore contains several vulnerable sections open to large waves.

The time series of wave properties in the nearshore, reconstructed numerically with a spatial resolution of about 0.25 nautical miles (470 m), form the starting-point of the analysis. This data set is used to (i) identify the coastal sections prone to the highest set-up in Paper I, (ii) analyse the timing of the highest offshore water levels and very large wave set-up events in Paper III and (iii) establish the wind directions associated with the most dangerous situations in which the total water level at the waterline considerably exceeds the all-time maximum for the offshore water level in Paper III. The analysis allows highlighting the link between particular storms and stretches where an unexpectedly high water level apparently occurred. It is shown that almost each coastal section had its “own” (perfect) storm in the last three decades that produced the 30-yr highest set-up in this section (Paper I). The results of the analysis suggest that the direction of storms has undergone some interesting decadal-scale variations, first of all the rotation of the approach direction of the largest waves from the beginning of the 1980s.

1.1. Reconstruction of wave properties

A number of recent studies have focused on the basic properties of the wave climate and fluctuation of the water levels in the Baltic Sea basin. A thorough overview of the relevant results is presented by Hünicke et al. (2015). The majority of such studies have not related these phenomena to each other. This viewpoint is to some extent justified for regions where strong waves and high sea levels normally do not occur simultaneously. This is the case, for example, for many sections of the western Baltic Sea coast where strong winds usually blow in the offshore direction.

The situation is more complicated in regions where high waves and elevated water levels may occur simultaneously. An example of such a coastal section is the vicinity of Tallinn Bay in the north-eastern Baltic Sea at the southern coast of the Gulf of Finland (Figure 3). This region has extremely complicated geometry. Its coastal sections are open to various directions, from the west over the north to the east. The area also includes low-lying urbanised segments that are most vulnerable

to extreme events. Therefore, even a moderate additional water level rise may cause problems in this area.

The typical tidal range in this part of the Baltic Sea is a few centimetres (Leppäranta and Myrberg, 2009) and water level fluctuations in the entire Gulf of Finland are mostly governed by atmospheric forcing. On the one hand, the ever highest recorded water level is 1.52 m above the long-term mean (1.55 m according to Hünicke et al. (2015)). These values have been measured at the entrances to Tallinn Old Harbour and Muuga Harbour (Figure 3). As the water depth in these locations is >10 m, the discussed values are not affected by wave set-up and characterise the offshore water level (called sea level in what follows). On the other hand, significant wave height, e.g., in the interior of Tallinn Bay may exceed 4 m in the strongest north-north-western (NNW) storms. Such waves may create set-up heights up to 1 m in ideal conditions (Dean and Dalrymple, 1991).

The evaluation of possible events of wave-induced set-up requires detailed information about wave properties, first of all the significant wave height, wave period and propagation direction. As the coastline in the vicinity of the city of

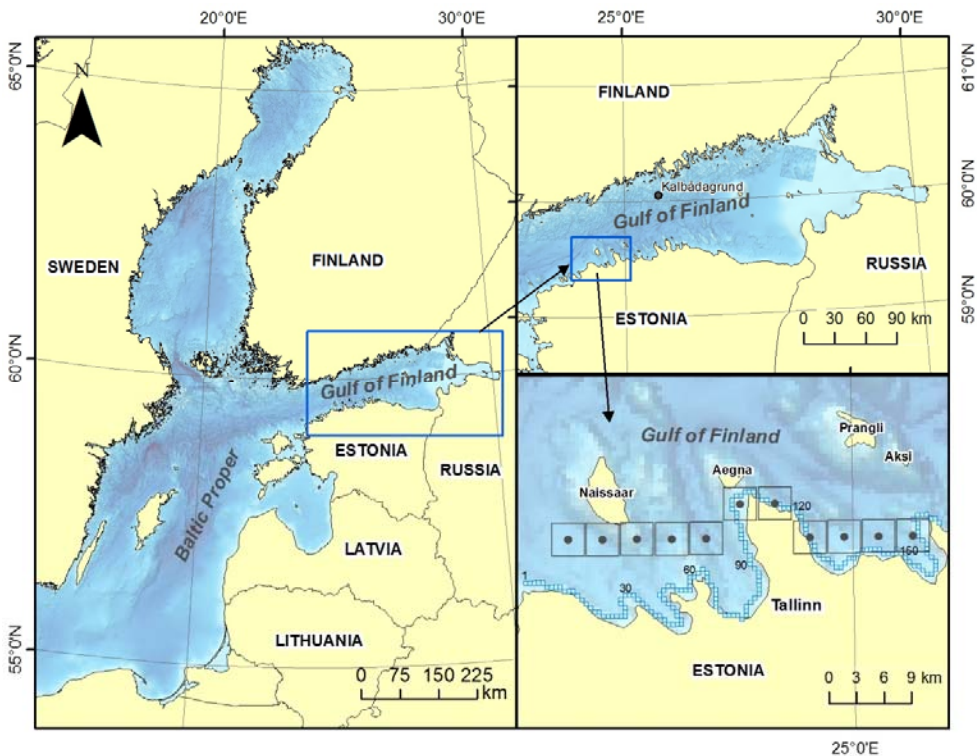


Figure 3. Computational areas of the sequence of wave models designed to evaluate the time series of wave properties in the Tallinn Bay area. Small cyan squares along the coast in the lower right panel reflect the grid points from which the wave data are used in Paper I and Paper III. The offshore water level is represented by values evaluated in 11 nearshore grid cells (grey squares) of the Rossby Centre Ocean (RCO) circulation model (Paper III). Adapted from Paper III.

Tallinn is mostly curved, such information is needed separately for each short section of the shore.

Even though wave observations in Tallinn Harbour have a long history (Soomere, 2005), the existing visually observed and instrumentally measured data do not have the spatial resolution necessary for adequate estimates of wave set-up properties. For this reason contemporary wave models are used in this thesis to reconstruct wave properties in the nearshore of the study area.

The wave properties necessary for the analysis of the “climate” of wave set-up were calculated using a triple-nested version of the third-generation spectral wave model WAM (Komen et al., 1994). This model was originally constructed for open ocean conditions and for relatively deep water (Komen et al., 1994). Its earlier versions are known to overestimate the wave height at very small depths in the study area (Alari and Raudsepp, 2010). However, with an enhanced spatial resolution the model is capable of producing auspicious results even in the archipelago conditions of the northern Gulf of Finland (Soomere et al., 2008a; Tuomi et al., 2011, 2012, 2014).

Large ocean waves have often periods of 12–15 s. Such waves start to lose part of their energy owing to wave–bottom interactions at depths of 50–60 m (Ardhuin et al., 2003). Typical Baltic Sea waves with a period of 5.5 s develop the same near-bottom orbital velocity at a much smaller depth (about 17 m, Soomere and Eelsalu, 2014). Due to relatively small typical wave periods in the Baltic Sea (Broman et al., 2006; Soomere and Räämet, 2011) compared to open ocean swells, the WAM model for the Baltic Sea gives acceptable results at much smaller depths. As waves are usually even shorter in semi-enclosed sub-basins of the Baltic Sea, the WAM model is able to passably describe the wave properties until depths of about 5 m, that is, usually at a distance of about 200–300 m from the coastline (Soomere, 2005).

The analysis in Paper I and Paper III uses the same configuration of the wave model. A relatively coarse grid (with a spatial step of about 5.5 km) covered the whole of the Baltic Sea (Figure 3). The results of the wave model run for this grid were used to provide information about wave properties at the entrance to the Gulf of Finland. A model with a grid step of about 1.8 km was implemented for this gulf. The bathymetry data used in these two modes is based on the data collection of Seifert et al. (2001), with a resolution of 1' along latitudes and 2' along longitudes. At each grid cell, 600 components of the two-dimensional wave spectrum were calculated. These components represent wave components propagating in 24 evenly spaced directions and having 25 discrete frequencies ranging from 0.042 to 0.41 Hz with an increment of 1.1.

It is commonly understood that to resolve the major local topographic and bathymetric features in most of the nearshore of Estonia and, consequently, for adequate representation of the nearshore wave fields, it is necessary to evaluate wave properties with a spatial resolution of at least 500 m. For this reason we employed a wave model with a spatial resolution of about 470 m (1/4' along latitudes and 1/2' along longitudes) in the Tallinn Bay area. The bathymetry data

for this model grid are constructed using the maps provided by the Maritime Administration of the Republic of Estonia (Soomere, 2005; Andrejev et al., 2010). The frequency range of this nearshore wave model was extended to 2.08 Hz (42 evenly spaced frequencies) for wind speeds ≤ 10 m/s in order to reasonably represent the wave growth in low wind and short fetch conditions (Soomere, 2005). A detailed description of the model is provided in Paper I where wave parameters are calculated for years 1981–2012. Paper III uses the same model but covers the years 1981–2014.

The quality of wave reconstructions critically depends on the quality of wind information used for wave modelling. The reliability of wind information seems to be the largest bottleneck in wave studies in the Baltic Sea region where simulations of wave climate performed using different wind data may lead to largely deviating results (Nikolkina et al., 2014). The problem is even more complicated if one wishes to have long temporal coverage. The main reason is the complicated geometry of the Baltic Sea and high elevations in many of its surrounding areas. As a result, surface-level offshore winds are often influenced by the mainland. The global wind data have a rather low resolution. For the use of wave modelling this information has to be downscaled (Schmager et al., 2008; Samuelsson et al., 2011) and artificially modified (e.g., using simulated gustiness to adequately replicate the air–sea interaction in the Baltic Sea region (Höglund et al., 2009)). All these steps may introduce distortions. As a result, some wind data sets are only reliable in the vicinity of the country that has produced them (Räämet et al., 2009). Another problem is that modelled high-resolution winds, especially those coupled with properties of windseas, are homogeneous only during very limited time intervals (Tuomi et al., 2012).

The situation is even more complicated due to rather specific features of the wind and wave regime of the Gulf of Finland (Soomere et al., 2008b; Pettersson et al., 2010). The strongest winds tend to blow obliquely across this water body. It is the most likely reason for the frequent mismatch in the direction of even the best modelled wind fields and high-quality wind records (Keevallik and Soomere, 2010). As wave set-up largely depends on the wave approach directions, this mismatch is a crucial problem in the reconstruction of wave set-up.

To avoid problems related to insufficient accuracy of representation of wind directions by numerical models in the study area, the triple-nested wave model described above was forced with high-quality marine wind data. Such data from a location that is practically not affected by the mainland are available from a measurement site operated by the Finnish Meteorological Institute at the caisson lighthouse of Kalbådagrund. This lighthouse is located in the central part of the Gulf of Finland at a distance of several tens of kilometres from the mainland (Figure 1, 59°59' N, 25°36' E; Figure 3).

The automatic weather station is mounted at the lighthouse at a height of 32 m above the mean sea level. The factors to reduce the recorded wind speed to a reference height of 10 m are 0.91 for neutral, 0.94 for unstable and 0.71 for stable stratifications in this region (Launiainen and Laurila, 1984). Following the

experience of simulations of wave climate in this region (Soomere, 2005), the constant factor 0.85 was used in the computations in this thesis.

To speed up wave calculations, I employed a simplified scheme of the evaluation of wave properties based on the speed, direction and duration of wind conditions (Soomere, 2005). Such schemes are applicable to relatively small sea areas (such as the Gulf of Finland) because of two favourable features. Firstly, the properties of strong winds (that create all significant wave events) are often highly homogeneous over such water bodies. In other words, wind speed and direction change insignificantly in different areas of the sea. It is therefore acceptable to assume that wind properties are constant over the entire study area and to use one-point wind data as the input for the wave model in the entire area in question.

Secondly, wave fields have a relatively short memory (normally no longer than 12 h in the Gulf of Finland) of wind history (Soomere, 2005). Consequently, to a first approximation, an instant wave field in Tallinn Bay is basically a function of a short section of the wind dynamics. This feature allows splitting the wave calculations into sections with a duration of 3, 6, 9 or 12 h and with almost constant wind properties. The geometry of the Baltic Proper and the Gulf of Finland is such that the waves excited in the Baltic Proper by most wind directions (except for western winds) normally do not propagate into the Gulf of Finland. It is therefore acceptable to assume that remote wind conditions in the open Baltic Sea insignificantly contribute to the local wave field in Tallinn Bay even if the properties in the Baltic Sea deviate significantly from those measured at Kalbådagrund. The wave fields excited by western winds are reconstructed based on the assumption that the wind properties in the northern part of the Baltic Proper match those observed at Kalbådagrund. These assumptions are correct in Tallinn Bay for about 99.5% cases (Soomere, 2005). The entire wind data-set covers the time interval of 01.01.1981–04.02.2014 and contains 93 016 measurements. In 8554 cases (less than 10%) either wind speed or direction was missing. These data were left out of further analysis.

The presence of ice was ignored in wave calculations. The mean number of ice days varies from 70 to 80 annually (Climatological Ice Atlas, 1982; Sooäär and Jaagus, 2007) and ice is present during a large part of the windiest season (Mietus, 1998). This simplification therefore leads to a certain bias in the results, in general, to a certain overestimation of the reconstructed wave and set-up heights. The computed parameters of wind waves and wave set-up are somewhat overestimated and represent average wave properties realistic for the years with no extensive ice cover.

The wind information starting from 1981 was at first available only once in 3 h. In order to keep the reconstructed wave time series homogeneous, only wind data with the temporal resolution of 3 h were used in all calculations of wave set-up. Thus, I employed the time series of significant wave height, peak period and mean wave direction that were evaluated once every three hours. The extracted data set of the time series of nearshore wave properties in the Gulf of Finland serves as the basis of the analysis in Paper I and Paper III.

1.2. The highest waves in the nearshore of Tallinn

The geometry of the nearshore of the urban area of Tallinn and its vicinity is fairly complicated. The study area contains four relatively large bays (Tallinn Bay, Kopli Bay, Kakumäe Bay and Muuga Bay, Figure 4) that are deeply cut into the mainland and are open to greatly different directions (north-west, NNW and north-east). Winds from the NNW are somewhat less frequent than south-western winds but contain the strongest winds in the northern Baltic Proper (Soomere, 2001). Easterly winds are usually thought to be less frequent and weaker than westerly or NNW winds (Soomere and Keevallik, 2003) but extremely strong eastern winds may occur in the area (Pettersson et al., 2013).

The coasts of the interior of Tallinn Bay are relatively well protected against most directions. Muuga Bay is widely open to the north-east. Beaches at the bayheads of the two other bays and along the Viimsi Peninsula are open to some of the predominant wind directions. Many coastal stretches possess the features that are favourable for the formation of high set-up. Some such stretches are adjacent to low-lying existing and planned residential areas.

The nearshore of the study area (Figure 4) was divided into 174 sections with a typical length of 0.5 km (Paper III). In Paper I, only 105 sections located to the

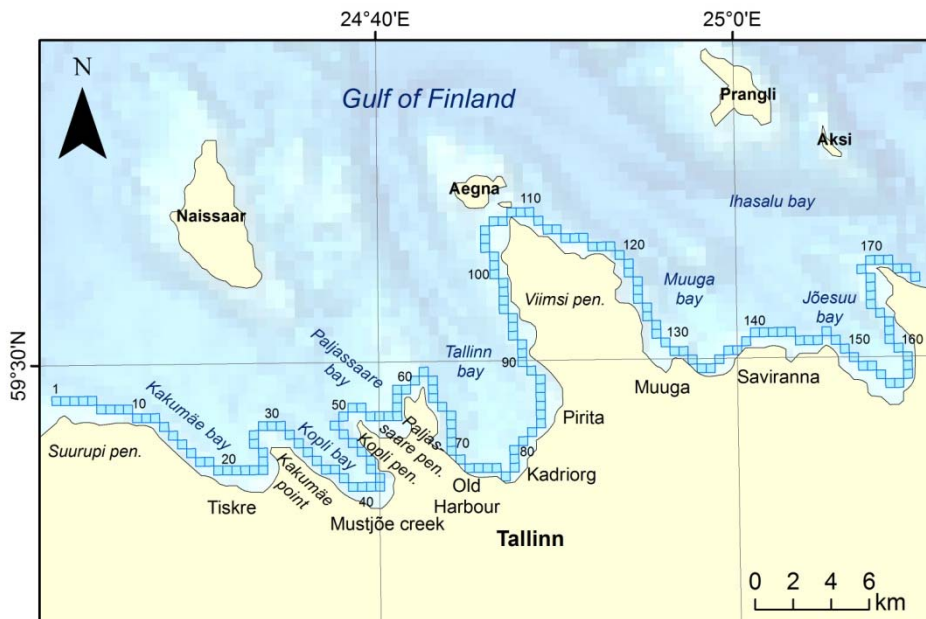


Figure 4. Study area in the vicinity of the city of Tallinn. The selected nearshore grid points of the wave model are numbered from west to east. Analyses in Paper I are performed for the grid cells 1–105. The study area is extended until grid cell 174 in Paper III. Reproduced from Paper III.

west of the Viimsi Peninsula were considered. The average orientation of the coast was defined for each section. The sections roughly correspond to the nearshore computational cells of the innermost wave model with a resolution of about 470 m.

The quality of reconstructions of wave properties can be implicitly evaluated by considering the spatial pattern of the highest waves along the selected nearshore sections. The overall maximum modelled wave height h_{\max} reached 5.4 m (Figure 5) during a furious storm on 18–19 October 1998. This estimate reflects well the properties of extreme waves in the central part of the Gulf of Finland. A significant wave height of 5.2 m has been recorded twice in the neighbourhood of the study area: in November 2001 in a western storm and on 30 November 2012 in an eastern storm (Pettersson et al., 2013).

The wind speed in the westerly storm on 18–19 October 1998 was 25 m/s during two sequential recordings, so over at least 3 h. The relevant nearshore area has a depth of 13 m and is completely open to the west, north-west and north, that is, to the directions of the largest waves. Figure 5 suggests that severe waves with a significant wave height >2.5 m may occur in the interior of Tallinn Bay at Pirita Beach and along the eastern coast of the Viimsi Peninsula. This reflects the anisotropy of wind fields in the area and the common understanding that western and NNW storms usually produce the largest waves in the study area.

The propagation direction of the highest waves varies considerably in the study area, from east to south-south-west (Figure 6). Figure 4 demonstrates that different coastal segments are open to the waves approaching from different directions. This signals that the overall highest waves that occur in different segments are usually

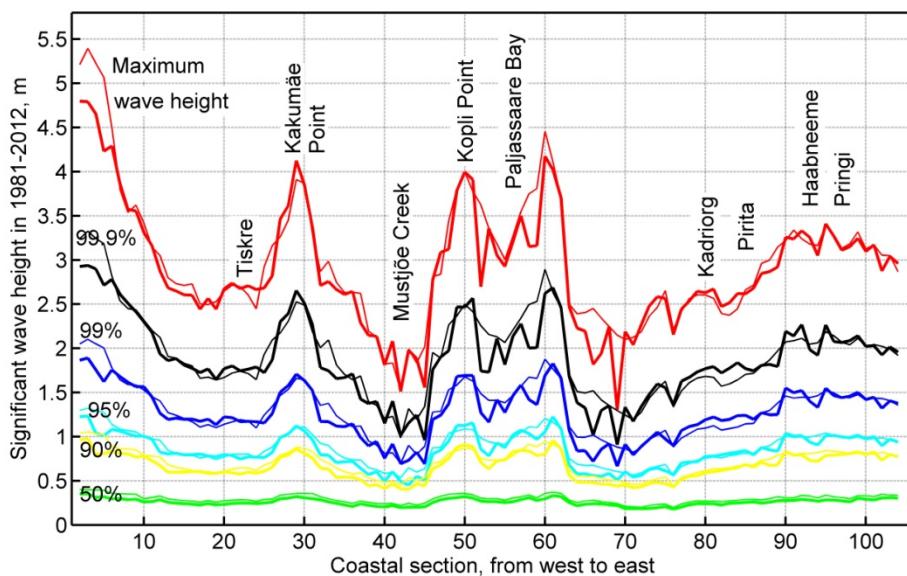


Figure 5. Maximum wave heights, higher quantiles and median wave height in the nearshore of the study area in 1981–2012. Thin lines indicate the modelled wave heights and bold lines show values for the breaking wave heights calculated from Eq. (5). Geographical locations are indicated in Figure 4. Reproduced from Paper I.

produced by various storms. This feature, in essence, simply mirrors the complex coastal geometry of the study area and the possibility of having large waves approaching from various directions in different storms.

All the reconstructed highest ever waves occurred in six storms in the study area (Figure 7). Among these, the storm of 15–16 November 2001 established the all-time highest waves in the Gulf of Finland (significant wave height 5.2 m, Pettersson and Boman, 2002) and set the all-time second highest maximum water level (1.35 m) in Tallinn Bay (Suursaar et al., 2006a). Three of the listed storms created the highest waves in most of the study area. The storm of 29 November 1999 produced the highest waves in four coastal sections of deeply cut bays that were usually sheltered against high storm waves.

Probably the most famous storm of this century on 8–9 January 2005 produced the all-time highest water levels in many parts of the eastern Baltic Sea (Suursaar et al., 2006b) and excited unusually high waves in the northern Baltic Proper (Soomere et al., 2008a). Interestingly, it did not bring very high waves to any section of the study area. Figure 7 shows that all the highest waves have occurred in the study area during the last two decades after the year 1995. This feature may reflect an increase in the wind speed in strong storms. However, below I shall demonstrate that a more adequate explanation is that the predominant wind direction during the strongest storms has rotated over the time interval in question.

1.3. Joint impact of shoaling and refraction

The WAM model does not reproduce the properties of waves in the surf zone. To adequately estimate the properties of wave set-up, the model grid cells should be chosen as close to the coast as possible but still offshore from the surf zone in the area where the wave model adequately reflects the parameters of waves. In other words, the water depth in the model grid cells should be larger than the breaking depth of waves.

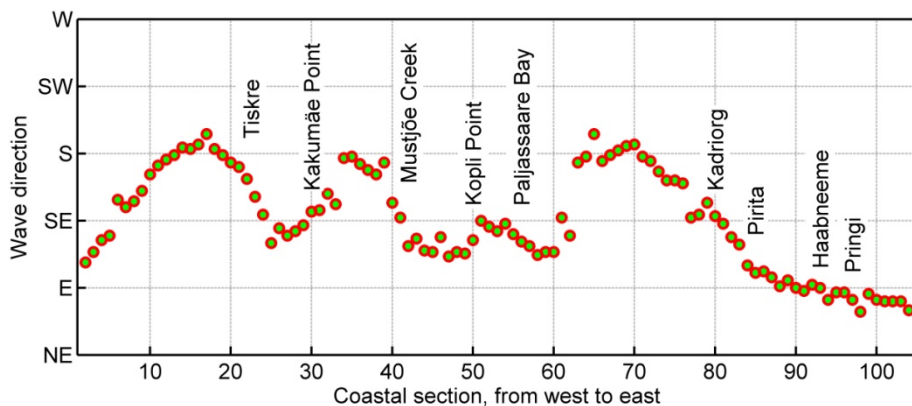


Figure 6. Propagation directions of the highest numerically simulated waves in single segments of the study area in 1981–2012. Notice that wave models traditionally indicate the direction in which waves propagate. Reproduced from Paper I.

Figure 5 and earlier numerical simulations indicate that strong storms may produce significant wave heights >4 m in grid cells that are open to the north and north-west. For example, a strong NNW storm (wind direction 330°, 23 m/s) on 15–16 November 2001 apparently created wave fields with the significant wave height around 4 m in a large part of the interior of Tallinn Bay (Soomere, 2005). The significant wave height in another very strong storm on 8–9 January 2005 was 4.5 m to the west of Naissaar (Soomere et al., 2008a).

Therefore, the nearshore grid cells in coastal segments where the nearshore wave heights may exceed 3 m should be chosen in at least 5–6 m deep water where waves are not yet intensively breaking. The water depth may be smaller in other segments but still at least 4 m. To follow these arguments, the wave data were mostly calculated for nearshore grid cells that had the water depth of 4–8 m. In a few locations near headlands or at points which are not vulnerable to high set-up for other reasons, the water depth in the selected cells was 20–27 m.

The classic estimates of wave set-up heights rely on the wave height at the seaward border of the surf zone (Dean and Dalrymple, 1991). While in some cases the output of the wave model adequately reflects the properties of (almost) breaking waves, in the majority of occasions the numerically simulated wave properties are valid at a distance of hundreds of metres from the surf zone. To properly evaluate the wave set-up height it is therefore necessary to take into account the transformation of waves from the grid cells to the breaker line.

It is assumed in earlier applications that waves approach the shoreline under a small angle with respect to the breaking line. This property makes it possible to use simplified approximations of shoaling and refraction (Dean and Dalrymple, 1991).

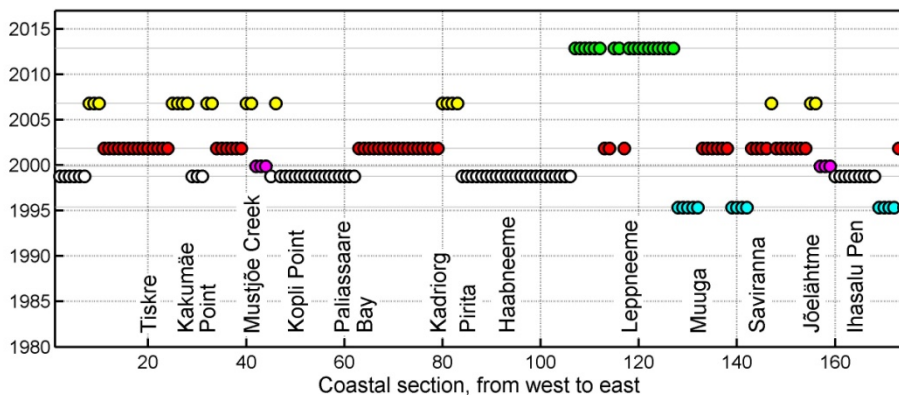


Figure 7. Six storms that caused the highest waves in different coastal sections of the study area in 1981–2014. The horizontal lines indicate the storms that produced the highest wave set-up in at least one section. Each storm is marked with a different colour. The colours vary cyclically. Note that wind records are missing in the Kalbådgrund data set during the maximum and aftermath of an extreme eastern storm on 29–30 November 2012 when the all-time highest significant wave height of 5.2 m was recorded for the second time in the Gulf of Finland (Pettersson et al., 2013). Therefore the largest waves approaching from the east may be missing in our reconstructions. See Figure 4 for the numbering of coastal sections. Adapted from Paper III.

The shoreline of the study area (Figure 4) has extremely complicated geometry and its different segments are open to very different directions. This means that in many coastal segments high waves may often approach the shoreline under large angles. In such occasions the simplified representations of refraction (Lopez-Ruiz et al., 2014, 2015) may lead to large errors. To properly evaluate the magnitude of wave set-up it is necessary to take into account full refraction and shoaling in the nearshore (Viška and Soomere, 2013; Paper I, Paper III).

The technique for the evaluation of changes in wave properties owing to the joint effect of shoaling and refraction during wave propagation from the grid cells to the breaking line was presented, to my knowledge, for the first time in Paper I. The presentation here follows this paper. The changes are evaluated using the following assumptions: (1) the numerically evaluated wave field is monochromatic, (2) the wave height is equal to the modelled significant wave height, (3) the wave period is equal to the modelled peak period and (4) the wave propagation direction matches the evaluated mean direction. It is also assumed that within each coastal section the isobaths seaward of the breaker line are straight and parallel to the average orientation of the coastline (Figure 8).

If one denotes the height, group speed and celerity (phase speed) of such a monochromatic wave field at a given nearshore grid cell as h_0 , c_{g0} and c_{f0} , respectively, then the height h_b of waves that are about to break is (Dean and Dalrymple, 1991)

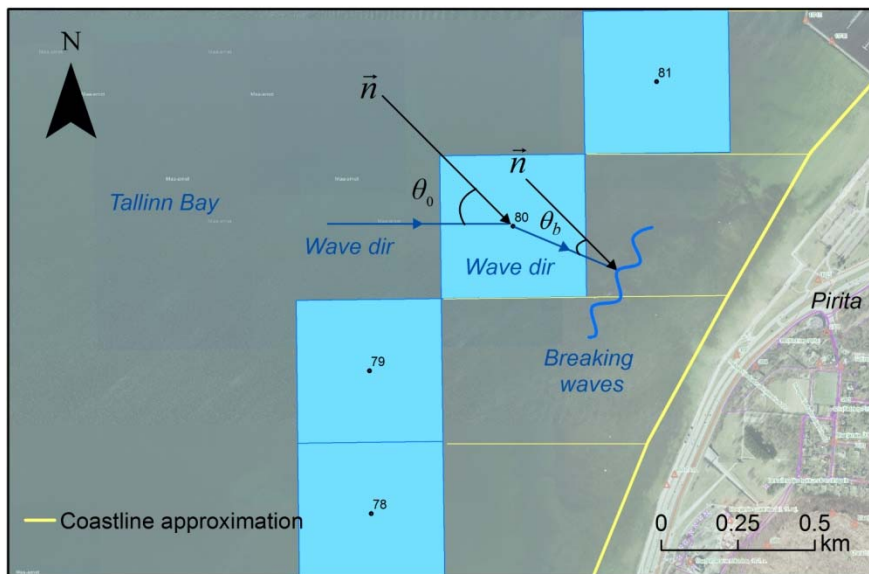


Figure 8. Wave transformation from the grid cell where wave properties were calculated until the breaking point of waves. Source for the background: Estonian Land Board WMS service, www.maaamet.ee.

$$h_b = h_0 \left(\frac{c_{g0} \cos \theta_0}{c_{gb} \cos \theta_b} \right)^{1/2}. \quad (1)$$

Here θ_0 is the angle between the wave direction and the normal to the coastline (attack angle) at the calculation point, θ_b is the similar angle at the breaking line (Figure 8) and c_{gb} is the group speed at the breaking line.

Equation (1) can be reduced to a relatively simple relationship for the breaking wave height under the assumption that the waves that approach the coast always break when their height exceeds a certain depth called breaking depth d_b . This assumption is usually expressed via the so-called breaking index γ_b that expresses the relationship between the breaking wave height and water depth. We employ the commonly used assumption that the ratio $\gamma_b = h_b/d_b$ between the breaking wave height and water depth is constant (Dean and Dalrymple, 1991). A discussion of the validity of this assumption is presented in Paper I and Paper III.

Changes in the wave height in the process of refraction are expressed via Snell's law. This law requires $\sin \theta/c_f = \text{const}$ along the wave rays. It is commonly assumed that breaking waves are long waves, consequently, their group speed and phase speed are equal: $c_{gb} = \sqrt{gd_b} = \sqrt{gh_b/\gamma_b}$, $c_{fb} = c_{gb}$. This assumption makes it possible to considerably simplify the appearance of Snell's law for waves at the breaker line and to write

$$\sin \theta_b = \sin \theta_0 \frac{c_{fb}}{c_{f0}} = \sin \theta_0 \frac{\sqrt{gh_b/\gamma_b}}{c_{f0}}, \quad (2)$$

where g is acceleration due to gravity. Substituting Eq. (2) into Eq. (1) yields the following equation for the breaking wave height h_b (Paper I):

$$F(h_b) = h_b^6 \frac{g^2 \sin^2 \theta_0}{\gamma_b^2 c_{f0}^2} - h_b^5 \frac{g}{\gamma_b} + h_0^4 c_{g0}^2 (1 - \sin^2 \theta_0) = 0. \quad (3)$$

Equation (3) is an algebraic equation of 6th order with respect to the breaking wave height h_b . Out of its three non-zero terms, the coefficient at the leading term and the constant term have the same sign while the coefficient at h_b^5 has the opposite sign. Therefore, Eq. (3) has maximally two real positive solutions (Kangro, 1962). Real solutions exist if

$$6^6 g^4 h_0^4 c_{g0}^2 \sin^{10} \theta_0 (1 - \sin^2 \theta_0) \leq 5^5 \gamma_b^4 c_{f0}^{10}. \quad (4)$$

Equation (3) has a double real solution if the expressions at the right- and left-hand sides of Eq. (4) are equal. As shown in Viška and Soomere (2013), an estimate of the breaking wave height is given by the smaller real solution (Figure 9).

The described solution is a straightforward generalisation of a simpler expression for the breaking wave height that is commonly used for open ocean

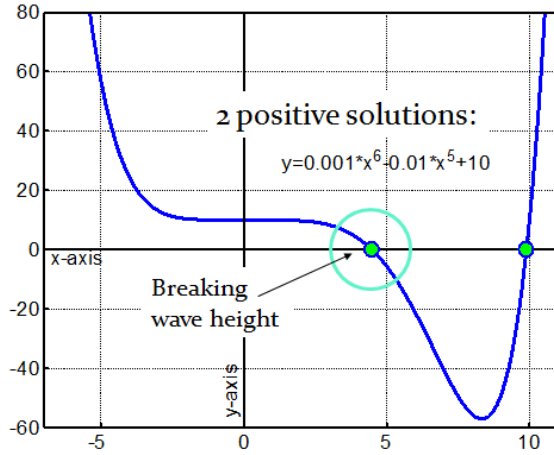


Figure 9. A typical shape of the graph of the polynomial in Eq. (3).

conditions. The constant term of Eq. (3) vanishes for incident waves, for which $\theta_0 = 0$. In this case there is no refraction and Eq. (3) reduces to

$$h_b^5 \frac{g}{\gamma_b} = h_0^4 c_{g0}^2, \quad (5)$$

from which the breaking depth can be expressed as $h_b = (h_0^4 c_{g0}^2 g \gamma_b)^{1/5}$ (Dean and Dalrymple, 1991).

The output of the wave model is presented in terms of the wave period T . To evaluate the wave number k , in Paper I and Paper III the linear dispersion relation of surface waves $\omega = 2\pi/T = \sqrt{gk \tanh kd}$, where ω is the angular frequency and d is the water depth at the cell of the WAM model, is solved with the precision of replication of decimal numbers in a 32-bit computer (that is, with about seven correct decimal digits). The values of the wave number were used to calculate the phase and group speed of the modelled waves in this cell. To replicate the behaviour of the largest waves, I used the peak period calculated by the WAM model. In a few cases of very small waves the root-finding subroutine failed and then an approximate value corresponding to the solution of Eq. (3) with a zero constant term was applied.

1.4. Evaluation of wave-induced set-up

The classic concept of wave set-up (Longuet-Higgins and Stewart, 1964) relates the local increase in water level with the onshore component of radiation stress. For a small depth (incl. the area near the breaker line) the beaching waves can be described using the approximation of long waves and this component of radiation stress can be approximated as follows:

$$S_{xx} \approx \left(\frac{1}{2} + \cos^2 \theta \right) E . \quad (6)$$

Here $E = \rho g h_{rms} / 8 = \rho g h_s / 8$ is the wave energy, ρ is water density, g is acceleration due to gravity, h_{rms} is the root mean square wave height and h_s is the significant wave height.

A scheme of variations in the nearshore water level owing to surface waves is presented in Figure 10. The phenomenon of wave set-down (Dean and Dalrymple, 1991) to some extent decreases the effective water depth under large waves in relatively shallow water. The magnitude of this effect is (Longuet-Higgins and Stewart, 1964)

$$\Delta d = -\frac{h^2 k}{8 \sinh 2kd} , \quad (7)$$

where h is the wave height and d is the undisturbed water depth in the absence of waves. This phenomenon is active seawards from the breaker line and usually has the largest impact in the immediate vicinity of this line.

In the surf zone the mechanism of wave set-up generates an increase in the average water level. A straightforward estimate of this increase can be derived under the assumption that waves gradually break in the nearshore. Similarly to the above, it is assumed that the so-called breaking index $\gamma_b = h_b/d_b$ remains constant in the entire surf zone. If the beach is impermeable and has a planar shape, and waves propagate directly onshore ($\theta = 0$), the maximum set-up height (McDougal and Hudspeth, 1983; Dean and Dalrymple, 1991) is

$$\bar{\eta}_{\max} = \frac{5}{16} \gamma_b h_b . \quad (8)$$

Therefore, even though radiation stress (1) and wave set-down (7) are, similarly to

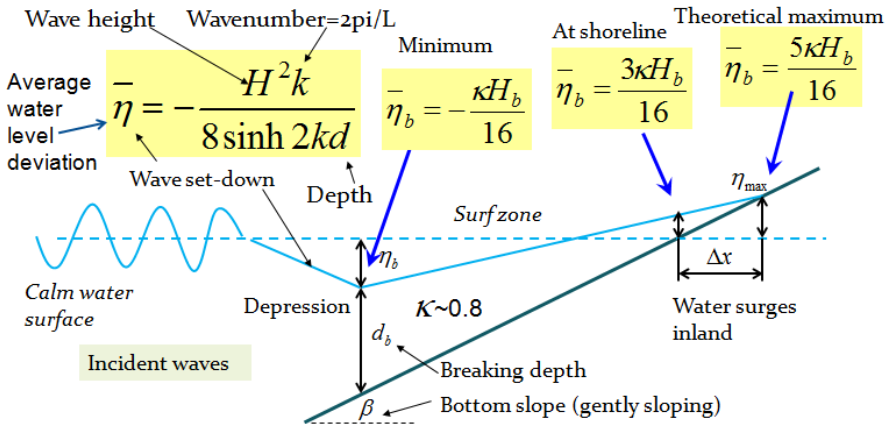


Figure 10. Wave-driven variations in the average water level in the nearshore.

wave energy, quadratic functions of the wave height, the set-up height (8) is a linear function of the wave height.

A thorough discussion of the validity of these assumptions is provided in Paper I and Paper III. In fact, the breaking index γ_b is not necessarily constant across the surf zone (Raubenheimer et al., 1996; Power et al., 2010). There is some evidence that the breaking index probably increases shorewards (Raubenheimer et al., 2001; Yemm, 2004). This feature may affect the resulting set-up heights but apparently does not change the location of the areas of high and low set-up heights.

There is also no consensus about the particular value of the breaking index. It is often assumed in practice that $\gamma_b \approx 0.78$ (Dean and Dalrymple, 1991, 2002). For several types of beaches (strongly reflecting steep shores) the breaking index may reach values ~ 1.5 . For very gently sloping and mostly dissipative beaches γ_b is in the range of 0.55–0.6 (Nelson, 1994; Massel, 1996). For sandy beaches a version of Eq. (2) $\bar{\eta}_{\max} \approx 0.17h_s$ is often used. Here h_s is the significant wave height at a depth of 10 m (Guza and Thornton, 1981; Coastal Engineering Manual, 2002).

As mentioned above, there is no consensus today about to what degree the parameters of wave set-up depend on the offshore wave properties and particular features of the nearshore. Moreover, the conversion of wave-driven momentum into onshore motions of water masses is highly sensitive with respect to the appearance of the nearshore (Dean and Bender, 2006). For example, wave propagation over vegetated coastal areas may result in a negative set-up (that is, a decrease in the local water level; Dean and Bender, 2006). Similarly, various modelling efforts (e.g., using SWAN) show that the modelled values of set-up heights substantially depend on the model resolution and details of the beach (Nayak et al., 2012). For example, concave coastal stretches host relatively large values of maximum wave set-up.

It is important to understand how large this effect could be in unfavourable conditions. This knowledge is crucial for the identification of the potential areas of high set-up. As many segments of the study area are mostly sedimentary, with gently sloping profiles resembling Dean’s Equilibrium Profile, the commonly used value $\gamma_b = 0.8$ is employed in Paper I and Paper III to evaluate the maximum set-up height. This choice leads to the following approximation for the evaluation of set-up height:

$$\bar{\eta}_{\max} \approx 0.25h_b . \quad (9)$$

The described approach contains several sources of uncertainties associated with the approximate nature of the reconstructed wave properties, and variations in the conditions for the formation of high set-up. Therefore, the results of the presented calculations should be interpreted as indicative. The material in Paper I and Paper III focuses on the properties of wave set-up that are less sensitive with respect to the listed uncertainties but may have important applications in the management of the coastal area: (i) the potential locations of high set-up, (ii) possible changes in the properties of set-up events and (iii) the timing of typical storms that may produce high set-up.

1.5. Almost-incident waves and endangered areas

The analysis performed in Section 1.2 presented results for waves approaching from any direction. High waves that approach the coast under large angles mostly produce longshore current (Apotsos et al., 2008). The highest set-up occurs when the wave approach direction almost matches the normal to the coastline (Figure 8). It is thus likely that extreme set-up heights are produced by severe waves that propagate almost directly onshore. If the height of such wave fields is much lower than the all-time highest waves, large set-up heights are unlikely.

Figure 11 demonstrates that both extreme and average heights of waves that approach the coast from a narrow direction range, with respect to the shore normal, are much lower than those presented in Figure 5. A few headlands receive severe waves from the shore normal direction but many coastal sections are implicitly (geometrically) protected (Caliskan and Valle-Levinson, 2008).

The areas that are likely to be endangered by high wave set-up are relatively open coastal sections with a convex shape and gently sloping beach. These considerations together with the analysis of the occurrence of severe wave fields lead to the following description of areas potentially endangered by maximum wave set-up heights occurring once in a 30-yr period (Figure 12). High levels of wave set-up are likely in the residential area of Tiskre and along the western coast of the Viimsi Peninsula.

The danger is relatively low but still non-negligible at the mouth of the Mustjõe

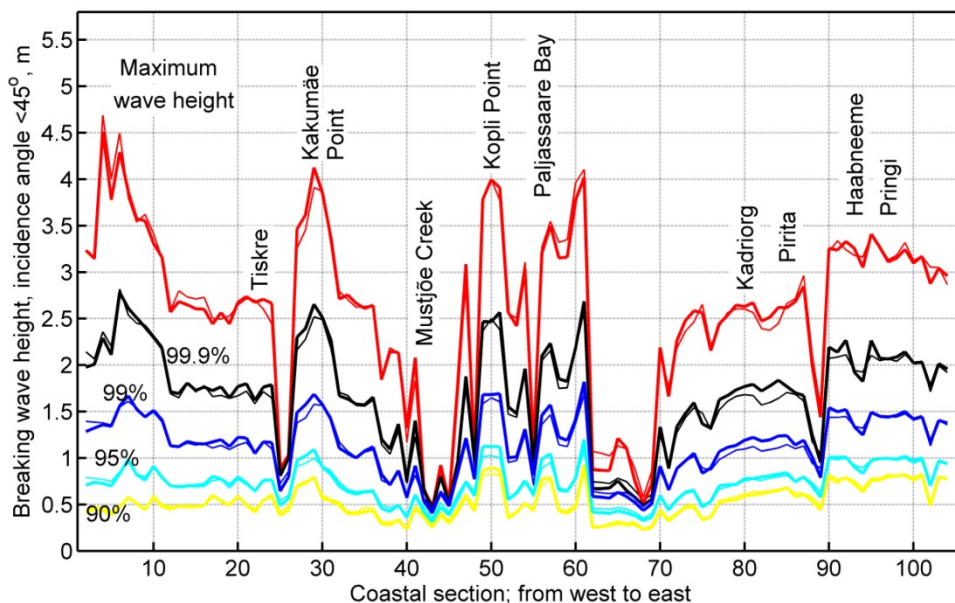


Figure 11. Maximum wave heights, higher quantiles and median wave height for waves approaching from a direction of maximally $\pm 45^\circ$ with respect to the normal to the coast. Thin lines indicate the modelled wave heights and bold lines show values for the breaking wave heights calculated from Eq. (4). Reproduced from Paper I.

Creek. This area is implicitly protected by a favourable combination of the geometry and bathymetry of Kopli Bay. Theoretically, high wave set-up may occur along the north-eastern coast of the Kakumäe Peninsula. However, the highly variable orientation of its coastline suggests that very high set-up events are unlikely in this area. The hazards associated with high set-up are apparently minor along the coastal section from Old City Harbour to Pirita. The shoreline of this segment is protected by a reflecting seawall.

Another view of the level of the danger in question provides an estimate of the highest quantiles for the theoretical set-up heights (Figure 13). As the probability of having severe wave fields from a particular narrow direction is lower than the probability of just high waves, it is natural to expect that very high set-up events are isolated, rare phenomena. In this context it is worth mentioning that in several segments of the study area the 99.9%-ile of the set-up height is quite high, close to 0.4 m. For Tallinn Bay it means a frequent addition (on average, three times a year) of about 25% to the all-time highest open sea water level. As discussed below and in Paper III, these events are not necessarily associated with high sea level. However, the simultaneous presence of high open sea water level and extreme wave set-up is likely in some locations (Paper III).

The results confirm that wave set-up serves as an important constituent of marine-induced coastal hazard in the vicinity of Tallinn Bay and evidently along many segments of the shores of the Baltic Sea. The key conclusion is that wave set-

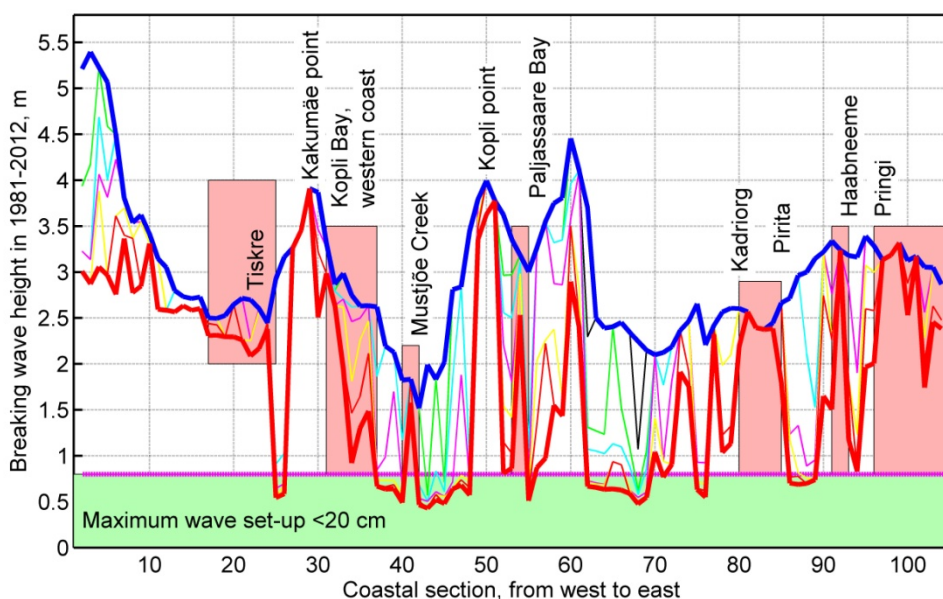


Figure 12. The highest breaking waves (coloured lines) approaching from different ranges of directions with respect to the coast normal in the study area. The bold blue line shows the all-time highest waves approaching from any direction and the bold red line shows the all-time highest almost incident waves ($\pm 10^\circ$ with respect to the coast normal). The light red bars indicate the regions with a gently sloping coast in which the maximum set-up likely exceeds 0.4 m. Reproduced from Paper I.

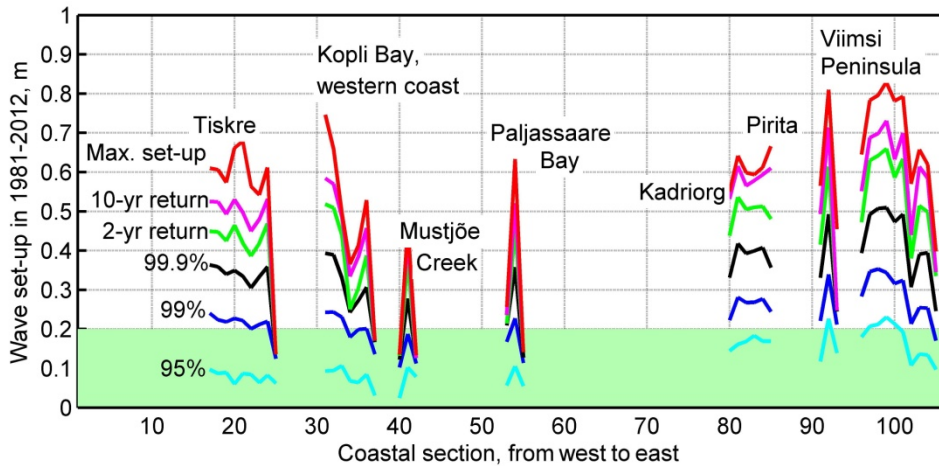


Figure 13. Maximum wave set-up values and higher quantiles of set-up heights for the coastal sections where high set-up is an issue. Reproduced from Paper I.

up may considerably increase the water level and provide up to one third of the overall maximum water level in areas that are open to predominant wind directions. The contribution of this phenomenon may be particularly large in micro-tidal regions that experience a relatively small range of sea level fluctuations, such as the Baltic Sea, Black Sea or the Mediterranean Sea.

The analysis of the “climate” of high set-up events in areas with complex geometry has many similar features with the problem of adequate description of the statistics of winds from particular directions. The return period of unfavourable combinations of wind and wave properties is substantially larger than that of just high waves. Thus much longer time series of wave set-up are necessary in order to reach adequate statistics of this phenomenon. The intermittent character of the location of coastal stretches which experience high set-up in different storms is a major challenge. While wave heights are nowadays adequately predicted, there are still issues with the forecast of wave periods and especially wave propagation directions in sea areas with complicated geometry (Pettersson et al., 2010).

The approaching waves do not always create high set-up. For example, this phenomenon is normally insignificant for strongly reflective shores, e.g., if the coast is protected by a seawall. Also, natural roughness of the coastal zone (reed, bushes and stones) largely damps this phenomenon (Dean and Bender, 2006).

This phenomenon creates particularly serious hazards in low-lying urban environments (Figure 14). It may have significant implications on the infrastructure, including the availability of evacuation roads. A concealed danger is that the presented estimates are valid also for elevated background water levels. During a considerable storm surge the waves will break much landwards from the beach. Therefore, developed areas (e.g., lawned gardens, parking areas) may become sources of increased risk in terms of extensive wave set-up during strong surge events. The potentially affected areas form in total about 50% of the study area (Figure 14, Paper I, Paper III).

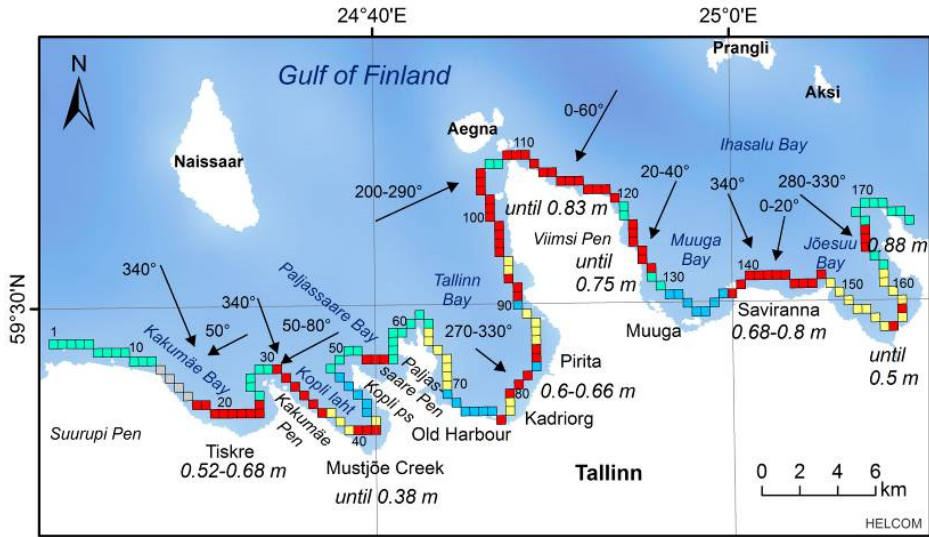


Figure 14. Coastal sections potentially affected by high wave set-up (red squares) in the urban area of the city of Tallinn based on wind data from 1981–2014. The arrows indicate the directions of wave propagation associated with the highest set-up for single coastal segments. Yellow squares indicate coastal stretches where the maximum wave set-up is $<0.2\text{ m}$, green squares – areas where high wave set-up is evidently not possible because of the convex shape of the shoreline and blue squares – areas containing various engineering structures. Reproduced from Paper III.

1.6. Evidence of the rotation of wind direction in strong storms

The analysis in Section 1.3 indicates that all events of the largest significant wave heights in all 174 shore segments were produced by six storms (Figure 7). All these storms occurred starting from the mid-1990s. In particular, the heights of wave fields in storms of 1999–2006 have been larger than in many earlier storms. This feature signals that certain changes in storm activity may have occurred over the last two decades.

Interestingly, the pattern of storms that produced the highest wave set-up has been radically different and substantially varied over recent years. The number of storms that brought to the coast waves whose propagation direction was at a relatively small angle to the coast normal increased rapidly when the range of the approach angles became narrower. For example, as presented in Paper I, 18 storms produced the all-time highest waves approaching the coast at an angle less than $\pm 45^\circ$ with respect to the shore normal in the interior of Tallinn Bay in 1981–2012. The number of such storms increased to 32 when the range of the approach angles was less than $\pm 30^\circ$ from the shore normal, and to 41 for almost-incident waves ($\pm 10^\circ$ from the shore normal). A similar increase was observed for the entire study area in Paper I. Therefore, in contrast with the all-time highest wave heights, each

short segment of the shore has its own "perfect storm" that creates the all-time highest wave set-up (Paper I).

Apart from the increase in the number of such storms, their distribution changes radically in time. Remarkably, a large number of the all-time highest almost-incident waves occurred in the 1980s (Paper I). The stormy years at the beginning of the 1980s were followed by the less stormy years 1983–1989. The years 1990–1994 were apparently particularly calm. These variations match the course of various storm indices for Stockholm (Rutgersson et al., 2014). Many coastal sections around Tallinn were not open to the public in the 1980s. It is therefore likely that the associated events of high set-up remained unnoticed.

Analogous temporal patterns became evident in the advanced estimates of the all-time highest set-up events over an extended study area and temporal coverage (until February 2014, Paper III). Similarly to the above, until October 2012 about a third of the all-time highest wave set-up values along the entire study area were created in the 1980s (Paper III).

The extension of the analysis performed in Paper III to the mid-2010s considerably modifies the pattern of storms responsible for the highest wave set-up values. Many records of set-up heights stemming from 1981–1982 were overridden during the time interval from November 2012 to February 2014. During these two windy seasons 24 different storms created new all-time (since 1981) highest wave set-up values whereas 18 such storms occurred in 2013. The total number of storms responsible for the highest wave set-up changed to a lesser extent: from 50 (January 1981–October 2012) to 58 (January 1981–February 2014, Paper III).

As explained above, sea ice is ignored in the described calculations. The extent of sea ice was relatively large in the 1980s (Climatological Ice Atlas, 1982). Therefore, it is likely that during some storms of this decade the presence of ice

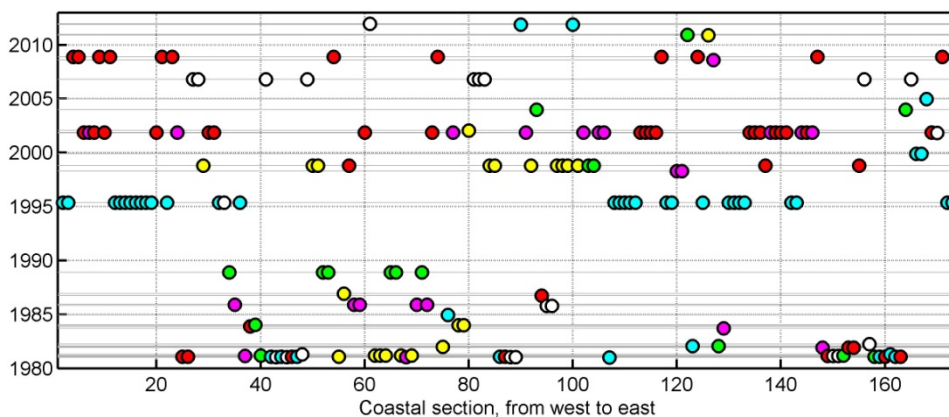


Figure 15. Scheme of 50 storms that caused the highest wave set-up ($\pm 15^\circ$ from the shore normal) in different segments of the study area in January 1981–October 2012. The horizontal lines indicate single storms that produced the highest wave set-up in at least one section. Each storm is marked with a different colour. The colours vary cyclically. Reproduced from Paper III.

damped waves and prevented the development of set-up. On the contrary, the area covered by sea ice was relatively small in the Gulf of Finland in winters 2012/2013 and 2013/2014. It is therefore likely that the reconstructed wave parameters match well the properties of actual wave fields and high set-up events really occurred.

The described extensive spatio-temporal variation in the largest set-up heights highlights substantial dependence of the development of set-up on the match of the wave propagation direction and the geometry of the coastline. This feature is particularly accentuated in domains with the complex geometry of the coastline. The analysis shows that dangerously high set-up events generally occur in different coastal sections in different storms, and thus may be easily overlooked.

The described patterns give an interesting insight into certain features of the local climate change. Figure 7 produces an impression that the 1980s and 1990s were relatively mild and that storms in the Baltic Sea have become stronger since the end of the 1990s. Figure 15 provides an alternative interpretation. It demonstrates that the strongest storms blowing from certain directions in 1981–2012 occurred at the beginning of the 1980s.

Paper III presents evidence showing that this process reversed in the 2010s and strong eastern storms returned to the area. A comparison of Figure 16 representing the time interval of 1981–2016 with Figure 15 suggests that many new all-time highest set-up events were generated since the autumn of 2012 in locations open to the east, particularly along the eastern Viimsi Peninsula near Leppneeme.

The changes in this pattern that occurred in 2012–2014 indicate the presence of strong (north-)easterly winds in the Gulf of Finland. This viewpoint is supported by *in situ* wave measurements. Namely, the all-time highest significant wave height of 5.2 m in the Gulf of Finland was measured for the second time during a strong eastern storm on 29–30 November 2012 (Pettersson et al., 2013). More generally,

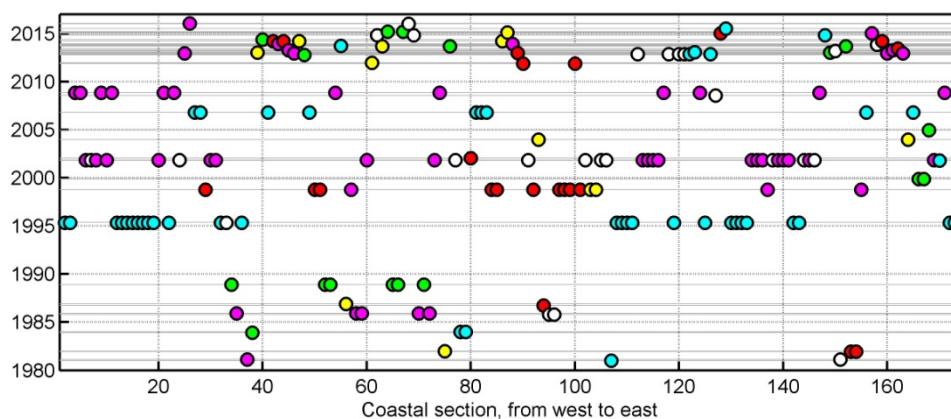


Figure 16. Scheme of 58 storms that caused the highest wave set-up ($\pm 15^\circ$ from the shore normal) in different segments of the study area in January 1981–February 2014. The horizontal lines indicate single storms that produced the highest wave set-up at least in one section. Each storm is marked with a different colour. The colours vary cyclically. Reproduced from Paper III.

the discussed pattern of changes signals that the approach directions of many severe wave systems have rotated in the Gulf of Finland. This is consistent with changes in the directional structure of winds recorded in Estonia (Jaagus, 2009). The identified changes also match the presence of quasiperiodic decadal or long-term (25–30 yr) cycles in the Baltic Sea storminess (Suursaar et al., 2015). The background reason for the changes may be a shift of the North Atlantic storm track to the north-east (Lehmann et al., 2011).

The importance of changes in the wind direction seems to be underrated today in various analyses of climate change. The related changes in the wave propagation direction may radically affect, e.g., the course of coastal processes (Räämet et al., 2010; Charles et al., 2012a, b; Viška and Soomere, 2012). A deceptive feature is the period of relatively low wave activity in the 1990s, which shows the importance of taking account of as long time series as possible. This position is necessary to avoid misleading interpretation of, e.g, a rapid increase in a certain type of wave activity at the turn of the millennium.

2. Contribution of wave set-up to extreme water levels

The results presented in Chapter 1 stress the importance of wave set-up in the formation of the nearshore water level in many segments of the Estonian coast. Several long-term water level measurement sites are placed in locations that may be regularly affected by this phenomenon. Distinguishing the contribution of wave set-up from other components of measured water levels is complicated. An indirect way to detect the presence of wave set-up is to compare the data measured in locations that may reflect the local effects (e.g., in small harbours such as Ristna (Figure 17) open to some directions of high waves) with modelled sea level data (that reflect the offshore water level before depth-induced wave breaking).

It is likely that the impact of the systematic presence of wave set-up influences most notably the projections of extreme values of water level. To identify this influence, Paper II introduces a simple approach for building an ensemble of such projections in the framework of the block maxima method. The analysis is based on seasonal and annual maximum water levels in three independent data sets, which include both observed and simulated water levels. The approach is tested on four very different regions of the Estonian coast (Figure 17) and reveals a substantial contribution from wave set-up to the total water level in one location that is open to severe seas. By combining the approach presented in Chapter 1 and numerically simulated offshore water levels, the analysis in Paper III explores the potential contribution of wave set-up to water level maxima in the vicinity of the city of Tallinn.

2.1. Observed water levels

Water level measurements in coastal waters of Estonia have a long tradition and extensive temporal coverage. The oldest records in the Tallinn site have been made in 1809. Regular estimates of the monthly mean water level based on observations reach back to 1842 (Suursaar et al., 2011).

From a wide range of contemporary water level measurement sites (Jaagus and Suursaar, 2013), Paper II focuses on four locations (Figure 17). These sites are representative for the majority of the Estonian coastline. The shores in the vicinity of Narva-Jõesuu characterise widely open bays that are exposed to large-scale storm surges during western and especially north-western winds. The coastline in the Tallinn region represents an area typical of the North Estonian coast with complex geometry as also described above. The observation site in the Western Estonian archipelago (Ristna) is representative for a rather straight coastal segment where offshore water level extremes are fairly limited but very high waves may frequently modify the water level at the shoreline. The fourth site in Pärnu Bay is located in an area that is particularly vulnerable with respect to storm surge. Specific wind events from a certain limited direction range can generate remarkable floodings in the entire bay (Suursaar et al., 2003). The largest

difference between the maxima and minima of water levels in Estonian waters has also been recorded in Pärnu Bay (Suursaar and Sooäär, 2007).

These coastal stretches have been extensively considered in earlier studies performed for Estonian coasts (Suursaar and Sooäär, 2007). Records of monthly extreme values at all sites are available from the end of the 19th century. Regular observations have been performed since 1945–1950 (depending on the observation site) two or four times per day, later observations are performed once an hour. The recordings are performed using the Estonian official height system named Baltic Height System BK77. The reference zero-benchmark was defined as the mean water level in Kronstadt in 1825–1840 (Lazarenko, 1986).

Several changes in the observation procedure, temporal resolution and timing may affect the homogeneity of the resulting data set of single observations. Even so the monthly maxima of water levels are likely not significantly affected by most of minor changes such as an increase in the frequency of observations or a shift from the Moscow time to the Greenwich (GMT) time.

The observations sites have been unchanged in Ristna, Narva-Jõesuu and Pärnu (Figure 17) but the site in Tallinn was relocated in 1996. Until 1996 observations were performed in Tallinn Old Harbour in the bayhead of Tallinn Bay (Figure 4) by the Estonian Meteorological and Hydrological Institute (EMHI) according to the World Meteorological Organisation (WMO) guidelines. Then the observation site was moved to Muuga Harbour in the bayhead of Muuga Bay (Figure 4). The measurements continued under the auspices of the EMHI. The Tallinn Harbour Enterprise continued with the measurements in Tallinn Old Harbour. In 2004 the



Figure 17. Location scheme of the four sites used in this study. Red circles indicate the observation sites and green rectangles – the associated points of the circulation model. Reproduced from Paper II.

Marine Systems Institute (MSI) at Tallinn University of Technology (TTÜ) installed the automatic water level tracking system (Lagemaa et al., 2011). Therefore, the data set that reflects water levels in the Tallinn area consists of several parts with different temporal resolution and has been recorded using various techniques. Implications of the potential inhomogeneity on the projections of extreme water levels are discussed in Lagemaa et al. (2013). More detailed information about the measurement sites, observation procedures and the data sets used in the analysis is presented in Paper II.

2.2. Modelled water levels

Modelled offshore water level time series in the nearshore of Estonia were extracted from two different circulation models. The Rossby Centre Ocean Model (RCO), developed and implemented by the Swedish Meteorological and Hydrological Institute (SMHI), provided a data set with a temporal resolution of 6 h. The other modelled data set we used, which has the temporal resolution of 1 h, was based on the same basic set-up.

The basic features of the RCO model and information about its implementation and validation have been comprehensively described in the scientific literature (Meier, 2001; Meier et al., 2003). The data were provided to the Wave Engineering Laboratory in the framework of BONUS BalticWay cooperation (Soomere et al., 2014). Details of the version of the model that was used to produce the data set employed in Paper II, Paper III and Paper IV are described in Meier and Höglund (2013). The key features are as follows. The horizontal resolution of the model is 2×2 nautical miles. The water column is divided into 41 levels with a thickness of 3–12 m and represented in classic z -coordinates. These parameters are commonly considered to be acceptable for an adequate reproduction of the large-scale motions and major statistical features of mesoscale motions in the Baltic Sea and its larger sub-basins such as the Gulf of Finland or the Gulf of Riga (Myrberg et al., 2010). The model is coupled to a sea ice model. Water level data were saved once 6 h for May 1961–May 2005.

The RCO model was forced with a high-resolution regionalized re-analysis of the ERA-40 atmospheric data set. The horizontal resolution of the forcing data was 22 km. To improve the wind statistics, wind adjustment was modified using simulated gustiness (Samuelsson et al., 2011). The results of the hindcast and forecast are analysed in Meier et al. (2004). The model reasonably replicates the wind-driven gentle slope in the average sea surface height towards the eastern and northern ends of the Baltic Sea but has problems with the replication of storm surge maxima in the western area of the Baltic Sea (Meier et al., 2004). In the light of Paper II and the analysis presented in this chapter it is possible that the mismatch was partly caused by wave set-up that was not taken into account in the calculations. The rest of the time series and statistical properties of the water level are acceptably represented.

The modelled water level is linked with the sea level in the Atlantic Ocean at the open boundary of the model in the northern Kattegat (Figure 1). The sea level data in this area follow the height system NH60 (Meier et al., 2004). Therefore, it is natural to interpret the model output in the same system. The zero level in the RCO model is defined with respect to the seabed. Its location is prescribed based on so-called Warnemünde topography. As this data set of water depths has been constructed using several maps based on different height systems (Seifert et al., 2001), the modelled water level cannot be directly associated with any particular height system.

Land up/downlift is ignored in the model implementation. This feature may to some extent modify the accuracy of modelled water levels in the northernmost part of the sea. As the Estonian coast only experiences weak uplift (Figure 1) that is more or less compensated by the increase in the global sea level during the modelled time interval, this feature apparently does not substantially affect the quality of modelled data in Estonian waters. The model works in spherical coordinates, neglecting the ellipticity of the Earth and the shape of the geoid. The sea surface provided by the model deviates from the geodetic solution by about 20–30 mm (Ekman and Mäkinen, 1996).

The RCO model follows the classic principle of volume conservation in ocean modelling. This means that the impact of variable salinity and temperature of sea water on the water level is neglected. The resulting systematic deviation of the modelled water level from the measured ones may reach 0.3–0.35 m in low-salinity parts of the sea such as the Gulf of Bothnia and Gulf of Finland (Ekman and Mäkinen, 1996). This basically constant difference is immaterial from the viewpoint of studies in this thesis because extreme water levels, their return periods and possible changes are counted from the long-term mean water level similarly to the measured extreme values in Estonian waters. Extracted water level time series were used after de-meaning without any further adjustment.

Alternatively, a semi-synthetic data set was constructed by merging measured water levels with the output of the operational Baltic Sea circulation model HIROMB (High-Resolution Operational Model for the Baltic Sea). The operational BS01 setup of this model (Funkquist, 2001) has a spatial resolution of one nautical mile (Lagemaa et al., 2011). The family of three-dimensional ocean circulation models where HIROMB belongs to was initially created in Germany by the Federal Maritime and Hydrographic Agency (BSH; Kleine, 1994), further developed by the Danish Meteorological Institute, SMHI and adjusted for the Baltic Sea by the HIROMB consortium. An overview of different versions of the model and its set-up for the Gulf of Finland is presented in Gästgifvars et al. (2008).

Paper II employs hourly output of the operational version of this model (Lagemaa et al., 2011) in four locations from January 1961 to December 2005. The location of water level observation sites in Figure 17 does not coincide with the HIROMB grid cells. To minimise possible errors in modelled water levels due to too low spatial resolution for the nearshore area, the locations in question are intentionally selected at a certain distance offshore from the observation sites. The

distance between the observation site and the relevant offshore location is about 10 km for Tallinn, 15 km for Pärnu, 20 km for Ristna and 40 km for Narva-Jõesuu. The time series of water level data from the observation sites were transformed to the open sea water level using a linear regression. The regression coefficients were evaluated from matching monthly maximum water levels with the similar water levels provided by the HIROMB model for 2006–2013. The relevant Pearson correlation coefficients were $R > 0.99$ for all sites. These values suggest that the applied regression model works acceptably. In the following text the resulting monthly maximum values are referred to as observed data. To make the data range comparable with the output of the offshore water level from the RCO model, only observed data from the time interval 1961–2005 are applied.

The empirical distributions of the frequency of occurrence of different water levels built on modelled and observed water levels (Figure 18) both resemble a

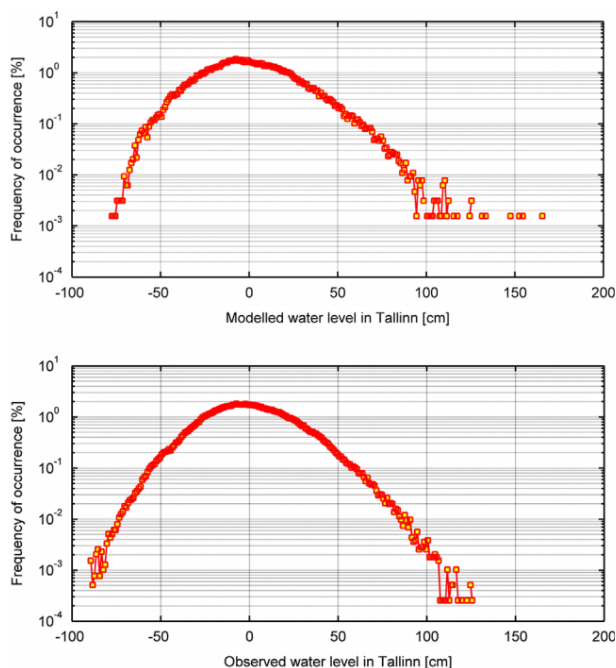


Figure 18. Frequency of occurrence of deviations of the water level from the long-term mean in the RCO simulations (6-h values in 1961–2005, upper panel) and in measurements in Tallinn Harbour (1945–15.05.1995). As the measurement site was relocated from Tallinn Old Harbour to Muuga Harbour in 1996, the distribution of observed values does not contain the highest examples in the 2000s (1.35 m in 2001; 1.52 m in 2005). The recordings of the largest values after the turn of the millennium raised the question of whether the overall dynamics of the water level may have changed since 1996. A similar change has been registered in the statistics of wave-driven set-up in the vicinity of Tallinn for 1981–2012. All the highest waves have occurred after 1995 but the highest set-up apparently occurred in many locations before 1995 (Paper I). A probable reason is a change in the wind direction in the strongest storms, with obvious changes in the local water level dynamics. Reproduced from Paper II.

Gaussian distribution. This kind of distribution of water levels is typical for the eastern part of the Baltic Sea (Johansson et al., 2001; Suursaar and Sooäär, 2007). The main difference from the classic Gaussian distribution is the asymmetric shape of distributions in Figure 18. Very high water levels tend to appear more frequently than low water levels with the same deviation from the long-term average. This feature apparently reflects the predominance of westerly winds among strong winds in the northern Baltic Sea. The distributions are moderately skewed: their peaks are almost at the long-term mean water level and, for example, the skewness of the 6-h RCO modelled data for Tallinn is 1.23.

The kurtosis of this distribution is 3.09, which insignificantly differs from the kurtosis of the Gaussian distribution (3.0). Therefore, the probability of very large positive or negative values almost coincides with the expected properties of the Gaussian-distributed data. The empirical distribution of the frequency of occurrence of different observed water levels in Tallinn Old Harbour has a similar shape (Figure 18).

Importantly, the high-value ends of the empirical distributions in question contain considerable scatter and/or single outliers (Figure 18). This feature substantially complicates the problem of the evaluation of extreme water levels and their return periods because it is not clear beforehand which extreme value distribution at best describes the properties of extreme water levels. The particular values of outliers may have different impact on the applicability of classic extreme value distributions (Suursaar and Sooäär, 2007).

2.3. Extreme value distributions

A common feature of the course of the water level in the eastern Baltic Sea is the occurrence of a few exceptionally high water levels (Figure 18). It is customary for the entire north-eastern part of the Baltic Sea (Johansson et al., 2001) as well as for the Estonian coastal areas (Suursaar et al., 2006a, b; Suursaar and Sooäär, 2007). High water levels are often associated with a specific feature of the Baltic Sea, namely, with sequences of storms which may force large volumes of water from the North Sea to the Baltic Sea and remarkably increase the sea level of the entire Baltic Sea (Johansson et al., 2001). Strong storms that affect the already increased water volume may lead to unusually high water levels (Suursaar and Sooäär, 2007). Such outliers (that usually form <0.01% of the water level recordings) have insignificant impact on the resulting distribution but may substantially modify the appearance of distributions of extreme water levels (Suursaar and Sooäär, 2007).

To evaluate extreme sea levels and respective return periods, Paper II employs the classic extreme value distributions to develop an ensemble of projections. The analysis relies on the method of block maxima. The main pillar of this method is the proof that independent maxima or minima of a random process (e.g., maximum water level values over long enough time intervals) follow under fairly general conditions one of the three theoretical limiting distributions (Coles, 2001). The exact match is only reached when the sample size increases infinitely. The family

of so-called extreme value distributions consists of the Gumbel, Fréchet and Weibull distributions. They can be considered as particular cases of the Generalized Extreme Value (GEV) distribution having the following cumulative distribution function:

$$G(y) = \exp \left\{ - \left[1 + \xi \left(\frac{y - \mu}{\sigma} \right) \right]^{-1/\xi} \right\}. \quad (10)$$

Here y has the meaning of, e.g., annual maximum water level and μ , σ and ξ are called the location, scale and shape parameters of the GEV distribution (Coles, 2001). If these parameters are known, the return period $T(\hat{y})$ for a particular water level \hat{y} is given by the $[1 - 1/T(\hat{y})]$ -th percentile of the cumulative distribution function $G(y)$:

$$T(\hat{y}) = \frac{1}{1 - G(\hat{y})}. \quad (11)$$

For $\xi \rightarrow 0$ the GEV distribution reduces to the Gumbel distribution with the following cumulative distribution function:

$$G(y) = \exp \left\{ - \exp \left[- \left(\frac{z - \mu}{\sigma} \right) \right] \right\}. \quad (12)$$

In oceanographic applications frequently $\xi < 0$ in Eq. (10). In this case the GEV distribution matches the Weibull distribution

$$G(y) = \exp \left\{ - \left[- \left(\frac{z - \mu}{\sigma} \right)^\alpha \right] \right\}, \quad z < \mu \quad \text{and} \quad G(y) = 1, \quad z \geq \mu. \quad (13)$$

The case $\xi > 0$ leads to the Fréchet distribution that is typical, e.g., in finance market problems and is not used in Paper II. The Weibull distribution is most suitable to for describing the properties of extremes of so-called light-tailed (very rapidly decaying) distributions. The Gumbel distribution is widely used in meteorology for the description of wind speed extremes and other quantities whose values decay approximately exponentially (e.g., having a Gaussian distribution).

The Gumbel distribution has an exponentially decreasing tail in semi-logarithmic coordinates that were used to create Figure 18. Therefore it is not obvious whether this distribution is able to match the very large positive outliers located far to the right of the main set of values in that figure and thus the long-term extremes may be underestimated (cf. Suursaar and Sooäär, 2007). The tail of the Weibull distribution decays as a power law in semi-logarithmic coordinates depicted in Figure 18. It is obvious from this figure that no power law is able to adequately follow the location of outliers of modelled water levels.

A feasible way to circumvent this problem and to reach the most credible outcome is to use an ensemble of estimates of extreme water levels and their return

periods. Paper II explores a simple approach of creating such an ensemble based on the existing data and different classical extreme value distributions. The idea is to apply three distributions – GEV, Gumbel and Weibull – to building a cluster of projections of extreme values and their return periods based on three data sets (one measured and two modelled) and several methods for the evaluation of the parameters of the extreme value distributions.

Doing so leads to an ensemble of projections. The applicability of a certain average of this ensemble in practice is, strictly speaking, only justified if the errors of different projections are random. This property is not tested rigorously in Paper II. This paper focuses on the identification of different regimes of extreme water levels in Estonian coastal waters based on the appearance of the entire ensemble. As I also rely on a specific qualitative feature of the resulting ensemble, the testing of the above property is out of the scope of this thesis.

The parameters for all mentioned distributions were calculated using the open source software tool *Hydrognomon* (<http://hydrognomon.org/>) that is part of the openmeteo.org framework. The resulting ensembles of different projections do not contain any visibly obvious outliers (i.e., curves that are clearly separated from the other members of the ensemble).

2.4. Projections based on block maxima

An important precondition for the use of the block maxima method (e.g., Haigh et al. 2010a; Arns et al., 2013) and extreme value distributions such as the GEV, Gumbel or Weibull distributions is that the time series of maxima of water levels over certain time intervals must be uncorrelated. In the Baltic Sea conditions the monthly maximum water levels are often correlated. The main reason is the long reaction time of the entire Baltic Sea water volume to atmospheric forcing that creates very low or highly elevated sea levels for time periods of several weeks (Leppäranta and Myrberg, 2009) as described above. Another reflection of this phenomenon is a substantial time lag between the occurrence of large-scale atmospheric patterns and the reaction of water level in terms of monthly means (Johansson et al., 2014). To attain uncorrelated block maxima it is necessary to divide the observed and modelled time series into much longer sections than a month.

Several studies have chosen the water level maxima for calendar years as the set of block maxima (e.g., Lagemaa et al., 2013; Ribeiro et al., 2014). Paper II uses this set as one example of almost uncorrelated block maxima. However, strong seasonal variations in atmospheric forcing may introduce spurious correlation of the annual maxima of the Baltic Sea water level in some occasions. For instance, the maximum water level that occurs in December of one year and the next maximum in January of the consecutive year may both be created by the same cluster of storms. For this reason Paper II makes use of an alternative set of block maxima. All the highest water levels in the Estonian coastal segments occur during the stormy season from August to March. During the calm spring season the

coastal areas usually do not experience high water levels (Johansson et al., 2001; Suursaar et al., 2002; Jaagus and Suursaar, 2013). Therefore, the set of block maxima, defined as the highest water levels during stormy seasons (from the beginning of June until the end of subsequent May), is apparently absolutely uncorrelated.

The difference between single values of the two sets of block maxima is insignificant. However, the projections of extreme water levels and respective return periods based on these sets differ significantly (Figure 19). For water levels with the return period of 200 yr deviations between the projections based on the RCO model data reach about 0.2 m. The projections of extreme water levels based on stormy season maxima are mostly higher than the ones calculated using annual maxima. The differences between projections that are based on observed data are somewhat smaller and reach about 0.1 m for the return period of 200 yr.

The described deviation of the distributions of modelled and observed water levels and large spreading of these projections for longer return periods indicate that probably none of the classical extreme value distributions is able to accurately project the extreme water levels for long return periods. A common understanding is that the projections provided by a GEV distribution frequently outperform the projections obtained from other distributions (Lowe et al., 2001; Wroblewski,

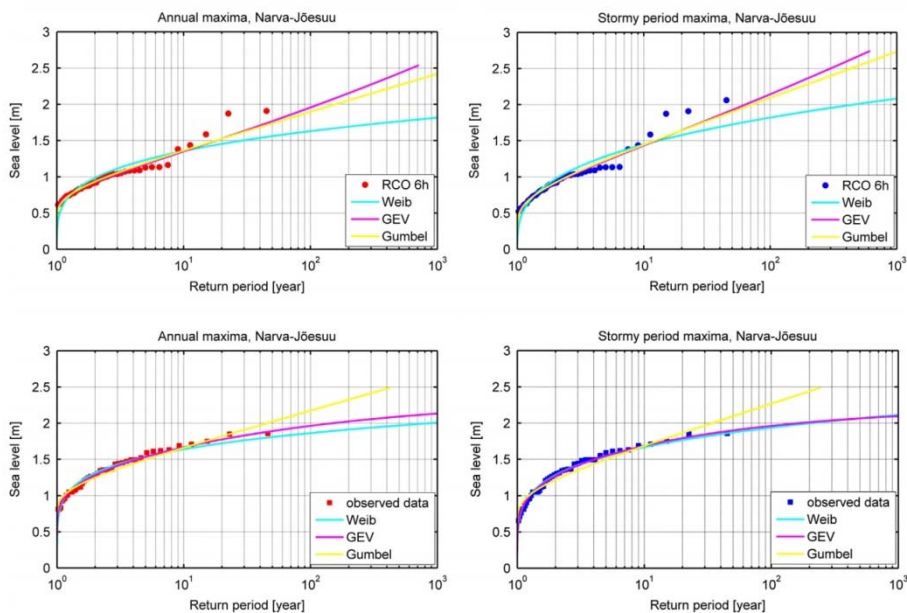


Figure 19. Return periods of extreme water levels at Narva-Jõesuu according to the results of the 6-h RCO data (upper panels) and the observed 1-h data set (lower panels). Note that the latter data constitute a semi-synthetic data set obtained based on actual observations and the output of HIROMB as explained above. The left panels correspond to projections based on annual maxima, the right panels – to projections based on maxima over stormy seasons. Single markers represent the set of block maxima. Reproduced from Paper II.

2001; van den Brink et al., 2005). The situation with the water levels on the Estonian coast may be different. Figure 19 indicates that the projections using the GEV distribution and different sets of block maxima have a much larger spreading than the projections based on Weibull or Gumbel distributions.

Paper II exploits the idea of the application of an ensemble of various projections to reach a reasonable estimate of the extreme values of water levels and their return periods. In other words, the idea is to use all of these distributions simultaneously. This approach implicitly assumes that errors of projections using different data sets and extreme value distributions are distributed randomly. This assumption is to some extent supported by the appearance of the projections using different distributions (Figure 19). For example, if the 6-h RCO data are used, the GEV distribution projects relatively large extreme water levels similarly to a Gumbel distribution. If, however, the observed data are used, the GEV distribution projects relatively modest values that almost coincide with the outcome of a Weibull distribution.

2.5. Projected water levels and contribution of wave set-up

Paper II addresses the properties of ensembles of 18 projections of extreme water levels and their return periods that consist of the outcome of the use of Weibull, Gumbel and GEV distributions built based on annual and stormy-season maxima of 6-h RCO, 1-h RCO and 1-h observed water level data in four locations. The assumption is that the appearance and particularly the spreading of these projections may carry valuable information about certain properties of water levels.

The analysis suggests that not one of the classic extreme value distributions (GEV, Gumbel, Weibull) replicates the observed and modelled extreme water levels adequately, especially for longer return periods. The Gumbel fit, in comparison with the Weibull fit, projects larger extreme levels for longer return periods. The GEV fit provides mostly intermediate values and the projections based on different sets of block maxima vary extensively, matching sometimes a Gumbel and sometimes a Weibull fit.

Even though the appearance of the resulting ensembles of projections of extreme water levels differs notably for the four chosen sites, the total spreading of projections of extreme water levels at all sites once in 200 yr is almost the same. The differences between projections are rather small for the Tallinn area (Figure 20). The total spreading within the ensemble is about 0.2 m for water levels with the return period of 5–10 yr, 0.25 m for the water levels with the return period of 20 yr, 0.5 m for the return period of 100 yr and around 0.8 m for the return period of 1000 yr. This level of spreading is considered to be minor in comparison with other similar studies (Sterl et al., 2009).

Several features can be interpreted as indicating a good consistency of the underlying data and adequacy of the entire approach in some locations. The set of different projections for Tallinn is nearly uniformly distributed between the highest and lowest projections. The lines representing different projections frequently cross

one another. No single projection is located clearly above or below the rest of the ensemble. It is therefore likely that for this particular location the average value or median of the ensemble is a suitable tool for evaluating the highest water levels and respective return periods (Paper II). This conjecture is consistent with the fact that observations in Tallinn were performed at the entrance to a relatively large harbour. The observation site is located in the area where water depth is around 10 m. Therefore it is likely that the measurements correctly reflect the offshore sea level while wave-induced changes are minor.

The overall appearance of the ensemble in question in Pärnu is similar to the one described above. This site is famous for statistically almost impossible extreme storm surges (Suursaar et al., 2006a; Suursaar and Sooäär, 2007) that reached 2.75 m in 2005 and 2.53 m in 1967. Even though they seem to not obey any of the existing theoretical extreme value distributions, such values are not exceptionally high for the Baltic Sea conditions (Figure 1). Figure 20 indicates that these outliers noticeably influence the GEV and Gumbel projections (cf. Suursaar and Sooäär,

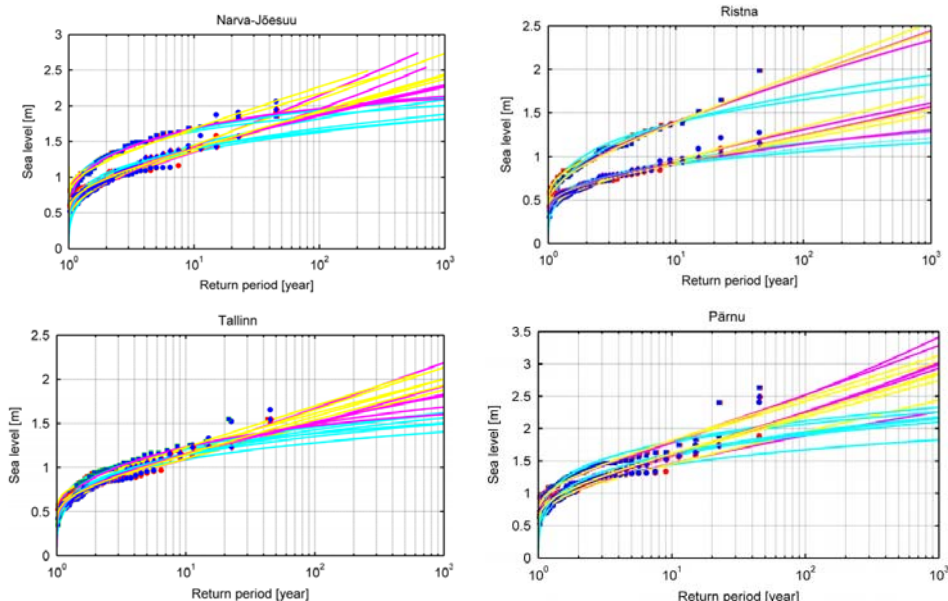


Figure 20. Return periods of extreme water levels according to different projections in Narva-Jõesuu, Ristna, Tallinn and Pärnu. Block maxima: red circles – annual maxima of the RCO 6-h data, blue circles – stormy-season maxima of the RCO 6-h data; red rhombi – annual maxima of the RCO 1-h data, blue rhombi – stormy-season maxima of the RCO 1-h data; red squares – annual maxima of the observed data set; blue squares – stormy-season maxima of the observed data set. The markers showing the block maxima derived from the 1-h RCO data almost coincide with those for the RCO 6-h data set. Yellow lines: projections using the Gumbel distribution, magenta – GEV distribution; cyan – Weibull distribution. Note that the difference between the observed and hindcast block maxima corresponding to the calendar years (red) or to stormy seasons (blue) does not become evident in the scale of the image but considerably impacts the relevant projections starting from return periods of about 20 yr. Reproduced from Paper II.

2007), whereas the Weibull fit tends to be mostly governed by the other block maxima. In Pärnu the observation site is slightly upstream of the Pärnu River. The observations apparently reflect adequately the water level at the end of about 1 km long jetties where contemporary circulation models reasonably replicate the water level.

The spread for the set of projections for Pärnu (Figure 20) is slightly larger than for Tallinn. Similarly to Tallinn, the “corridor” filled by different projections is narrow for short return periods (~10 yr) and widens for larger return periods. The spread is about 0.5 m for the return period of 20 yr, increases to 0.8 m for 100-yr return periods and reaches 1.5 m once in 500 yr. Despite the larger spread for Pärnu in comparison with Tallinn, the different projections are comparably homogeneously spread over this corridor; however, there is some indication that the ensemble splits into two subsets for return periods >100 yr.

In Narva-Jõesuu the deviations of different block maxima for small return periods of 2–10 yr are quite large – the observed values are up to 0.5 m higher than modelled ones. This difference disappears for larger return periods whereas the overall maxima of the two data sets differ by less than 0.2 m. The block maxima of modelled and recorded data sets seem to represent two populations of water levels (Figure 20). The two clusters of projections representing these populations are clearly separated until return periods of 20 yr. The populations almost coincide for the return period of 45 yr. The corresponding projections intersect for certain longer time instances. The projections are almost evenly distributed within the covered corridor from about the return period of 30 yr. The total spreading of the projections is comparable with the similar spreading in Pärnu: it is about 0.4 m for the return period of 20 yr and reaches close to 1 m for once in 500 yr.

A likely reason for the presence of two clusters of projections is that the observations were performed about 200 m upstream of the Narva River (Figure 21). The water level in this location is often substantially modified by the interaction of morphodynamic processes with hydrodynamic activity. Namely, obliquely approaching waves systematically cause the formation of a sandbar in the Narva River mouth. This feature grows in summer and almost blocks the river flow during certain seasons (Laanearu et al., 2007). It is also likely that extensive wave set-up is often formed along the smoothly sloping seabed near the river mouth that is open to the prevailing direction of wave propagation. These local effects are not resolved in the RCO model but may frequently modify the water level recordings. Nevertheless, the contribution of local effects to very high water levels and longer return periods is apparently modest because the behaviour of the measured block maxima is consistent with the predictions of the relevant extreme value distribution (Suursaar and Sooäär, 2007).

In Ristna (Figure 21) a radical difference occurs between block maxima of the observed and modelled water levels. The difference is 0.3 m for the return period of 2 yr and reaches close to 0.9 m for the return period of 45 yr. The overall maximum observed water level value (2.07 m) is considered not representative (Suursaar et al., 2006b, Suursaar and Sooäär, 2007). Even if the highest value is

excluded, the difference between the observations and modelled data is massive. The projections form two strongly separated clusters. Single projections from different clusters do not intersect even for water levels that appear once in 1000 yr. For the return periods up to 25 yr the spread of the projections within each cluster is modest and usually below 0.1 m. The spreading within clusters reaches 0.25–0.3 m for water levels that occur once in 100 yr and increases to 0.4–0.6 m for return periods of 500 yr. This fairly limited spreading indicates that both the observed and modelled data sets are internally consistent.

It is likely that the great difference between the observed and modelled data sets and respective projections is the result of local effects that contribute substantially to the observed water level in Ristna. This difference in turn affects the projections of extreme water levels. The measurements are performed in a small Kalana Harbour (Figure 21) lying on the Kõpu Peninsula at the southern coast of Hiiumaa. This coastal section is completely open to large waves generated by predominant south-western winds. The slope of the seabed is rather steep. The water depth at a distance of about 200 m from the land is 5 m, and already 10 m at a distance of 300 m.

Such geometry is not favourable for the generation of extensive local wind surge but allows for rather large waves to travel close to the harbour without breaking. Large waves that approach the harbour often along the shore normal may produce considerable wave set-up and thus form much higher water levels in the interior of the Kalana Harbour in comparison with the offshore water level in this region. Significant wave heights often exceed 4 m in the offshore of this region (Tuomi et al., 2011). The approach direction of these waves is usually from the south-west, that is, directly to the shoreline of the Kalana Harbour.

In ideal conditions 4 m high waves may cause about 1 m high wave set-up (Dean and Bender, 2006). The geometric centres of the two clusters differ by about 0.6 m for return periods of 45 yr (Figure 20). This value roughly matches the rule

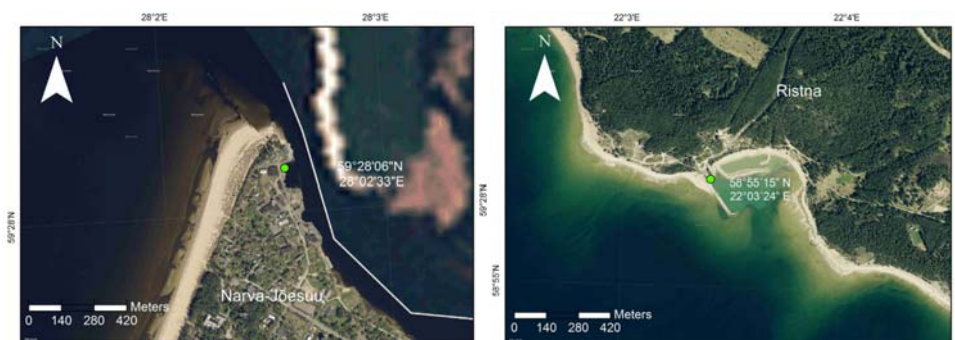


Figure 21. Left panel: Location of the water level observation peel (green circle) in Narva-Jõesuu at the left bank of the Narva River. The white line to the east of the observation site indicates the border between Estonia and Russia. The right bank of the river is blurred by the image provider. Right panel: Location of the water level observation peel (green circle) in Ristna (Kalana Harbour). Source: Estonian Land Board, www.maaamet.ee. Reproduced from Paper II.

of thumb that has been used for the contribution of wave set-up to the overall maximum water levels at open ocean coasts, where it contributes about 1/3 of the total water level maximum at the waterline (Dean and Bender, 2006).

On the one hand, the situation in Ristna carries a strong message that in some locations of the eastern Baltic Sea coast the ensemble approach for projections of extreme water levels and their return periods may be inoperable or even misleading. The reason is that a straightforward use of the modelled or observed data sets of water levels for such projections may ignore crucial components of coastal floodings. On the other hand, this approach is able to recover systematic differences in different data sets. In such situations the ensemble approach can be effectively used to identify the contribution of local effects (first of all wave set-up) to the formation of the total water level. Therefore, the systematic use of this approach enables much more explicit analyses of the local effects like wave set-up and their possible impact.

As discussed in Chapter 1, the contribution of wave set-up varies largely along shores with complicated geometry. Figure 21 demonstrates that the orientation of the coastline of the Kõpu Peninsula turns considerably over a short distance. It is therefore likely that the contribution from wave set-up to the total water level and thus the total water level itself vary extensively in different locations of the Kõpu Peninsula. This variation is apparently characteristic of many coastal stretches of Estonia and substantially complicates the analysis and projections of the extreme water level and its return periods on our shores.

2.6. Synchronisation of high wave set-up and offshore water level

As discussed above, the population of extreme values (outliers) of the water level is driven by joint impact of several effects (cf. Haigh et al., 2014). The sequences of storms from certain directions that force large water volumes into the Baltic Sea contribute about 40–50% of the total water level extremes (Soomere et al., 2015b). This contribution of the water volume of the sea is usually not distinguished from the offshore water level data. It is addressed in more detail in Chapter 3 and Paper IV. The presented analysis suggests that wave set-up may substantially strongly affect the water level in selected measurement sites. Paper I confirms that this mechanism is apparently often active along many sections of the eastern Baltic Sea coast. However, events of high wave set-up are sensitive with respect to the wave approach direction and thus not necessarily synchronised with the highest offshore water levels.

The analysis in Paper III makes an attempt to estimate how often high offshore water levels occur simultaneously with high set-up events. Particular focus is on the proportion of wave set-up in the total extreme water levels, the timing and synchronization of extreme offshore water levels and the highest wave set-up events. The study area extend from the interior of Tallinn Bay, used as the study area in Paper I, to a large coastal section to the east of Tallinn that is open to the north-east. The calculation scheme of numerically simulated wave properties

follows the one described in Sections 1.1 and 1.3. The water level data are extracted from the simulations using the RCO model for years 1961–2005 described in Section 2.2.

Another goal was to analyse the sensitivity of the locations with the highest wave set-up with respect to the possible rotation of wind directions in strong storms from the beginning of the 1980s (Section 1.6). It is also necessary to establish the wind directions associated with the situations when the total water level at the waterline considerably exceeds the all-time maximum for the offshore water level.

The largest coastal floodings occur if the maximum wave set-up develops simultaneously with very high sea levels. The latter are interpreted here as water levels modelled using an ocean circulation model at a distance of a few kilometres from the shoreline where local wave-driven effects are negligible. The water level time series (once in 6 h) is extracted for 11 offshore locations (Figure 3) from the output of the RCO model.

The overall highest offshore water levels in the study area were generated by only two storms (Figure 22). In most of the coastal segments the water level reached its all-time maximum during the storm on 8–9 January 2005 (Soomere et al., 2008). The modelled maximum water levels reached 1.6–1.7 m. These values are slightly larger than the observed maximum water level of 1.52 m in Tallinn Old Harbour (Suursaar et al., 2006b) and 1.55 m in Muuga Harbour (Hünicke et al., 2015).

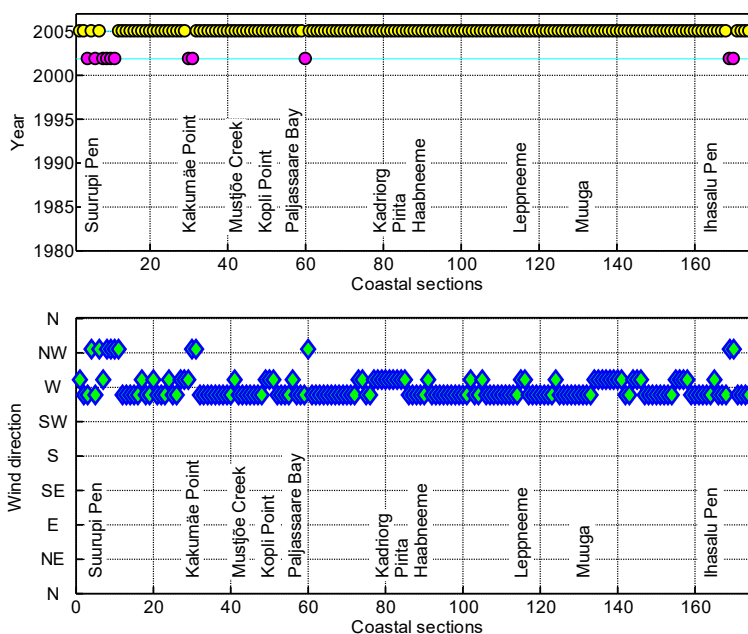


Figure 22. Storms (above) and wind directions (below) that were responsible for the highest total water levels at the shoreline. See Figure 4 for the numbering of coastal sections. Reproduced from Paper III.

The highest modelled wave set-up in single coastal segments varies between 0.26 and 0.96 m (Figure 14). This phenomenon actually does not appear in some areas where the theoretical value of wave set-up may be very high due to the nature of the coastal segment. The modelled maximum wave set-up reaches almost 1 m for some segments that are exposed to high waves on the Suurupi Peninsula. As the area has a steep scarp at the waterline, this value is unrealistic.

The predominant winds are blowing from westerly directions in this region. These winds may induce high wave set-up in coastal segments that are open to the west, north-west or north. Although north-eastern winds are comparatively rare in the Gulf of Finland (Soomere et al., 2008a), the resulting wave set-up may be rather high in the coastal segments of Muuga Bay that are open to the easterly directions (Figure 14).

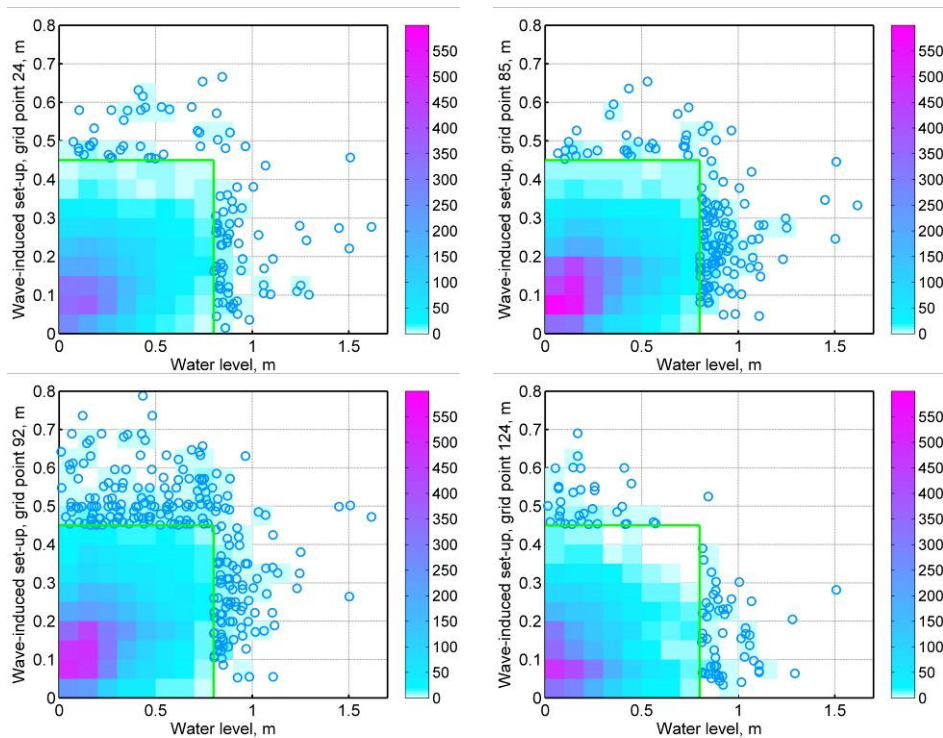


Figure 23. Scatter diagrams of the occurrence of different offshore water levels and various wave set-up values at four representative sections of the study area: section 24 (Tiskre, a bayhead open to the north-west and partially to the west), section 85 (Pirita Beach, open only to the north-west), section 92 (western coast of the Viimsi Peninsula; open to the west) and section 124 (eastern coast of the Viimsi Peninsula; open to the north-east). The colour code corresponds to ≥ 2 occasions (otherwise the area is left white) with a particular wave set-up (with a step of 0.05 m) and water level (with a step of 0.1 m). Single cases of wave set-up > 0.45 m and water levels > 0.8 m (outside the rectangle bordered by green lines) are represented as separate circles. The situations with zero wave set-up (waves propagating offshore) and cases with offshore water levels below the long-term average are not shown. Reproduced from Paper III.

The estimations of the total water level at the waterline in Paper III are found by adding the modelled offshore water levels from the RCO model to the instantaneous wave set-up height. The two data sets cover the years 1981–2005. The water level information is provided once in 6 h (Section 2.2) and wave set-up is calculated once for every 3 h (Section 1.1). To match the course of wave heights and water levels, the highest value of set-up within 6 subsequent hours is used in Paper III.

Figure 23 signals that the maximum wave set-up never appears simultaneously with the highest offshore water level. This feature reflects the specific combination of the orientation of the coastline and the directional structure of the predominant waves. Large waves that approach the northern coast of Estonia are mostly generated by strong northerly winds whereas the highest offshore water levels are driven by strong westerly winds.

This mismatch of the highest offshore water levels and high set-up events is particularly evident in coastal segments open to the east (Figure 23). The total water levels that exceed 1.4 m in such segments are mainly driven by the offshore water level and contain only minimal contribution from set-up. The largest offshore water levels never occur simultaneously with set-up values higher than 0.3 m. In other words, all remarkably high wave set-up events occur when the offshore water level remains moderately elevated (Figure 23).

In coastal segments that are exposed to the westerly directions high wave set-up may relatively often occur during high offshore water levels. The shape of the scatter diagram of wave set-up and offshore water level is elongated towards high water levels and set-up heights. It extends from the origin to the water levels of about 1 m and wave set-up heights of 0.4 m. Offshore water levels >1 m often

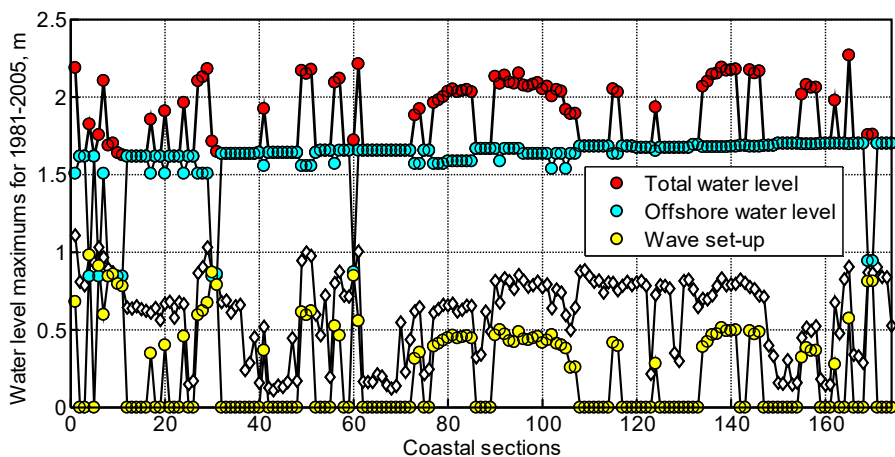


Figure 24. The contribution of the hindcast instantaneous offshore water level and wave set-up to the all-time highest water level at the shoreline. The modelled all-time offshore water level maximum (not shown) varies insignificantly (from 1.6 to 1.7 m) along the shore. White diamonds indicate the all-time highest set-up values. Reproduced from Paper III.

appear together with set-up over 0.3 m. The highest water levels that reach ~ 1.6 m may occur simultaneously with relatively large (up to 0.5 m) wave set-up events.

Therefore, the presence of wave set-up may substantially increase the total water level at the waterline during strong storms in sections open to the west. In contrast, in coastal segments that are open to the east the contribution of wave set-up to the extreme water levels is mostly negligible.

The largest values of the total water level were 1.6–2.3 m along the study area in 1981–2005 (Figure 24). The offshore water level contributed 0.9–1.7 m to these values. The all-time highest water level was governed exclusively by offshore water level in more than half of the coastal sections (99 out of 174). Extremely large offshore water levels in all these locations were accompanied by waves that either approached the coast under large angles or propagated offshore.

In some coastal segments exposed to the easterly directions large offshore water levels are systematically accompanied with insignificant set-up events (Figure 24). As a result, the largest total water levels either were equal to or only insignificantly exceeded the all-time highest offshore water levels in these sections. The reason for this feature is that during easterly winds (when the approaching waves were high)

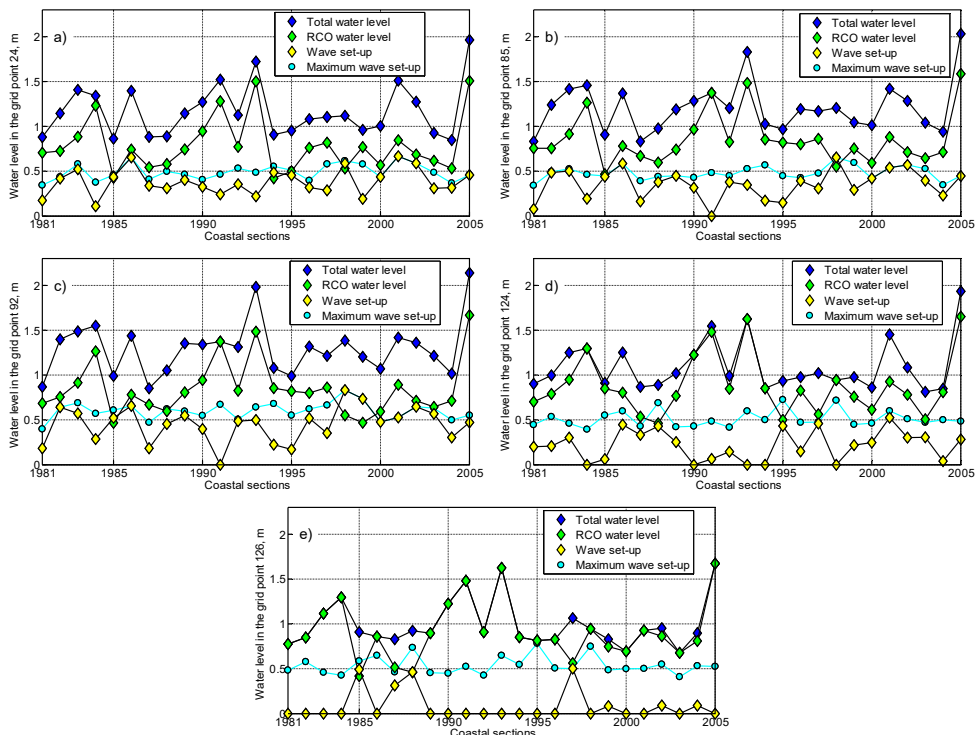


Figure 25. The proportion of wave set-up and offshore water level in the formation of annual maxima of the total water level at the shoreline at five representative sections of the study area: a) Tiskre (section 24), b) Pirita (85), c) Viimsi (92), d) Muuga (124), e) a location close to Muuga Harbour (126) where wave set-up almost does not contribute. See Figure 2 for the numbering of coastal sections. Reproduced from Paper III.

the offshore water level remained well below the all-time highest values. On the contrary, in coastal segments open to the north, north-west or west the contribution of wave set-up to the all-time maximum total water level is up to 0.5 m (Figure 24).

The time series of contributions of the offshore water level and wave set-up to the annual water level maxima follow a similar pattern. Large contributions of wave set-up to water level maxima systematically occur in the coastal segments that are open to the north-west (Figure 25). Therefore the total water level at the waterline often exceeds the offshore water level (Figure 25a, b).

Interestingly, annual maximum contributions of wave set-up to the total water level are often equal with the annual highest set-up values in these segments. This means that very high waves approach directly the coast during the storms that create the highest offshore water levels. The situation is opposite in coastal segments that are open to the east. The contribution of set-up to the total water level is generally smaller and vanishes in some years (Figure 25c, d, e).

3. Spatial variability in trends in extreme water levels

The maximum offshore water levels at the Baltic Sea coast exhibit overall increasing trends. The magnitude (slope) of these trends varies largely (from 2 to 9 mm/yr) in different measurement sites on the Estonian coast (Suursaar and Sooäär, 2007). This increase rate several times exceeds the global ocean level rise. As the overall storminess in the Baltic Sea basin has not shown any radical increase over the 20th century (Hünicke et al., 2015), the reasons for such a rapid increase are of great interest. Moreover, it is also not clear which component of the water level is responsible for the increase in these extremes.

An attempt to shed light on these questions is presented in Paper IV. This paper addresses separately the two components of the offshore water level that may be responsible for the increase in the extremes. The analysis is based on the annual and stormy-season maxima of the offshore water level. The idea is to separate the course of the total offshore water level into the local storm surge and the weekly-scale component that characterises the water volume of the entire Baltic Sea as recommended in Soomere et al. (2015b).

3.1. Trends in the annual maxima of the total water level

The focus in this chapter and in the underlying Paper IV is on the spatial patterns of changes in the two contributors to the annual maximum offshore water levels. Measurements and observations of the water level in the coastal region provide not only the most essential information for understanding the processes behind devastating floodings but also better predictions and a strong background for the relevant risk assessments. Unfortunately the spatial coverage of observed water level data sets usually does not provide enough information for making conclusions that are appropriate for the entire coastline. The network of tide gauges has major gaps even in the areas where their coverage is relatively dense (Arns et al., 2015; Hünicke et al., 2015). In some cases, as shown in Section 2.5 and in Paper II, the data from tide gauges may contain the contribution of local effects such as wave set-up. Therefore the measured time series do not necessarily provide spatially adequate values of the water level (Brakenridge et al., 2013).

For the above reasons the analysis in Paper IV is largely based on simulated water levels. The water level data along the study area (the coast of Estonia and the northern part of Latvia, Figure 26) is extracted from simulations using the RCO model for years 1961–2005. The technical information about the model and its forcing, and the basics of the simulations are presented in Section 2.2. An overview of the complementary data set of water level time series from four observation sites along the Estonian coast, used also in Chapter 2 and Paper III, is presented in Section 2.1.

The grid cells of the RCO model used in the analysis were chosen along the coast (Figure 26) mostly in 6–30 m deep water. This water depth is generally large enough to avoid local distortions in the shape of the water surface caused by

unresolved bathymetric features in shallow areas and other local effects. The focus is on the temporal course of extreme deviations of water levels from the long-term mean value. Comparisons of the modelled data sets with observed values suggest that the role of local effects in measurements may be significant in some locations (Section 2.5).

The slopes of trends in the observed long-term average water level vary in the range of 2–3 mm/yr on Estonian coasts (Suursaar and Sooäär, 2007; Suursaar et al., 2015). Spatial variations in the rate of increase in the mean water level are fairly small in the entire eastern Baltic Sea. The slopes of trends in the annual maxima are much larger (3.2–9 mm/yr, Jaagus and Suursaar, 2013) in Estonian coastal waters. As Paper IV addresses the variations in the maximum deviations of water level from the long-term mean, the trend in the mean water level is removed from both the observed and modelled data sets by simple de-trending.

Trends in the maxima of water level are analysed based on the concept of block maxima that is described in more detail in Section 2.4 and Paper II. Similarly to the approach in Section 2.4, two sets of block maxima are specified. Firstly, the maxima over the largest values of water level that occur once during each calendar year are evaluated. Secondly, the largest values over the stormy period from June to May of the subsequent year are singled out. As discussed above, the latter set contains negligible correlations between the subsequent values. The main object of study is the pool of trendlines for these two sets of maxima for the RCO model grid cells shown in Figure 26.

Both sets of block maxima show comprehensive interannual variability (Figure 27). The formal linear trends are evaluated with the classic approach of

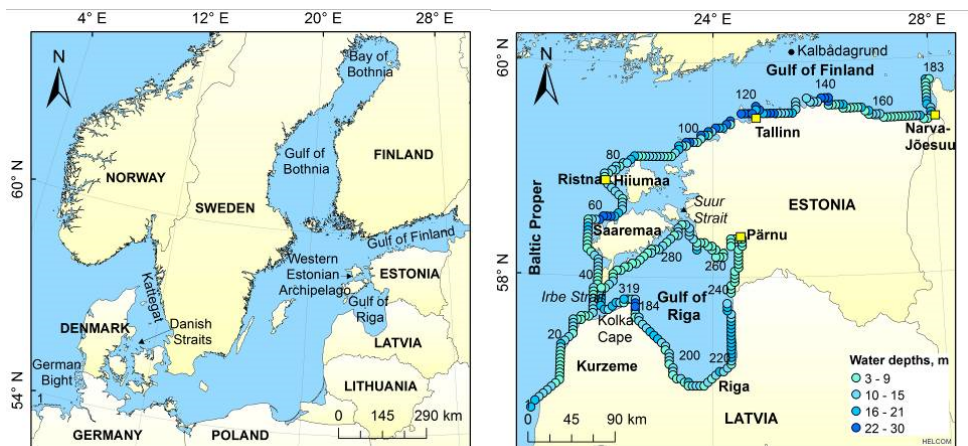


Figure 26. Left panel: Scheme of the Baltic Sea. Right panel: Water depth at the selected RCO model grid cells in the eastern Baltic Sea (colour scale) and locations of water level gauges (yellow squares in Pärnu, Ristna, Tallinn and Narva-Jõesuu) used in the analysis. The grid cells are numbered consecutively from the western coast of Latvia to the eastern Gulf of Finland, and then counter-clockwise along the coast of the Gulf of Riga starting from Cape Kolka. Reproduced from Paper IV.

linear regression. In addition, the Theil–Sen estimator is applied to detect trends with the nonzero slope. The Theil–Sen estimator is less sensitive to outliers than trendlines evaluated using classic approximations and generally provides more adequate estimates of statistical significance of the nonzero trends.

The increase rate of both sets of block maxima is about 7 mm/yr near Tallinn (Figure 27). Although the individual values of different block maxima are at times largely different (e.g., for the years 2004/2005 in Figure 27), the slopes of the two trendlines differ insignificantly and the lines mostly overlap (Figure 27). This increase is about twice as rapid as the increase in the water level maxima extracted from the observed data for years 1948–1995 (Suursaar and Sooäär, 2007). The described difference in the increase rates is apparently mostly induced by the different temporal coverage of the observed and simulated time series. Nevertheless, this difference is consistent with the recent acceleration of the increase in the water level extremes during 1980s–2000s (Suursaar and Sooäär, 2007).

Both the modelled maxima of the total water level for the calendar years and over the stormy seasons exhibit a rapid and statistically significant (99%) increase for all grid cells in the study area. The increase in the total water level maxima (equivalently, the slope of the relevant trend) is between 5 and 10 mm/yr (Figure 28). This estimate is consistent with the results of Suursaar and Sooäär (2007) derived using the observed and measured water levels in several locations of the Estonian coast. The values and spatial patterns for the increase in the maxima over a calendar year and over the storm season are rather similar. The slopes of the relevant trends mostly coincide in the eastern part of the Gulf of Finland and also on the Latvian coast of the Baltic Proper. The coastal areas in the eastern Gulf of Finland and the eastern Gulf of Riga exhibit the largest increase up to 8–10 mm/yr.

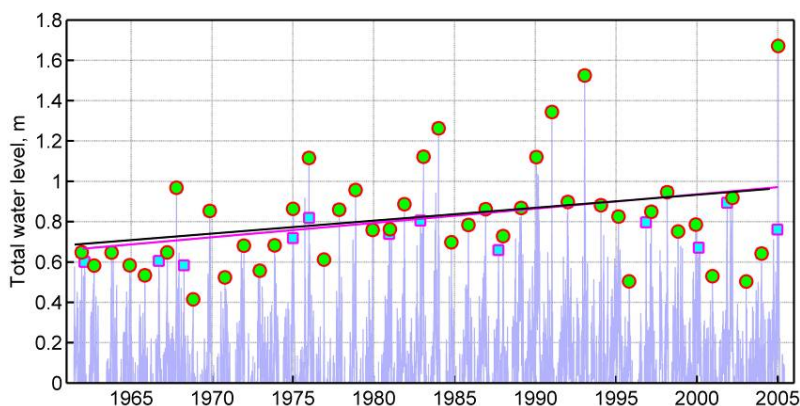


Figure 27. Trends in stormy-season (green circles, 7.1 mm/yr, red line) and annual (cyan squares, visible if different from the stormy-season maxima, 6.4 mm/yr, black line) modelled water level maxima near Tallinn (Figure 28) in 1961–2004. The Sen’s slope for both trends is 6.4 mm/yr. The confidence intervals for the Sen’s slope of stormy-season maxima and for the annual maxima are [0.9, 11.6] mm/yr and [2.3, 9.8] mm/yr, respectively. Reproduced from Paper IV.

The coastal areas of the eastern Baltic Proper and the entrance to the Gulf of Finland show smaller increasing trends of about 5–7 mm/yr. The western coast of Saaremaa hosts the smallest trend slopes below 5 mm/yr. This area is open to predominant strong south-western winds. The German North Sea coast exhibits a similar trend slope (Mudersbach et al., 2013).

3.2. Maxima of storm surge heights and weekly average water levels

It is of great interest to understand how much the two major components of water level (volume of the Baltic Sea and local storm surge) contribute to the increase in the water level maxima. Many methods are available for separating the impact of the two processes, including simple averaging and filtering methods (e.g., Haigh et al., 2010a, b) or approaches based on the use of wavelet techniques (Percival and Mofjeld, 1997).

Soomere et al. (2015b) have demonstrated that a meaningful separation of the impact of the two major aperiodic water level drivers for the Baltic Sea conditions can be obtained by a straightforward averaging of the de-trended water level time series over a certain time interval and subsequent removing of the resulting average from the total water level. A suitable time window for averaging is about 8 days. The averaged water level reflects the water volume of the entire Baltic Sea that changes on scales of a few weeks (Figure 29) and follows a quasi-Gaussian distribution. The residual (when the described weekly-scale average is removed from the total water level) reflects to some extent the height of storm surges (Figure 29). The link between this residual and the height of the local storm surge is, however, not straightforward. The residual expresses more or less adequately the height of a surge created by a single storm after a calm period (e.g., on 10 February 1990, Figure 29). For a longer series of storms the maximum value of the residual is approximately half the storm surge height.

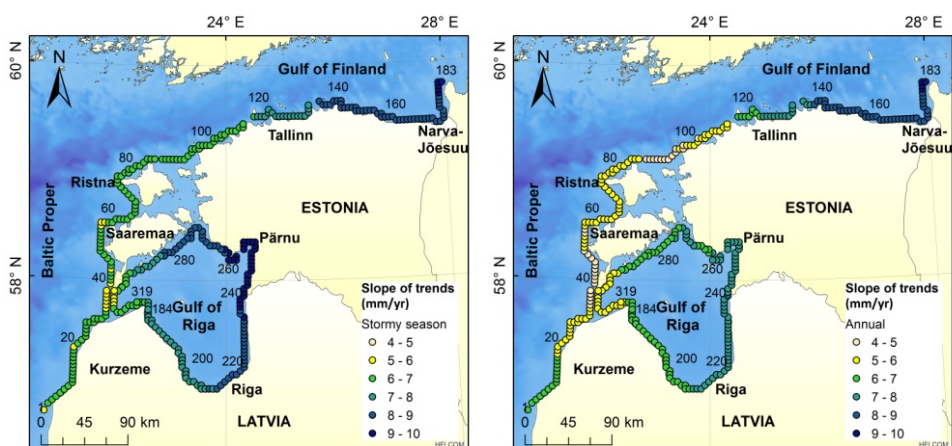


Figure 28. Slope (mm/yr) of trends in the stormy-season and annual maxima of total water level in 1961–2004. Reproduced from Paper IV.

The shape of the distribution of this residual suggests that the drivers of surge events follow a Poisson distribution (Soomere et al., 2015b). As I address the water level maxima, only positive storm surges are considered in this thesis. Storm surges have a typical duration of one day. Even though wave set-up may have a large impact on the observed water levels at some sites (Ristna, Paper II), its role is not taken into account in Paper IV and this chapter focuses on the offshore water level.

The overall appearance of the temporal course of both components of the water level resembles the course of the total water level (Figure 30). They all exhibit strong seasonality as well as comprehensive intra- and interannual variations all over the research area. As expected, the temporal variability of the weekly average water level is much lower than that of the total water level. For example, the standard deviation (std) of the weekly average water level in Tallinn (std 0.067 m) is only about 25% of this measure for the total water level (std 0.25 m) and for the storm surge height (std 0.23).

The annual maxima of the weekly average water level (from about 0.2 m to 0.8 m) are basically in the same range as the annual maxima of storm surge heights (Figure 30). Nevertheless, these maxima have largely different distributions. The most common values of the annual and stormy-season (see Section 2.4 for definitions) maxima of the weekly average are 0.5–0.6 m while the values in the range of 0.2–0.35 m are infrequent. Similar maxima for the residual of the water level (below called storm surge maxima) are commonly close to 0.3–0.4 m, rarely over 0.45 m and just a couple of examples exceed 0.7 m (Figure 30). This feature probably reflects a specific nature of the applied separation of the water level components. Namely, it assigns all very large values (positive outliers) of the annual water level maxima to the time series of storm surge heights (Soomere et al., 2015b). The std of the annual and stormy-season maxima of the total water level (0.22 m and 0.27 m, respectively) are approximately equal to the std of the relevant time series. The temporal variation in the maxima of the water level components is different from the variation in their time series. The std for the maxima of the weekly average and of the storm surge height are 0.13–0.16 m and 0.12–0.14 m, respectively.

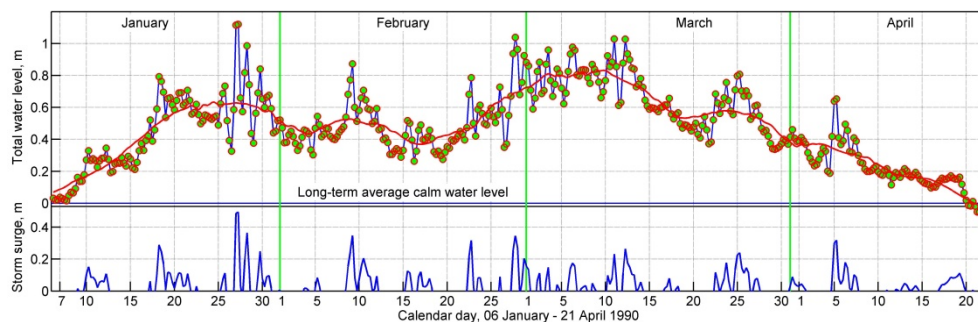


Figure 29. Numerically simulated total water level (green circles connected with a blue line), its 198-h (8.25-day) average (red) and the positive part of the residual (the total water level minus the 8.25-day average, interpreted as the positive storm surge, blue, lower panel) near Tallinn. Reproduced from Paper IV.

3.3. Spatial distribution of slopes of trends

The maxima of both components of the water level, evaluated over calendar years and over stormy seasons, also increase in time in the entire study area (Figure 31). The spatial patterns of their variations are radically different. The slopes of trendlines of single water level components vary largely along the shores of Estonia and northern Latvia. The increase in the maxima of the weekly average water level and of the storm surge are comparable (about 3–4 mm/yr as suggested by Figure 30) only in a small stretch of the central part of the northern coast of the Gulf of Finland and in the eastern Gulf of Riga. The storm surge maxima exhibit an almost twice faster increase in the eastern part of the Gulf of Finland (Narva-Jõesuu) than the weekly average maxima. The increase in the storm surge maxima is several times slower in the coastal areas open to the Baltic Proper (e.g., Ristna).

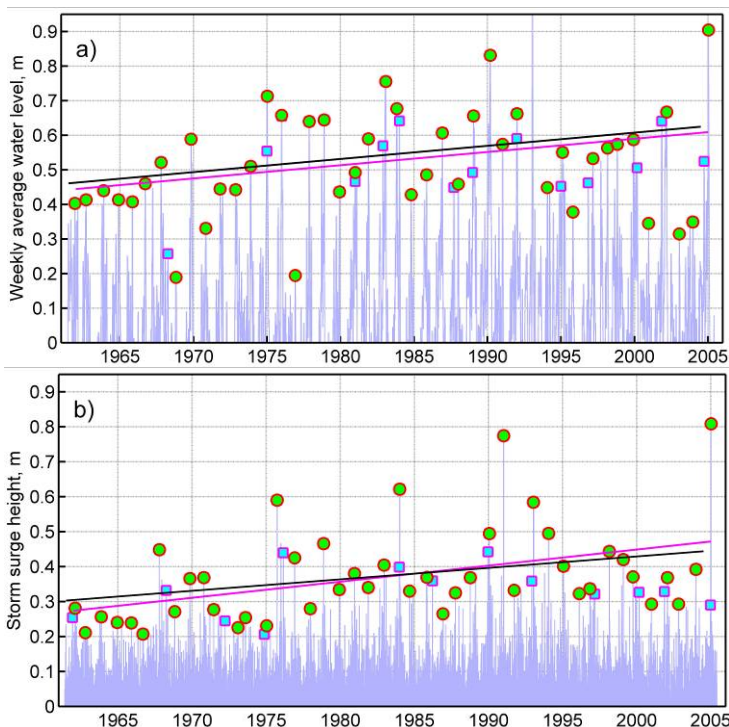


Figure 30. Trends in the maxima of water level components near Tallinn in 1961–2005. a) Trends in stormy-season (circles, 3.8 mm/yr, Sen's slope 4.0 mm/yr, 95% confidence interval [0.0, 7.4] mm/yr; red trendline) and annual (squares, visible only if different from the stormy-season maxima, 3.8 mm/yr, Sen's slope 3.5 mm/yr, 95% confidence interval [1.3, 6.8] mm/yr; black trendline) maxima of the weekly average water level; b) trends in stormy-season maxima (circles, 4.6 mm/yr, Sen's slope 3.7 mm/yr, 95% confidence interval [1.6, 5.8] mm/yr; red trendline) of the (relative) storm surge heights and in similar annual maxima (squares, visible only if different from the stormy-season maxima, 3.3 mm/yr, Sen's slope 2.9 mm/yr, 95% confidence interval [0.7, 5.1] mm/yr; black trendline). Reproduced from Paper IV.

The trendlines evaluated for the storm surge height maxima differ to some extent, depending on whether they have been found for stormy-season maxima or calendar year maxima (Figure 31 and Figure 32). The slopes of trends of annual maxima are by 10–15% smaller for most of the study area and spatially more variable than those for stormy season maxima. The two slopes differ insignificantly only on the Latvian coast of the Baltic Proper. This feature indicates that the maxima over calendar years may be correlated in some coastal segments.

Importantly, both these slopes vary extensively over the study area (Figure 31) from from zero to 7.3 mm/yr. The maxima of storm surges increase rapidly in the eastern Gulf of Finland and eastern Gulf of Riga at a rate well above 5 mm/yr (Figure 32). The increase is much slower in the western part of the Gulf of Riga.

Most interestingly, the maxima of storm surges have increased only very little, by about 1 mm/yr in some locations on the shores of the Western Estonian archipelago open to the predominant strong wind directions (Figure 31, Figure 32). Consequently, in these locations the increase in the maxima of total water levels is driven exclusively by changes in the weekly average water level. Although the latter measure does not perfectly reflect the volume of the whole of the Baltic Sea, it confirms that the contribution from the water volume of the entire sea governs the formation of the local water level maxima in these spots. The increase in storm surge maxima was also comparatively slow (3–4 mm/yr) on the north-western shore of Latvia.

The spatial pattern of the slopes of trends in the weekly average water level is qualitatively similar to that of the total water level maxima (Paper IV, Figure 32). The increase in these maxima has been the fastest in the eastern Gulf of Finland and in the Gulf of Riga. The relevant spatial variations are much smaller than the variations in the slopes of total water level maxima as well as similar properties of storm surge heights. The slopes estimated from the annual and stormy-season

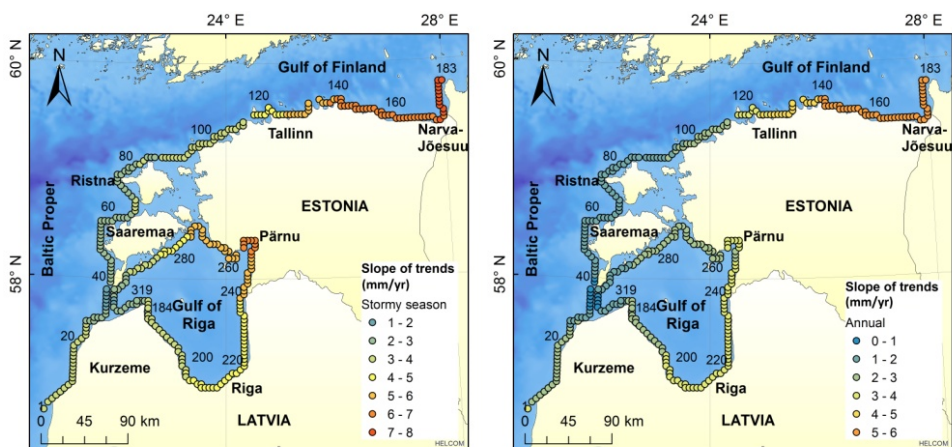


Figure 31. Slope (mm/yr) of trends in the stormy-season and annual maxima of storm surge heights (total water level minus 8.25-day average) in 1961–2004. Reproduced from Paper IV.

maxima almost coincide. However, the full range of their variations is less than 1 mm/yr. The slopes of all these trends are close to 4 mm/yr. Therefore, the long-term increase in the water volume maxima of the Baltic Sea has contributed about 4 mm/yr to the maxima of total water levels in the entire study area. This rate is almost three times as large as the global sea level increase rate.

An important conjecture from this result is that the impact of basically wind-driven events of large-scale inflow of the North Sea waters into the Baltic Sea has increased considerably and almost steadily since the 1970s. An increase in the water volume that flows through the Danish straits may be caused either by growth of the wind speed during such inflow events or by longer duration of these events. The above has shown that the maxima of local wind-driven surge heights have not increased in the locations of the Western Estonian archipelago that are completely open to the predominant strong wind directions. Consequently, it is unlikely that wind speed in strong storms has increased in the Baltic Proper. It is likely that the same conjecture applies to the area of the Danish straits. Therefore, an increase in the water volume maxima of the Baltic Sea most likely reflects an increase in the duration of the sequences of storms that push the North Sea water into the southern Baltic Sea (Paper IV).

The slopes of trends evaluated from the water level observations and from the results of numerical simulations coincide only in the vicinity of Tallinn (Figure 32). The increase rates of the maxima of weekly average and storm surge (Figure 32). The increase rates of the maxima of weekly average and storm surge

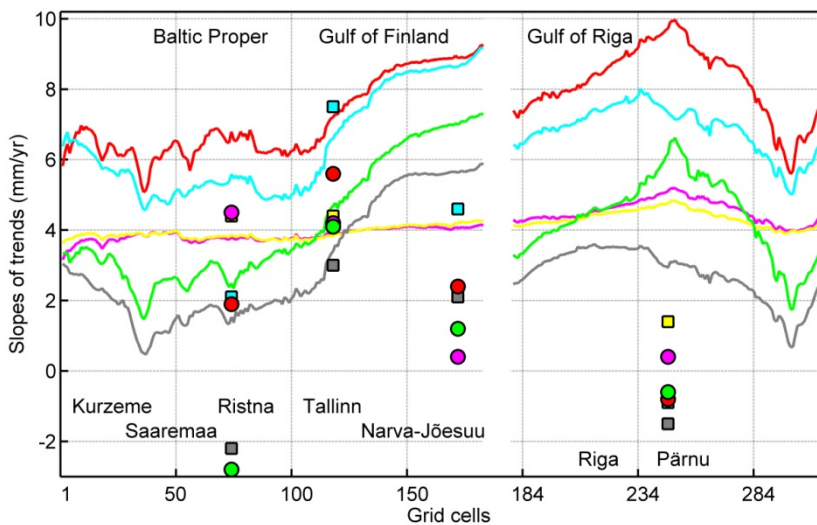


Figure 32. Alongshore variation in the slopes of trends (mm/yr) of water level components in 1961–2004. Red and cyan: total water level, stormy seasons and calendar year, respectively; magenta and yellow: 8.25-day average, stormy seasons and calendar year, respectively; green and grey: storm surge, stormy seasons and calendar year, respectively. For the observed data sets the colours are the same, circles indicate trends for stormy-season maxima and squares – trends for annual maxima. The typical width of 95% confidence intervals for various slopes is ± 2 mm/yr. The numbering of grid cells follows Figure 4. Adapted from Paper IV.

heights almost exactly match each other whereas the match is acceptable for the increase rates of the total water level maxima. A likely reason for such a match is that the water level measurements in Tallinn were performed at the entrance to Tallinn Old Harbour, where the water is sufficiently deep (~10 m) and local wave- and wind-driven effects are negligible. Moreover, the observation and measurement site is open to the NNW and is thus protected against the majority of storm winds. Therefore, the role of local effects is rather small and the observed water levels reflect the offshore water levels well.

In three other locations (Narva-Jõesuu, Ristna and Pärnu) the slopes for the observed and modelled data diverge. It is likely that the mismatch is driven by certain local factors that affect the water level readings. For example, water level observations in Ristna are strongly influenced by local wave set-up (Paper II). This phenomenon greatly contributes to the storm surge created by strong south-western winds in this site (Figure 21). It is thus not unexpected that the slopes of total water level maxima for observations and for modelled data differ remarkably and have even opposite signs. However, wave set-up is rapidly relaxed when the wave height decreases and the “memory” of the Baltic wave fields is relatively short (usually well below 12 h). Therefore, it should have a much weaker influence on the maxima of weekly average water levels. Indeed, Figure 32 shows a very good match of the “observed” and “modelled” slopes of weekly-scale water levels.

The match of the slopes in question is very poor in Narva-Jõesuu and Pärnu. A likely reason is that observations are performed at both sites in large river mouths. The highest storm surges in these two locations are driven by winds from particular directions (Suursaar et al., 2003). Therefore, even relatively small deviations of the modelled wind directions in the atmospheric forcing used in the RCO model from the actual wind direction may lead to great differences in the reproduction of the local storm surge during the strongest storms. There is, however, no straightforward explanation for the large mismatch of trend slopes for the maxima of the weekly-scale water level. Even though the water level in Narva-Jõesuu may often be modified due to joint impact of wave set-up and a sill at the river mouth (Laanearu et al., 2007), this mismatch requires further investigation.

3.4. The role of the averaging interval

The averaging interval used to single out the impact of short-term storm surges has a strong effect on trend slopes. This is an expected feature because the annual maxima of the weekly average water level may contain a significant contribution from local storm surges (Figure 29). In this sense it is remarkable that the contribution of the weekly average water level maxima to the increase in the total water level maxima is almost constant for the entire study area (Figure 32) even though some sections of the shore are heavily impacted by local storm surges.

An analysis of the impact of the varying length of the averaging intervals used for the separation of the two major water level components sheds additional light on the interplay of these components in the study area (Figure 33). It is natural that

in the case of short averaging intervals the behaviour of the average water level largely follows the total water level. The local values, spatial variation and slopes of trendlines of the maxima of the average water level, obtained using averaging lengths of 1–3 days are qualitatively and quantitatively comparable to similar properties of the maxima of the total water level (Figure 33). Interestingly, the trends of the average water level maxima evaluated over calendar years and stormy seasons are notably different in the case of averaging over short intervals. This feature probably reflects the presence of frequent correlation of the relevant maxima in consecutive years that are essentially produced by the same sequence of winter storms in December–January.

Longer averaging intervals lead to a decrease in spatial variations in the slopes of trendlines for maxima over both calendar years and stormy seasons (Figure 33). While the slopes of trendlines of maxima over stormy seasons vary by about 3 mm/yr for the averaging interval of 18 h, the variation is much smaller, about 1.5 mm/yr, when the averaging interval is 4.25 days. The spatial variation continues to decrease for even longer averaging intervals. For averaging intervals longer than 6 days the decrease in the spatial variability of the slopes is faster in the Gulf of Riga. It is likely that a large part of the remaining variation of about 1 mm/yr reflects the contribution of local storm surges. This feature signals once more that the weekly average local water level may include some part of storm surges and therefore is not a precise proxy of the water volume of the Baltic Sea.

Gradual increase in the length of the averaging interval yields a sophisticated mutual variation in the slopes of trendlines of the two sets of maxima (Paper IV, Figure 33). The slopes for the maxima of stormy seasons exhibit a monotonous and more rapid decrease than similar slopes for the annual maxima. The two slopes are almost equal for a certain length of the averaging interval. This length is different for different segments of the study area. It is about 6 days for the shores of the Baltic Proper and the Gulf of Finland and 10 days for the Gulf of Riga. The typical slopes of the relevant trendlines are about 3.5–4 mm/yr in the Baltic Proper and in the Gulf of Finland, 4–4.7 mm/yr in the Gulf of Riga and up to 5.2 mm/yr in the interior of Pānu Bay. This difference in the “balancing” lengths of the averaging interval suggests that the water level maxima in the Gulf of Riga may have another component. A likely reason is that the water volume of the entire Gulf of Riga may be increased for a few days by specific sequences of storms.

An increase in the averaging period to 16–24 days results in the continuous decrease in the slopes of trends of water level maxima over stormy seasons because longer averaging intervals suppress to some extent all short-term maxima. Interestingly, in the case of even longer averaging intervals the trends of maxima over calendar years (Figure 33) show an increase. The minima of these slopes appear when the smoothing interval is 7–8 days on the Kurzeme coast (Figure 33) and in the eastern Gulf of Riga, and about 10–11 days in the Gulf of Finland. A likely reason behind this increase is that the maxima of subsequent years are levelled off towards the larger values for long averaging intervals.

In the Gulf of Riga the slopes of the trends in question notably and systematically exceed the similar slopes in the rest of the study area. Consistently with the above-described difference in the lengths of the “balancing” averaging intervals, this feature may also be interpreted as reflecting a peculiar delay in the formation and persistence of very high water levels in the Gulf of Riga. The delay is caused by the slow flow through the shallow and narrow Irbe Strait and Suur Strait (Figure 26) between the Baltic Sea and the Gulf of Riga. Owing to this configuration the water level in the Gulf or Riga may rise higher than in the rest of the Baltic Sea during specific storms. Strong westerly winds may push the water into the gulf and therefore support the long-term elevated water level there similarly to the impact of sequences of storms that push water into the Baltic Sea via the Danish straits. The described process cannot appear in the Gulf of Finland and northern part of the Baltic Proper. The signal of changes in the water level generally moves in these areas with the wave speed in shallow water and reaches the eastern part of the gulf in 6–7 h.

3.5. Possible changes in the directional structure of forcing

The results presented in Section 1.6 and Paper I indicate that certain nontrivial changes in the atmospheric forcing of the wave field may have taken place in the

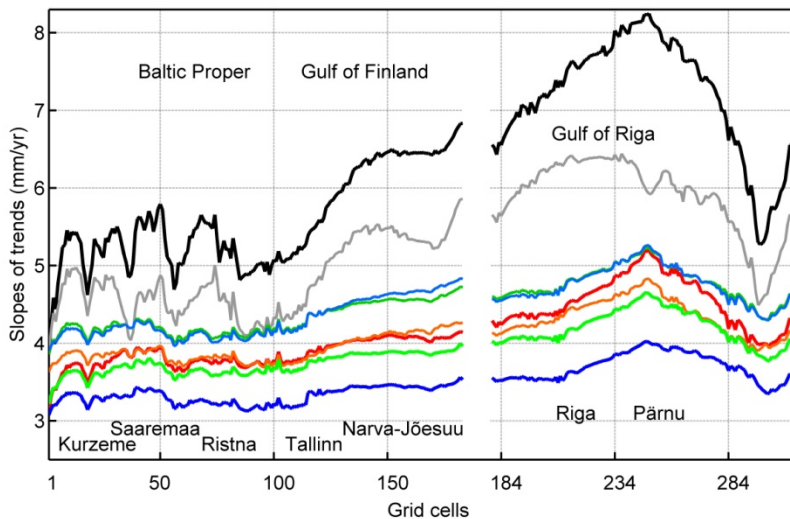


Figure 33. Spatial variations in the slope of the trendline of the maxima of the average water level for different averaging lengths. Dark and light grey: 18-h average, stormy-season and annual maxima, respectively; red and orange: 8.25-day (198-h) average stormy-season and annual maxima, respectively (equivalent to yellow and pink lines in Figure 32); light and dark green: 16.25-day (390-h) average stormy-season and annual maxima, respectively; blue and cyan: 24.25-day (582-h) average stormy-season and annual maxima, respectively. The lines representing slopes for stormy-season maxima are wider than their counterparts for annual maxima. The numbering of grid cells follows Figure 26. Adapted from Paper IV.

Gulf of Finland during the simulation time (since 1981). The assumption of a change in the wind direction during selected strong storms in the eastern Baltic Sea (Paper I) is supported by the established spatial structure of the slopes of the trendlines of water level maxima (Figure 32). The decrease in the observed maxima of water levels over stormy seasons in Ristna also supports this hypothesis.

The relevant conjecture relies on the significant contribution of wave set-up to water level observations in Ristna (Paper II). Figure 32 suggests that the local storm surge maxima have not increased in the vicinity of Ristna. Therefore, it is likely that wind speeds have remained basically on the same level since the 1970s. A possible reason for a decrease in the observed water level maxima is thus a decrease in the contribution from wave set-up. As wave set-up height largely depends on the wave approach direction, a turn in the wind directions in selected storms may explain the decrease in the observed water level maxima.

The major qualitative difference in the properties of spatial variation in the trendlines of the maxima of the two water level components also signals a rotation of strong winds in selected storms. The analysis in Section 3.3 reveals that the wind speed has not increased substantially in the Baltic Sea basin. However, the maxima of storm surges have increased significantly in the eastern Gulf of Finland and the eastern Gulf of Riga. As storm surge height also depends on the dimensions of the sea area, it is likely that, differently from the past, some storms blow almost along the Gulf of Finland nowadays. This sort of rotation of the wind direction explains well the increase in the storm surge maxima in the eastern part of this water body.

This conjecture is consistent with the increasing evidence of the rotation of wind directions in the Baltic Sea basin. Changes have been noted in the wind, air flow and wave approach directions all over the Baltic Sea (Soomere and Viška, 2014; Soomere et al., 2015a). Several studies report a more frequent occurrence of south-western winds in several Estonian observation sites in 1966–2005 (Jaagus, 2009; Jaagus and Kull, 2011). The predominant wind direction has turned 20° to the west during 1966–2011 (Suursaar, 2013, 2015). All these changes are

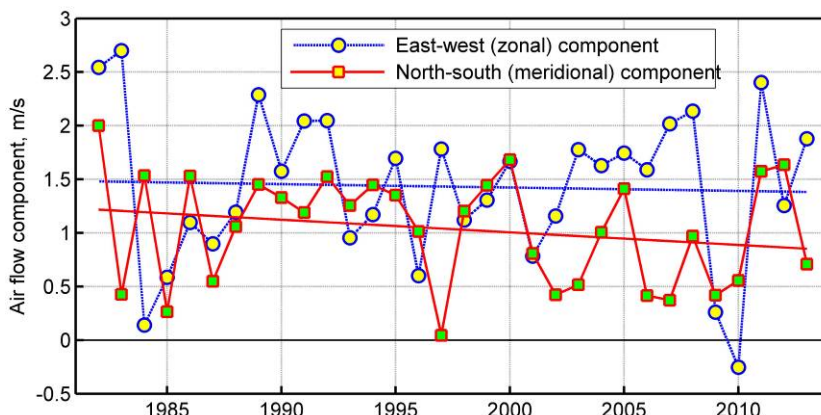


Figure 34. Annual average zonal and meridional air-flow components and their trendlines for 1982–2013 at Kalbådgrund in the Gulf of Finland. Reproduced from Paper IV.

eventually reflected in the wave properties. For example, the formal prevailing direction of the approach of observed waves in Narva-Jõesuu has changed more than 90° in 1954–2008 (Räämet et al., 2010). There is evidence that these changes also impact wave heights. For example, the modelled wave heights show a decrease about 60 km to the south from Ristna (Suursaar, 2015).

The described changes are, if at all, only weakly represented in standard time series of wind properties and classic wind statistics (Keevallik and Soomere, 2014). The highest water levels develop in severe storms which occur irregularly and are hardly visible in the bulk of long-term wind measurements. Such changes are much more clearly highlighted in terms of air flow or its components. For example, at the end of the 1980s an abrupt rotation by 40° occurred in the annual average geostrophic air flow over the southern Baltic Sea (Soomere et al., 2015a). This is also visible in the analysis of air flow on the latitudes of the Gulf of Finland (Keevallik and Soomere, 2014). The components of average air flow are components of mean wind speed over a certain time period. The average air flow gives an idea of the speed and direction of the average air motion. As it involves information about wind velocity, it also carries information about changes in the wind direction during strong storms.

Paper IV makes an attempt to detect such a change in the marine wind in the Gulf of Finland. As extreme water levels reflect open sea wind properties, the analysis uses the wind information from a caisson lighthouse at Kalbådagrund (Figure 3, 59°59' N, 25°36' E). The same wind information is used in Paper I and Paper II. The wind properties measured in this location are almost not affected by the mainland. The data set is described in more detail in Section 1.1. As I am interested in the changes in wind direction, the height correction is not performed.

Consistently with Soomere et al. (2010) the annual mean wind speed decreased slightly (~0.1 mm/s per year) over 1982–2013 (Paper IV). The magnitude of zonal and meridional components (1.43 m/s and 1.03 m/s; positive to the east and north, respectively) shows the prevalence of south-westerly winds (Figure 34). The zonal component exhibits a very small decrease of 3 mm/s per year which is statistically insignificant. Therefore, this component has practically not changed in 1982–2013. On the contrary, the meridional component has a negative trend of –11 mm/s per year. The decrease was almost 30% (from ~1.2 m/s to ~0.8 m/s) of the average value in 1982–2013.

As both components of air flow vary remarkably on the interannual scale (Figure 34), it is appropriate to use the Theil–Sen estimator to evaluate the statistical significance of their potential changes. This estimator confirms that no trend exists in the zonal component whereas the decrease in the meridional component is even steeper (–13.5 mm/s per year) and statistically significant at a 80% level. Despite a low statistical significance of this trend, its presence still supports the assumption of the rotation of the wind direction in a part of severe storms in the eastern Baltic Sea.

Conclusions

Summary of the results

The presented studies address properties of three major components of the nearshore water level in the Baltic Sea (water volume in the entire sea, the local storm surge and wave-induced set-up) and spatio-temporal variations in their contributions to the total water level extremes on the Estonian coasts. The central objectives were to (i) quantify the contribution of wave set-up to the nearshore water levels at the coastline of the city of Tallinn, (ii) evaluate the extent of spatio-temporal variations in typical and maximum set-up heights and identify the pattern of storms responsible for extreme wave set-up, (iii) detect the wave set-up from standard water level observations and modelling efforts, (iv) establish the contribution of the three major components to the increasing trends in the extreme water level on the eastern coast of the Baltic Sea.

As waves often approach the Baltic Sea shores under a relatively large angle, a method is developed to analytically evaluate the height and direction of breaking waves in such occasions. This method is used to estimate the typical and maximum wave set-up heights in ideal conditions in the vicinity of the City of Tallinn. The properties of approaching waves are evaluated based on a high-resolution triple-nested wave model WAM, forced with high-quality wind data obtained at Kalbådagrund in 1981–2014.

About 50% of coastal segments in this relatively low-lying urbanised area may potentially be endangered by wave set-up. Single coastal segments are sensitive with respect to high waves approaching from various directions and therefore experience high wave set-up during different storms. The maximum set-up heights may have reached 0.8 m on the eastern coast of the Viimsi Peninsula and 0.65 m in Pirta Beach and on the coast of Tiskre.

The all-time highest waves in the study area were generated by 6 different storms which all occurred after 1995. In contrast, over 50 storms were responsible for the highest set-up events in 1981–2012 whereas many of these storms occurred in the 1980s. Storms in 2012–2014 overrode many previous maxima of set-up heights. This pattern of changes suggests the presence of a complicated pattern of the rotation of wind direction during selected strong storms and an increase in the intensity of eastern storms since 2012.

An indirect method of distinguishing the influence of wave set-up from the measured water level is developed. It relies on the comparison of projections of extreme water levels and their return periods based on block maxima of the historical observations of water level at harbours and the offshore water level extracted from the ocean circulation model. The contribution of wave set-up is evident from the appearance of an ensemble of such projections for longer return periods. It is shown that in some locations of the Estonian coast, most notably in Ristna, the observed water levels apparently have substantial contribution from wave set-up. The extensive mismatch of projections based on measurements and

hindcasts in some locations signals that numerically simulated water levels may completely overlook essential components of coastal flooding such as wave set-up.

The interplay of the directional distribution of strong winds and the geometry of the northern coast of Estonia leads to complicated interrelations between high offshore water level and extensive set-up. The contribution of set-up may, theoretically, reach >50% of the offshore water level. The highest wave set-up, however, almost never occurs simultaneously with very high offshore water levels in this region. The largest contribution of set-up to the total water level is below 0.5 m in ideal conditions. The contribution of set-up to total water level maxima is frequently significant in coastal segments that are open to (north-)westerly storms. In these locations the total water level may occasionally exceed the all-time maximum offshore water level. The segments that are open to the east almost never experience high waves during very high offshore water levels.

The input of different mechanisms of the formation of offshore water levels into the increasing trends in the water level maxima is evaluated using the classic technique of linear trendlines that was applied to the results of the Rossby Centre Ocean (RCO) model. The input from the storm surges is separated from that of the water volume of the entire Baltic Sea using a simple averaging technique.

In 1961–2005 the annual maxima of the total water level increased, on average at a spatially different rate of 4–10 mm/yr in the eastern Baltic Sea. The described separation technique of the two components highlights the driver behind this increase. The water level in the eastern part of the Gulf of Finland and in the Gulf of Riga exhibits the fastest increase whereas the increase rate on the open Baltic Proper coast is the smallest.

The contribution of the water volume of the entire sea to this increase is more or less constant, about 4 mm/yr, all over the study area. Therefore, the impact of basically wind-driven events of large-scale inflow of the North Sea waters into the Baltic Sea has considerably and almost steadily increased since the 1970s. This indicates that either wind speed in selected storms has increased or the sequences of storms that force the North Sea water into the Baltic Sea have become longer.

The contribution of storm surges to the water level extremes varies remarkably along the shores of Estonia and northern Latvia. It is the lowest, often below 1 mm/yr, in some locations of the open segments of the shores of the Western Estonian archipelago. This feature signals that an increase in the wind speed in strong storms in this area is unlikely.

The contribution of storm surges to the water level extremes is the highest, up to 6 mm/yr in the eastern bayheads of the Gulf of Finland and Gulf of Riga. The revealed spatial pattern of this increase signals that the wind direction in a part of strong storms may have changed so that the fetch length for the marine wind in selected storms has become longer. This change is highlighted using the concept of air-flow that characterises to some extent both the wind direction and speed. The annual average direction of air flow at Kalbådagrund has changed from the south-west towards a more westerly direction in 1981–2014 at an 80% level of statistical significance.

Main conclusions proposed to defend

1. A method is developed to analytically evaluate the height and direction of breaking waves in the case when waves approach a homogeneous beach under a relatively large angle.
2. The contribution of wave set-up to the total water level may be up to 0.8 m in several locations of the shoreline in the vicinity of Tallinn in ideal conditions. This makes up to 50% of the maximum offshore water levels caused by other factors.
3. About 50% of coastal segments in the vicinity of Tallinn may experience high wave set-up. As the area has complicated coastal geometry, each coastal segment is endangered by wave set-up during a different storm. The pattern of reaching new maxima of wave set-up heights indicates a substantial change in the wind direction in selected storms and an increase in the intensity of easterly winds since 2012.
4. The highest wave set-up almost never occurs simultaneously with very high offshore water levels on the northern coast of Estonia. The maximum contribution of set-up to the total water level reaches up to 0.5 m. High offshore water levels are frequently accompanied by large set-up events in coastal segments open to the west or north-west. These two phenomena are often in antiphase in sections open to the east.
5. The ensemble approach used for building projections of extreme water levels reveals a relatively large contribution of local effects (eventually wave set-up) to the formation of very high water levels in several locations on the Estonian coast.
6. The increase rate of modelled extreme water levels varies in the range of 4–10 mm/yr along the Estonian coast. The increase is largest in the eastern Gulf of Riga and the Gulf of Finland. A gradual increase in the water volume extremes of the whole of the Baltic Sea contributes about 4 mm/yr to the increase in the extreme water levels along the entire coast of Estonia. The contribution of local storm surges is highly variable, from almost zero on the Baltic Proper coast of the Western Estonian archipelago up to 6 mm/yr in the eastern Gulf of Riga and the Gulf of Finland.
7. The separation of these two components of extreme water levels highlights the driver behind the increase in the annual offshore water level maxima in the eastern Baltic Sea. Wind speed in strong storms has not substantially increased in the northern Baltic Proper whereas the sequences of storms that force water into the Baltic Sea have become longer and wind directions in some storms have rotated. The annual average direction of air flow at Kalbådagrund has changed in 1981–2014 at an 80% level of statistical significance.

Recommendations for further work

The analysis performed first of all reveals that numerical estimates of the maxima of wave set-up heights are relatively sensitive with respect to the particular way of evaluating the impact of radiation stress and the transformation of wave properties in the nearshore. The magnitude of the related effects largely depends on the appearance of bathymetry. The impact of refraction can easily override the purely geometric effects of shoreline orientation changes and redirect substantial levels of wave energy into seemingly sheltered shore sections.

This feature calls for the necessity of using high-resolution information about wind properties (incl. wind directions) and bathymetry together with advanced methods for the evaluation of the propagation and impact of radiation stress in the nearshore in operational and hindcast models of coastal flooding. A natural extension of the research presented in this thesis would be the implementation of techniques that could resolve the changes in the propagation direction of breaking waves. It is likely that these techniques will provide a much higher certainty of the estimates of wave set-up heights.

Recent research has shown that typical probability distributions of different constituents of extreme water levels may be fundamentally different (Soomere et al., 2015b). As discussed above, the distribution of observed and numerically simulated water levels is usually close to a Gaussian one. The component that reflects the local storm surge may have an exponential distribution. The probabilities of the occurrence of different single wave heights are at best approximated either by a Rayleigh or a Tayfun distribution. The probability distribution of run-up heights usually follows the relevant distribution for incident wave heights or can be approximated by a Rayleigh distribution. The empirical probabilities of average or significant wave heights usually resemble either a Rayleigh or a Weibull distribution.

However, nothing is known about the appearance and properties of empirical distributions of wave-driven local water level set-up. Research in this direction may also shed new light on the distribution of wind speeds from a particular unfavourable direction. While the overall distribution of all wind speeds commonly matches well a Rayleigh distribution in north-western Europe, similar distributions for single directions often deviate from the Rayleigh one.

Further development of the ensemble approach technique has a variety of important implications and applications. This approach has a potential to lead to reasonable projections of extreme water levels in areas where the measured or observed signal contains an unknown share of local effects.

It is necessary and straightforward to extend the presented results about the specific role of the contributions of the two major mechanisms that drive the water level to the entire Baltic Sea shoreline. In particular, the described difference in the “balancing” lengths of the averaging interval suggests that water level maxima in the Gulf of Riga may have another component, namely, the water volume of this gulf that may be increased for a few days by specific sequences of storms. Strong winds from westerly directions may push the water into the Gulf and therefore

support the long-term elevated water level there similarly to the impact of sequences of storms that push water into the Baltic Sea via the Danish straits. The described process cannot appear in the Gulf of Finland and northern part of the Baltic Proper but may add an extremely dangerous feature to the formation of extreme water levels in large low-lying cities such as Riga and Pärnu.

Bibliography

- Alari V., Kõuts T. 2012. Simulating wave-surge interaction in a non-tidal bay during cyclone Gudrun in January 2005. In: *Proceedings of the IEEE/OES Baltic 2012 International Symposium "Ocean: Past, Present and Future. Climate Change Research, Ocean Observation & Advanced Technologies for Regional Sustainability," May 8–11, Klaipėda, Lithuania.* IEEE Conference Publications.
- Alari V., Raudsepp U. 2010. Depth induced breaking of wind generated surface gravity waves in Estonian coastal waters. *Boreal Environment Research*, 15, 295–300.
- Andrejev O., Sokolov A., Soomere T., Värvi R., Viikmäe B. 2010. The use of high-resolution bathymetry for circulation modelling in the Gulf of Finland. *Estonian Journal of Engineering*, 16, 187–210.
- Apotsos A., Raubenheimer B., Elgar S., Guza R.T. 2008. Wave-driven setup and alongshore flows observed onshore of a submarine canyon. *Journal of Geophysical Research – Oceans*, 113, C07025.
- Apotsos A., Raubenheimer B., Elgar S., Guza R.T., Smith J.A. 2007. Effect of wave rollers and bottom stress on wave setup. *Journal of Geophysical Research – Oceans*, 112, C02003.
- Araújo M.B., New M. 2006. Ensemble forecasting of species distributions. *Trends in Ecology & Evolution*, 22, 42–47.
- Ardhuin F., O'Reilly W.C., Herbers T.H.C., Jessen P.F. 2003. Swell transformation across the continental shelf. Part I: attenuation and directional broadening. *Journal of Physical Oceanography*, 33, 1921–1939.
- Arns A., Wahl T., Haigh I.D., Jensen J. 2015. Determining return water levels at ungauged coastal sites: a case study for northern Germany. *Ocean Dynamics*, 65, 539–554.
- Arns A., Wahl T., Haigh I.D., Jensen J., Pattiaratchi C. 2013. Estimating extreme water level probabilities: a comparison of the direct methods and recommendations for best practise. *Coastal Engineering*, 81, 51–66.
- Averkiev A.S., Klevanny K.A. 2010. A case study of the impact of cyclonic trajectories on sea-level extremes in the Gulf of Finland. *Continental Shelf Research*, 30, 707–714.
- Barbosa S.M. 2008. Quantile trends in Baltic Sea level. *Geophysical Research Letters*, 35 (Art. No, L22704).
- Bastos A., Trigo R.M., Barbosa S.M. 2013. Discrete wavelet analysis of the influence of the North Atlantic oscillation on Baltic Sea level. *Tellus A*, 65, Art. No. 20077.

- Batstone C., Lawless M., Tawn J., Horsburgh K., Blackman D., McMillan A., Worth D., Laeger S., Hunt, T. 2013. A UK best-practice approach for extreme sea-level analysis along complex topographic coastlines. *Ocean Engineering*, 71, 28–39.
- Bechle A.J., Kristovich D.A.R., Wu C.H. 2015. Meteotsunami occurrences and causes in Lake Michigan. *Journal of Geophysical Research – Oceans*, 120, 8422–8438.
- Bertin X., Fortunato A.B., Oliveira A. 2009. A modeling-based analysis of processes driving wave-dominated inlets. *Continental Shelf Research*, 29, 819–834.
- Bosley K.T., Hess K.W. 2001. Comparison of statistical and model-based hindcasts of subtidal water levels in Chesapeake Bay. *Journal of Geophysical Research – Oceans*, 106(C8), 16869–16885.
- Brakenridge G.R., Syvitski J.P.M., Overeem I., Higgins S.A., Kettner A.J., Stewart-Moore J.A., Westerhoff R. 2013. Global mapping of storm surges and the assessment of coastal vulnerability. *Natural Hazards*, 66, 1295–1312.
- Broman B., Hammarklint T., Rannat K., Soomere T., Valdmann A. 2006. Trends and extremes of wave fields in the north-eastern part of the Baltic Proper. *Oceanologia*, 48, 165–184.
- Caliskan H., Valle-Levinson A. 2008. Wind-wave transformations in an elongated bay. *Continental Shelf Research*, 28, 1702–1710.
- Cariot J.M., Suanez S. 2009. Method of mapping flood hazard in low-lying coasts. *Houille Blanche*, 2, 52–58.
- Cazenave A., Dieng B., Meyssignac B., von Schuckmann K., Decharme B., Berthier E. 2014. The rate of sea-level rise. *Nature Climate Change*, 4, 358–361.
- Charles E., Idier D., Delecluse P., Deque M., Le Cozannet G. 2012a. Climate change impact on waves in the Bay of Biscay, France. *Ocean Dynamics*, 62, 831–848.
- Charles E., Idier D., Thiebot J., Le Cozannet G., Pedreros R., Arduin F., Planton S. 2012b. Present wave climate in the Bay of Biscay: spatiotemporal variability and trends from 1958 to 2001. *Journal of Climate*, 25, 2020–2039.
- Cheng X.T., Evans E.P., Wu H.Y., Thorne C.R., Han S., Simm J.D., Hall J.W. 2013. A framework for long-term scenario analysis in the Taihu Basin, China. *Journal of Flood Risk Management*, 6, 3–13.
- Cheung K.K.W. 2001. A review of ensemble forecasting techniques with a focus on tropical cyclone forecasting. *Meteorological Applications*, 8, 315–332.
- Christiansen B., Schmith T., Thejll P. 2010. A surrogate ensemble study of sea level reconstructions. *Journal of Climate*, 23, 4306–4326.
- Climatological Ice Atlas for the Baltic Sea, Kattegat, Skagerrak and Lake Vänern (1963–1979)*. 1982. Swedish Meteorological and Hydrological Institute,

- Norrköping, Sweden, and Institute of Marine Research, Helsinki, Finland, Norrköping.
- Coastal Engineering Manual*. 2002. U. S. Army Corps of Engineers (US-ACE), Manual EM 1110-2-1100.
- Coles S. 2001. *An Introduction to Statistical Modeling of Extreme Values*. Springer, London.
- Dailidienė I., Davulienė L., Tilickis B., Stankevičius A., Myrberg K. 2006. Sea level variability at the Lithuanian coast of the Baltic Sea. *Boreal Environmental Research*, 11, 109–121.
- Dailidienė I., Tilickis B., Stankevičius A. 2004. General peculiarities of long-term fluctuations of the Baltic Sea and the Kurshiu Marios lagoon water level in the region of Lithuania. *Environmental Research, Engineering and Management. Technologija*, 4, 3–10.
- Darwin R.F., Tol R.S.J. 2001. Estimates of the economic effects of sea level rise. *Environmental and Resource Economics*, 19, 113–129.
- Dawson R.J., Speight L., Hall J.W., Djordjevic S., Savic D., Leandro J. 2008. Attribution of flood risk in urban areas. *Journal of Hydroinformatics*, 10, 275–288.
- Dean R.G., Bender C.J. 2006. Static wave set-up with emphasis on damping effects by vegetation and bottom friction. *Coastal Engineering*, 53, 149–165.
- Dean R.G., Dalrymple R.A. 1991. *Water Wave Mechanics for Engineers and Scientists*. World Scientific.
- Dean R.G., Dalrymple R.A. 2002. *Coastal Processes with Engineering Applications*. Cambridge University Press, Cambridge.
- Donner R.V., Ehrcke R., Barbosa S.M., Wagner J., Donges J.F., Kurths J. 2012. Spatial patterns of linear and nonparametric long-term trends in Baltic sea-level variability. *Nonlinear Processes in Geophysics*, 19, 95–111.
- Dube S.K., Jain I., Rao A.D., Murty T.S. 2009. Storm surge modelling for the Bay of Bengal and Arabian Sea. *Natural Hazards*, 51, 3–27.
- Dukhovskoy D.S., Morey S.L. 2011. Simulation of the Hurricane Dennis storm surge and considerations for vertical resolution. *Natural Hazards*, 58, 511–540.
- Eelsalu M., Soomere T., Pindsoo K., Lagemaa P. 2013. Ensemble approach for projections of return periods of extreme water levels in Estonian waters. *Continental Shelf Research*, 91, 201–210.
- Ekman M., Mäkinen J. 1996. Mean sea surface topography in the Baltic Sea and its transition area to the North Sea: A geodetic solution and comparisons with oceanographic models. *Journal of Geophysical Research – Oceans*, 101, 11993–11999.
- Fawcett L., Walshaw D. 2016. Sea-surge and wind speed extremes: optimal estimation strategies for planners and engineers. *Stochastic Environmental Research and Risk Assessment*, 30, 463–480.

- Feistel R., Nausch G., Wasmund N. (eds.). 2008. *State and evolution of the Baltic Sea 1952–2005*. Wiley, Hoboken, New Jersey.
- Feng X., Tsimplis M.N., Quartly G.D., Yelland M.J. 2014. Wave height analysis from 10 years of observations in the Norwegian Sea. *Continental Shelf Research*, 72, 47–56.
- Filipot J.-F., Cheung K.F. 2012. Spectral wave modeling in fringing reef environments. *Coastal Engineering*, 67, 67–79.
- Forristall G.Z. 1978. 2014. Statistical distribution of wave heights in a storm. *Journal of Geophysical Research – Oceans*, 83, 2353–2358.
- Funkquist L. 2001. HIROMB, an operational eddy-resolving model for the Baltic Sea. *Bulletin of the Marine Institute in Gdańsk*, 28, 7–16.
- Gästgifvars M., Müller-Navarra S., Funkquist L., Huess V. 2008. Performance of operational systems with respect to water level forecasts in the Gulf of Finland. *Ocean Dynamics*, 58, 139–153.
- Geist E.L., ten Brink U.S., Gove M. 2014. A framework for the probabilistic analysis of meteotsunamis. *Natural Hazards*, 74, 123–142.
- Gönnert G. 2003. Storm tides and wind surge in the German Bight: character of height, frequency, duration, rise and fall in the 20th century [Sturmfluten und Windstau in der Deutschen Bucht Charakter, Veränderungen und Maximalwerte im 20. Jahrhundert]. *Küste*, 67, 185–366.
- Guannel G., Tissot P., Cox D.T., Michaud P. 2001. Local and remote forcing of subtidal water level and setup fluctuations in coastal and estuarine environments. In: *Coastal Dynamics 2001: 4th Conference on Coastal Dynamics; Lund, Sweden, 11–15 June 2001*. ASCE, 443–452.
- Guza R.T., Thornton E.B. 1981. Wave set-up on a natural beach. *Journal of Geophysical Research – Oceans*, 86, 4133–4137.
- Haigh I. D., Nicholls R., Wells N. 2010a. A comparison of the main methods for estimating probabilities of extreme still water levels. *Coastal Engineering*, 57, 838–849.
- Haigh I., Nicholls R., Wells N., 2010b. Assessing changes in extreme sea levels: application to the English Channel, 1900–2006. *Continental Shelf Research*, 30, 1042–1055.
- Haigh I.D., Wijeratne E.M.S., MacPherson L.R., Pattiaratchi C.B., Mason M.S., Crompton R.P., George S. 2014. Estimating present day extreme water level exceedance probabilities around the coastline of Australia: tides, extra-tropical storm surges and mean sea level. *Climate Dynamics*, 42, 121–138.
- Hall J.W., Dawson R.J., Barr S.L., Batty M., Bristow A.L., Carney S., Dagoumas A., Ford A.C., Harpham C., Tight M.R., Walsh C.L., Watters H., Zanni A.M. 2010. City-Scale integrated assessment of climate impacts, adaptation, and mitigation. In: Bose R.K. (ed.), *Energy Efficient Cities: Assessment Tools and Benchmarking Practices*, The World Bank, 63–83.

- Hallegatte S., Green C., Nicholls R.J., Corfee-Morlot J. 2013. Future flood losses in major coastal cities. *Nature Climate Change*, 3, 802–806.
- Harff J., Meyer M. 2011. Coastlines of the Baltic Sea – zones of competition between geological processes and a changing climate: examples from the Southern Baltic. In: Harff J., Björck S., Hoth P. (eds.), *The Baltic Sea Basin*. Springer-Verlag, Berlin, Heidelberg, 149–164.
- Harper B., Hardy T., Mason L., Fryar R. 2009. Developments in storm tide modelling and risk assessment in the Australian region. *Natural Hazards*, 51, 225–238.
- Hawkes P.J., Gouldby B.R., Tawn J.A., Owen M.W. 2002. The joint probability of waves and water levels in coastal engineering design. *Journal of Hydraulic Research*, 40, 241–251.
- Heidarzadeh M., Bonneton P., Bonneton N., Tissier M. 2009. Field observations of wave-induced set-up on the french Aquitanian coast. In: *Proceedings of the 28th International Conference on Ocean, Offshore and Arctic Engineering (OMAE 2009)*, Honolulu, 31 May–5 June 2009, vol. 4. ASME, 233–241.
- Hoeke R.K., McInnes K.L., Kruger J.C., McNaught R.J., Hunter J.R., Smithers S.G. 2013. Widespread inundation of Pacific islands triggered by distant-source wind-waves. *Global and Planetary Change*, 108, 128–138.
- Höglund A., Meier H.E.M., Broman B., Kriezi E. 2009. *Validation and Correction of Regionalised ERA-40 Wind Fields Over the Baltic Sea using the Rossby Centre Atmosphere Model RCA3.0*. Rapport Oceanografi, No. 97, Swedish Meteorological and Hydrological Institute, Norrköping, Sweden.
- Howard T., Pardaens A.K., Bamber J.L., Ridley J., Spada G.L., Hurkmans R.T.W., Lowe J.A., Vaughan D. 2014. Sources of 21st century regional sea-level rise along the coast of northwest Europe. *Ocean Science*, 10, 473–483.
- Hsu T.-W., Hsu J.R.-C., Weng W.-K., Wang S.-K., Ou S.-H. 2006. Wave setup and setdown generated by obliquely incident waves. *Coastal Engineering*, 53, 865–877.
- Hünicke B. 2010. Contribution of regional climate drivers to future winter sea-level changes in the Baltic Sea estimated by statistical methods and simulations of climate models. *International Journal of Earth Sciences*, 99, 1721–1730.
- Hünicke B., Zorita E. 2008. Trends in the amplitude of Baltic Sea level annual cycle. *Tellus A*, 60, 154–164.
- Hünicke B., Zorita E., Soomere T., Madsen K. S., Johansson M., Suursaar, Ü. 2015. Recent change – sea level and wind waves. In: The BACC II Author Team, *Second Assessment of Climate Change for the Baltic Sea Basin, Regional Climate Studies*. Springer, 155–185.
- Irish J.L., Canizares R. 2009. Storm-wave flow through tidal inlets and its influence on bay flooding. *Journal of Waterway, Port, Coastal, and Ocean Engineering Ocean*, 135, 52–60.

- Jaagus J. 2009. Long-term changes in frequencies of wind directions on the western coast of Estonia. *Publications of Institute of Ecology, Tallinn University*, 11, 11–24 (in Estonian).
- Jaagus J., Kull A. 2011. Changes in surface wind directions in Estonia during 1966–2008 and their relationships with large-scale atmospheric circulation. *Estonian Journal of Earth Sciences*, 60, 220–231.
- Jaagus J., Suursaar Ü. 2013. Long-term storminess and sea level variations on the Estonian coast of the Baltic Sea in relation to large-scale atmospheric circulation. *Estonian Journal of Earth Sciences*, 62, 73–92.
- Jain I., Rao A.D., Jitendra V., Dube S.K. 2010a. Computation of expected total water levels along the east coast of India. *Journal of Coastal Research*, 26, 681–687.
- Jain I., Rao A.D., Ramesh K.J. 2010b. Vulnerability assessment at village level due to tides, surges and wave set-up. *Marine Geodesy*, 33, 245–260.
- Johansson M. 2014. Sea level changes on the Finnish coast and their relationship to atmospheric factors. *Finnish Meteorological Institute Contributions*, 109, 1–132 (PhD thesis, University of Helsinki).
- Johansson M., Boman H., Kahma K., Launiainen J. 2001. Trends in sea level variability in the Baltic Sea. *Boreal Environmental Research*, 6, 159–179.
- Johansson M., Kahma K., Pellikka H. 2011. Sea level scenarios and extreme events on the Finnish coast. In: Puska E.K., Suolanen V. (eds.), *SAFIR2010, The Finnish Research Programme on Nuclear Power Plant Safety 2007–2010*. VTT Research Notes 2571, 570–578.
- Johansson M., Pellikka H., Kahma K., Ruosteenoja K. 2014. Global sea level rise scenarios adapted to the Finnish coast. *Journal of Marine Systems*, 129, 35–46.
- Kangro G. 1962. *Kõrgem algebra (Higher algebra)*. Eesti Riiklik Kirjastus, Tallinn (in Estonian).
- Keevallik S., Soomere T. 2010. Towards quantifying variations in wind parameters across the Gulf of Finland. *Estonian Journal of Earth Sciences*, 59, 288–297.
- Keevallik, T., Soomere T. 2014. Regime shifts in the surface-level average air flow over the Gulf of Finland during 1981–2010. *Proceedings of the Estonian Academy of Sciences*, 63, 428–437.
- Kleine E. 1994. *Das operationelle Modell des BSH für Nordsee und Ostsee. Konzeption und Übersicht*. Bundesamt für Seeschifffahrt und Hydrographie.
- Komen, G.J., Cavaleri, L., Donelan, M., Hasselmann, K., Hasselmann, S., Janssen, P.A.E.M. 1994. *Dynamics and Modelling of Ocean Waves*. Cambridge University Press, Cambridge.
- Kulikov E.A., Medvedev I.P. 2013. Variability of the Baltic Sea level and floods in the Gulf of Finland. *Oceanology*, 53, 145–151.

- Laanearu J., Koppel T., Soomere T., Davies P.A. 2007. Joint influence of river stream, water level and wind waves on the height of sand bar in a river mouth. *Nordic Hydrology*, 38, 287–302.
- Lagemaa P., Elken J., Kõuts T. 2011. Operational sea level forecasting in Estonia. *Estonian Journal of Engineering*, 17, 301–331.
- Lagemaa P., Raudsepp U., Kõuts T., Allik A., Elken J. 2013. *Tallinna linna Haabersti, Põhja-Tallinna ja Kakumäe linnaosade meretasemete stsenaariumite modelleerimine (Modelling of water level scenarios for City of Tallinn)*. Research report, Marine Systems Institute at Tallinn University of Technology, Tallinn (in Estonian).
- Larson M., Hoan L.X., Hanson H. 2010. Direct formula to compute wave height and angle at incipient breaking. *Journal of Waterway, Port, Coastal, and Ocean Engineering*, 136, 119–122.
- Launiainen J., Laurila T. 1984. Marine wind characteristics in the northern Baltic Sea. *Finnish Marine Research*, 250, 52–86.
- Lazarenko N.N. 1986. Variations of mean level and water volume of the Baltic Sea. In: *Proceedings of the Water Balance of the Baltic Sea Environment*, 16, 64–80.
- Lehmann A., Post P. 2015. Variability of atmospheric circulation patterns associated with large volume changes of the Baltic Sea. *Advances in Science and Research*, 12, 219–225.
- Lehmann A., Getzlaff K., Harlaß J. 2011. Detailed assessment of climate variability in the Baltic Sea area for the period 1958 to 2009. *Climate Research*, 46, 185–196.
- Lehmann A., Hoefflich K., Post P., Myrberg K. 2017. Pathways of deep cyclones associated with large volume changes (LVCs) and major Baltic inflows (MBIs). *Journal of Marine Systems*, 167, 11–18.
- Lehmann A., Myrberg K., Höflich K. 2012. A statistical approach to coastal upwelling in the Baltic Sea based on the analysis of satellite data for 1990–2009. *Oceanologia*, 54, 369–393.
- Leppäranta M., Myrberg K. 2009. *Physical Oceanography of the Baltic Sea*. Springer, Berlin.
- Longuet-Higgins M.S. 1952. On the statistical distribution of the heights of sea waves. *Journal of Marine Research*, 11, 1245–1266.
- Longuet-Higgins M.S., Stewart R.W. 1964. Radiation stresses in water waves: a physical discussion with applications. *Deep-Sea Research*, 11, 529–562.
- Lopez-Ruiz A., Ortega-Sanchez M., Baquerizo A., Losada M.A. 2014. A note on alongshore sediment transport on weakly curvilinear coasts and its implications. *Coastal Engineering*, 88, 143–153.

- Lopez-Ruiz A., Solari S., Ortega-Sanchez M., Losada M. 2015. A simple approximation for wave refraction – application to the assessment of the nearshore wave directionality. *Ocean Modelling*, 96, 324–333.
- Losada I.J., Reguero B.G., Méndez F.J., Castanedo S., Abascal A.J., Mínguez R. 2013. Long-term changes in sea-level components in Latin America and the Caribbean. *Global and Planetary Change*, 104, 34–50.
- Lowe J.A., Gregory J.M., Flather R.A. 2001. Changes in the occurrence of storm surges around the United Kingdom under a future climate scenario using a dynamic storm surge model driven by the Hadley Centre climate models. *Climate Dynamics*, 18, 179–188.
- Masina M., Lamberti A. 2013. A nonstationary analysis for the Northern Adriatic extreme sea levels. *Journal of Geophysical Research – Oceans*, 118, 3999–4016.
- Masina M., Lamberti A., Archetti, R. 2015. Coastal flooding: a copula based approach for estimating the joint probability of water levels and waves. *Coastal Engineering*, 97, 37–52.
- Massel S.R. 1996. On the largest wave height in water of constant depth. *Ocean Engineering*, 23, 553–573.
- McDougal W.G., Hudspeth R.T. 1983. Wave setup/setdown and longshore current on non-planar beaches. *Coastal Engineering*, 7, 103–117.
- McInnes K.L., O’Grady J.G., Hubbert G.D. 2009. Modelling sea level extremes from storm surges and wave set-up for climate change assessments in southeastern Australia. *Journal of Coastal Research*, Special Issue, 56, 1005–1009.
- Medvedev I.P. 2014. Seasonal fluctuations of the Baltic Sea level. *Russian Meteorology and Hydrology*, 39, 814–822.
- Meier H.E.M. 2001. On the parameterization of mixing in three-dimensional Baltic Sea models. *Journal of Geophysical Research – Oceans*, 106, C30997–C31016.
- Meier H.E.M., Höglund A. 2013. Studying the Baltic Sea circulation with Eulerian tracers. In: Soomere T., Quak E. (eds.), *Preventive Methods for Coastal Protection*. Springer, Cham Heidelberg, 101–130.
- Meier H.E.M., Broman B., Kjellström E. 2004. Simulated sea level in past and future climates of the Baltic Sea. *Climate Research*, 27, 59–75.
- Meier H.E.M., Döscher R., Faxén T. 2003. A multiprocessor coupled ice-ocean model for the Baltic Sea: application to salt inflow. *Journal of Geophysical Research – Oceans*, 108, 32–73.
- Mel R., Sterl A., Lionello P. 2013. High resolution climate projection of storm surge at the Venetian coast. *Natural Hazards and Earth System Science*, 13, 1135–1142.
- Melet A., Almar R., Meyssignac B. 2016. What dominates sea level at the coast: a case study for the Gulf of Guinea. *Ocean Dynamics*, 66, 623–636.

- Meyer V., Becker N., Markantonis V., Schwarze R., van den Bergh J.C.J.M., Bouwer L.M., Bubeck P., Ciavola P., Genovese E., Green C., Hallegatte S., Kreibich H., Lequeux Q., Logar I., Papyrakis E., Pfurtscheller C., Poussin J., Przyłuski V., Thieken A.H., Viavattene C. 2013. Review article: assessing the costs of natural hazards – state of the art and knowledge gaps. *Natural Hazards and Earth System Science*, 13, 1351–1373.
- Mietus M. 1998. (ed.). *The climate of the Baltic Sea Basin. Marine Meteorology and Related Oceanographic Activities*. Rep. No. 41, World Meteorological Organization, Geneva.
- Moghimi S., Klingbeil K., Gräwe U., Burchard H. 2013. A direct comparison of a depth-dependent Radiation stress formulation and a Vortex force formulation within a three-dimensional coastal ocean model. *Ocean Modelling*, 70, 132–144.
- Mudersbach C., Jensen J. 2009. Extreme value statistical analysis of historical, observed and modeled water levels on the German Baltic Sea coast [Extremwertstatistische Analyse von Historischen, Beobachteten und Modellierten Wasserständen an der Deutschen Ostseeküste]. *Küste*, 75, 131–161 (in German).
- Mudersbach C., Wahl T., Haigh I.D., Jensen J. 2013. Trends in high sea levels of German North Sea gauges compared to regional mean sea level changes. *Continental Shelf Research*, 65, 111–120.
- Muraleedharan G., Rao A.D., Kurup P.G., Nair N.U., Sinha M. 2007. Modified Weibull distribution for maximum and significant wave height simulation and prediction. *Coastal Engineering*, 54, 630–638.
- Myrberg K., Ryabchenko V., Isaev A., Vankevich R., Andrejev O., Bendtsen J., Erichsen A., Funkquist L., Inkala A., Neelov I., et al. 2010. Validation of three-dimensional hydrodynamic models in the Gulf of Finland based on a statistical analysis of a six-model ensemble. *Boreal Environmental Research*, 15, 453–479.
- Nayak S., Bhaskaran P., Venkatesan R. 2012. Near-shore wave induced set-up along Kalpakkam coast during an extreme cyclone event in the Bay of Bengal. *Ocean Engineering*, 55, 52–61.
- Nelson R.C. 1994. Depth limited design wave heights in very flat regions. *Coastal Engineering*, 23, 43–59.
- Nikolkina I., Soomere T., Räämet A. 2014. Multidecadal ensemble hindcast of wave fields in the Baltic Sea. In: *The 6th IEEE/OES Baltic Symposium Measuring and Modeling of Multi-Scale Interactions in the Marine Environment, May 26–29, Tallinn Estonia*. IEEE Conference Publications.
- O’Grady J.G., McInnes K.L. 2010. Wind waves and their relationship to storm surges in northeastern Bass Strait, *Australian Meteorological and Oceanographic Journal*, 60, 265–275.

- O'Grady J.G., McInnes K.L., Hoeke R.K. 2015. Forecasting maximum wave setup hazards around Australia. In: *Coasts & Ports Conference 2015, 15–18 September 2015, Pullman Hotel, Auckland*. Engineers Australia and IPENZ, Auckland, 636–641.
- Olbert A.I., Nash S., Cunnane C., Hartnett M. 2013. Tide–surge interactions and their effects on total sea levels in Irish coastal waters. *Ocean Dynamics*, 63, 599–614.
- Orimolade A.P., Haver S., Gudmestad O.T. 2016. Estimation of extreme significant wave heights and the associated uncertainties: a case study using NORA10 hindcast data for the Barents Sea. *Marine Structures*, 49, 1–17.
- Pattiaratchi C., Wijeratne E.M.S. 2014. Observations of meteorological tsunamis along the south-west Australian coast. *Natural Hazards*, 74, 281–303.
- Pellikka H., Rauhala J., Kahma K.K., Stipa T., Boman H., Kangas A. 2014. Recent observations of meteotsunamis on the Finnish coast. *Natural Hazards*, 74, 197–215.
- Percival D.B., Mofjeld H.O. 1997. Analysis of subtidal coastal sea level fluctuations using wavelets. *Journal of American Statistical Association*, 92, 868–880.
- Pettersson H., Boman H. 2002. *High Waves and Sea Level During the November Storm*. Annual report 2001, Finnish Institute of Marine Research, Helsinki.
- Pettersson H., Kahma K.K., Tuomi L. 2010. Wave directions in a narrow bay. *Journal of Physical Oceanography*, 40, 155–169.
- Pettersson H., Lindow H., Brüning T. 2013. Wave climate in the Baltic Sea 2012. *HELCOM Baltic Sea Environment Fact Sheets 2012*, <http://helcom.fi/baltic-sea-trends/environment-fact-sheets/hydrography/wave-climate-in-the-baltic-sea/>.
- Pindsoo K., Soomere T., 2015. Contribution of wave set-up into the total water level in the Tallinn area. *Proceedings of the Estonian Academy of Sciences*, 64(3S), 338–348.
- Post P., Kõuts T. 2014. Characteristics of cyclones causing extreme sea levels in the northern Baltic Sea. *Oceanologia*, 56, 241–258.
- Power H.E., Hughes M.G., Aagaard T., Baldock T.E. 2010. Nearshore wave height variation in unsaturated surf. *Journal of Geophysical Research – Oceans*, 115, C08030.
- Pugh D., Vassie J. 1978. Extreme sea-levels from tide and surge probability. In: *Proceedings of the 16th Coastal Engineering Conference (Hamburg), vol. 1*. ASCE, New York, 911–930.
- Pugh D., Vassie J. 1980. Applications of the joint probability method for extreme sea-level computations. *Proceedings of Institution of Civil Engineers*, 69, 959–975.

- Purvis M.J., Bates P.D., Hayes C.M. 2008. A probabilistic methodology to estimate future coastal flood risk due to sea level rise. *Coastal Engineering*, 55, 1062–1073.
- Pycroft J., Abrell J., Ciscar J.C. 2016. The global impacts of extreme sea-level rise: a comprehensive economic assessment. *Environmental and Resource Economics*, 64, 225–253.
- Räämet A., Soomere T., Zaitseva-Pärnaste I. 2010. Variations in extreme wave heights and wave directions in the north-eastern Baltic Sea. *Proceedings of the Estonian Academy of Sciences*, 59, 182–192.
- Räämet A., Suursaar Ü., Kullas T., Soomere T. 2009. Reconsidering uncertainties of wave conditions in the coastal areas of the northern Baltic Sea. *Journal of Coastal Research*, Special Issue, 56, 257–261.
- Raubenheimer B., Guza R.T., Elgar S. 1996. Wave transformation across the inner surf zone. *Journal of Geophysical Research – Oceans*, 101, 25589–25597.
- Raubenheimer B., Guza R.T., Elgar S. 2001. Field observations of set-down and set-up. *Journal of Geophysical Research – Oceans*, 106, 4629–4638.
- Raudsepp U., Toompuu A., Kõuts T. 1999. A stochastic model for the sea level in the Estonian coastal area. *Journal of Marine Systems*, 22, 69–87.
- Ribeiro A., Barbosa S.M., Scotto M.G., Donner R.V. 2014. Changes in extreme sea-levels in the Baltic Sea. *Tellus A*, 66, Art. No. 20921.
- Richter A., Groh A., Dietrich R. 2012. Geodetic observation of sea-level change and crustal deformation in the Baltic Sea region. *Physics and Chemistry of the Earth*, 53–54, 43–53.
- Roland A., Cucco A., Ferrarin C., Hsu T.-W., Liao J.-M., Ou S.-H., Umgiesser G., Zanke U. 2009. On the development and verification of a 2-D coupled wave-current model on unstructured meshes. *Journal of Marine Systems*, 78, S244–S254.
- Rueda A., Camus P., Mendez F.J., Tomas A., Luceno A. 2016a. An extreme value model for maximum wave heights based on weather types. *Journal of Geophysical Research – Oceans*, 121, 1262–1273.
- Rueda A., Camus P., Tomas A., Vitousek S., Mendez F.J. 2016b. A multivariate extreme wave and storm surge climate emulator based on weather patterns. *Ocean Modelling*, 104, 242–251.
- Rutgersson A., Jaagus J., Schenk F., Stendel M. 2014. Observed changes and variability of atmospheric parameters in the Baltic Sea region during the last 200 years. *Climate Research*, 61, 177–190.
- Samuelsson P., Jones C.G., Willén U., Ullerstig A., Gollvik S., Hansson U., Jansson C., Kjellström E., Nikulin G., Wyser, K. 2011. The Rossby Centre Regional Climate Model RCA3: Model description and performance. *Tellus A*, 63, 4–23.

- Särkkä, J., Kahma, K.K., Kämäräinen, M., Johansson, M.M., Saku, S. 2017. Simulated extreme sea levels at Helsinki. *Boreal Environment Research*, 22, 1797–2469.
- Schmager G., Fröhle P., Schrader D., Weisse R., Müller-Navarra S. 2008. Sea state, tides. In: Feistel R., Nausch G., Wasmund N. (eds.), *State and Evolution of the Baltic Sea 1952–2005*. Wiley, Hoboken, New Jersey, 143–198.
- Scotto M.G., Barbosa S.M., Alonso A.M. 2009. Model-based clustering of Baltic sea-level. *Applied Ocean Research*, 31, 4–11.
- Seifert T., Tauber F., Kayser B. 2001. A high resolution spherical grid topography of the Baltic Sea, 2nd Ed., Baltic Sea Science Congress, Stockholm 25–29 November 2001. Poster #147, available at: www.io-warnemuende.de/iowtopo.
- Serafin K.A., Ruggiero P. 2014. Simulating extreme total water levels using a time-dependent, extreme value approach. *Journal of Geophysical Research – Oceans*, 119, 6305–6329.
- Shi F., Kirby J.T. 2008. Discussion of “Wave setup and setdown generated by obliquely incident waves” by T.-W. Hsu et al. *Coastal Engineering*, 53, 865–877, 2006. *Coastal Engineering*, 55, 1247–1249.
- Socquet-Juglard H., Dysthe K., Trulsen K., Krogstad H.E., Liu J.D. 2005. Probability distributions of surface gravity waves during spectral changes. *Journal of Fluid Mechanics*, 542, 195–216.
- Sooäär J., Jaagus J. 2007. Long-term variability and changes in the sea ice regime in the Baltic Sea near the Estonian coast. *Proceeding of the Estonian Academy of Sciences, Engineering*, 13, 189–200.
- Soomere T. 2001. Extreme wind speeds and spatially uniform wind events in the Baltic Proper. *Proceedings of the Estonian Academy of Sciences, Engineering*, 7, 195–211.
- Soomere T. 2005. Wind wave statistics in Tallinn Bay. *Boreal Environment Research*, 10, 103–118.
- Soomere T., Eelsalu M, 2014. On the wave energy potential along the eastern Baltic Sea coast. *Renewable Energy*, 71, 221–233.
- Soomere T., Keevallik S. 2003. Directional and extreme wind properties in the Gulf of Finland. *Proceedings of the Estonian Academy of Sciences, Engineering*, 9, 73–90.
- Soomere T., Pindsoo K. 2016. Spatial variability in the trends in extreme storm surges and weekly-scale high water levels in the eastern Baltic Sea. *Continental Shelf Research*, 115, 53–64.
- Soomere T., Räämet A. 2011. Spatial patterns of the wave climate in the Baltic Proper and the Gulf of Finland. *Oceanologia*, 53, 335–371.
- Soomere T., Viška M. 2014. Simulated wave-driven sediment transport along the eastern coast of the Baltic Sea. *Journal of Marine Systems*, 129, 96–105.

- Soomere T., Behrens A., Tuomi L., Nielsen J.W. 2008a. Wave conditions in the Baltic Proper and in the Gulf of Finland during windstorm Gudrun. *Natural Hazards and Earth System Science*, 8, 37–46.
- Soomere T., Bishop S.R., Viška M., Räämet A. 2015a. An abrupt change in winds that may radically affect the coasts and deep sections of the Baltic Sea. *Climate Research*, 62, 163–171.
- Soomere T., Döös K., Lehmann A., Meier H.E.M., Murawski J., Myrberg K., Stanev E. 2014. The potential of current- and wind-driven transport for environmental management of the Baltic Sea. *Ambio*, 43, 94–104.
- Soomere T., Eelsalu M., Kurkin A., Rybin A. 2015b. Separation of the Baltic Sea water level into daily and multi-weekly components. *Continental Shelf Research*, 103, 23–32.
- Soomere T., Myrberg K., Leppäranta M., Nekrasov A. 2008b. The progress in knowledge of physical oceanography of the Gulf of Finland: a review for 1997–2007. *Oceanologia*, 50, 287–362.
- Soomere T., Pindsoo K., Bishop S.R., Käär A., Valdmann A. 2013. Mapping wave set-up near a complex geometric urban coastline. *Natural Hazards and Earth System Sciences*, 13, 3049–3061.
- Soomere T., Zaitseva-Pärnaste I., Räämet A., Kurennoy D. 2010. Spatio-temporal variations of wave fields in the Gulf of Finland. *Fundamental and Applied Hydrophysics*, 4(10), 90–101 (in Russian).
- Starr V.P. 1947. A momentum integral for surface waves in deep water. *Journal of Marine Research*, 6, 126–135.
- Sterl A., van den Brink H., de Vries H., Haarsma R., van Meijgaard E. 2009. An ensemble study of extreme storm surge related water levels in the North Sea in a changing climate. *Ocean Science*, 5, 369–378.
- Stigebrandt A., Gustafsson B. 2003. Response of the Baltic Sea to climate change – theory and observations. *Journal of Sea Research*, 49, 243–256.
- Stockdon H.F., Holman R.A., Howd P.A., Sallenger A.H. 2006. Empirical parameterization of set-up, swash, and runup. *Coastal Engineering*, 53, 573–588.
- Stramska M. 2013. Temporal variability of the Baltic Sea level based on satellite observations. *Estuarine, Coastal and Shelf Science*, 133, 244–250.
- Stramska M., Chudziak N. 2013. Recent multiyear trends in the Baltic Sea level. *Oceanologia*, 55, 319–337.
- Stramska M., Kowalewska-Kalkowska H., Świrgoń M. 2013. Seasonal variability in the Baltic Sea level. *Oceanologia*, 55, 787–807.
- Sun J., Zuo J., Huang L., Cai X., Li Q. 2013. Characteristics and causes of typhoon and storm surge along coast of East China Sea. *Journal of Hohai University*, 41, 461–465.

- Suursaar Ü. 2013. Locally calibrated wave hindcasts in the Estonian coastal sea in 1966–2011. *Estonian Journal of Earth Science*, 62, 42–56.
- Suursaar Ü. 2015. Analysis of wave time series in the Estonian coastal sea in 2003–2014. *Proceedings of the Estonian Academy of Science*, 64, 289–304.
- Suursaar Ü., Sooäär J. 2007. Decadal variations in mean and extreme sea level values along the Estonian coast of the Baltic Sea. *Tellus A*, 59, 249–260.
- Suursaar Ü., Jaagus J., Kullas T. 2006a. Past and future changes in sea level near the Estonian coast in relation to changes in wind climate. *Boreal Environmental Research*, 11, 123–142.
- Suursaar Ü., Jaagus J., Tõnisson H. 2015. How to quantify long-term changes in coastal sea storminess? *Estuarine, Coastal and Shelf Science*, 156, 31–41.
- Suursaar Ü., Kullas T., Otsmann M. 2002. A model study of the sea level variations in the Gulf of Riga and the Vainameri Sea. *Continental Shelf Research*, 22, 2001–2019.
- Suursaar Ü., Jaagus J., Kullas T., Tõnisson H. 2011. Estimation of sea level rise and storm surge risks along the coast of Estonia, Baltic Sea – a tool for coastal management. *Littoral*, 12005.
- Suursaar Ü., Kullas T., Otsmann M., Kõuts T. 2003. Extreme sea level events in the coastal waters of western Estonia. *Journal of Sea Research*, 49, 295–303.
- Suursaar Ü., Kullas K., Otsmann M., Saaremäe I., Kuik J., Merilain M. 2006b. Cyclone Gudrun in January 2005 and modelling its hydrodynamic consequences in the Estonian coastal waters. *Boreal Environmental Research*, 11, 143–159.
- SWAN Technical Documentation* 2007. Delft University of Technology. The Netherlands.
- Talke S.A., Orton P., Jay D.A. 2014. Increasing storm tides in New York Harbor 1844–2013. *Geophysical Research Letters*, 41, 3149–3155.
- Torresan S., Critto A., Rizzi J., Marcomini A. 2012. Assessment of coastal vulnerability to climate change hazards at the regional scale: the case study of the North Adriatic Sea. *Natural Hazards and Earth System Science*, 12, 2347–2368.
- Torres-Freyermuth A., Marino-Tapia I., Coronado C., Salles P., Medellín G., Pedrozo-Acuña A., Silva R., Candela J., Iglesias-Prieto R. 2012. Wave-induced extreme water levels in the Puerto Morelos fringing reef lagoon. *Natural Hazards and Earth System Science*, 12, 3765–3773.
- Trenhaile A.S. 2009. Modeling the erosion of cohesive clay coasts. *Coastal Engineering*, 56, 59–72.
- Tuomi L., Kahma K. K., Fortelius C. 2012. Modelling fetch-limited wave growth from an irregular shoreline. *Journal of Marine Systems*, 105, 96–105.

- Tuomi L., Kahma K.K., Pettersson H. 2011. Wave hindcast statistics in the seasonally ice-covered Baltic Sea. *Boreal Environmental Research*, 16, 451–472.
- Tuomi L., Pettersson H., Fortelius C., Tikka K., Bjorkqvist J.V., Kahma K.K. 2014. Wave modelling in archipelagos. *Coastal Engineering*, 83, 205–220.
- Ullmann A., Pirazzoli P.A., Tomasin A. 2007. Sea surges in Camargue: trends over the 20th century. *Continental Shelf Research*, 27, 922–934.
- Valdmann A., Käär A., Kelpšaitė L., Kurennoy D., Soomere T. 2008. Marine coastal hazards for the eastern coasts of the Baltic Sea. *Baltica*, 21, 3–12.
- van den Brink H.W., Konnen G.P., Opsteegh J.D. 2005. Uncertainties in extreme surge level estimates from observational records. *Philosophical Transactions of the Royal Society of London A*, 363, 1377–1386.
- Vetter O., Becker J.-M., Merrifield M.A., Pequignet A.-C., Aucan J., Boc S.J., Pollock C.E. 2010. Wave set-up over a Pacific Island fringing reef. *Journal of Geophysical Research – Oceans*, 115, C12066.
- Vilibic I. 2006. The role of the fundamental seiche in the Adriatic coastal floods. *Continental Shelf Research*, 26, 206–216.
- Vilibic I., Monserrat S., Rabinovich A.B. 2014. Meteorological tsunamis on the US East Coast and in other regions of the World Ocean. *Natural Hazards*, 74, 1–9.
- Viška M., Soomere T. 2012. Hindcast of sediment flow along the Curonian Spit under different wave climates. In: *Proceedings of the IEEE/OES Baltic 2012 International Symposium “Ocean: Past, Present and Future. Climate Change Research, Ocean Observation & Advanced Technologies for Regional Sustainability,” May 8–11, Klaipėda, Lithuania*. IEEE Conference Publications.
- Viška M., Soomere T. 2013. Simulated and observed reversals of wave-driven alongshore sediment transport at the eastern Baltic Sea coast. *Baltica*, 26, 145–156.
- Wadey M.P., Brown J.M., Haigh I.D., Dolphin T., Wisse P. 2015. Assessment and comparison of extreme sea levels and waves during the 2013/14 storm season in two UK coastal regions. *Natural Hazards and Earth System Science*, 15, 2209–2225.
- Weisse R., Bellafiore D., Menéndez M., Méndez F., Nicholls R.J., Umgiesser G., Willems P. 2014. Changing extreme sea levels along European coasts. *Coastal Engineering*, 87, 4–14.
- Weisse R., von Storch H., Niemeier H.D., Knaack H. 2012. Changing North Sea storm surge climate: an increasing hazard? *Ocean & Coastal Management*, 68, 58–68.
- Wilson M., Meyers S.D., Luther M.E. 2014. Synoptic volumetric variations and flushing of the Tampa Bay estuary. *Climate Dynamics*, 42, 1587–1594.

- Wiśniewski B., Wolski T. 2011. A long-term trend, fluctuations and probability of the sea level at the southern Baltic coast. *Journal of Coastal Research*, Special Issue 64, 255–259.
- Wong K.-C., Moses-Hall J.E. 1998. On the relative importance of the remote and local wind effects to the subtidal variability in a coastal plain estuary. *Journal of Geophysical Research – Oceans*, 103, 18393–18404.
- Wroblewski A. 2001. A probabilistic approach to sea level rise up to the year 2100 at Kolobrzeg, Poland. *Climate Research*, 18, 25–30.
- Xu S., Huang W. 2013. Effects of sea level rise on frequency analysis of 1% annual maximum water levels in the coast of Florida. *Ocean Engineering*, 71, 96–102.
- Yemm S.P. 2004. *Field Observation of Set-up*. M.S. Thesis, Naval Post-graduate School, USA.

Acknowledgements

I owe my deepest gratitude to my supervisor Prof. Tarmo Soomere for the guidance, support and encouragement during my PhD study. This thesis would not have been possible without his thorough knowledge, enthusiasm, timely suggestions and inspiring educating speeches.

It is my privilege to thank the people from the Laboratory of Wave Engineering for the countless times they provided me with necessary advice, technical suggestions and good company during my research. My sincere thanks to my great colleagues and dearest friends Maris Eelsalu, Dr. Andrea Giudici and Dr. Maija Viška. I also thank Dr. Nicole Delpeche-Ellmann, Katri Kartau, Dr. Nadezhda Kudryavtseva, Rain Männikus, Dr. Artem Rodin, Dr. Bert Viikmäe, and all whom I have inadvertently left out.

I thank the Finnish Meteorological Institute for providing Kalbådgrund wind information and the Swedish Meteorological and Hydrological Institute for providing the Rossby Center Ocean water level data.

I take this opportunity to express my greatest appreciation to my family Lauri Viigand, Ene Pindsoo, Ain Aasa, Karmen Aasa and Karen Aasa for the love, support, inspiration and wisdom they are sharing with me.

* * *

The studies were supported by the institutional block grant IUT33-3 of the Estonian Ministry of Education, the Estonian Science Foundation grant 9125 and the “Sebastian Checkpoints – Lot 3 Baltic” project of the call MARE/2014/09 “Sea-basin check-points”.

The underlying research was partially supported by the small grants scheme project “Effects of climate changes on biodiversity in the coastal shelves of the Baltic Sea” 2015–2016 via European Economic Area (EEA) grant no. 2/EEZLV02/14/GS/022 and the ERA-NET+ RUS project EXOSYSTEM (grant no. ETAG16014).

Abstract

The thesis addresses the properties of three mechanisms that contribute the most to the formation of extreme water levels on the Estonian coasts: the water volume of the Baltic Sea, the local storm surge and the wave-driven increase in water level known as wave set-up.

The set-up heights are evaluated for the shores in the vicinity of the city of Tallinn using the wave properties computed with a triple nested WAM model forced by one-point open-sea wind data (obtained at Kalbådagrund) for 1981–2014. About 50% of the coastline of Tallinn may potentially be endangered by wave set-up. The maximum set-up has reached 0.8 m at some locations. The all-time highest waves were generated by 6 different storms after 1995. The highest set-up events were generated by more than 50 storms in 1981–2012 whereas many of these occurred in the 1980s. Many previous set-up maxima were overridden in the years 2012–2014. A likely reason for such a pattern of changes is the rotation of the wind direction in selected storms and the reappearance of strong eastern winds starting from 2012.

The highest offshore water levels are only infrequently synchronised with extreme set-up events in this area. The contribution of set-up to the extreme values of water level is the largest on the northern coast of Estonia during western and north-western storms in coastal segments open to the west and north-west.

A method to distinguish the presence of wave set-up is developed. It relies on the comparison of projections of extreme water levels based on water level observations and modelled water level data. For this purpose the offshore water level was extracted from the Rossby Center Ocean (RCO) model for the Estonian coasts for 1961–2005. The contribution of set-up is remarkable in some locations such as Ristna where it may provide up to 1/3 of the water level maxima.

Changes in the annual extremes of water level in the eastern Baltic Sea are evaluated based on the output of the RCO model. Water level extremes have increased by 4–10 mm/yr along the entire coast of Estonia and Latvia. The increase occurs jointly owing to higher storm surges and increased water volumes of the whole of the Baltic Sea. The contribution of the water volume of the entire sea to this increase is about 4 mm/yr everywhere. The contribution of storm surges into the water level extremes varies largely. It is almost zero in the open segments of the shores of the Western Estonian archipelago and up to 6 mm/yr in the eastern Gulf of Finland and the Gulf of Riga. It is likely that the described spatial pattern of the increase reflects the rotation of wind direction in a part of strong storms and a longer duration of events that force the North Sea water into the Baltic Sea.

Resüme

Doktoritöö käsitleb kolme peamist tegurit, mille panus on määrav Eesti rannikul esinevate ekstreemsete veetasemete kujunemisel: i) vee hulk Läänemeres, ii) kohalik tormiaju ning iii) lainetuse poolt põhjustatud veetõus, mis on tuntud ka kui laineaju. Nende kolme mehhanismi koosmõjul tekkivad ülikõrged veetasemed ohustavad kõige enam madalaid keeruka rannajoone kujuga linnastunud piirkondi, sh mitmeid Tallinna uusehituste rajooni.

Laineaju teoreetilisi väärtusi hinnati ligikaudu 90 km pikkusel rannalõigul Tallinna ümbruses ja Muuga lahes lainemudeli WAM kolmeastmelise versiooniga arvutatud laineparameetrite abil. Tugineti ühes punktis (Kalbådagrundil) 1981–2014 mõõdetud tuultele, mis esindavad adekvaatselt tuule omadusi Soome lahe avaosas. Tallinna ja Muuga lahes on ligi 50% rannajoonest kõrge laineaju poolt ohustatud. Maksimaalne modelleeritud laineaju ulatus üksikutes Viimsi poolsaare rannalõikudes 0.8 meetrini. Kõrgeimad lained kogu uuringuala kõigis segmentides olid tekkinud kuue tormi tagajärjel, mis kõik esinesid peale 1995. aastat. Kõrgeimad laineaju väärtused tekkisid aga enam kui 50s erinevas tormis. Paljud neist leidsid aset 1980ndatel. Aastatel 2012–2014 ületati enamuses varasemaid laineaju maksimume, sh suur osa ida poole avatud segmentides. Kirjeldatud muster viitab, et mõnedes tugevates tormides alates 2012 on tuul puhunud ebatavalisest suunast ning et on alates 2012. aastast on Soome lahel olnud mitmeid tugevaid idatorme.

Töötati välja meetod laineaju mõju identifitseerimiseks ekstreemsete veetasemete projektsioonide võrdlemise alusel. Selleks kasutati veetaseme mõõdistusi Eesti rannikul ning nn RCO mudeli abil aastaiks 1961–2005 rekonstrueeritud avamere veetasemete andmestikke. Laineaju panus ilmneb erinevatest allikatest pärinevate andmete alusel konstrueeritud ekstreemsete veetasemete projektsioonides pikemate korduvusperioodide jaoks. Näidati, et Eesti rannikul võib laineaju nt Ristnas panustada kuni 1/3 maksimaalsest veetasemest.

Maksimaalsed laineaju väärtused Eesti põhjarannikul ei esine üldiselt üheaegselt kõrgeimate veetasemetega. Kõrgeimad summaarsed veetasemed tekivad Tallinna ja Muuga lahe rannas üldjuhul lääne- ja loodetormides, kus üsna kõrge veetase ning laineaju võivad üheaegselt esineda.

Läänemere idaosa avamere veetaseme aastased maksimumid kasvavad RCO mudeli andmete põhjal keskmise kiirusega 4–10 mm/aastas. Sellesse panustavad nii aasta maksimaalne tormiaju kui ka Läänemere taustveetaseme maksimumide suurenemine. Läänemeres taustveetaseme panus ekstreemumite kasvu on kogu Eesti rannikul ligikaudu 4 mm/aastas. Tormiaju panus veetaseme maksimumidesse varieerub märkimisväärselt piki randa praktiliselt nullist Lääne-Eesti saarestiku avatud osas tasemeni 6 mm/aastas Soome lahe ja Riia lahe idaosas. Sellise mustri põhjuseks võib olla vett Põhjamerest Läänemerele suruvate tormiseeriade pikenemine koos tuule pöördumisega mõnedes tormides, mis on tekitanud väga kõrgeid tormiajusid Soome lahe või Liivi lahe idaosades.

Appendix A: Curriculum Vitae

1. Personal data

Name	Katri Pindsoo
Date and place of birth	15.05.1988, Tartu, Estonia
Address	Akadeemia tee 21, 12618 Tallinn
Phone	(+372) 534 88 734
E-mail	katri.pindsoo@ioc.ee

2. Education

Educational institution	Graduation year	Education (field of study / degree)
Tallinn University of Technology	2013	Earth Science / Master's Degree
Estonian Maritime Academy	2011	Hydrography/ Applied higher education

3. Language competence/skills

Language	Level
Estonian	Native language
English	Fluent
Russian	Basic skills

4. Special courses and further training

Period	Educational or other organisation
September 2016	<i>Baltic Earth International Summer School on Climate change in the Baltic Sea region (Askö Laboratory, Sweden)</i>
February 2016	<i>Course in Process modelling of natural hazards (Enschede, Netherlands)</i>
August–September 2015	<i>Visit to James Cook University in Australia, courses on Coastal and Catchment Geomorphology and Coastal management (Townsville, Australia)</i>
November 2014	<i>Intense course Wave dynamics and coastal processes (Klaipėda, Lithuania)</i>
September 2011	<i>Practical training course in Marine science in Estonia and Finland (Seili, Finland)</i>
September 2011	<i>International Summer School on Preventive methods for coastal protection (Klaipėda, Lithuania)</i>

5. Professional employment

Period	Organisation	Position
Sept 2013–to date	Tallinn University of Technology, Institute of Cybernetics (from 01.01.2017: School of Science, Department of Cybernetics)	Early stage researcher
April 2011– Sept 2013	Tallinn University of Technology, Institute of Cybernetics	Technician

6. Research activity

6.1. Publications

Articles indexed by the Web of Science and Scopus database (1.1):

Soomere T., Männikus R., **Pindsoo K.**, Kudryavtseva N., Eelsalu M. 2017. Modification of closure depths by synchronisation of severe seas and high water levels. *Geo-Marine Letters*, 37, 35–46.

Soomere T., **Pindsoo K.** 2016. Spatial variability in the trends in extreme storm surges and weekly-scale high water levels in the eastern Baltic Sea. *Continental Shelf Research*, 115, 53–64.

Pindsoo K., Soomere T. 2015. Contribution of wave set-up into the total water level in the Tallinn area. *Proceedings of the Estonian Academy of Sciences*, 64, 338–348.

Eelsalu M., Soomere T., **Pindsoo K.**, Lagemaa P. 2014. Ensemble approach for projections of return periods of extreme water levels in Estonian waters. *Continental Shelf Research*, 91, 201–210.

Tõnisson H., Suursaar Ü., Kont A., Orviku K., Rivis R., Szava-Kovats R., Vilumaa K., Aarna T., Eelsalu M., **Pindsoo K.**, Palginõmm V., Ratas U. 2014. Field experiments with different fractions of painted sediments to study material transport in three coastal sites in Estonia. *Journal of Coastal Research*, Special Issue 70, 229–234.

Soomere T., **Pindsoo K.**, Bishop S.R., Käard A., Valdmann A. 2013. Mapping wave set-up near a complex geometric urban coastline. *Natural Hazards and Earth System Sciences*, 13, 3049–3061.

Didenkulova I., Soomere T., **Pindsoo K.**, Suuroja S. 2013. On the occurrence of non-reflecting cross-shore profiles along Estonian coasts of the Baltic Sea. *Estonian Journal of Engineering*, 19, 110–123.

Peer-reviewed articles in other international journals (1.2) and collections (3.1):

Soomere T., Viška M., **Pindsoo K.** 2017. Retrieving the signal of climate change from numerically simulated sediment transport along the eastern Baltic Sea Coast. In: Harff J., Furmańczyk K., von Storch H. (eds.), *Coastline Changes of the Baltic Sea from South to East: Past and Future Projection*, 327–361. Springer, Cham. (Coastal Research Library; 19).

Käär A., Valdmann A., Eelsalu M., **Pindsoo K.**, Männikus R., Soomere T. 2016. Preventive management of undesired changes in alongshore sediment transport in planning of waterfront infrastructure. In: Galiano-Garrigos A., Brebbia C.A. (eds.), *The Sustainable City XI : [Proceedings of the 11th International Conference on Urban Regeneration and Sustainability (SC 2016), Alicante, Spain]*. WIT Press, Ashurst Southampton, 419–430. (WIT Transactions on Ecology and the Environment; 204).

Pindsoo K., Eelsalu M., Soomere T., Tõnisson H. 2014. An estimate of the impact of vessel wakes on coastal processes: a case study for Aegna, Estonia. 2014 In: *2014 IEEE/OES Baltic International Symposium, 26–29 May 2014, Tallinn, Estonia, Proceedings*. IEEE Conference Proceedings.

Soomere T., **Pindsoo K.**, Bishop S.R., Käär A., Valdmann A. 2013. Mapping wave set-up near a complex geometric urban coastline. *Natural Hazards and Earth System Sciences Discussions*, 1, 1651–1688, 10.

Pindsoo K., Soomere T., Zujev M. 2012. Decadal and long-term variations in the wave climate at the Latvian coast of the Baltic Proper In: *IEEE/OES Baltic 2012 International Symposium, 8–11 May 2012, Klaipėda, Lithuania, Proceedings*. IEEE Conference Proceedings.

Articles published in other conference proceedings (3.4):

Pindsoo K., Eelsalu M., Soomere T. 2016. Spatial variation of statistical properties of extreme water levels along the eastern Baltic Sea. In: Reckermann M., Köppen S. (eds.), *1st Baltic Earth Conference Multiple Drivers for Earth System Changes in the Baltic Sea Region: 13–17 June 2016, Nida, Curonian Spit, Lithuania; Conference Proceedings*. International Baltic Earth Secretariat Publication Geesthacht, Germany, 9, 126–127.

Soomere T., Eelsalu M., **Pindsoo K.** 2016. Water level extremes signal changes in the wind direction in the north-eastern Baltic Sea. In: Reckermann M., Köppen S. (eds.), *1st Baltic Earth Conference Multiple Drivers for Earth System Changes in the Baltic Sea Region: 13–17 June 2016, Nida, Curonian Spit, Lithuania; Conference Proceedings*. International Baltic Earth Secretariat Publication Geesthacht, Germany, 9, 132–133.

Pindsoo K., Soomere T. 2014. Signal of wave climate change reflected by wave set-up height. In: Witkowski A., Harff J., Reckermann M. (eds.), *2nd International Conference on Climate Change – The Environmental and Socio-Economic Response in the Southern Baltic Region, 12–15 May 2014, Szczecin, Poland; Conference Proceedings*. International Baltic Earth Secretariat Publication, Geesthacht, Germany, 2, 67–68.

Soomere T., Eelsalu M., **Pindsoo K.**, Zujev M. 2013. Lessons from the almost seven decades of visual wave observations from the eastern Baltic Sea coast. In: Reckermann M., Köppen S. (eds.), *7th Study Conference on BALTEX, 10–14 June 2013, Borgholm, Island of Öland, Sweden, Conference Proceedings*. International BALTEX Secretariat Publication, 53, 91–92.

Abstracts of conference presentations (5.2):

Pindsoo K., Soomere T. 2017. Trends in the extreme water levels of the Baltic Sea. *11th Baltic Sea Science Congress: Living along gradients: Past, Present, Future, 12–16 June 2017, Rostock, Germany, Abstract Book*. 90.

Viška M., **Pindsoo K.** 2017. Sea level rise and its impact on sediment dynamics along the south-eastern Baltic Sea coast. In: *11th Baltic Sea Science Congress: Living along Gradients: Past, Present, Future, 12–16 June 2017, Rostock, Germany, Abstract Book*. 248.

Pindsoo K., Soomere T. 2017. Wave set-up in the urban area of the city of Tallinn, Estonia. In: *11th Baltic Sea Science Congress: Living along Gradients: Past, Present, Future, 12–16 June 2017, Rostock, Germany, Abstract Book*. 252.

Pindsoo K., Eelsalu M., Soomere T. 2016. Spatial variation of statistical properties of extreme water levels along the eastern Baltic Sea coast. In: *1st Baltic Earth Conference: Multiple drivers for Earth system changes in the Baltic Sea region, 13–17 June 2016, Nida, Curonian Spit, Lithuania, Abstract Book*. 126.

Soomere T., Eelsalu M., **Pindsoo K.** 2016. Water level extremes signal changes in the wind direction in the north-eastern Baltic Sea. In: *1st Baltic Earth Conference: Multiple Drivers for Earth System Changes in the Baltic Sea Region, 13–17 June 2016, Nida, Curonian Spit, Lithuania, Abstract Book*. 132.

Pindsoo K., Soomere T., Rocha E. 2016. Spatial variation of statistical properties of extreme water levels along the eastern Baltic Sea. In: *Geophysical Research Abstracts*, 18, EGU2016-9679.

Pindsoo K., Soomere T. 2016. Trends in the components of extreme water levels signal a rotation of winds in strong storms in the eastern Baltic Sea. In: *Geophysical Research Abstracts*, 18, EGU2016-9378.

Pindsoo K., Soomere T. 2015. Contribution of wave induced set-up into total water level in the urban area of Tallinn. In: *Climate Modelling and Impacts from the Global to the Regional to the Urban Scale: An International Scientific Seminar at HafenCity University Hamburg, 10 March 2015, Poster Abstracts*. Baltic Earth; HCU, 15.

Pindsoo K., Soomere T. 2015. Contribution of wave set-up into the total water level in the Tallinn area. In: *10th Baltic Sea Science Congress: Science and Innovation for Future of the Baltic and the European Regional Seas, 15-19 June 2015, Riga, Latvia, Abstract Book*. 87.

Eelsalu M., Soomere T., **Pindsoo K.**, Lagemaa P. 2015. Ensemble approach for the projections of extreme water levels reveals bias in water level observations. *10th Baltic Sea Science Congress: Science and Innovation for Future of the Baltic and the European Regional Seas, 15–19 June 2015, Riga, Latvia, Abstract Book*. 85.

Pindsoo K., Soomere T., Eelsalu M., Tõnisson H. 2015. Quantification of the impact of vessel wakes on a shingle-gravel beach. In: *10th Baltic Sea Science Congress: Science and Innovation for Future of the Baltic and the European Regional Seas, 15–19 June 2015, Riga, Latvia, Abstract Book*. 201.

Mingelaitė T., Eelsalu M., **Pindsoo K.**, Soomere T., Dailidienė I. 2015. Return periods of extreme water levels along Lithuanian sea coast based on a simple ensemble of projections. In: *10th Baltic Sea Science Congress: Science and Innovation for Future of the Baltic and the European Regional Seas, 15–19 June 2015, Riga, Latvia, Abstract Book*. 238.

Pindsoo K., Soomere T. 2015. Trends in extreme water levels of the eastern Baltic Sea. In: *10th Baltic Sea Science Congress: Science and Innovation for Future of the Baltic and the European Regional Seas, 15–19 June 2015, Riga, Latvia, Abstract Book*. 76.

Pindsoo K., Eelsalu M., Tõnisson H. 2014. An estimate of the impact of vessel wakes on coastal processes: a case study for Aegna, Estonia. In: *Measuring and Modeling of Multi-Scale Interactions in the Marine Environment: IEEE/OES Baltic Symposium, 26–29 May 2014, Tallinn, Estonia, Book of Abstracts*. Tallinn, Tallinn University of Technology, 97.

Pindsoo K., Soomere T. 2014. Changing wave set-up climate in the urban area of Tallinn. In: *MEME'2014: Mathematics and Engineering in Marine and Earth Problems, 22–25 July 2014, Aveiro, Portugal, Book of Abstracts*. 130–132.

Tõnisson H., Kont A., Suursaar Ü., Orviku K., Eelsalu M., **Pindsoo K.**, Suuroja S. 2014. Painted sediment experiments in studies of coastal processes. In: *The 12th Colloquium on Baltic Sea Marine Geology, Warnemünde, Germany, September 8–12, 2014*. 37.

Lagemaa P., Eelsalu M., **Pindsoo K.**, Soomere T. 2014. Properties of an ensemble of projections of extreme water levels near Tallinn. In: *Measuring and Modeling of Multi-Scale Interactions in the Marine Environment: IEEE/OES Baltic Symposium 2014, May 26–29, 2014, Tallinn, Estonia, Book of Abstracts*. Tallinn, Tallinn University of Technology, 64.

Pindsoo K., Eelsalu M., Soomere T. 2014. Quantification of the impact of vessel wakes on the transport of coarse sediment. In: *Baltic Earth - Gulf of Finland Year 2014 Modelling Workshop "Modelling as a Tool to Ensure Sustainable Development of the Gulf of Finland-Baltic Sea Ecosystem", Finnish Environment Institute, Helsinki 24–25 November 2014, Programme, Abstracts, Participants*. Geesthacht, Germany: Helmholtz-Zentrum Geesthacht, 16. (International Baltic Earth Secretariat Publication; 4).

Pindsoo K., Soomere T., Eelsalu M., Tõnisson H. 2014. Vessel wakes effectively transport gravel, cobbles and pebbles. In: *MEME'2014: Mathematics and Engineering in Marine and Earth Problems, 22–25 July 2014, Aveiro, Portugal, Book of Abstracts*, 103–105.

Pindsoo K., Soomere T. 2014. Wave set-up climatology in the city of Tallinn, Estonia. In: Salupere A., Maugin G.A. (eds.), *IUTAM Symposium on Complexity of Nonlinear Waves: 8–12 September, Tallinn 2014, Book of Abstracts*. Tallinn: Institute of Cybernetics at Tallinn University of Technology, 91.

Didenkulova I., **Pindsoo K.**, Suuroja S. 2013. Power laws for the cross-shore profiles along Estonian coasts. In: *BSSC 9th Baltic Sea Science Congress 2013: New Horizons for Baltic Sea Science, 26–30 August, 2013, Klaipeda, Lithuania, Abstract Book*. Klaipeda: Coastal Research and Planning Institute of Klaipeda University (KU CORPI), 157.

Pindsoo K., Soomere T. 2013. Wave set-up in the urban area of the City of Tallinn, Estonia. In: *BSSC 9th Baltic Sea Science Congress 2013: New Horizons for Baltic Sea Science, 26–30 August, 2013, Klaipeda, Lithuania, Abstract Book*. Klaipeda: Coastal Research and Planning Institute of Klaipeda University (KU CORPI), 224.

Pindsoo K., Soomere T., Zujev M. 2012. Decadal and long-term variations in the wave climate at the Latvian coast of the Baltic Proper. In: *2012 IEEE/OES Baltic International Symposium "Ocean: Past, Present and Future. Climate Change Research, Ocean Observation & Advances Technologies for Regional Sustainability": Klaipeda, Lithuania, May 8–11, 2012, Presentation Abstracts*. Klaipeda: Baltic Valley, 13.

Pindsoo K., Soomere T. 2012. Interannual, decadal and long-term variations in the wave fields at the Latvian coast of the Baltic proper. In: Virtasalo J., Vallius H. (eds.), *11th Colloquium on Baltic Sea Marine Geology: Helsinki 19th–21st September 2012, Abstract Book*. Espoo, Juvenes Print, 54–55. (Geological Survey of Finland; Guide 57).

Other creative activities (6.7):

Soomere T., **Pindsoo K.**, Eelsalu M. 2016. Veetasemete ekstreemumid ja korduvusperioodid Eesti rannikul. [Tallinn]: Tallinna Tehnikaülikooli Küberneetika Instituut.

Soomere T., Eelsalu M., **Pindsoo K.** 2014. Rannasetete bilanss Miidurannast Tallinna Vanasadamani. Tallinn: Tallinna Tehnikaülikooli Küberneetika Instituut.

Soomere T., **Pindsoo K.**, Eelsalu M. 2013. Kopli lahe suudmes esinevate kõrgete veetasemete tõenäosuse ja korduvuse hinnang. (30). Tallinn: Tallinna Tehnikaülikooli Küberneetika Instituut.

Appendix B: Elulookirjeldus

1. Isikuandmed

Ees- ja perekonnanimi Katri Pindsoo
Sünniaeg ja -koht 15.05.1988, Tartu, Eesti
Aadress Akadeemia tee 21, 12618 Tallinn, Eesti
Telefon (+372) 534 88 734
E-mail katri.pindsoo@ioc.ee

2. Hariduskäik

Õppeasutus	Lõpetamise aeg	Haridus (eriala / kraad)
Tallinna Tehnikaülikool	2013	Maateadused / magister
Eesti Mereakadeemia	2011	Hüdrograafia / rakenduskõrgharidus

3. Keelteoskus

Keel	Tase
eesti	emakeel
inglise	kõrgtase
vene	algtase

4. Täiendõpe

Õppimise aeg	Täiendõppe läbivijja nimetus
September 2016	Rahvusvaheline suvekool <i>Baltic Earth International Summer School on Climate change in the Baltic Sea region</i> (Askö laboratoorium, Rootsi)
Veebruar 2016	Kursus <i>Process modelling of natural hazards</i> (Enschede, Holland)
August–September 2015	Kahekuuline visiit James Cooki Ülikooli Austraalias, kursused <i>Coastal and Catchment Geomorphology</i> ja <i>Coastal management</i> (Townsville, Austraalia)
November 2014	Intensiivkursus <i>Wave dynamics and coastal processes</i> (Klaipėda Ülikool, Leedu)
September 2011	Rahvusvaheline suvekool <i>Preventive methods for coastal protection</i> (Klaipėda, Leedu)
September 2011	Rahvusvaheline suvekool <i>Practical training course in Marine science in Estonia and Finland</i> (Seili, Soome)

5. Teenistuskäik

Töötamise aeg	Tööandja nimetus	Ametikoht
September 2013– tänapeni	Tallinna Tehnikaülikooli Küberneetika Instituut	Nooremteadur
Aprill 2011–September 2013	Tallinna Tehnikaülikooli Küberneetika Instituut	Tehnik

4. Teadustegevus

Avaldatud teadusartiklite ja konverentsiteeside ning peetud konverentsiette-kannete loetelu on toodud ingliskeelse CV juures.

Paper I

Soomere T., **Pindsoo K.**, Bishop S.R., Käär A., Valdmann A. 2013. Mapping wave set-up near a complex geometric urban coastline. *Natural Hazards and Earth System Sciences*, 13(11), 3049–3061, doi:10.5194/nhess-13-3049-2013.



Mapping wave set-up near a complex geometric urban coastline

T. Soomere^{1,2}, K. Pindsoo¹, S. R. Bishop³, A. Käär⁴, and A. Valdmann⁴

¹Institute of Cybernetics at Tallinn University of Technology, Tallinn, Estonia

²Estonian Academy of Sciences, Tallinn, Estonia

³Mathematics Department, University College London, London, UK

⁴Municipal Engineering Services Department, Tallinn, Estonia

Correspondence to: T. Soomere (soomere@cs.ioc.ee)

Received: 3 April 2013 – Published in Nat. Hazards Earth Syst. Sci. Discuss.: 24 April 2013

Revised: 9 September 2013 – Accepted: 24 October 2013 – Published: 29 November 2013

Abstract. Wave induced set-up is a process that leads to increased water levels in coastal regions. When coupled with storm conditions, wave set-up – or, for brevity, set-up – can significantly increase the risk of flooding or structural damage and therefore is of particular importance when considering coastal management or issues related to the planning of nearshore infrastructures. Here, we investigate the effects of set-up in the coastal region of the Gulf of Finland in the Baltic Sea, close to Tallinn, Estonia, although the results will have wider relevance for many other areas. Due to a lack of continuous wave data we employ modelling to provide input data using a calculation scheme based on a high-resolution (470 m) spectral wave model WAM to replicate spatial patterns of wave properties based on high-quality, instrument-measured wind data from the neighbourhood of the study site. The results indicate that for the specific geometry of coastline under consideration, there is a variation in set-up which is strongly affected by wind direction. The maximum set-up values are up to 70–80 cm in selected locations. This is more than 50 % of the all-time maximum water level and thus may serve as a substantial source of marine hazard for several low-lying regions around the city. Wind directions during storms have changed in recent years and, with climate variability potentially increasing, these results will encourage further tests which may be used in a policy setting regarding defences or other structures in and around coastlines. In particular, with urban development now taking place in many coastal regions (including the one within this study) these results have implications for local planners. They may also be incorporated into new storm warning systems.

1 Introduction

Worldwide, cities are faced with the challenge of adapting to the effects of climate change. The interaction of the synergies and conflicts in the objectives of mitigation and adaptation are most vivid in urban areas, where they play out through land use, infrastructure systems, and the built environment (e.g. Hall et al., 2010). This interaction becomes even sharper, for coastal cities for which the collection of marine hazards and especially the risk of coastal flooding may be radically amplified by the potential influence of future global climate changes (e.g. as reported in Cheng et al., 2013; O’Grady and McInnes, 2010; Torresan et al., 2012; among many others).

Dangerous water levels are normally produced by an unfortunate combination of high tide, low atmospheric pressure, strong wind-driven surge of seas as well as wave-induced set-up. While usually the wind surge and inverted barometric effect (customarily called storm surge together) lead to the majority of the elevated water levels, wave set-up can contribute substantially under certain conditions.

It is well known that even almost linear ocean waves produce a mass transport that is proportional to the squared wave height (Starr, 1947), which is an example of so-called second-order effects. The propagation of such waves results in a decrease in the average water level (set-down) in areas of finite depth (Dean and Dalrymple, 1991). For waves approaching a coast, the water level minimum occurs at the seaward border of the surf zone.

As opposed to wave set-down, wave-driven set-up is a strongly non-linear phenomenon within the surf zone. It results in a rise in the mean water level in the nearshore owing

to the release of momentum in the process of waves breaking. Theoretically, wave set-up can be quantified in terms of changes to the onshore component of the radiation stress (Longuet-Higgins and Stewart, 1964).

The prediction of wave set-up, and/or the quantification of its magnitude, is crucial during extreme events because its impact adds to other factors producing a high water level. To protect life and property, advance warning and detailed knowledge of wave set-up are vital in the design of coastal and nearshore structures vulnerable to high waves and water levels.

As yet, there is no consensus about the exact relationship between the offshore wave properties and the parameters of wave set-up (Hsu et al., 2006; Shi and Kirby, 2008; Nayak et al., 2012). Relevant estimates diverge radically (Stockdon et al., 2006), probably because the conversion of wave-driven momentum is very sensitive with respect to a multitude of factors. On the one hand, the properties of set-up substantially depend on the nature of the bottom (Apostos et al., 2007). There is theoretical evidence that the set-up height may even be negative in the presence of vegetation and/or very rough bottom on the seabed (Dean and Bender, 2006). This is perhaps why users of the SWAN model broadly believe that the set-up height is in the range of 10–15 % of the offshore wave height (Filipot and Cheung, 2012; Nayak et al., 2012). On the other hand, in particular conditions, the set-up may reach about 1/3 of the offshore wave height (Vetter et al., 2010), and extreme values of set-up up to 2 m above the offshore water level have been observed being influenced by large storm waves (Heidarzadeh et al., 2009). A subtle but important impact of wave set-up under very rough seas is an increase in the water level at the entrance of wave-dominated inlets or lagoons (Bertin et al., 2009; Irish and Canizares, 2009; Torres-Freyermuth et al., 2012), a process that may considerably enhance the dangers, e.g. in the “*aqua alta*” in Venice (L. Cavaleri, personal communication, 2010).

Wave set-up is thus one of the core marine-induced hazards along many of our coasts. Its importance is relatively large at steep coasts with limited tidal range, where people are used to a more moderate range of variation in the water level. For example, in Florida wave set-up can be 30 % to 60 % of the total 100 yr storm surge (Dean and Bender, 2006). In areas with relatively narrow continental shelves (more generally, in regions where the wind surge remains moderate) wave set-up can be an even larger contributor to extreme water levels during major storms (Dean and Bender, 2006). A natural reflection of this situation is the trend to include the analysis of the potential of wave set-up into various methods of the mapping of flood hazards for low-lying coastal regions (see Cariolet and Suanez, 2009; Harper et al., 2009; Jain et al., 2010a, b; among many others), especially in the context of potential changes in climate (McInnes et al., 2009) and for the purposes of estimates of the erosion of higher parts of the beach (Trenhaile, 2009).

While the properties of set-up are apparently more or less homogeneous and relatively easy to predict on long, basically straight, coastal sections, for coasts with complicated geometry this process has the potential to create unexpectedly high water levels in specific locations where storm waves directly approach the coast. As each storm may have a somewhat different wind direction, and the transformation of wave direction in the nearshore also depends on the wave periods, the most dangerous locations may vary considerably from one storm to another. (Note that, when describing wind properties, the wind direction is given by the direction from which the wind originates, but wave direction is usually given as the direction in which the waves propagate; thus an easterly wind produces a westerly wave). For city planning purposes, or estimates of the maximum inundation etc., this complicates the estimation of the maximum water level along coastal stretches with complicated geometry (Valdmann et al., 2008). In particular, this requires the use of a long-time climatology of wave properties to properly resolve effects caused by the directional distribution of the wave approach direction for different storms.

This problem is very acute in micro-tidal, semi-enclosed seas and shelf seas that are vulnerable not only to the potential increase in the overall water level but also to changes in the wave approach directions that have been recently identified for several regions (Räämet et al., 2010; Charles et al., 2012b). The problem is furthermore complicated in urban areas where flooding represents a particular challenge to modellers and flood risk managers because of the complex interactions of surface and sewer flows since, in practice, urban flooding systems involve tens of thousands of variables (Dawson et al., 2008).

The study area of the current paper is Tallinn Bay (Fig. 1), in Estonia. This area, similarly to the entire Baltic Sea, is micro-tidal (tidal range less than 5 cm) and water level fluctuations are mostly governed by atmospheric forcing. As the predominant wind direction is from the south-west, and the city is located at the southern coast of the Gulf of Finland, the coasts of the urban area are implicitly sheltered from the most furious wave storms in this area. This feature is reflected in the relatively modest all-time maximum water level (1.52 m) since the end of the 19th century, whereas Saint Petersburg, for example, has experienced flooding heights up to 4.21 m and Pärnu 2.75 m (Suursaar et al., 2006). In Tallinn, some parts of the city are not protected even against a moderate water level rise. For example, when the water level rose to 1.52 m on 8–9 January 2005, several low-lying areas (such as the 1980 Olympic sailing centre) were flooded. Typically water levels in this area are about 0.7–0.9 m above the long-term mean during several weeks in the autumn stormy season. As the critical water level of several infrastructure facilities of the city of Tallinn is about 1 m, even a moderate wave set-up, say, about 0.5 m, may lead to serious consequences.

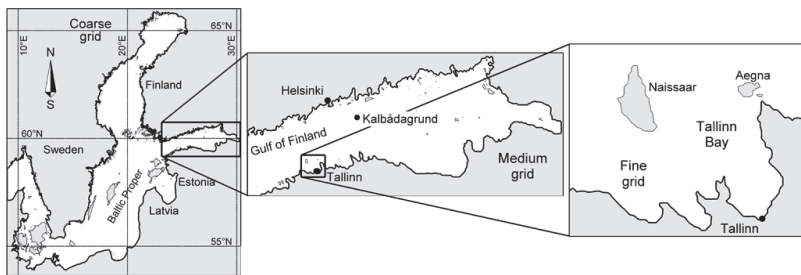


Fig. 1. Computational areas of the triple-nested wave model applied to the Tallinn Bay area.

The situation along the coastline of the entire urban area of Tallinn is even more complicated because of the particular geometry of Tallinn Bay and its neighbouring small bays. The three largest bays, Tallinn Bay itself, Kopli Bay and Kakumäe Bay to the west, are open to the north-west or north-north-west (NNW). Winds from these directions are somewhat less frequent than south-western winds but contain the strongest winds in the north-eastern part of the Baltic (Soomere, 2001). While the coasts of the interior of Tallinn Bay are relatively well protected, beaches at the bayheads of the two other bays and along the Viimsi Peninsula have an open shape, and many stretches possess the features that are favourable for producing high set-up adjacent to low-lying existing and planned residential areas.

The study area chosen here is an example of a wave-dominated micro-tidal coastline which is locally almost straight (for scales up to few 100s of metres or, at some locations, up to a kilometre or two), but on larger scales (from a few kilometres) the coast contains large peninsulas and bays deeply cut into the mainland. In essence, this is a relatively young coast which is actively in the process of straightening (Raukas and Hyvärinen, 1992). The process of wave set-up crucially depends on the wave height and propagation direction (the attack angle), and, since the bays are open in different directions, the magnitude of wave set-up not only exhibits extensive variability along the coast but also reaches the largest values in different bayheads during different storms.

The objective of this paper is to evaluate the “climatology” of the set-up heights along this example of urban coast formed by a complicated geometry and hosting several vulnerable sections. First we reconstruct the statistics of wave conditions in the nearshore with a spatial resolution of about 0.25 nautical miles (~ 470 m) for the years 1980–2012. This data set will then be used to identify the coastal sections prone to the highest set-up and, more importantly, to highlight the link between particular storms and stretches which have suffered from unexpectedly high water levels. The analysis reveals that the direction of storms has undergone some interesting decadal-scale variations. Perhaps the

most unexpected feature is that almost each coastal section had its “own” (perfect) storm in the last three decades that produced the 30 yr highest set-up in this section.

2 Data and methods

2.1 Reconstruction of wave properties

Although weather and wave observations covering Tallinn Harbour extend back to 1805 (Soomere, 2005), the older part of the data contains only visual estimates of wave properties. These data adequately represent wave fields in the proximity of the harbour but fail to describe the wave regime in other parts of the bay and, importantly, fail to identify the swell-dominated conditions (which actually form about a half of all wave conditions); consequently these data also fail to find the predominant wave direction (Orlenko et al., 1984). Therefore, it is natural to use a contemporary wave-modelling system to reconstruct the time series of wave properties in the nearshore.

Wave properties were calculated using a triple-nested version of the third-generation spectral wave model called WAM (Komen et al., 1994). A coarse-resolution model was run for the whole Baltic Sea based on a regular grid with a discretisation of about 3 nautical miles (5.5 km) (see Fig. 1). At each sea point, 600 spectral components (24 evenly spaced directions and 25 frequencies ranging from 0.042 to 0.41 Hz with an increment of 1.1) were calculated. A medium-resolution model was run for the Gulf of Finland with a grid step of about 1.8 km. The bathymetry of the model is based on data from Seifert et al. (2001) with a resolution of 1' along latitudes and 2' along longitudes. Additionally, a fine-resolution model with a grid step of about 470 m (1/4' along latitudes and 1/2' along longitudes) resolving the major local topographic and bathymetric features was run for the Tallinn Bay area. The frequency range was extended to 2.08 Hz (42 evenly spaced frequencies) for wind speeds ≤ 10 m s⁻¹ to better represent the wave growth in low-wind and short-fetch conditions.

The WAM model, although constructed for open-ocean conditions and for relatively deep water (Komen et al., 1994), gives good results in the Baltic Sea basin provided the model resolution is appropriate and the wind information is correct. Extensive information about the model performance and validation for the Baltic can be found in Soomere et al. (2008a), Räämet et al. (2009), and Tuomi et al. (2011, 2012). Waves are relatively short in the Baltic Sea. Common wave periods are 3–6 s in the open Baltic proper (Broman et al., 2006) and usually even shorter (2–4 s) in its semi-enclosed sub-basins (Soomere and Räämet, 2011). They very occasionally reach 8–10 s in strong storms in the Baltic proper but almost never reach these levels in the Gulf of Finland or in Tallinn Bay (Soomere et al., 2008a, b). For a 1 m-high wave with a rather long (in this context) period of 6 s the Ursell number in 5 m-deep water is about 11. Therefore, Stokes' theory is applicable up to about 3.5 m high waves with periods of 6 s in such conditions. As will be noted below, significant wave heights exceeding 3.5 m have not occurred in any of the areas prone to high set-up during the last three decades.

Moreover, the relatively shallow (less than 20 m deep) nearshore is fairly narrow, usually less than 1 km wide in most of the study area. The wave field thus experiences various non-linear shallow-water effects (such as the frequency shift and spectral shape changes as water depth decreases or the impact of triad interactions) for a limited time and only during the propagation over a few 100s of metres. Therefore, it can be assumed that the chosen triple-nested implementation of the WAM wave model, run in the finite-depth mode, allows a satisfactory description of wave properties in the coastal zone, down to depths of about 5 m and as close to the coast as about 200–300 m in the study area. The output of this implementation has been compared with in situ measurements in Tallinn Bay in Soomere (2005).

Successful numerical wave modelling requires reliable marine wind information. The quality of wind data is a major issue in wave modelling in the Baltic Sea region, which has a large and complex-shaped water body that greatly influences surface-level winds and results in a high variability of the local climate in its vicinity. The existing global wind data sets have relatively low resolution and have to be downscaled for the use in the Baltic Sea conditions (Samuelsson et al., 2011; Schmager et al., 2008) but also artificially adjusted (e.g. using simulated gustiness) in order to properly replicate the air–sea interaction (Höglund et al., 2009). Local (national) wind data sets are only reliable in the vicinity of each country (Räämet et al., 2009), and high-resolution modelled winds, optionally coupled with wind sea properties, suffer from being substantially inhomogeneous over time (Tuomi et al., 2012). Furthermore, the Gulf of Finland has a specific wind and wave regime (Pettersson et al., 2010; Soomere et al., 2008b) mainly because the strongest winds blow obliquely across this water body with respect to the topography. The biggest problem in the reconstruction of wave set-up is the mismatch in the direction of even the best modelled versions

of wind fields compared with high-quality measured data (Keevallik and Soomere, 2010).

A favourable feature is that the dimensions of the Gulf of Finland are smaller than the typical spatial extension of high and persistent wind events in the area. Thus the wind fields that produce the highest waves in this water body are approximately uniform over the entire gulf.

Based on the reasons listed, we consequently force the wave model with a spatially homogeneous wind field that matches the wind measured in fully marine conditions, at a location that is not affected by the presence of the mainland. Such a wind measurement site in the gulf is Kalbådgrund, a caisson lighthouse in the central part of the Gulf of Finland (Fig. 1, 59° 59' N, 25° 36' E). The wind measurements are performed at the height of 32 m above the mean sea level. Height correction factors, to reduce the recorded wind speed to the reference height of 10 m, are 0.91 for neutral, 0.94 for unstable and 0.71 for stable stratifications (Laurila and Laurila, 1984). To the first approximation, the factor 0.85 was used in the computations that follow.

The wave time series in the nearshore of the entire study area were estimated using a simplified scheme for long-term wave hindcasting. The basic idea of speeding up the wave computations consists of reducing long-term calculations of the sea state to an analysis of a cluster of wave field maps pre-computed with the use of single-point wind data. A favourable feature of the study area is that wave fields rapidly become saturated here and have relatively short memory (normally no longer than 12 h) of wind history (Soomere, 2005). This feature makes it possible to split the wave calculations into a number of short independent sections of 3–12 h. To the first approximation, it was assumed that an instant wave field in Tallinn Bay is a function of a short section of the wind dynamics. Moreover, it was implicitly assumed that remote wind conditions in the open Baltic Sea did not significantly contribute to the local wave field in Tallinn Bay. A comparison of the results of modelling using the triple-nested wave model and the described method for reconstruction of wave fields (Soomere, 2005) suggests that the listed assumptions are valid in Tallinn Bay for about 99.5% of cases and thus the reconstructed wave properties are a good approximation to measured data.

The nearshore of the study area was divided into 105 sections with a typical length of 0.5 km. For each section the average orientation of the coast and the limits of its variation were defined. The sections roughly correspond to the nearshore computational cells of the innermost, fine-resolution wave model (Fig. 2).

The choice of cells used to evaluate the set-up height was based on estimates of the extreme wave heights in the Tallinn Bay area. For adequate estimates of the wave set-up, the cells should be as close to the coast as possible, but the modelled mean water depth in these cells should be bigger than the breaking depth for the largest waves. In many nearshore locations few storms produce significant wave heights of ~4 m.

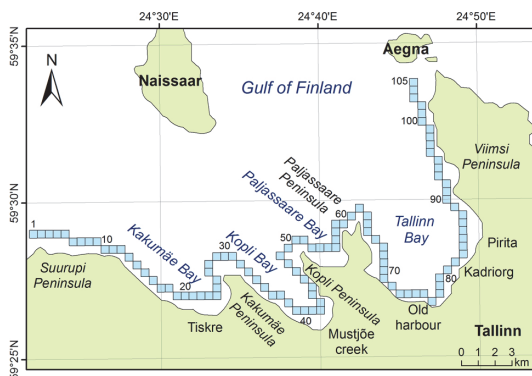


Fig. 2. Selected nearshore grid cells of the wave model. The cells are numbered sequentially starting from the westernmost point.

For example, on 15–16 November 2001, when the all-time high of the significant wave height of the Gulf of Finland (5.2 m) was recorded during a NNW storm (wind direction 330° , 23 m s^{-1}), the significant wave height in the interior of Tallinn Bay, and at the entrance to the two smaller bays, reached 4 m (Soomere, 2005). The significant wave height in an exceptional storm on 8–9 January 2005 was 4.5 m to the west of Naissaar (Soomere et al., 2008a). Therefore, waves in cells with a depth $< 4 \text{ m}$ may already be intensively breaking, and the use of wave data from these would severely underestimate the set-up height. Based on the listed reasons, the wave data were mostly used from nearshore cells that had a model water depth in the range of 4–8 m. With this selection, the highest waves (producing also the highest set-up) were already close to the breaking stage in some computational cells. In a few cells that were associated with headlands, or points which are not vulnerable to high set-up, the water depth in the selected cells is, in some cases, up to 20–27 m. A detailed analysis of further shoaling and refraction was performed to evaluate the breaking height and the approach angle at the seaward border of the surf zone based on the average orientation of the sections of the coast corresponding to the selected grid cells.

From the output of the WAM model, time series of the significant wave height, peak period and mean wave direction were evaluated once every 3 h from 1 January 1981 to 31 October 2012 for each selected coastal section. The set of wind data contained 93 016 measurements. In 8554 cases either the wind speed or wind direction was missing. These incomplete data points were subsequently left out of the analysis, which was then based on the remaining 84 462 measurements. The presence of ice was ignored. Doing so leads to a certain bias of the results, because the mean number of ice days varies from 70 to 80 annually (Climatological Ice Atlas, 1982; Soõäär and Jaagus, 2007). Statistically, the ice cover damps wind waves either partially or totally during the winter

season, which is normally windier (Mietus, 1998). Therefore, the computed annual mean parameters of wind waves (as well as the corresponding extreme set-up) are somewhat overestimated and represent average wave properties during the years with no extensive ice cover.

2.2 Evaluation of wave set-up

As mentioned above, there is no consensus today about the exact relationship between the offshore wave properties and the parameters of wave set-up. The situation is actually even more complicated as the conversion of wave-driven momentum is very sensitive with respect to details of the nearshore (Dean and Bender, 2006), and the results of its modelling (e.g. using SWAN) show extensive dependence of the results on the model resolution and the slope of the beach (Nayak et al., 2012). The resolution used here gives a fair estimate (about 90 % of the actual values) of wave set-up for gentle slopes (about 1 : 80), whereas it may fail to characterise this process for steeper slopes (about 1 : 20) (Nayak et al., 2012). The concave coastal stretches that host large values of maximum wave set-up are located in bayheads where the sediment is comparatively fine and the beach profiles have a relatively gentle slope in the surf zone (Soomere et al., 2007).

Given several uncertainties in the data set, limited knowledge about the nature of the particular nearshore areas, possible shortages in the evaluation of the wave parameters in single extreme storms and unresolved questions of the estimates of the set-up height, we specifically focus on the parameters of the climatology of wave set-up that are less sensitive with respect to the listed uncertainties but have a crucial role in the future management (including more detailed modelling) of the related issues. These are (i) the potential locations of the high set-up, (ii) a comparative climatology of set-up events and (iii) the properties and timing of typical storms that may produce high set-up in specific sections.

Solving the listed tasks, to a first approximation, is feasible using relatively simple parameterisations of the set-up height based on the primary wave properties. A straightforward estimate can be derived using the simplest concept of gradual wave breaking in the nearshore, namely that the ratio of the breaking-wave height H_b to the associated depth d_b – the so-called breaking index $\gamma_b = H_b/d_b$ – remains constant in the entire surf zone (Lentz and Raubenheimer, 1999). In ideal conditions the maximum set-up height (Dean and Dalrymple, 1991) would be

$$\bar{\eta}_{\max} = \frac{5}{16} \gamma_b H_b. \quad (1)$$

The assumption of the constant value of γ_b across the surf zone has been questioned by several authors (Raubenheimer et al., 1996; Power et al., 2010). On the one hand, there is some evidence that it probably increases shoreward (Raubenheimer et al., 2001; Yemm, 2004). But on the other hand, several observations in the surf zone have indicated that γ_b may

be much smaller there (Lentz and Raubenheimer, 1999), and often only in the range of $0.2 \leq \gamma_b \leq 0.5$ (Sallenger and Holman, 1985; Raubenheimer et al., 1996). This change may, to some extent, affect the numerical values of the wave set-up at specific, individual locations but evidently does not change the location of areas of high and low values of the set-up.

A commonly used assumption in coastal engineering is that a wave approaching a natural beach breaks when its height is 78 % of the water depth at this location, so that equivalently the breaking index is $\gamma_b \approx 0.78$ (Dean and Dalrymple, 1991, 2002). For strongly reflecting and/or steep beaches the breaking index may reach values ~ 1.5 , while for domains with an almost horizontal bed it is in the range of 0.55–0.6 (Nelson, 1994; Massel, 1996). On sandy beaches $\bar{\eta}_{\max} \approx 0.17 H_{S10}$, where H_{S10} is the significant wave height at a depth of 10 m (Guza and Thornton, 1981; Coastal Engineering Manual, 2002). These variations in the parameterisation of the maximum set-up evidently have a larger impact on the identification of the potential areas of high set-up. As the coasts in the study area considered here are mostly sedimentary with gently sloping profiles resembling Dean's equilibrium profile, the use of $\gamma_b = 0.8$ (Dean and Dalrymple, 1991) and, consequently, $\bar{\eta}_{\max} \approx 0.25 H_b$ is justified for our purposes.

The time series of wave properties are calculated for a selection of grid cells located offshore the surf zone at different depths (Fig. 2). At many locations the water depth is much larger than the breaking depth for the waves generating the highest set-up; therefore it is necessary to account for the transformation of waves from the grid cells to the breaker line. The processes of shoaling and refraction during the wave propagation from the grid cells to the breaking line are evaluated using the common assumptions that (i) the numerically evaluated wave field is monochromatic, with (ii) the wave height equal to the modelled significant wave height, (iii) the period equal to the peak period, and (iv) wave directions matching the evaluated mean direction. This latter assumption implicitly means that the directional spreading of natural wave fields is ignored in the analysis; consequently, the onshore component of the radiation stress is overestimated by about 10–12 % (Feddersen, 2004). Moreover, we assume that within a particular coastal section the depth isolines seaward of the breaker line are straight and parallel to the average orientation of the coastline. This set of assumptions allows the use of linear wave theory for estimates of the breaking-wave height.

Let the wave height, group speed and celerity at a calculation point be H_0 , c_{g0} and c_{f0} , respectively. The height H_b at the breaking line is

$$H_b = H_0 \left(\frac{c_{g0} \cos \theta_0}{c_{gb} \cos \theta_b} \right)^{1/2}, \quad (2)$$

where θ_0 is the attack angle at the calculation point and θ_b is the attack angle at the breaking line. Breaking waves are

normally long waves and thus their group speed is $c_{gb} = \sqrt{g d_b} = \sqrt{g H_b / \gamma_b}$, where g is the acceleration due to gravity. The impact of refraction can be estimated from Snell's law $\sin \theta / c_f = \text{const}$ along the wave rays. For the breaking waves the phase speed $c_{fb} = c_{gb}$ and thus

$$\sin \theta_b = \sin \theta_0 \frac{c_{fb}}{c_{f0}} = \sin \theta_0 \frac{\sqrt{g H_b / \gamma_b}}{c_{f0}}, \quad (3)$$

from which we reach the following equation with respect to the breaking height:

$$H_b^4 c_{gb}^2 \left(1 - \frac{c_{fb}^2}{c_{f0}^2} \sin^2 \theta_0 \right) = H_b^4 \frac{g H_b}{\gamma_b} \left(1 - \frac{g H_b}{\gamma_b} \frac{\sin^2 \theta_0}{c_{f0}^2} \right) = H_0^4 c_{g0}^2 (1 - \sin^2 \theta_0). \quad (4)$$

Equation (4) is an algebraic equation of 6th order with respect to H_b with three non-zero coefficients. The leading term and the constant term have the same sign, while the coefficient of H_b^5 has the opposite sign. The relevant polynomial with respect to H_b has exactly one minimum at $H_b = 5 \gamma_b c_{f0}^2 / (6g \sin^2 \theta_0)$ and tends to positive infinity if $H_b \rightarrow \pm \infty$. Therefore, Eq. (4) has exactly two real positive solutions provided that

$$6^6 g^4 H_0^4 c_{g0}^2 \sin^{10} \theta_0 (1 - \sin^2 \theta_0) \leq 5^5 \gamma_b^4 c_{f0}^{10}. \quad (5)$$

It has a double, real solution if the expressions at the right- and left-hand side of Eq. (5) are equal, and has no real solutions for other combinations of the wave parameters and water depth. An estimate of the breaking-wave height is given by the smaller real solution. For almost-incident waves (for which the breaking angle θ_b may be assumed zero and $\cos \theta_b = 1$) Eq. (4) can be reduced to an explicit formula for H_b . The resulting expression under-predicts the breaking-wave height by approximately 12 % (Dalrymple et al., 1977; Dean and Dalrymple, 1991). This under-prediction to some extent counterbalances the over-prediction of the onshore radiation stress stemming from the assumption of unidirectional waves.

Physical arguments suggest that Eq. (4) should always have real solutions if the modelled wave height is $H_0 < d_b / \gamma_b$, that is, the waves are not yet breaking. The domain of existence of real solutions to Eq. (4) is actually somewhat more limited by the inequality Eq. (5). This feature can be, to some extent, speculative as no rigorous proof seems to be easily available, attributed to the impact of the wave set-down in relatively shallow waters. This phenomenon to some extent decreases the effective water depth under large waves. The magnitude of this effect is (Longuet-Higgins and Stewart, 1964)

$$\Delta d = - \frac{H_0^2 k}{8 \sinh 2kd}, \quad (6)$$

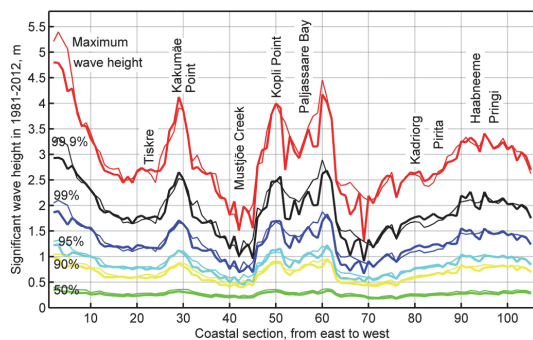


Fig. 3. Maximum wave heights, higher quantiles and median wave height in the nearshore of the study area in 1981–2012. Thin lines indicate the modelled wave heights, and bold lines show values for the breaking-wave heights calculated from Eq. (4). Geographical locations and the position of the coastal sections are indicated in Fig. 2.

where k is the wave number and d is the undisturbed water depth in the absence of waves. In our calculations, real valued solutions always exist if the modelled wave height was such that $H_0 < (d + \Delta d)/\gamma_b$.

The leading term of Eq. (4) vanishes for incident waves. In this case there is no refraction, and condition (2) reduces to $H_b^2 = H_0^2 c_{g0}/c_{gb} = H_0^2 c_{g0} \sqrt{\gamma_b}/(g H_b)$, from which the breaking depth can be explicitly expressed as $H_b = (H_0^4 c_{g0}^2 \gamma_b / g)^{1/5}$ (Dean and Dalrymple, 1991).

In calculations, the linear dispersion relation $\omega = 2\pi/T = \sqrt{gk \tanh kd}$, where ω is the angular frequency and T is the wave period, is solved exactly (that is, with about 7 correct decimal digits, which is the precision of replication of decimal numbers in a 32-bit computer) for wave number k and water depth d at the cell of the WAM model. These values were used to calculate the phase and group speed of the numerically modelled waves. In order to optimally replicate the behaviour of the largest waves, the peak period calculated by the WAM model was used as the wave period.

There were a few cases when the incoming wave height was very small (well below 10 cm) and the ratio of the constant term to the coefficient of the leading term was also small, of the order of 10^{-7} . In these cases the root-finding subroutine of the 32-bit computer failed to produce a solution, and an approximate value corresponding to the exact solution of Eq. (5) with a zero constant term was applied. These cases were, in any case, irrelevant for our purposes, as low wave heights do not lead to any real danger.

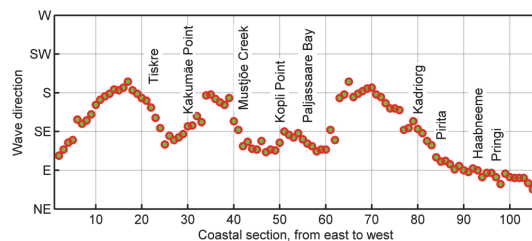


Fig. 4. Wave propagation directions corresponding to the highest waves that occurred in the study area in 1981–2012. Differing from meteorology, wave modellers indicate the direction in which waves propagate.

3 Results

3.1 The highest waves

The overall maximum wave height H_{\max} in the study area was 5.4 m (Fig. 3). This value was reached only once at the westernmost section during a furious storm on 18–19 October 1998 when a westerly wind reached 25 m s^{-1} during two sequential measurement points in time, so over at least three hours. This coastal section (with a depth of 13 m in the model grid) is completely open to the west, north-west and north, that is, to the directions of the largest waves. The largest waves, not unexpectedly, occurred at the three headlands. The possibility of occurrence of quite high waves in the interior of Tallinn Bay (at Pirita Beach) and along the eastern coast of the Viimsi Peninsula reflects the predominance of western and NNW storms among those which produce large waves in the study area.

The wave propagation direction in the storms that have produced the highest waves in individual coastal sections varies considerably, from east to south-south-west. The results of Fig. 4 suggest that each section has its own perfect storm in which the largest waves occur. Such an extensive variation of the approach direction of the highest waves obviously reflects the complexity of the geometry of the study area and simply mirrors the fact that different coastal sections are open to waves from different directions.

All the highest-ever waves in the study occurred in four storms (Fig. 5): western storm on 18–19 October 1998 (maximum wind speed 25 m s^{-1} , direction 260° – 280°), WSW to WNW storm on 29 November 1999 (25 m s^{-1} , 220° – 290°), NNW storm on 15–16 November 2001 (23 m s^{-1} , 320° – 340°), and NW storm of 27–28 October 2006 (23 m s^{-1} , 300° – 320°). Among these, the storm of 15–16 November 2001 set the previous maximum water level (1.35 m) in Tallinn Bay (Suursaar et al., 2006). The peak periods (not shown) were all in the range of 7–9 s in these events. Three of the listed storms created the highest waves in most of the study area, whereas the storm of 29 November 1999 produced the highest waves only in three coastal sections.

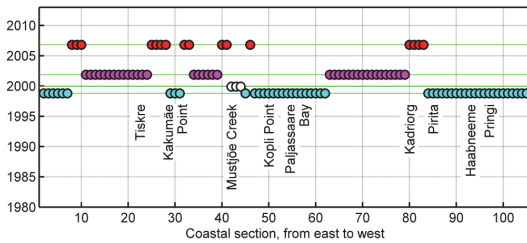


Fig. 5. Four storms (marked with different colours) that caused the highest waves in the study area in 1981–2012.

Interestingly, the “one-hundred-year storm” on 8–9 January 2005 that produced the all-time peak water level for many sites in the eastern Baltic Sea (Suursaar et al., 2006), and also very high waves in the Gulf of Finland (Soomere et al., 2008a), did not produce very high waves in any section of the study area. Another interesting feature of Fig. 5 is that all of the highest waves have occurred during the last decade. This may be indicative of an increase in the overall wind speed. However, another explanation – that the predominant wind direction in the strongest storms has changed over the decades – seems to be a more adequate explanation as will be discussed below.

The ratio of the maximum wave height and the 99.9 percentile (not shown) varies by about 30% in the study area, from 1.42 to 1.78. This level of variation signals that in this region the distributions of different wave heights may have quite different properties for different sections. Although not unexpected, this feature also indicates that the straightforward use of the classical estimates for properties in the nearshore (such as the closure depth or the width of the equilibrium beach profile), developed for open-ocean coasts, may lead to considerable errors for Baltic Sea conditions. For example, the simplified estimate (Houston, 1996) for the closure depth based on the annual average significant wave height implicitly assumes that the ratio of the 99.863 percentile ($H_{0.137\%}$ or threshold for the wave height that is exceeded 12 h a year) and the annual average wave height H_{mean} is 4.5. This ratio varies from about 3.7 to 6.1, whereas its average over the study area is about 5.

3.2 Almost-incident waves

The analysis performed here was for waves approaching from any direction. The approach angle of such waves varies from almost zero up to 90° for several sections located at headlands and even up to 135° for one section (Fig. 6). Waves that approach the coast obliquely mostly produce longshore current rather than high set-up because the cross-shore component of the radiation stress is mostly responsible for set-up (Apotsos et al., 2008). The highest set-up occurs when waves approach the coast almost perpendicularly (i.e. normal to the

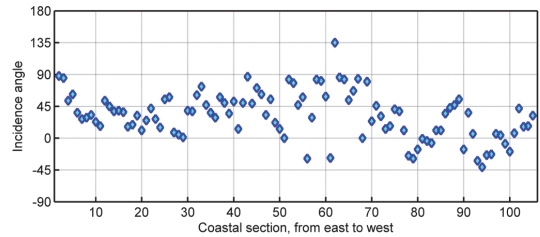


Fig. 6. The angle between the normal to the coast and wave approach direction for the highest waves in the study area in 1981–2012.

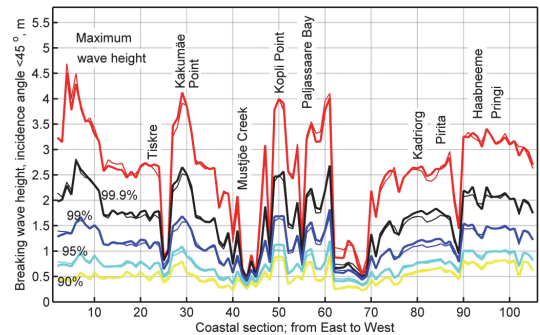


Fig. 7. Maximum wave heights, higher quantiles and median wave height for waves approaching from the direction of maximally $\pm 45^\circ$ with respect to the normal to the coast. Thin lines indicate the modelled wave heights, and bold lines show values for the breaking-wave heights calculated from Eq. (4).

coastline). The crucial parameter for extreme set-up height is the maximum height of waves that approach a coastal section from a narrow range of direction. If the height of such almost-incident waves is much lower than the all-term highest waves, the onshore component of the radiation stress in such waves is relatively limited and the problem with high set-up may not occur at all.

Not surprisingly, both extreme and average wave heights from a narrow direction range, with respect to the normal to the coast (Fig. 7), are much lower than those pictured in Fig. 3. The largest decrease occurs in semi-sheltered sections of the coast, whereas such wave heights for a few headlands remain almost unchanged. Several such sections are implicitly protected by the geometrical shape of the bays (Caliskan and Valle-Levinson, 2008), or by intense refraction of wave fields that redirects part of the wave energy towards the coastal stretches that are located relatively close to the entrance of the bay and, in this way, reduces the wave height in the bay interior.

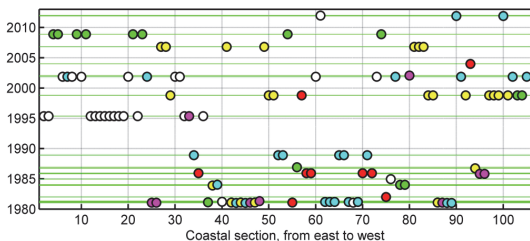


Fig. 8. Pattern of storms generating the highest waves approaching from the direction of $\pm 15^\circ$ with respect to the normal to the coast. The horizontal lines indicate storms that produced the highest almost-normal waves at least in one coastal section. Each storm is marked with a single colour. The colours vary cyclically.

Given the highly variable orientation of the coastline, it is natural to expect that for certain coastal sections the highest waves that approach the coast directly are generated by storms that are not among the strongest ones. Somewhat surprisingly, the collection of storms that produce the highest waves changes radically if waves whose propagation direction is at a relatively small angle to the coast normal are considered. While only four storms were responsible for the all-time highest waves in the study area, 18 different storms produce the all-time highest waves approaching the coast at an angle less than $\pm 45^\circ$ with respect to the normal to the coast. The number of different storms increases to 32 if only waves approaching the coast at an angle less than $\pm 30^\circ$ are considered and increases to 41 for almost-incident waves ($\pm 10^\circ$). Apart from the increase in the number of such storms, their distribution over the time period in question changes radically. For example, for the highest waves approaching from the direction of $\pm 15^\circ$ (Fig. 8), the four storms depicted in Fig. 5 are only responsible for the all-time highest set-up in about 1/3 of the coastal sections. The above-mentioned storm in January 2005 does not feature in this measure at all.

A large number of all-time highest almost-incident waves (and thus of the all-time highest wave set-up in the relevant section) occurred in the 1980s. As many coastal sections around Tallinn (which was much smaller then) were not open to the public, these events evidently remained unnoticed and therefore are not accounted for in contemporary statistics (which started after Estonia obtained independence in the beginning of the 1990s). A particularly deceptive feature of the short-term statistics for decision-makers is the period of relatively low wave activity in the 1990s from the directions to which the coasts of the city of Tallinn are open. It is thus not surprising that the statistics of storms and high wave-induced set-up can be misleadingly interpreted as showing a rapid increase in a certain type of wave activity at the turn of the millennium. A much more appropriate explanation is that the directional structure of strong storms exhibits decadal-scale variations in the region of the Gulf of Finland.

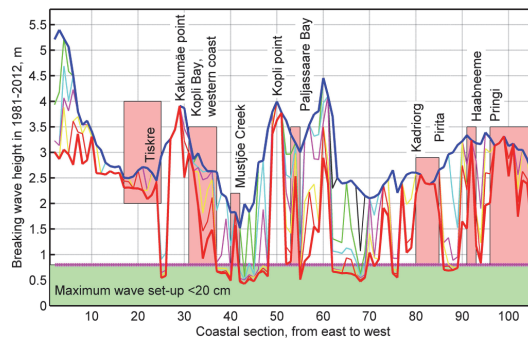


Fig. 9. Highest breaking waves (coloured lines) approaching from different ranges of directions with respect to the coast normal in the study area. The bold blue line shows the all-time highest waves approaching from any direction, and the bold red line shows the all-time highest almost-incident waves ($\pm 10^\circ$ with respect to the coast normal). The light red bars indicate the regions with gently sloping coast in which the maximum set-up likely exceeds 40 cm.

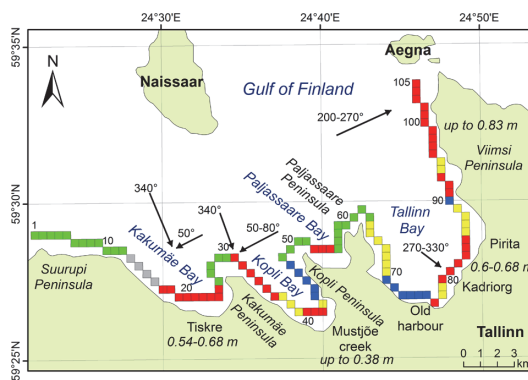


Fig. 10. Areas around Tallinn potentially affected by high wave set-up (red squares indicate the maximum set-up) with the respective directions of wave propagation (arrows). Yellow squares indicate coastal stretches where the maximum wave set-up is less than 20 cm, green squares indicate areas where high set-up is evidently not possible because of the convex shape of the coastline, grey squares indicate areas naturally protected by a cliff and blue squares represent areas containing various engineering structures.

3.3 The endangered areas

The areas endangered by high wave set-up are coastal sections with a convex shape that are often affected by high almost-incident waves. Areas satisfying the latter condition can be easily identified by gradually narrowing the range of directions of high waves (Fig. 9). A decision about whether dangerous values of wave set-up may actually occur also requires the geographical map of the area (Fig. 10) and data

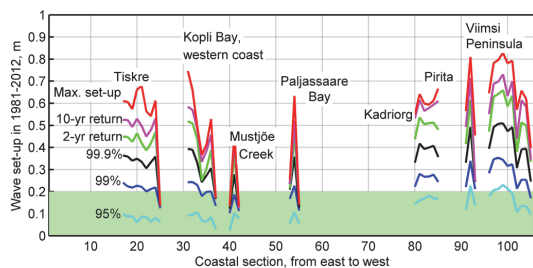


Fig. 11. Maximum wave set-up values, higher quantiles of set-up heights and 2 yr and 10 yr return values of set-up heights for the coastal sections where high set-up is an issue.

about the nature of particular sections of the coastline. It turns out that substantial levels of wave set-up are likely in the residential area of Tiskre and specifically along the western coast of the Viimsi Peninsula. The danger is relatively low at the mouth of Mustjõe Creek – an area that technically is open to high waves but which apparently is implicitly protected by a favourable combination of the geometry and bathymetry of Kopli Bay.

It is not clear whether or not the danger of high wave set-up actually occurs along the north-eastern coast of the Kakumäe Peninsula. The related hazards are apparently minor along the coastal section from Old City Harbour to Piritä, where the coastline is protected by a seawall that reflects the wave energy and prevents set-up.

The above results have been presented and discussed in terms of maximum wave set-up heights occurring once in a 30 yr period. A somewhat better indication of the realistic level of danger for the coastal stretches that may be affected by high wave set-up provides an estimate of the highest quantiles for the set-up (Fig. 11). While it is expected that the all-time highest values of set-up are an isolated phenomenon, in several areas the 99.9 percentile of the set-up height is quite high, close to 40 cm. For the particular conditions of Tallinn Bay it means that an addition of the magnitude of 25 % of the all-time highest open sea water level occurs in these locations, on average, three times a year. Although these events are not necessarily associated with the overall high water level, such a high occurrence suggests that simultaneous attack of high open sea water level and wave set-up is very likely in these locations. This conjecture is supported by relatively large 2 yr and 10 yr return values of the set-up height in some locations (Fig. 11).

4 Conclusions and discussion

The analysis presented here confirms the well-known conjecture that wave set-up serves as an important constituent of marine-induced coastal hazard. Although several assumptions made in the analysis may, to some extent, oversimplify

the situation and the individual estimates may have quite large uncertainty, the key conclusion is that the contribution of wave set-up may be up to 50 % of the maximum water levels caused by other factors in areas that are open to predominant wind and wave directions. In other words, wave set-up may frequently form about 1/3 of the total water level increase during specific storms. This results in a considerable increase in the risk of coastal flooding in regions that normally experience a relatively small range of the fluctuations of the local water level such as the Baltic Sea, Black Sea or the Mediterranean Sea.

The extensive variation given here of the climatological properties of set-up heights along the study area highlights a particularly insidious feature of this phenomenon – its substantial dependence on the match of the wave propagation direction and the geometry of the coastline. This feature is probably not decisive along open-ocean coasts, where high waves usually approach the coast under small incidence angles and produce high set-up in long coastal stretches. It is, however, accentuated in semi-sheltered domains with complex geometry of the coastline where the location of high set-up may substantially vary, depending not only on the storm wind direction but also on the wave period (which affects the intensity of refraction and thus also the wave approach direction). The resulting, dangerously high, set-up in selected coastal sections may be easily overlooked or, especially in urban areas, associated with other phenomena (e.g. heavy rainfall, snow melt or flash flooding of a river).

The analysis of the climatology of high set-up events in such areas with complex geometry is thus additionally complicated because the return period of unfavourable combinations of wind and wave properties is substantially larger than that of just high waves or water levels alone. On the one hand, this peculiarity requires us to obtain much longer time series of wave set-up in order to reach adequate statistics of this phenomenon in coastal sections that are orientated differently, similarly to the proper evaluation of statistics of winds from particular directions. On the other hand, this phenomenon, if it occurs, contains particularly large hazards in low-lying urban environments, with possibly significant implications on the functioning of infrastructure in neighbouring areas and on the availability of evacuation roads.

There are several simple ways to avoid high wave set-up. For example, this phenomenon normally does not occur if the coast is protected by a seawall. Another, option is to use “soft” measures, e.g. the ability of natural roughness of the coastal zone (reed, bushes and stones) to substantially damp out this phenomenon. As high set-up is dangerous in combination with high water levels, this means that it is sensible to keep naturally occurring bushes at the level of the maximum expected storm surge, an option that is not always easy to explain to the decision-makers, the public and especially to developers. This is thus a challenge for smart and sustainable planning and management of urban coastal areas, but it

is a natural, low-cost measure to mitigate this type of marine coastal hazard.

The numerical values of the set-up climatology presented here have been evaluated in ideal conditions additionally using a number of approximations, and thus they should be interpreted as indicative values. The correspondence between the results and estimates derived from in situ observations suggests that the estimates are still realistic in cases when the set-up process is not unduly affected by wave reflection or damping. The danger here is that the estimates are invariant with respect to the background water level. In other words, even if the nearshore is stony, as it is in many locations of the coastline of Tallinn especially along the Viimsi Peninsula, then in the case of a considerable storm surge (say, about 1 m) the waves will break in a completely different location. Therefore, developed areas (e.g. lawned gardens, parking areas) theoretically within reach of high water may become sources of increased risk, in terms of extensive wave set-up. The analysis above shows that potentially affected areas form in total about 50 % of the entire coastline. This estimate, although very rough, simply expresses the balance between the convex- and concave-shaped sections of the coastline.

The intermittent character of the location of coastal stretches which experience high set-up, and the strong dependence of the areas with highest set-up on the properties of a particular storm, is a major challenge for any crisis management team. Although the parameters of approaching waves can be predicted with quite good quality nowadays, the prediction of high set-up requires a proper replication of wave periods (which is a challenge anyway even for the very best contemporary wave models) and wave propagation directions. In essence, this problem is equivalent to the exact forecast of a hurricane landing point, where there is still some room for improvement.

Apart from the analysis of the properties of hazard for this intricate coastline, the results included here give an interesting insight into some potentially deceptive features of wave statistics. If one concentrates on the properties of the highest waves, Fig. 5 produces an impression that the 1980s and 1990s were relatively mild and that the wave climate has become considerably more severe since the end of the 1990s. Figure 8 clarifies the picture by demonstrating that, for many directions, the strongest wave storms occurred at the beginning of the 1980s. Moreover, it suggests that the wave climate (in terms of the number of coastal sections in a particular year where the all-time highest wave set-up has been reached) has become clearly milder now than it was in the 1980s. In essence, this controversy basically reflects the core property of climate changes in the northern Baltic Sea and probably in many other areas in the world: changes become more evident in the wind direction rather than in the wind strength. This aspect of climate change is perhaps underrated today, although the related changes in the wave propagation direction eventually have major consequences on the coastal processes (Charles et al., 2012a, b; Räämet et al., 2010). A

more detailed analysis of various wave phenomena may thus give some extremely interesting insight into this still unidentified feature of climate change.

Acknowledgements. This study was a part of the project “Science-based forecast and quantification of risks to properly and timely react to hazards impacting Estonian mainland, air space, water bodies and coasts” (TERIKVANT) supported by the European Union (European Regional Development Fund, ERDF) and managed by the Estonian Research Council in the framework of the environmental technology R&D programme KESTA. The research was partially supported by the targeted financing of the Estonian Ministry of Education and Research (grant SF0140007s11), by the Estonian Science Foundation (grant no. 9125), and through support of the ERDF to the Centre of Excellence in Non-linear Studies (CENS) and the Mobilitas project MTT63. The authors are deeply grateful to the Finnish Meteorological Institute for providing Kalbådagrund wind data. Financial contribution of the city of Tallinn towards detailed analysis of wave properties in particularly endangered coastal stretches is gratefully acknowledged.

Edited by: I. Didenkulova

Reviewed by: two anonymous referees

References

- Apotsos, A., Raubenheimer, B., Elgar, S., Guza, R. T., and Smith, J. A.: Effect of wave rollers and bottom stress on wave setup, *J. Geophys. Res.-Oceans*, 112, C02003, doi:10.1029/2006JC003549, 2007.
- Apotsos, A., Raubenheimer, B., Elgar, S., and Guza, R. T.: Wave-driven setup and alongshore flows observed onshore of a submarine canyon, *J. Geophys. Res.-Oceans*, 113, C07025, doi:10.1029/2007JC004514, 2008.
- Bertin, X., Fortunato, A. B., and Oliveira, A.: A modeling-based analysis of processes driving wave-dominated inlets, *Cont. Shelf Res.*, 29, 819–834, 2009.
- Broman, B., Hammarklint, T., Rannat, K., Soomere, T., and Valdmann, A.: Trends and extremes of wave fields in the north-eastern part of the Baltic Proper, *Oceanologia*, 48, 165–184, 2006.
- Caliskan, H. and Valle-Levinson, A.: Wind-wave transformations in an elongated bay, *Cont. Shelf Res.*, 28, 1702–1710, 2008.
- Cariolet, J.-M. and Suarez, S.: Method of mapping flood hazard in low-lying coasts, *Houille Blanche*, 2, 52–58, 2009.
- Charles, E., Idier, D., Thiebot, J., Le Cozannet, G., Pedreros, R., Ardhuin, F., and Planton, S.: Present wave climate in the Bay of Biscay: Spatiotemporal variability and trends from 1958 to 2001, *J. Climate*, 25, 2020–2039, 2012a.
- Charles, E., Idier, D., Delecluse, P., Deque, M., and Le Cozannet, G.: Climate change impact on waves in the Bay of Biscay, France, *Ocean Dynam.*, 62, 831–848, 2012b.
- Cheng, X. T., Evans, E. P., Wu, H. Y., Thorne, C. R., Han, S., Simm, J. D., and Hall, J. W.: A framework for long-term scenario analysis in the Taihu Basin, China, *J. Flood Risk Manage.*, 6, 3–13, 2013.
- Climatological Ice Atlas for the Baltic Sea, Kattegat, Skagerrak and Lake Vänern (1963–1979), Swedish Meteorological and Hydro-

- logical Institute, Norrköping, Sweden, and Institute of Marine Research, Helsinki, Finland, Norrköping, 1982.
- Coastal Engineering Manual: U. S. Army Corps of Engineers (USACE), Manual EM 1110-2-1100, 2002.
- Dalrymple, R. A., Eubanks, R. A., and Birkemeier, W. A.: Wave-induced circulation in shallow basins, *J. Waterw. Ports Coast. Ocean Div. ASCE*, 103, 117–135, 1977.
- Dawson, R. J., Speight, L., Hall, J. W., Djordjevic, S., Savic, D., and Leandro, J.: Attribution of flood risk in urban areas, *J. Hydroinform.*, 10, 275–288, 2008.
- Dean, R. G. and Bender, C. J.: Static wave set-up with emphasis on damping effects by vegetation and bottom friction, *Coast. Eng.*, 53, 149–165, 2006.
- Dean, R. G. and Dalrymple, R. A.: *Water wave mechanics for engineers and scientists*, World Scientific, 1991.
- Dean, R. G. and Dalrymple, R. A.: *Coastal Processes with Engineering Applications*, Cambridge University Press, Cambridge, 2002.
- Fedderson, F.: Effect of wave directional spread on the radiation stress: comparing theory and observations, *Coast. Eng.*, 51, 473–481, 2004.
- Filipot, J.-F. and Cheung, K. F.: Spectral wave modeling in fringing reef environments, *Coast. Eng.*, 67, 67–79, 2012.
- Guza, R. T. and Thornton, E. B.: Wave set-up on a natural beach, *J. Geophys. Res.-Ocean Atmos.*, 86, 4133–4137, 1981.
- Hall, J. W., Dawson, R. J., Barr, S. L., Batty, M., Bristow, A. L., Carney, S., Dagoumas, A., Ford, A. C., Harpham, C., Tight, M. R., Walsh, C. L., Watters, H., and Zanni, A. M.: City-scale integrated assessment of climate impacts, adaptation, and mitigation, in: *Energy efficient cities: assessment tools and benchmarking practices*, edited by: Bose, R. K., The World Bank, 63–83, 2010.
- Harper, B., Hardy, T., Mason, L., and Fryar, R.: Developments in storm tide modelling and risk assessment in the Australian region, *Nat. Hazards*, 51, 225–238, 2009.
- Heidarzadeh, M., Bonneton, P., Bonneton, N., and Tissier, M.: Field observations of wave-induced set-up on the french Aquitanian coast, in: *Proceedings of the 28th International Conference on Ocean, Offshore and Arctic Engineering (OMAE 2009)*, Honolulu, 31 May–5 June 2009, ASME, vol. 4, 233–241, 2009.
- Höglund, A., Meier, H. E. M., Broman, B., and Kriezi, E.: Validation and correction of regionalised ERA-40 wind fields over the Baltic Sea using the Rossby Centre Atmosphere Model RCA3.0, *Rapport Oceanografi No. 97*, Swedish Meteorological and Hydrological Institute, Norrköping, Sweden, 2009.
- Houston, J. R.: Simplified Dean's method for beach-fill design, *J. Waterw. Port C-ASCE* 122, 143–146, 1996.
- Hsu, T.-W., Hsu, J. R.-C., Weng, W.-K., Wang, S.-K., and Ou, S.-H.: Wave setup and setdown generated by obliquely incident waves, *Coast. Eng.*, 53, 865–877, 2006.
- Irish, J. L. and Canizares, R.: Storm-wave flow through tidal inlets and its influence on bay flooding, *J. Waterw. Port C-ASCE*, 135, 52–60, 2009.
- Jain, I., Rao, A. D., Jitendra, V., and Dube, S. K.: Computation of expected total water levels along the east coast of India, *J. Coastal Res.*, 26, 681–687, 2010a.
- Jain, I., Rao, A. D., and Ramesh, K. J.: Vulnerability assessment at village level due to tides, surges and wave set-up, *Mar. Geod.*, 33, 245–260, 2010b.
- Keevallik, S. and Soomere, T.: Towards quantifying variations in wind parameters across the Gulf of Finland, *Estonian J. Earth Sci.*, 59, 288–297, 2010.
- Komen, G. J., Cavaleri, L., Donelan, M., Hasselmann, K., Hasselmann, S., and Janssen, P. A. E. M.: *Dynamics and modelling of ocean waves*, Cambridge University Press, Cambridge, 1994.
- Launiainen, J. and Laurila, T.: Marine wind characteristics in the northern Baltic Sea, *Finnish Mar. Res.*, 250, 52–86, 1984.
- Lentz, S. and Raubenheimer, B.: Field observations of wave setup, *J. Geophys. Res.-Oceans*, 104, 867–875, 1999.
- Longuet-Higgins, M. S. and Stewart, R. W.: Radiation stresses in water waves: a physical discussion with applications, *Deep-Sea Res.*, 11, 529–562, 1964.
- Massel, S. R.: On the largest wave height in water of constant depth, *Ocean Eng.*, 23, 553–573, 1966.
- McInnes, K. L., O'Grady, J. G., and Hubbert, G. D.: Modelling sea level extremes from storm surges and wave set-up for climate change assessments in southeastern Australia, *J. Coastal Res., Special Issue*, 56, 1005–1009, 2009.
- Mietus, M. (Ed.): *The climate of the Baltic Sea Basin. Marine meteorology and related oceanographic activities*, Rep. No. 41, World Meteorol. Org. Geneva, 64 pp., 1998.
- Nayak, S., Bhaskaran, P., and Venkatesan, R.: Near-shore wave induced set-up along Kalpakkam coast during an extreme cyclone event in the Bay of Bengal, *Ocean Eng.*, 55, 52–61, 2012.
- Nelson, R. C.: Depth limited design wave heights in very flat regions, *Coastal Eng.*, 23, 43–59, 1994.
- O'Grady, J. G. and McInnes, K. L.: Wind waves and their relationship to storm surges in northeastern Bass Strait, *Aust. Meteorol. Oceanogr. J.*, 60, 265–275, 2010.
- Orlenko, L. R., Lopatukhin, L. I., and Portnova, G. L. (Eds.): *Studies of hydrometeorological regime of Tallinn Bay, Gidrometeoizdat, Leningrad*, 1984 (in Russian).
- Pettersson, H., Kahma, K., and Tuomi, L.: Wave directions in a narrow bay, *J. Phys. Oceanogr.*, 40, 155–169, 2010.
- Power, H. E., Hughes, M. G., Aagaard, T., and Baldock, T. E.: Nearshore wave height variation in unsaturated surf, *J. Geophys. Res.-Oceans*, 115, C08030, doi:10.1029/2009JC005758, 2010.
- Räämet, A., Suursaar, Ü., Kullas, T., and Soomere, T.: Reconsidering uncertainties of wave conditions in the coastal areas of the northern Baltic Sea, *J. Coastal Res., Special Issue*, 56, 257–261, 2009.
- Räämet, A., Soomere, T., and Zaitseva-Pärnaste, I.: Variations in extreme wave heights and wave directions in the north-eastern Baltic Sea, *Proc. Estonian Acad. Sci.*, 59, 182–192, 2010.
- Raubenheimer, B., Guza, R. T., and Elgar, S.: Wave transformation across the inner surf zone, *J. Geophys. Res.-Oceans*, 101, 25589–25597, 1996.
- Raubenheimer, B., Guza, R. T., and Elgar, S.: Field observations of set-down and set-up, *J. Geophys. Res.-Oceans*, 106, 4629–4638, 2001.
- Raukas, A. and Hyvärinen, H. (Eds.): *Geology of the Gulf of Finland, Valgus, Tallinn*, 1992 (in Russian).
- Sallenger, A. H. and Holman, R. A.: Wave energy saturation on a natural beach of variable slope, *J. Geophys. Res.-Oceans*, 90, 11939–11944, 1985.
- Samuelsson, P., Jones, C. G., Willén, U., Ullerstig, A., Gollvik, S., Hansson, U., Jansson, C., Kjellström, E., Nikulin, G., and

- Wyser, K.: The Rossby Centre Regional Climate Model RCA3: Model description and performance, *Tellus A*, 63, 4–23, 2011.
- Schmager, G., Fröhle, P., Schrader, D., Weisse, R., and Müller-Navarra, S.: Sea state, tides, in: State and evolution of the Baltic Sea 1952–2005, edited by: Feistel, R., Nausch, G., and Wasmund, N., Wiley, Hoboken, New Jersey, 143–198, 2008.
- Seifert, T., Tauber, F., and Kayser, B.: A high resolution spherical grid topography of the Baltic Sea, 2nd Edn., Baltic Sea Science Congress, Stockholm 25–29 November 2001, Poster #147, available at: www.io-warnemuende.de/iowtopo, 2001.
- Shi, F. and Kirby, J. T.: Discussion of “Wave set-up and setdown generated by obliquely incident waves” by T.-W. Hsu et al., *Coastal Engineering*, 53, 865–877, 2006, *Coast. Eng.*, 55, 1247–1249, 2008.
- Sooäär, J. and Jaagus, J.: Long-term variability and changes in the sea ice regime in the Baltic Sea near the Estonian coast, *Proc. Estonian Acad. Sci. Eng.*, 13, 189–200, 2007.
- Soomere, T.: Wind wave statistics in Tallinn Bay, *Boreal Environ. Res.*, 10, 103–118, 2005.
- Soomere, T.: Wave regimes and anomalies off north-western Saaremaa Island, *Proc. Estonian Acad. Sci. Eng.*, 7, 157–173, 2001.
- Soomere, T. and Räämet, A.: Spatial patterns of the wave climate in the Baltic Proper and the Gulf of Finland, *Oceanologia*, 53, 335–371, 2011.
- Soomere, T., Kask, A., Kask, J., and Nerman, R.: Transport and distribution of bottom sediments at Pirita Beach, *Estonian J. Earth Sci.* 56, 233–254, 2007.
- Soomere, T., Behrens, A., Tuomi, L., and Nielsen, J. W.: Wave conditions in the Baltic Proper and in the Gulf of Finland during windstorm Gudrun, *Nat. Hazards Earth Syst. Sci.*, 8, 37–46, doi:10.5194/nhess-8-37-2008, 2008a.
- Soomere, T., Myrberg, K., Leppäranta, M., and Nekrasov, A.: The progress in knowledge of physical oceanography of the Gulf of Finland: a review for 1997–2007, *Oceanologia*, 50, 287–362, 2008b.
- Starr, V. P.: A momentum integral for surface waves in deep water, *J. Mar. Res.*, 6, 126–135, 1947.
- Stockdon, H. F., Holman, R. A., Howd, P. A., and Sallenger, A. H.: Empirical parameterization of set-up, swash, and runup, *Coast. Eng.*, 53, 573–588, 2006.
- Suursaar, Ü., Kullas, K., Otsmann, M., Saaremäe, I., Kuik, J., and Merilain, M.: Hurricane Gudrun and modelling its hydrodynamic consequences in the Estonian coastal waters, *Boreal Environ. Res.*, 11, 143–159, 2006.
- Torresan, S., Critto, A., Rizzi, J., and Marcomini, A.: Assessment of coastal vulnerability to climate change hazards at the regional scale: the case study of the North Adriatic Sea, *Nat. Hazards Earth Syst. Sci.*, 12, 2347–2368, doi:10.5194/nhess-12-2347-2012, 2012.
- Torres-Freyermuth, A., Marín-Tapia, I., Coronado, C., Salles, P., Medellín, G., Pedrozo-Acuña, A., Silva, R., Candela, J., and Iglesias-Prieto, R.: Wave-induced extreme water levels in the Puerto Morelos fringing reef lagoon, *Nat. Hazards Earth Syst. Sci.*, 12, 3765–3773, doi:10.5194/nhess-12-3765-2012, 2012.
- Trenhaile, A. S.: Modeling the erosion of cohesive clay coasts, *Coast. Eng.*, 56, 59–72, 2009.
- Tuomi, L., Kahma, K. K., and Pettersson, H.: Wave hindcast statistics in the seasonally ice-covered Baltic Sea, *Boreal Environ. Res.*, 16, 451–472, 2011.
- Tuomi, L., Kahma, K. K., and Fortelius, C.: Modelling fetch-limited wave growth from an irregular shoreline, *J. Marine Syst.*, 105, 96–105, 2012.
- Valdmann, A., Käär, A., Kelpšaitė, L., Kurennoy, D., and Soomere, T.: Marine coastal hazards for the eastern coasts of the Baltic Sea, *Baltica*, 21, 3–12, 2008.
- Vetter, O., Becker, J.-M., Merrifield, M. A., Pequignet, A.-C., Aucan, J., Boc, S. J., and Pollock, C. E.: Wave set-up over a Pacific Island fringing reef, *J. Geophys. Res.-Oceans*, 115, C12066, doi:10.1029/2010JC006455, 2010.
- Yemm, S. P.: Field observation of set-up, M.S. Thesis, Naval Postgraduate School, USA, 45 pp., 2004.

Paper II

Eelsalu M., Soomere T., **Pindsoo K.**, Lagemaa P. 2013. Ensemble approach for projections of return periods of extreme water levels in Estonian waters. *Continental Shelf Research*, 91, 201–210, doi: 10.1016/j.csr.2014.09.012.



Research papers

Ensemble approach for projections of return periods of extreme water levels in Estonian waters

Maris Eelsalu^a, Tarmo Soomere^{a,*}, Katri Pindsoo^a, Priidik Lagemaa^b^a Institute of Cybernetics at Tallinn University of Technology, Akadeemia tee 21, 12618 Tallinn, Estonia^b Marine Systems Institute at Tallinn University of Technology, Akadeemia tee 15a, 12618 Tallinn, Estonia

ARTICLE INFO

Article history:

Received 22 June 2014

Received in revised form

30 August 2014

Accepted 24 September 2014

Available online 2 October 2014

Keywords:

Water level

Extreme value distributions

Ensemble approach

Baltic Sea

Block maxima method

Wave set-up

ABSTRACT

The contribution of various drivers to the water level in the eastern Baltic Sea and the presence of outliers in the time series of observed and hindcast water level lead to large spreading of projections of future extreme water levels. We explore the options for using an ensemble of projections to more reliably evaluate return periods of extreme water levels. An example of such an ensemble is constructed by means of fitting several sets of block maxima (annual maxima and stormy season maxima) with a Generalised Extreme Value, Gumbel and Weibull distribution. The ensemble involves projections based on two data sets (resolution of 6 h and 1 h) hindcast by the Rossby Centre Ocean model (RCO; Swedish Meteorological and Hydrological Institute) and observed data from four representative sites along the Estonian coast. The observed data are transferred into the grid cells of the RCO model using the HIROMB model and a linear regression. For coastal segments where the observations represent the offshore water level well, the overall appearance of the ensembles signals that the errors of single projections are randomly distributed and that the median of the ensemble provides a sensible projection. For locations where the observed water level involves local effects (e.g. wave set-up) the block maxima are split into clearly separated populations. The resulting ensemble consists of two distinct clusters, the difference between which can be interpreted as a measure of the impact of local features on the water level observations.

© 2014 Elsevier Ltd. All rights reserved.

1. Introduction

Flooding of low-lying nearshore areas is one of the largest threats for coastal countries. The associated risks are severely enhanced by the projected increase in the sea level. This increase will eventually over-ride the current postglacial uplift for all Estonian coasts (cf. Johansson et al., 2014). Some information about the changes may be extracted from long-term water level time series. This information, however, is of limited use because of extensive short-term climate variability (Weisse and von Storch, 2010) and associated flooding risks (Gaslikova et al., 2013). In other words, the properties of strong storms and associated surges may change aperiodically, often on a decadal scale, within quite a wide range. For the listed reasons estimates of extreme water levels and their return periods are often constructed using a combination of relatively short-term sets of recorded water level, numerical modelling and various statistical distributions of extreme values (van den Brink et al., 2005; Sterl et al., 2009,

among others). The estimates usually reveal extensive disparity depending on the particular method in use, set of underlying data and regional differences in the storm surge heights (Bardet et al., 2011). The discrepancies can be attributed to a number of reasons, from the shortness and inaccuracy of the observations up to the possible presence of a specific population of intense storms, properties of which do not obey the distribution of commonly occurring wind events (van den Brink et al., 2005; Suursaar and Sooäär, 2007).

The situation is particularly complicated in the Baltic Sea where such populations of extreme water levels in different sea areas are naturally created by the possibility of encountering relatively long-term aperiodic high water levels in the entire sea (Leppäranta and Myrberg, 2009). The predominance of westerly winds among strong wind events additionally modifies the course of water level in the eastern regions of this water body (Suursaar et al., 2006a; Averkiev and Klevanny, 2010). The distribution of deviations of the instantaneous water level from the long-term average is close to a normal distribution (Johansson et al., 2001; Suursaar and Sooäär, 2007). The difference from a Gaussian distribution is insignificant for moderate deviations of both signs. There are two important exceptions. Firstly, all extremely large deviations from the average level correspond to high water level events (Johansson et al., 2001). Secondly, the

* Corresponding author. Tel.: +372 6204176.

E-mail addresses: maris.eelsalu@ioc.ee (M. Eelsalu), soomere@cs.ioc.ee (T. Soomere), katrip@ioc.ee (K. Pindsoo), priidik.lagemaa@msi.ttu.ee (P. Lagemaa).

distribution is not exactly symmetric: relatively high water levels are more probable equivalent low water levels. These properties reflect the well-known asymmetry of water level in the Estonian waters: while high water levels are usually short-living transient events, low water levels often persist for relatively long time. The largest mismatch between a normal distribution and measured or modelled values is evident for extreme surges (Johansson et al., 2001; Suursaar and Sooäär, 2007).

The described deviations of the water level anomalies from a Gaussian distribution are unimportant for applications that address commonly occurring water levels (Stramska, 2013), their spatial and seasonal variations and trends (Hünicke and Zorita, 2008; Hünicke, 2010; Scotto et al., 2009; Stramska et al., 2013), or certain quantiles (Barbosa, 2008; Donner et al., 2012). The non-Gaussian population, however, may substantially affect the results of calculations of exceedance probabilities of rare events in coastal engineering and projections of extreme water levels and their return periods (Suursaar and Sooäär, 2007; Johansson et al., 2011). Such projections are commonly done by using extreme value statistics. In essence, they rely on extrapolations of the water levels beyond the time interval and range of observations or model hindcasts (see, e.g., Mudersbach and Jensen (2009) for a discussion of such methods for the Baltic Sea).

Different methods of this type exploit similar statistical parameters of observed or modelled values of water level and basically differ only in how the existing values are accounted for in the implementation of the particular model. These methods implicitly rely on the assumption that the measured or modelled water levels at least approximately follow certain classical (e.g., a Gaussian or Weibull) distribution. If this assertion is true, other classical statistical methods (such as a Gumbel distribution) can be used for evaluation of their extreme values.

If the empirical distribution of water level time series at a particular location substantially deviates from a Gaussian one, or has a substantial number of outliers, its extreme values not necessarily obey any classical (Fréchet, Weibull or Gumbel, Coles, 2001) extreme-value statistics. It is therefore not surprising that slightly different methods can yield significantly different predictions of extreme water levels and their return periods (e.g., Sterl et al., 2009). Moreover, even the use of the same technique may lead to large spreading of the results owing to the use of various weights of the rare measured values or various options for (the evaluation of) the model parameters (Arns et al., 2013). For example, even the initial de-trending of water level, often applied as a background procedure, may modify the results of the projections of extreme events. The long-term course of water levels in many locations is far from linear (Donner et al., 2012). An obvious shift in the water level trend was observed in the Baltic Sea in the 20th century (Johansson et al., 2001, 2014; Dailidiene et al., 2006). The above-discussed skewness of the distribution of water levels additionally complicates the problem and leads to a much higher increase in the annual maximum water levels compared to the changes in the mean values (Jaagus and Suursaar, 2013). Suursaar and Sooäär (2007) even conclude that no single commonly used extreme value distribution is able to adequately describe or predict extreme water level events in some locations of Estonia.

This situation calls for alternative approaches for the evaluation of extreme water levels and their return periods. A possible first-order solution to improve the performance of the projections of rare water level events is to use an ensemble approach (Christiansen et al., 2010). This approach has become a standard way of addressing of forecasts and projections that are highly sensitive with respect to the initial conditions or certain model parameters (Araújo and New, 2006). The basic idea is that a (possibly weighted) average of a cluster of projections is often a much better forecast than any single model could provide (Cheung, 2001). This approach is usually employed for projections of extreme surges via the construction of an ensemble of models for water level time series (e.g., Sterl et al., 2009; Mel et al.,

2013). In the Baltic Sea conditions it has been also applied to project the local mean sea level rise (Johansson et al., 2014).

In this paper we explore a simple way to create an ensemble for estimates of extreme water levels and their return periods from a viewpoint that offers considerable reduction of computational loads. Namely, instead of re-running atmospheric and water level models, we use three independent data sets (one measured and two modelled), several methods for their handling and a few methods for the assessment of extreme values and their return periods. Doing so is equivalent to implicitly perturbing the “weight” of single block maxima (e.g., annual water level maxima) in the measured or modelled data by using different extreme value distributions rather than perturbing the initial data of simulations. The obvious drawback is that the estimates of errors and uncertainties are not straightforward. However, the simplicity and transparency of this easy-to-use approach evidently counterbalances a certain loss of rigorosity.

The analysis is performed for four coastal regions (Fig. 1) that are representative for a large part of the entire coastline of Estonia and have been extensively considered in earlier studies (Suursaar and Sooäär, 2007). The location near the island of Hiiumaa is characteristic to relatively straight coastal sections and headlands in the north-eastern Baltic Proper where the extreme water levels are comparatively limited. The site near Tallinn portrays coastal segments of semi-enclosed subbasins of the Baltic Sea with highly complicated geometry. A site in Narva Bay represents widely open bays that are vulnerable with respect to large-scale storm surges for almost all westerly wind events. Finally, Pärnu Bay is particularly vulnerable with respect to specific wind events from a narrow direction range and offers one of the largest ranges of water levels in the Baltic Sea basin (Suursaar and Sooäär, 2007). We intentionally selected the grid cells of the used circulation models at a distance of a few km from the observation sites in order to avoid possible distortions of the modelled water level because of insufficient spatial resolution of the local bathymetry and geometry.

Heuristically, the use of an average over an ensemble of projections is only justified if the errors of various projections are random. This property can be to some extent tested (but of course not proved) by looking at the appearance of the entire ensemble. It is natural to expect that projections containing random errors are distributed more or less uniformly within the entire range of projected values. This is usually not the case in dynamical projections of climate change and associated sea level rise (e.g. Johansson et al., 2014) but should be so for projections based on statistical concepts and consistent initial data. In this context, an important outcome of our analysis is the demonstration that the resulting ensemble of projections does not contain any obvious outliers for several representative locations of the Estonian coast in which the observations adequately reflect the open-sea water level. Similar ensembles, however, may exhibit clearly separated clusters for locations where the contribution of local factors to the observed water level is significant.

The paper is organized as follows. Section 2 provides information about the data sets, methods of their handling and statistical distributions used to build the projections of extreme water levels and their return periods. The ensembles of projections for the sites in question and their properties are presented in Section 3. Section 4 discusses the outcome of these projections and possibilities of the practical use of the presented approach.

2. Data and methods

2.1. Hindcast and observed data

The ‘ground truth’ is represented by water level measurements at the four sites that have been performed for many decades

(Suursaar and Sooäär, 2007). For example, the oldest water level records in Tallinn reach back to the year 1809 and regular monthly mean water level records start from the year 1842 (Suursaar et al., 2011). The monthly extreme values have been filed at these sites since the end of the 19th century (Table 1). Time series of regular observations are available from the middle of the 20th century (Table 1) two or four times a day (once in 12 or 6 h) and later on once an hour. As the observation intervals have changed in the course of time, none of the observed time series is completely homogeneous; however, it is likely that various sources of inhomogeneity of the time series do not significantly affect the monthly maxima.

The observed (or measured) values at these sites are presented in the official height system used in Estonia which is called the Baltic Height System BK77 with its reference zero-benchmark at

the Kronstadt near St. Petersburg. The Kronstadt zero is defined as the average water level in Kronstadt in 1825–1840 (Lazarenko, 1986).

Water level observations in three sites (Table 1) have performed in the same location for a long time while one station (Tallinn) has been relocated in 1996. For this reason the data for Tallinn stem from three different sources. The observations up to the year 1996 were performed by the Estonian Meteorological and Hydrological Institute (EMHI) in Tallinn Old Harbour. Since then the water level observations at this site by the EMHI were terminated due to the construction works and moved to Muuga Harbour. However, the Tallinn Harbour Enterprise continued the observations until the water level mooring buoy operated by Marine Systems Institute at Tallinn University of Technology (MSI) was installed. Therefore, a combined dataset from EMHI,



Fig. 1. Location scheme of the four sites used in this study. Red circles indicate the observation sites and green rectangles—the associated points of the circulation model (for interpretation of the references to colour in this figure legend, the reader is referred to the web version of this article).

Table 1

Co-ordinates of observation sites, centroids of the associated model grid cells in Fig. 1, model water depth at these cells and the mean water level in simulations. Years in brackets indicate the start of recording of monthly extreme values at a particular site.

Location	Observations since	Co-ordinates	RCO (6 h)	Model water depth (m)	Mean level (cm)	HIROMB	Mean level (cm)
Narva-Jõesuu	(1899) 01.10.1950	59°28'06"N 28°02'32"E	59.49°N 27.25°E	24	19.17	59.5°N 27.25°E	5.93
Tallinn	(1899) 01.01.1945	59°26'39"N 24°45'49"E	59.49°N 24.583°E	27	17.24	59.5°N 24.58°E	-0.81
Ristna	(1922) 01.01.1950	58°55'14"N 22°03'23"E	59.06°N 21.98°E	42	14.66	59.0°N 22.0°E	-2.95
Pärnu	(1893) 01.11.1949	58°23'12"N 24°29'33"E	58.26°N 24.32°E	6	18.14	59.25°N 24.3°E	5.21

Tallinn Harbour Enterprise and MSI (Lagemaa et al., 2013) is used in this study. To comply with the modelled data range, only observations from the interval 1961–2005 are used.

The water levels at the grid cells indicated in Table 1 were extracted from the output of two different circulation models. Water level data simulated using the Rossby Centre Ocean Model (RCO, Swedish Meteorological and Hydrological Institute) were used without any adjustment except for de-meaning. We employed data from two different model runs with the same basic setup but with slightly different starting instance and duration. One of these data sets has a temporal resolution of 6 h and the other 1 h.

The RCO model has been thoroughly described, e.g., in (Meier et al., 2003) and we present here only its key features. Its horizontal resolution is 2×2 nautical miles and it uses 41 vertical levels (thickness 3–12 m) in z-co-ordinates. The model follows boundary information in the northern Kattegat and is coupled to a sea ice model. The particular model runs for 1961–2005 (May 1961–May 2005 by the 6 h dataset; January 1961–December 2005 by the 1 h dataset) was forced with high-resolution meteorological information from a regionalization of the ERA-40 re-analysis over Europe with a horizontal resolution of 22 km in which the wind is adjusted using simulated gustiness to improve the wind statistics (Samuelsson et al., 2011). Details of the model set-up and an extensive validation of its output are provided in (Meier et al., 2003; Meier and Höglund, 2013). The results of the water level hindcast and forecast are analysed in detail in (Meier et al., 2004). The model generally acceptable represents the time series and statistics of water levels but has some problems with replication of storm surges in the western Baltic Sea.

The zero water level in the RCO model is defined by the topography, i.e., connected with the bedrock. The model uses information from so-called Warnemünde topography (Seifert et al., 2001). As several different open sea maps have been used to construct this information, it is not straightforward to associate the model water level with a particular height system. In particular, land uplift is neglected in the model implementation. The study area experiences weak uplift that has been almost compensated by the global sea level rise during the last decades. The sea level data used to drive the model at the open boundary in Kattegat are based upon the height system NH60 (Meier et al., 2004). It is natural to interpret the model output in this system. The model, however, works in spherical co-ordinates and thus neglects several other factors that affect the water level such as the ellipticity of the Earth or the shape of the geoid. The modelled sea surface level follows the geodetic solution with an accuracy of 2–3 cm (Ekman and Mäkinen, 1996). However, the implementation of the principle of volume conservation in ocean modelling means that the impact of variable salinity and temperature of sea water on water level is often neglected in the models. This may lead to substantial systematic deviations of the modelled water level from the measured ones. These differences reach 30–35 cm in low-salinity parts of the Gulf of Bothnia and Gulf of Finland (Ekman and Mäkinen, 1996). In the context of extreme water levels and their return periods such a basically constant difference between the modelled and measured values is immaterial as the modelled extreme values are counted (similarly to the measured extreme values) from the long-term mean water level. To a first approximation, we consider in this study the de-meaned values of modelled water levels and call them hindcast data.

Alternatively, a semi-synthetic data set was generated by merging measured water levels with a hindcast of a higher-resolution operational circulation model. For this purpose we used the output of the HIROMB (High-Resolution Operational Model for the Baltic Sea) model (Funkquist, 2001) operational BS01 setup with a resolution of 1 nautical mile (Lagemaa et al., 2011). This

water level forecasting system in Estonia is operational since 08.08.2005 (Lagemaa et al., 2011). The model belongs to the family of 3D circulation models originally developed by the Federal Maritime and Hydrographic Agency (BSH), Germany (Kleine, 1994), later implemented also at the SMHI and Danish Meteorological Institute and further developed for the Baltic Sea conditions by the HIROMB consortium. An earlier overview of different model versions and their set-up in the Gulf of Finland is presented in (Gästgifvars et al., 2008).

As the grid cells of the HIROMB model do not coincide with the locations of water level observations, it was necessary to transform the existing measurements at the four sites to the open-sea water level at the locations of the selected grid cells of this model. The observed time series were transferred using the HIROMB model and a linear regression to a distance of about 10 km in Tallinn, 15 km in Pärnu, 20 km in Ristna and 40 km in Narva-Jõesuu. The regression coefficients were calculated by matching the monthly maximum water levels at the nearest observation site with the water level output of the HIROMB model in 2006–2013. The very high values of Pearson correlation coefficients ($R > 0.99$ for all sites) confirmed the suitability of this method. For the purposes of our study it was sufficient to apply the regression model to the monthly maximum values of measured water level data. The resulting values are called observed data.

2.2. Extreme value distributions

An ensemble of projections of extreme water levels and their return periods was constructed based on the commonly used distributions of extreme values. These distributions are theoretical limiting distributions for maximums or minimums (extreme values) of the relevant samples of independent, identically distributed random variables, and are only reached when the sample size increases infinitely. The family of the limiting (extreme value) distributions consists of the Gumbel, Fréchet and Weibull distributions. They can be considered as particular cases of the Generalized Extreme Value (GEV) distribution

$$G(y) = \exp\left\{-\left[1 + \xi\left(\frac{y - \mu}{\sigma}\right)\right]^{-1/\xi}\right\}. \quad (1)$$

Here y has the meaning of block maxima (e.g. annual maximum water levels) and μ , σ and ξ are called the location, scale and shape parameter (Coles, 2001). The return period $T(\hat{y})$ for a certain value \hat{y} is given by the $[1 - 1/T(\hat{y})]$ -th percentile of $G(y)$

$$T(\hat{y}) = \frac{1}{1 - G(\hat{y})}. \quad (2)$$

For $\xi \rightarrow 0$ the GEV distribution reduces to the Gumbel distribution $\Lambda(y) \sim \exp\{-\exp(-y)\}$, for $\xi < 0$ (which is frequent in oceanographic applications) it represents the Weibull distribution and for $\xi > 0$ (which is typical for finance market problems) the Fréchet distribution. The latter two distributions formally mirror each other but represent basically different physical situations. The Weibull distribution matches extremes of so-called light-tailed (very rapidly decaying) distributions while the Fréchet distribution is the limiting one of those which have polynomially (that is, relatively slowly) decaying tails. The Gumbel distribution is suitable for distributions possessing an exponential tail such as the Gaussian distribution.

The distributions of both modelled and measured water levels are typical for similar distributions in the north-eastern Baltic Sea (Johansson et al., 2001; Suursaar and Sooäär, 2007). They all resemble a Gaussian distribution but are usually skewed towards high water levels and thus have a maximum at or slightly below the long-term mean. For example, the distribution for the simulated water levels in the Tallinn Bay using the 6-h values from the RCO

model (Fig. 2) resembles a modified Gaussian distribution. It is moderately skewed (skewness 1.23). Its kurtosis (3.09, which is almost equal to the kurtosis of a Gaussian distribution) signals that the probability of very large values (either positive or negative water levels) insignificantly differs from their expectation for a Gaussian-distributed data set.

The distribution of measured water levels at Tallinn Old Harbour has a similar shape (Fig. 2). Its right-hand tail (extreme surges) is neither polynomial nor exponential. A typical feature of the coastal waters of Estonia (Suursaar et al., 2006a, b; Suursaar and Sooäär, 2007) and the entire north-eastern Baltic Sea (Johansson et al., 2001) is the presence of a few outliers. These are very high water levels (often regarded as values larger than the third quartile plus 1.5 times the difference between the first and third quartile) that are vividly represented in Fig. 2. This set may represent a specific population of water levels created by the interaction of sequences of storms that markedly increase the water volume of the Baltic Sea and a strong storm approaching when the entire Baltic Sea water level is unusually high (Suursaar and Sooäär, 2007).

The presence of a few such values (usually < 0.01% of the total water level recordings) insignificantly impacts the integral parameters of the overall (almost Gaussian-shaped) distribution. These values may still substantially affect the parameters of the associated extreme value distributions and projections of return periods of very large water levels (Suursaar and Sooäär, 2007). The use of a Gumbel distribution (which has an exponentially decreasing tail in semi-logarithmic co-ordinates) would eventually

underestimate the importance of positive outliers in Fig. 2 (and to lead to a certain underestimation of extremes). The use of a Weibull distribution would do the opposite because its tail decays as a power law in semi-logarithmic co-ordinates far to the right of the rightmost data depicted in Fig. 2. It is thus plausible to consider a set of various distributions for long-term projections.

To evaluate the parameters of the GEV, Gumbel and Weibull distributions we used *Hydrognomon*, a freely available general-purpose software tool for the processing and analysis of hydrological data (<http://hydrognomon.org/>). It is an open source application running on standard Microsoft Windows platforms, and also part of the *openmeteo.org* framework. This software employs typical hydrological applications, such as homogeneity tests, evapotranspiration modelling, stage-discharge analysis, areal integration of point data, of hydrometric data processing, and lumped hydrological modelling. We used only the statistical modules of *Hydrognomon* that provide numerical tools for data exploration, fitting of distribution functions, statistical prediction, Monte-Carlo simulation, determination of confidence limits, analysis of extremes, and construction of ombrian (intensity-duration-frequency) curves.

2.3. Projections based on block maxima

All constructed projections are built using so-called block maximum method (e.g., Arns et al., 2013). The monthly maximum values evidently cannot be assumed as uncorrelated because of substantial time lag between the impact of large-scale atmospheric patterns and the reaction of water level in terms of monthly means (Johansson et al., 2014). For this reason the hindcast and observed time series were divided into longer blocks of fixed length so that the maximum values within the blocks were uncorrelated. For each above-described data set we formed two sets of block maxima. Following the common practice in the Baltic Sea conditions (Lagemaa et al., 2013), the first set contained the extreme values in each calendar year.

In some cases, however, the obtained values may be correlated. For example, a maximum in December for one year and another in January of the subsequent year may reflect the impact of the same cluster of storms. The strong seasonal variation of water levels provides a natural way to construct an alternative set of block maxima of 1-yr intervals. Namely, stormy seasons (August–March) contain all annual highest water levels in the Estonian coastal waters and are clearly separated by calm spring seasons (Johansson et al., 2001; Suursaar et al., 2002; Jaagus and Suursaar, 2013). Therefore, the block maxima over such stormy seasons (equivalently, over the time intervals from a June until the subsequent May) are completely uncorrelated.

The two sets of block maxima generally differ insignificantly. The projections of extreme water levels and their return periods, however, show substantial differences (Fig. 3). For Estonian coastal waters the extreme water levels projected using the maxima of stormy seasons are usually higher than those based on the annual maxima. The differences are relatively large (about 20 cm for water levels that occur once in 200 yr) for the RCO data and somewhat smaller but still substantial (about 10 cm) for the observed data.

The above-discussed mismatch between the actual distributions of observed and hindcast water levels and a Gaussian one suggests that none of the extreme value distributions perfectly captures the extreme levels for longer return periods. The nature of deviations of the actual distributions from a Gaussian one is not known and thus the biases produced by the use of either of these distributions are also unknown. To resolve the problem at least to a first approximation it is reasonable to assume that the errors of each distribution are randomly distributed. This assumption is to

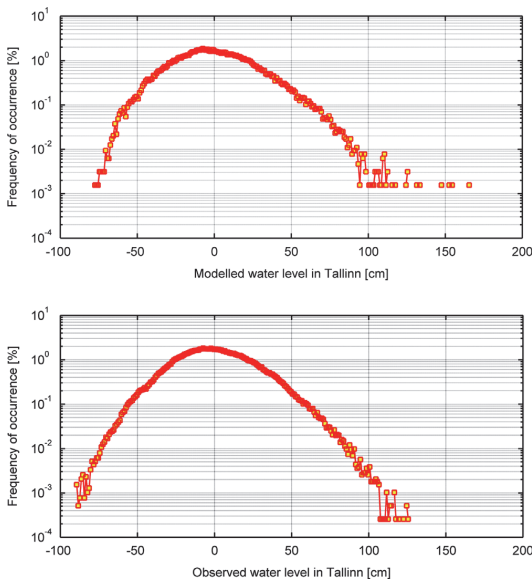


Fig. 2. Frequency of occurrence of deviations of the water level from the long-term mean in the RCO simulations (6-h values in 1961–2005, upper panel) and in measurements in Tallinn Harbour (1945–15.05.1995). As the measurement site was relocated from Tallinn Old Harbour to Muuga Harbour in 1996, the distribution of observed values does not contain the highest examples in the 2000 s (135 cm in 2001; 152 cm in 2005). The recordings of the largest values after the turn of the millennium raises the question whether the overall dynamics of the water level may have changed since 1996. A similar change has been found in the statistics of wave-driven setup in the vicinity of Tallinn for 1981–2012. All the highest waves have occurred after 1995 but the highest set-up apparently occurred in many locations before 1995 (Soomere et al., 2013). A probable reason is a change in the wind direction in strongest storms, with obvious changes to the local water level dynamics.

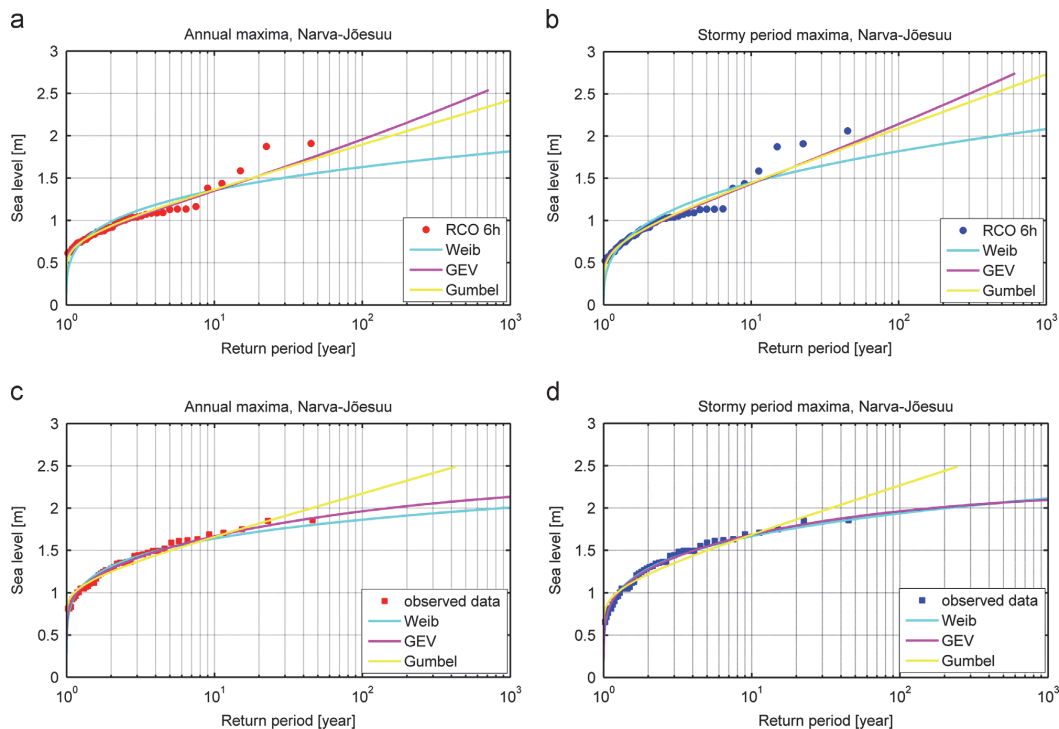


Fig. 3. Return periods of extreme water levels at Narva-Jõesuu according to the results of the 6-h RCO data (upper panels) and the observed data set (lower panels). Note that the latter data is actually a semi-synthetic data set obtained based on actual observations and the output of HIROMB as explained above. The panels at left correspond to projections based on annual maxima, the panels at right—to projections based on maxima over stormy seasons. Single markers represent the set of block maxima in the relevant data sets. Magenta line: the projection based on the GEV distribution, cyan line: Weibull distribution (Weib), yellow line: Gumbel distribution (for interpretation of the references to colour in this figure legend, the reader is referred to the web version of this article).

some extent supported by the appearance of the projections using different distributions (Fig. 3). For example, if the 6-h RCO data are used, the GEV distribution projects the largest extreme water levels that largely match the projection using a Gumbel distribution. If, however, the observed data is used, the GEV distribution projects the smallest values that almost coincide with the outcome of a Weibull distribution.

Given such an extensive variability of different projections, a feasible solution is the concurrent use of all these distributions. The average of such an ensemble of projections eventually provides a reasonable estimate of the true value. Following this conjecture, we include results obtained using the Gumbel and Weibull distributions into the ensemble of projections along with the outcome of the GEV distribution. Although the projections made using the GEV distribution often outperform the other approaches (Lowe et al., 2001; Wroblewski, 2001; van den Brink et al., 2005), the spreading of all three projections provides valuable additional information about their possible bias. Interestingly, the spreading of all four versions of projections of extreme water levels once in 200+ yr is almost the same.

3. Results

The empirical estimates of extreme water levels up to once in 45 yr from the hindcast and observed data differ markedly. The difference of these values for Tallinn (Fig. 4) is relatively small but still is about 20 cm for water levels once in 5–10 yr and reaches

30 cm for water levels once in 22 yr. In spite of these deviations, the different projections are located much closer to each other. They spread only by 25 cm for water levels once in 20 yr, by about 50 cm for water levels once in 100 yr and about 80 cm for water levels once in 1000 yr. This range is quite small compared to many other similar exercises (Sterl et al., 2009) and signals good consistency of the underlying data. Importantly, different projections are almost uniformly distributed within the entire ‘corridor’ formed by the largest and smallest projected extreme water level. Also, the lines corresponding to different projections often cross each other. These features suggest that the assumption of randomness of the error of each projection is not explicitly violated and that the median (or average value) of the ensemble of projections is a good estimate for the extreme water levels and return periods at this location.

The severest storm surges at Pärnu (2.75 m in 2005, 2.53 m in 1967) are extremely high in the context of the Baltic Sea. The total range of variations is as large as 4 m at Pärnu. The nature of such surges has been extensively discussed in the literature (Suursaar et al., 2006a; Suursaar and Sooäär, 2007, among others). The common opinion is that these values cannot be fit into any of the existing theoretical extreme value distributions. Fig. 5 suggests that the presence of these values markedly affects the appearance of the GEV and Gumbel fit (cf. Suursaar and Sooäär, 2007) while the Weibull fit seems to be largely governed by the rest of the block maxima.

The different sets of block maxima in Fig. 5 also deviate typically by 20 cm for return periods less than 15 yr but up to 60–70 cm for

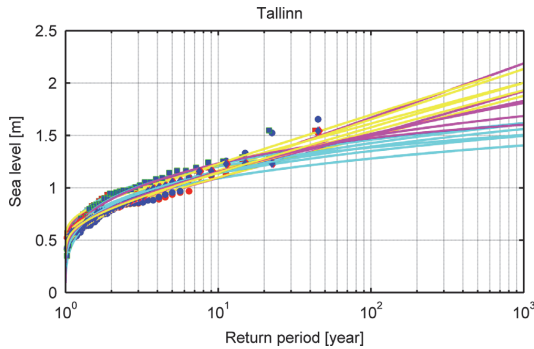


Fig. 4. Return periods of extreme water levels according to different projections at Tallinn. Block maxima: red circles—annual maxima of the RCO 6-h data, blue circles—stormy season maxima of the RCO 6-h data; red rhombi—annual maxima of the RCO 1-h data, blue rhombi—stormy season maxima of the RCO 1-h data; red squares—annual maxima of the observed data set; blue squares—stormy season maxima of the observed data set. The markers showing the block maxima derived from the 1-h RCO data almost coincide with those for the RCO 6-h data set. Yellow lines: projections using the Gumbel distribution, magenta—GEV distribution; cyan—Weibull distribution. Note that the difference between the observed and hindcast block maxima corresponding to the calendar years (red) or to stormy seasons (blue) does not become evident in the scale of the image but considerably impacts the relevant projections starting from return periods of about 20 yr (for interpretation of the references to colour in this figure legend, the reader is referred to the web version of this article).

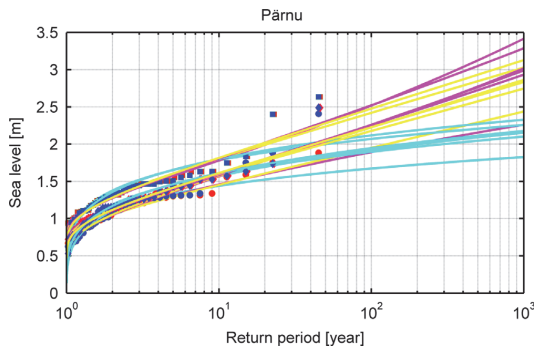


Fig. 5. Return periods of extreme water levels according to different projections at Pärnu. Notations are the same as for Fig. 4. As the RCO set does not cover the entire 2005 year, the surge in January 2005 is not reflected in the set of annual maxima of this data set.

return periods of 22 and 45 yr. This span is reflected in a somewhat larger spread of various projections than in Fig. 4. The spread is 40–50 cm for return periods of 10–20 yr and increases to 80 cm for return periods of 100 yr and to 150 cm for return period of 500 yr. Although the spread of the block maximum data is much larger for Pärnu than for Tallinn, the lines corresponding to different projections are relatively uniformly distributed within the corridor of all projections.

The deviations between the different values of block maxima for relatively short return periods (2–10 yr) are quite large at Narva-Jõesuu (Fig. 6). The observed values exceed the hindcast ones typically by up to 50 cm. The difference diminishes for the largest block maxima and the overall maxima of all three data sets only differ by less than 20 cm. The differences for the return periods of 2–10 yr evidently reflect local features of the measurement site. The observations were made using a staff mounted in the harbour located ca 200 m upstream of River Narva (Fig. 7). The river flow is occasionally blocked by a sand bar at the river mouth.

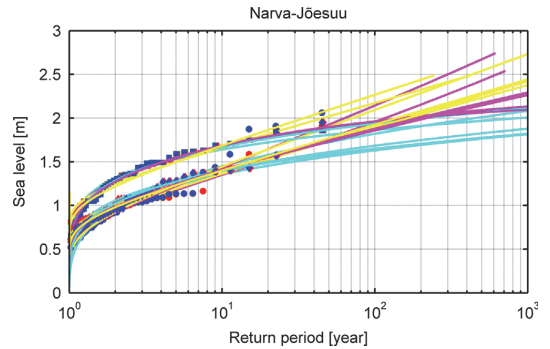


Fig. 6. Return periods of extreme water levels according to different projections at Narva-Jõesuu. Notations are the same as for Fig. 4.

The water depth at the sill usually varies in the range of 2–3 m (Laanearu et al., 2007). The gently sloping sandy seabed is favourable for the formation of relatively high local wind-driven surge and wave-induced set-up. These features are not resolved by the circulation models with a moderate spatial resolution like the RCO model. The entire river mouth area is open to the predominant wave propagation direction. It is thus likely that local wind-driven surge (similarly to Pärnu, Suursaar and Sooäär, 2007) and wave set-up (Dean and Bender, 2006) often substantially contribute to the observed water levels. The sill is gradually eroded by large discharge in spring and restored by wave-driven alongshore sand transport in late summer and autumn (Laanearu et al., 2007). Its dynamics may thus add considerable seasonality into the difference between the (hindcast) open sea level and the observed water level.

Under described circumstances it is not unexpected that the hindcast and measured block maxima form two distinct populations (Fig. 6). These populations, however, have almost matching values for the water level once in 45 yr. The presence of the two populations gives rise to two clusters of projections. These clusters are clearly separated for return periods of less than 20 yr but largely merge for longer return periods. Starting from return periods of about 30 yr they are more or less uniformly distributed between the largest and lowest projected water levels. The joint spread of the two sets of projections is about 40 cm for return periods of 20 yr, increases to about 60 cm for return periods of 100 yr and is close to 100 cm for return periods of about 500 yr. These values are comparable to those for Pärnu.

The situation is completely different at Ristna (Fig. 8). The measured and hindcast block maxima differ radically, from 30 cm for as short return periods as 2 yr up to almost 90 cm for the return period of 45 yr. Even if the overall highest observed value (209 cm, January 2005) is considered as not representative (Suursaar et al., 2006b, Suursaar and Sooäär, 2007), the deviations between the hindcast and observed block maxima are massive. Accordingly, the projections form two clearly separated clusters that do not overlap even for return periods of 1000 yr. The spreading of the projections within each cluster is fairly limited (below 10 cm) until return periods of about 25 yr and increases to 25–30 cm for return periods of 100 yr and to 40–60 cm for return periods of 500 yr. This modest spreading signals that both data sets (observed and hindcast) are internally consistent and that the all-time highest measured value (209 cm) is a valid member of the data set.

The described substantial deviation of the hindcast and observed data sets and associated projections signals that local features play a decisive role in the formation of the observed water level at Ristna.

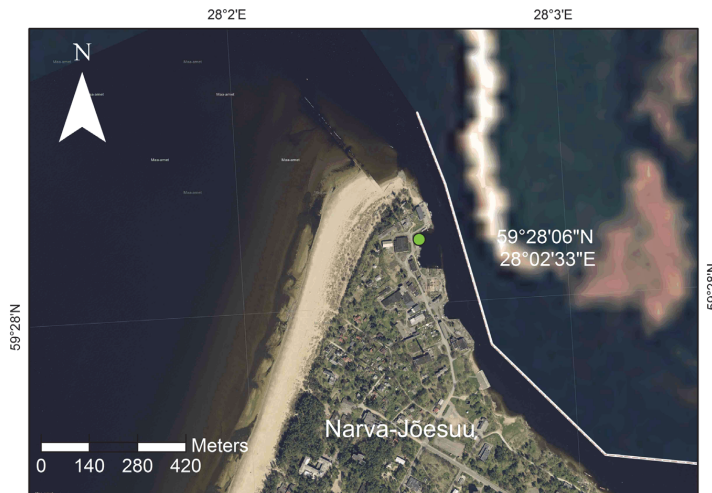


Fig. 7. Location of the water level observation peel (green circle) in Narva-Jõesuu at the left bank of the River Narva. The white line to the east of the observation site indicates the border between Estonia and Russia. The right bank of the river is blurred by the image provider. Source: Estonian Land Board, www.maaamet.ee (for interpretation of the references to colour in this figure legend, the reader is referred to the web version of this article).

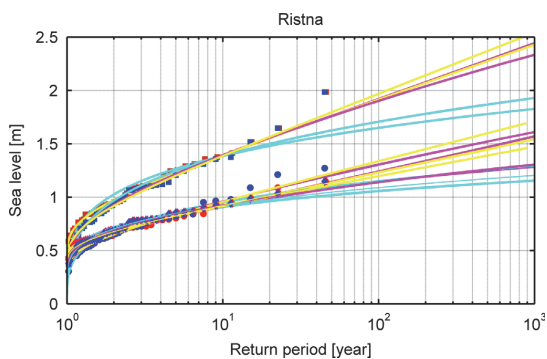


Fig. 8. Return periods of extreme water levels according to different projections at Ristna. Notations are the same as for Fig. 4.

The site is located in a small harbour of Kalana at the southern coast of the Kõpu Peninsula (Hiiumaa). The coastline is fully open to the predominant south-western winds and evidently to the largest waves that may reach the coasts of Hiiumaa. The geometry of the harbour (Fig. 9) is favourable for the formation of higher water levels in its interior under southern and south-western winds and by waves approaching from south-west. The seabed deepens relatively rapidly. It reaches a depth of 5 m at a distance of 150–200 m from the coast and 10 m at a distance of 300 m from the coast. Therefore, quite large waves may reach the immediate vicinity of the harbour and to produce substantial set-up. It is not uncommon that significant wave heights over 4 m reach this area (Tuomi et al., 2011). Such waves usually approach the coast from the south-west, that is, almost incidentally to the shoreline, and thus may create set-up heights up to 1 m in ideal conditions (Dean and Bender, 2006).

4. Conclusions and discussion

The analysis of the frequency of occurrence of various water levels along the Estonian coast suggests that none of the commonly used extreme value distributions (Generalised Extreme Value, Gumbel,

Weibull) is able to perfectly replicate the observed and hindcast extreme water levels. The Gumbel fit tends to produce larger projections of extreme levels for longer return periods than the Weibull fit. The GEV fit usually gives certain intermediate values but may match either Gumbel or Weibull fit, depending on the location and the method of building the block maxima. The typical spreading of the projections that employ six different sets of block maxima as the input to a particular distribution is fairly limited (below 10 cm) until return periods of about 25 yr. It increases to 25–30 cm for return periods of 100 yr and to 40–60 cm for return periods of 500 yr. The discrepancy apparently reflects the presence of a population of water levels that do not fit the general statistics and correspond to specific dynamically driven situations such as a high surge after a sequence of strong storms that have already increased the volume of the water in the Baltic Sea.

As hypothesized above, a feasible way to take into account the presence of this population is to employ the ensemble approach. If single projections of the extreme water levels are more or less uniformly distributed, a reasonable projection can be obtained as a median, average or weighted average of the ensemble members. This perception is largely met for coastal segments where the water level measurements or observations (that have been usually performed from certain coastal engineering structures) properly reflect the open-sea water level. This is the case for two substantially different locations such as Tallinn and Pärnu, to a lesser extent for Narva-Jõesuu but completely different for Ristna. For the first three locations, the spreading of the entire ensemble is < 50 cm for about 20 yr return periods and increases to 75 cm for about 100 yr and 125 cm for about 500 yr return period. Importantly, no clear outliers exist among predictions for these sites in the sense that no prediction is clearly above or below the cluster of other predictions. All projections of extreme water levels in the ensemble are generally homogeneously spread between the highest and the lowest one. Moreover, no prediction fits well the ensemble average. This appearance of the ensembles signals that the assumption of random distributions of errors of single projections is sensible. The median of the ensemble for 1 in 100 yr event corresponds almost exactly with the highest measured or hindcast water levels at Tallinn, Narva and Ristna. The two highest surges in Pärnu are 1 in 300–500 yr events (Suursaar and Sooäär, 2007).



Fig. 9. Location of the water level observation peel (green circle) in Ristna (Kalana Harbour). Source: Estonian Land Board, www.maaamet.ee (for interpretation of the references to colour in this figure legend, the reader is referred to the web version of this article).

It is likely that the described difference in the appearance of the ensembles of projections is associated with different contribution of local effects into the observed water levels. The observation site in Tallinn is located at the entrance to Tallinn Old Harbour. The water depth in its vicinity is > 10 m and the reading evidently reflects well the open-sea water level. The observation site at Pärnu is located a little bit upstream of the River Pärnu, in an ancient city moat. The depth of the River Pärnu mouth is kept at the level of about 5 m, which is comparable with the water depth in the entire Pärnu Bay. Therefore, wave set-up and local (near-shore) surge are both immaterial at the observation site. The observed water level reflects well the situation at the end of about 1 km long jetties that prevent the river mouth from silting. The water level at this location is reasonably reflected by contemporary circulation models. The observed water level data for Narva-Jõesuu evidently contain a certain contribution from the local effects (local surge, wave set-up, seasonally varying sill at the river mouth). Their impact is still moderate in the sense that the ensemble of projections for longer return periods has the same basic features as those for Tallinn and Pärnu.

The situation in Ristna is completely different. It is likely that local effects (first of all wave-induced set-up) substantially contribute to the formation of the observed block maxima. Fig. 8 suggest that their contribution is about 1/3 of the total water level. This estimate is supported by the large difference in the maximum water levels in January 2005 between Ristna (207 cm) and Dirhami (134 cm, Suursaar et al., 2006b) located about 80 km to the north-east (downwind for this storm) at the entrance of the Gulf of Finland (Fig. 1). This value is also consistent with the widely used rule of thumb for the open ocean coasts where wave set-up often provides 1/3 of the maximum surge at the waterline (Dean and Bender, 2006). It is likely that this locally induced contribution varies substantially along the coast of the Kõpu Peninsula already on scales of a few km depending on the orientation of the coast (cf. Soomere et al., 2013). This feature greatly complicates the analysis and projections of extreme water levels and their return periods compared to other coastal segments of Estonia.

Although extensive and rapid local changes in the water level are possible in the Gulf of Finland, strong spatial correlation of water level recordings extends to at least 150–200 km (Raudsepp

et al., 1999; Johansson et al., 2001). The typical de-correlation time is about two weeks (Raudsepp et al. 1999). These features suggest that the proposed ensemble approach is likely usable for the entire Gulf of Finland. In particular, the analysis of the Narva-Jõesuu data set advocates that it makes sense to approximate the observed extreme values in this gulf over a distance of tens of km to match them with the output of contemporary circulation models such as HIRLAM in studies of water levels in future climates. It is also likely that similar properties are valid for the eastern Gulf of Riga that has relatively regular geometry and bathymetry.

The extensive mismatch between the (offshore) hindcast and (coastal) observed water level data at Ristna not only renders the entire idea of building an ensemble of projections inoperable but possibly even misleading for locations of this type. More importantly, it emphasizes that numerically simulated water levels and associated projections of extreme surges and their return periods may completely overlook such essential components of storm surges as wave set-up and calls for much more detailed analysis of their possible role.

Another aspect is that the population of (positive) outliers in the water level time series may have several sources (cf. Haigh et al., 2014). The relatively well-known contributor to these is the possibility of pumping large volumes of water into the Baltic Sea by a sequence of strong storms (see Leppäranta and Myrberg, 2009 and references therein). Although it often provides 40–50% of the total storm surge, its contribution is commonly not singled out from the water level time series although the impact of this aperiodic mechanism not necessarily has a Gaussian-type distribution. The impact of local sources of extremely high water levels along the coast is often discussed but in a very few occasions separated from the total water level. It is unclear how to quantify their contribution even in statistical sense. A part of this contribution apparently mirrors the distribution of wind speeds from a particular unfavourable direction. While the overall distribution of all wind speeds commonly matches well a Rayleigh distribution in the north-western Europe (Troen and Petersen, 1989), similar distributions for single directions often deviate from the Rayleigh one (Soomere, 2001). Furthermore, the largest corrections to the water level (e.g. the highest wave set-up) is not necessarily synchronised with the course of the highest open-sea levels.

Acknowledgements

The research was a part of the project TERIKVANT (managed by the Estonian Research Council in the framework of the Environmental Technology R&D Programme KESTA and financed by the ERDF). The work was additionally supported by targeted financing SF0140007s11 of the Estonian Ministry of Education and Research, Grant 9125 by the Estonian Science Foundation and through support of the ERDF to the Centre of Excellence in Non-linear Studies CENS. The simulated hydrographic data were kindly provided by the Swedish Meteorological and Hydrological Institute in the framework of the BONUS BalticWay cooperation (Soomere et al., 2014).

References

- Arns, A., Wahl, T., Haigh, I.D., Jensen, J., Pattiaratchi, C., 2013. Estimating extreme water level probabilities: a comparison of the direct methods and recommendations for best practise. *Coast. Eng.* 81, 51–66.
- Araújo, M.B., New, M., 2006. Ensemble forecasting of species distributions. *Trends Ecol. Evol.* 22, 42–47.
- Averkiev, A.S., Klevanny, K.A., 2010. A case study of the impact of cyclonic trajectories on sea-level extremes in the Gulf of Finland. *Cont. Shelf Res.* 30, 707–714.
- Barbosa, S.M., 2008. Quantile trends in Baltic Sea level. *Geophys. Res. Lett.*, 35 (Art. No. 122704).
- Bardet, L., Duluc, C.-M., Rebour, V., L'Her, J., 2011. Regional frequency analysis of extreme storm surges along the French coast. *Nat. Hazards Earth Syst. Sci.* 11, 1627–1639.
- Cheung, K.K.W., 2001. A review of ensemble forecasting techniques with a focus on tropical cyclone forecasting. *Meteorol. Appl.* 8, 315–332.
- Christiansen, B., Schmith, T., Thejll, P., 2010. A surrogate ensemble study of sea level reconstructions. *J. Clim.* 23, 4306–4326.
- Coles, S., 2001. *An Introduction to Statistical Modeling of Extreme Values*. Springer, London.
- Dailidienė, I., Davulienė, L., Tilickis, B., Stankevicius, A., Myrberg, K., 2006. Sea level variability at the Lithuanian coast of the Baltic Sea. *Boreal Environ. Res.* 11, 109–121.
- Dean, R.G., Bender, C.J., 2006. Static wave set-up with emphasis on damping effects by vegetation and bottom friction. *Coast. Eng.* 53, 149–165.
- Donner, R.V., Ehrcke, R., Barbosa, S.M., Wagner, J., Donges, J.F., Kurths, J., 2012. Spatial patterns of linear and nonparametric long-term trends in Baltic sea-level variability. *Nonlinear Process. Geophys.* 19, 95–111.
- Ekman, M., Mäkinen, J., 1996. Mean sea surface topography in the Baltic Sea and its transition area to the North Sea: a geodetic solution and comparisons with oceanographic models. *J. Geophys. Res.–Oceans* 101 (C5), 11993–11999.
- Funkquist, L., 2001. HIROMB, an operational eddy-resolving model for the Baltic Sea. *Bull. Mar. Inst. (Gdańsk)* 28, 7–16.
- Gästgövars, M., Müller-Navarra, S., Funkquist, L., Huess, V., 2008. Performance of operational systems with respect to water level forecasts in the Gulf of Finland. *Ocean Dyn.* 58, 139–153.
- Gaslikova, L., Grabemann, L., Groll, N., 2013. Changes in North Sea storm surge conditions for four transient future climate realizations. *Nat. Hazard.* 66, 1501–1518.
- Haigh, I.D., Wijeratne, E.M.S., MacPherson, L.R., Pattiaratchi, C.B., Mason, M.S., Crompton, R.P., George, S., 2014. Estimating present day extreme water level exceedance probabilities around the coastline of Australia: tides, extra-tropical storm surges and mean sea level. *Clim. Dyn.* 42, 121–138. <http://dx.doi.org/10.1007/s00382-012-1652-1>.
- Hünicke, B., 2010. Contribution of regional climate drivers to future winter sea-level changes in the Baltic Sea estimated by statistical methods and simulations of climate models. *Int. J. Earth Sci.* 99, 1721–1730.
- Hünicke, B., Zorita, E., 2008. Trends in the amplitude of Baltic Sea level annual cycle. *Tellus A* 60, 154–164.
- Jaagus, J., Suursaar, Ü., 2013. Long-term storminess and sea level variations on the Estonian coast of the Baltic Sea in relation to large-scale atmospheric circulation. *Estonian J. Earth Sci.* 62, 73–92.
- Johansson, M., Boman, H., Kahma, K.K., Launinen, J., 2001. Trends in sea level variability in the Baltic Sea. *Boreal Environ. Res.* 6, 159–179.
- Johansson, M., Kahma, K., Pellikka, H., 2011. Sea level scenarios and extreme events on the Finnish coast. *VTT Tied. Valt. Tek. Tutk.* 2571, 570–578.
- Johansson, M.M., Pellikka, H., Kahma, K.K., Ruosteenoja, K., 2014. Global sea level rise scenarios adapted to the Finnish coast. *J. Mar. Syst.* 129, 35–46.
- Kleine, E., 1994. *Das operationelle Modell des BSH für Nordsee und Ostsee. Konzeption und Übersicht*. Bundesamt für Seeschifffahrt und Hydrographie.
- Laanearu, J., Koppel, T., Soomere, T., Davies, P.A., 2007. Joint influence of river stream, water level and wind waves on the height of sand bar in a river mouth. *Nordic Hydrol.* 38, 287–302.
- Lagemaa, P., Elken, J., Kõuts, T., 2011. Operational sea level forecasting in Estonia. *Estonian J. Eng.* 17, 301–331.
- Lagemaa, P., Raudsepp, U., Kõuts, T., Allik, A., Elken, J., 2013. Tallinna linna Haabersti, Põhja-Tallinna ja Kakumäe linnaosaade meretasemete stsenaariumite modelleerimine (Modelling of water level scenarios for City of Tallinn). Research report. Marine Systems Institute at Tallinn University of Technology, Tallinn (29 pp.).
- Lazarenko, N.N., 1986. Variations of mean level and water volume of the Baltic Sea. In: *Proceedings of the Water Balance of the Baltic Sea Environment*, 16, pp. 64–80.
- Lowe, J.A., Gregory, J.M., Flather, R.A., 2001. Changes in the occurrence of storm surges around the United Kingdom under a future climate scenario using a dynamic storm surge model driven by the Hadley Centre climate models. *Clim. Dyn.* 18, 179–188.
- Leppäranta, M., Myrberg, K., 2009. *Physical Oceanography of the Baltic Sea*. Springer, Berlin, pp. 378.
- Meier, H.E.M., Höglund, A., 2013. Studying the Baltic Sea circulation with Eulerian tracers. In: Soomere, T., Quak, E. (Eds.), *Preventive Methods for Coastal Protection*. Springer, Cham Heidelberg, pp. 101–130.
- Meier, H.E.M., Döschner, R., Faxén, T., 2003. A multiprocessor coupled ice-ocean model for the Baltic Sea: application to salt inflow. *J. Geophys. Res.–Oceans* 108 (C8), 32–73.
- Meier, H.E.M., Broman, B., Kjellström, E., 2004. Simulated sea level in past and future climates of the Baltic Sea. *Clim. Res.*, 59–75.
- Mel, R., Sterl, A., Lionello, P., 2013. High resolution climate projection of storm surge at the Venetian coast. *Nat. Hazards Earth Syst. Sci.* 13, 1135–1142.
- Mudersbach, C., Jensen, J., 2009. Extreme value statistical analysis of historical, observed and modeled water levels on the German Baltic Sea coast [Extremwertstatistische Analyse von Historischen, Beobachteten und Modellierten Wasserständen an der Deutschen Ostseeküste]. *Küste* 75, 131–161.
- Raudsepp, U., Toompuu, A., Kõuts, T., 1999. A stochastic model for the sea level in the Estonian coastal area. *J. Mar. Syst.* 22, 69–87.
- Samuelsson, P., Jones, C.G., Willén, U., Ullerstig, A., Gollvik, S., Hansson, U., Jansson, C., Kjellström, E., Nikulin, G., Wyser, K., 2011. The Rossby Centre Regional Climate Model RCA3: Model description and performance. *Tellus A* 63, 4–23.
- Seifert, T., Tauber, F., Kayser, B., November 25–29, 2001. A high resolution spherical grid topography of the Baltic Sea, revised edition. In: *Baltic Sea Science Congress*. Poster #147, Stockholm (www.iowarnemunde.de/iowtopo_resampling.html).
- Scotto, M.G., Barbosa, S.M., Alonso, A.M., 2009. Model-based clustering of Baltic sea-level. *Appl. Ocean Res.* 31, 4–11.
- Soomere, T., 2001. Extreme wind speeds and spatially uniform wind events in the Baltic Proper. *Proc. Estonian Acad. Sci. Eng.* 7, 195–211.
- Soomere, T., Pindsoo, K., Bishop, S.R., Kärd, A., Valdmann, A., 2013. Mapping wave set-up near a complex geometric urban coastline. *Nat. Hazards Earth Syst. Sci.* 13, 3049–3061.
- Soomere, T., Dööb, K., Lehmann, A., Meier, H.E.M., Murawski, J., Myrberg, K., Stanev, E., 2014. The potential of current- and wind-driven transport for environmental management of the Baltic Sea. *Ambio* 43, 94–104.
- Sterl, A., van den Brink, H., de Vries, H., Haarsma, R., van Meijgaard, E., 2009. An ensemble study of extreme storm surge related water levels in the North Sea in a changing climate. *Ocean Sci.* 5, 369–378.
- Stramska, M., 2013. Temporal variability of the Baltic Sea level based on satellite observations. *Estuar. Coast. Shelf Sci.* 133, 244–250.
- Stramska, M., Kowalewska-Kalkowska, H., Świrgoń, M., 2013. Seasonal variability in the Baltic Sea level. *Oceanologia* 55, 787–807.
- Suursaar, Ü., Sooäär, J., 2007. Decadal variations in mean and extreme sea level values along the Estonian coast of the Baltic Sea. *Tellus A* 59, 249–260.
- Suursaar, Ü., Kullas, T., Otsmann, M., 2002. A model study of the sea level variations in the Gulf of Riga and the Vainameri Sea. *Cont. Shelf Res.* 22, 2001–2019.
- Suursaar, Ü., Jaagus, J., Kullas, T., 2006a. Past and future changes in sea level near the Estonian coast in relation to changes in wind climate. *Boreal Environ. Res.* 11, 123–142.
- Suursaar, Ü., Kullas, T., Otsmann, M., Saaremäe, I., Kuik, J., Merilain, M., 2006b. Cyclone Gudrun in January 2005 and modelling its hydrodynamic consequences in the Estonian coastal waters. *Boreal Environ. Res.* 11, 143–159.
- Suursaar, Ü., Jaagus, J., Kullas, T., Tõnisson, H., 2011. Estimation of sea level rise and storm surge risks along the coast of Estonia, Baltic Sea—a tool for coastal management. *Littoral* 2010, 12005.
- Troen, I., Petersen, E.L., 1989. *European Wind Atlas*. Risø National Laboratory, Roskilde, Denmark.
- Tuomi, L., Kahma, K.K., Pettersson, H., 2011. Wave hindcast statistics in the seasonally ice-covered Baltic Sea. *Boreal Environ. Res.* 16, 451–472.
- van den Brink, H.W., Konnen, G.P., Oosteech, J.D., 2005. Uncertainties in extreme surge level estimates from observational records. *Phil. Trans. Roy. Soc. A* 363 (1831), 1377–1386.
- Weisse, R., von Storch, H., 2010. *Marine Climate and Climate Change. Storms, Wind Waves and Storm Surges*. Springer, Berlin, Heidelberg (220 pp.).
- Wroblewski, A., 2001. A probabilistic approach to sea level rise up to the year 2100 at Kolobrzeg. *Pol. Clim. Res.* 18, 25–30.

Paper III

Pindsoo K., Soomere T. 2015. Contribution of wave set-up into the total water level in the Tallinn area. *Proceedings of the Estonian Academy of Sciences*, 64, 338–348, doi: 10.3176/proc.2015.3S.03.



Contribution of wave set-up into the total water level in the Tallinn area

Katri Pindsoo^{a*} and Tarmo Soomere^{a,b}

^a Laboratory of Wave Engineering, Institute of Cybernetics at Tallinn University of Technology, Akadeemia tee 21, 12618 Tallinn, Estonia

^b Estonian Academy of Sciences, Kohtu 6, 10130 Tallinn, Estonia

Received 2 March 2015, accepted 15 May 2015, available online 28 August 2015

Abstract. Wave-induced set-up is a nonlinear phenomenon driven by the release of momentum from breaking waves. It may cause a systematic rise in the water level in certain coastal segments. We address the contribution of wave set-up into the formation of extreme water levels at the waterfront in the Tallinn area of the north-eastern Baltic Sea. The parameters of set-up are evaluated using the wave properties computed for 1981–2014 with a triple-nested WAM model with a horizontal resolution of about 470 m. The offshore water level is extracted from the output of the Rossby Centre Ocean (RCO) model. The maximum set-up may reach 0.7–0.8 m in some coastal sections and the all-time highest measured water level is 1.52–1.55 m in the study area. The high offshore water levels are only infrequently synchronized with extreme set-up events. Wave set-up may contribute to the all-time maximum water level at the shoreline by up to 0.5 m. This contribution considerably varies for different years. The largest contribution from set-up into extreme water levels usually occurs during north-westerly storms.

Key words: marine coastal hazards, flooding, wave set-up, water level.

1. INTRODUCTION

Effects of climate change have the most significant influence on urban areas [4] where they affect people's safety, the functioning of the existing infrastructure, new development projects, etc. A serious problem for low-lying urban areas is coastal flooding [5]. The water level at the shoreline of coastal segments that are open to high waves can be considerably higher than in neighbouring offshore locations because of wave-induced set-up. This non-linear phenomenon, hereafter denoted as wave set-up, occurs in the surf zone where the release of momentum of breaking waves may lead to an increase in the water level [13]. The magnitude of wave set-up is traditionally modelled and quantified using the variation in the onshore component of radiation stress (the tensor of excess horizontal momentum fluxes due to the presence of the waves) [13]. For open ocean coasts wave

set-up can contribute up 30–60% of the total height of the 100-year surge [2]. Extreme water levels are usually produced by an unfortunate combination of high tide (or water volume of a semi-enclosed sea [12]), low atmospheric pressure, and strong wind-driven surge. As wave set-up is added on top of their joint effect, its presence may cause extensive additional flooding of affected coastal sections [1] and may provide a significant threat to people and property.

The magnitude of wave set-up crucially depends on the approach angle of waves. Waves that approach the coast obliquely mostly produce a longshore current rather than high wave set-up [3]. Therefore, if high waves always approach a certain section of the shore under relatively large angles, wave set-up usually does not cause any substantial danger [28]. The wave set-up is the largest when waves propagate (almost) directly onto the shore. This is common on more or less straight open ocean coasts [3]. The situation is more complicated in semi-sheltered areas such as the Baltic

* Corresponding author, katrip@ioc.ee

Sea where the wave approach angle is often highly variable [33].

The existing flooding maps, operational water level forecasts, and warning systems often ignore wave set-up. The prediction of extreme wave set-up events is particularly difficult in coastal segments with complex geometry and bathymetry [1]. In such areas the wave approach direction may be considerably affected by wave–seabed interaction and specific effects such as slanted fetch [18]. As a consequence, the highest wave set-up in such coastal segments does not necessarily occur during the strongest storms [28]. Each storm may have a somewhat different wind direction and refraction-induced changes in the wave direction depend also on wave periods. It is thus natural that the locations hosting the highest wave set-up normally vary from one storm to another. This suggests that the highest water levels at a certain distance from the shoreline (hereafter named offshore water level although it corresponds to a distance of a few kilometres from the shore in this study) are only infrequently synchronized with extreme wave set-up events.

The vicinity of Tallinn Bay in the north-eastern Baltic Sea (Fig. 1) is an example of regions with extremely complicated geometry. Its coastal sections are open to a wide range of directions and include segments that are most vulnerable to extreme events. The typical tidal range is a few centimetres and water level fluctuations in the entire region are mostly governed by atmospheric forcing. The extreme water level measured at a single location has reached 1.52 m above the long-term mean [29], or 1.55 m according to [6]. These values have been measured at the entrances of major harbours (Tallinn Old Harbour, Muuga Harbour, Fig. 2) at water depths >10 m. They are thus not affected by wave set-up and can be considered as representative for the offshore water level. Therefore, even a moderate additional water level rise may cause problems in this area. The entire study area is almost completely open to the waves excited by north-westerly and northerly winds. The adjacent Muuga Bay (Fig. 2) is open to high

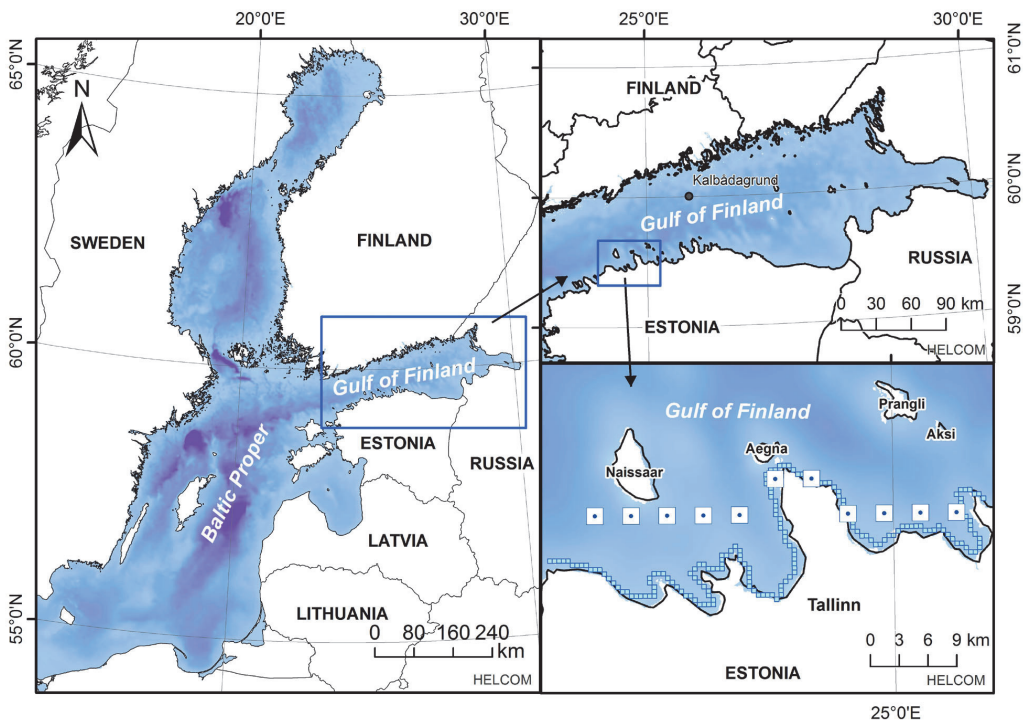


Fig. 1. Computational areas of the triple-nested wave model applied to the Tallinn Bay area. The small squares along the coast in the lower right panel indicate grid points of the wave model used in the analysis. The cells are numbered sequentially starting from the westernmost point (Fig. 2). The offshore water level is represented by 11 grid cells (white squares) of the RCO circulation model.

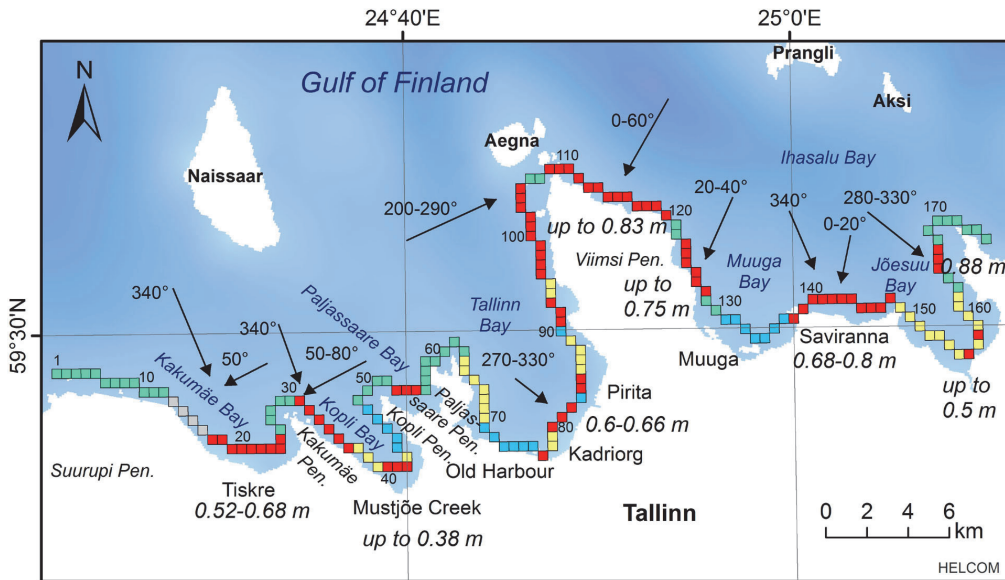


Fig. 2. Coastal sections potentially affected by high wave set-up (red squares) in the urban area of the City of Tallinn. The arrows indicate the associated directions of wave propagation. Yellow squares indicate coastal stretches where the maximum wave set-up is <20 cm, green squares are areas where high wave set-up is evidently not possible because of the convex shape of the shoreline, and blue squares refer to areas containing various engineering structures. Extended from [28] to cover areas to the east of the Viimsi Peninsula.

waves from the north-east. The maximum wave set-up may reach 0.7–0.8 m according to simplified reconstructions of wave fields in [28], and thus may substantially contribute to the resulting water level near the bayheads or along almost straight sections of the study area.

In this paper we address the contribution of wave set-up to the formation of very high water levels on the waterfront of the study area using numerically reconstructed wave properties and offshore water levels. The calculation scheme of wave time series and the method for the calculation of wave set-up height follows the material in [28]. Our focus is on the timing of the highest offshore water levels and very large wave set-up events. The study area involves also a large area to the east of Tallinn that is open to the north-east. We also further elaborate the analysis of sensitivity of the locations with the highest wave set-up in this complicated geometry with respect to the rotation of the approach direction of the largest waves from the beginning of the 1980s [28] and establish the wind directions associated with the most dangerous situations in which the total water level at the waterline considerably exceeds the all-time maximum for the offshore water level.

2. DATA AND METHODS

The study area is an about 80 km long coastal segment of Tallinn Bay and Muuga Bay from the Suurupi Peninsula to the Ihasalu Peninsula (Fig. 2). The parameters of wave set-up are evaluated from wave properties reconstructed using a triple-nested version of the WAM model with the resolution of the innermost grid about 470 m [24]. The WAM model was originally designed for open ocean conditions and for relatively deep water [9], but its latest versions reasonably replicate the Baltic Sea wave fields [6,22] and the model works properly even in Finnish archipelago areas [31,32]. To adequately represent the wave growth in low wind and short fetch conditions (which are frequent in the study area [24]), an increased frequency range of waves up to 2.08 Hz is implemented. The presence of sea ice is ignored. As there may be as many as 70–80 ice days annually [11,23], the hindcast extreme parameters of wave set-up may be somewhat overestimated. For details of the used bathymetry, the implementation, and validations of the used model version the reader is referred to [24]. The properties of simulated wave set-up statistics in Tallinn Bay are analysed in [28].

The quality of wave hindcast primarily depends on the adequacy of the wind information. Wave simulations were forced by one-point open-sea wind data for 33 years (1981–2014) according to the scheme developed in [24]. As wave set-up is very sensitive with respect to the wave propagation direction, it is important to use correct information about wind directions. Considering that atmospheric models often fail to adequately replicate wind directions in the Gulf of Finland [8], we used wind data measured at Kalbådgrund in the central part of this gulf (Fig. 1, 59°59' N, 25°36' E). The measurement devices were mounted on a caisson lighthouse located on the top of a shoal far offshore. The wind fields at this site are practically not affected by the shores and their use satisfactorily represents wave properties in the interior of Tallinn Bay [24]. The entire simulation interval contained 93 016 measurement instants with a time step of 3 h. In 8554 cases either wind speed or direction was missing. These time instants were excluded from the further analysis. As some of these instants involved quite strong winds, the analysis may underestimate the highest wave set-up events.

For an adequate estimation of wave set-up, we selected nearshore grid cells of the innermost wave model located as close to the shore as possible (Fig. 1) but still in a reasonable water depth so that the modelled waves were not yet breaking. The nearshore of the study area was divided into 174 sections with a typical length of 0.5 km that roughly correspond to the selected cells (Fig. 2). For each section the time series of the significant wave height, peak period, and mean wave direction were extracted from the output of the WAM model every 3 h from 1 January 1981 to 4 February 2014. The maximum simulated significant wave was usually lower than 4 m [24] but reached up to 5 m in a few locations [27]. These estimates are commensurable with the maximum measured values of 5.2 m in the open part of the Gulf of Finland at a distance of a few tens of kilometres from the study site [31]. To properly account for such wave heights, the grid points were chosen mainly in 4–8 m deep water. In a few cell locations with large bottom gradients the water depth is 20–27 m.

The joint impact of shoaling and refraction during the propagation of waves from the model grid points to the breaking line (the seaward border of the surf zone) was resolved in the framework of the linear wave theory following the approach developed in [28,33]. We assume that the numerically evaluated wave field is monochromatic, the wave height H_0 at the centre of the grid cell equals the modelled significant wave height, the period equals the peak period, and the approach direction equals the evaluated mean direction. We also assume that the nearshore is locally homogeneous along the direction of the shoreline and that the waves start to break when their height is 80% of the water depth d_b

(equivalently, the breaking index $\gamma_b = H_b/d_b = 0.8$). Then the wave height H_b at the breaking line satisfies the following equation [3]:

$$H_b = H_0 \left(\frac{c_{g0} \cos \theta_0}{c_{fb} \cos \theta_b} \right)^{1/2}, \quad (1)$$

where c_g is the group speed, c_f is the phase speed, and θ is the attack angle of the approaching waves. The subscripts '0' and 'b' indicate the relevant value at the particular wave model grid cell and at the breaker line, respectively. As breaking waves are long waves, their group and phase speeds are equal: $c_{gb} = c_{fb} = \sqrt{gd_b} = \sqrt{gH_b/\gamma_b}$, where g is the gravity acceleration. Applying Snell's law $\sin \theta/c_f = \text{const}$, Eq. (1) can be reduced to the following algebraic equation of 6th order [28,33]:

$$\frac{H_b^5 g}{H_0^4 \gamma_b} \left(1 - \frac{gH_b \sin^2 \theta_0}{\gamma_b c_{f0}^2} \right) = c_{g0}^2 (1 - \sin^2 \theta_0). \quad (2)$$

This equation has exactly two real positive solutions if $216g^2 H_0^2 c_{g0}^2 \sin^5 \theta_0 \cos \theta_0 < 25\sqrt{5} \gamma_b^2 c_{f0}^5$. The estimate of the breaking wave height H_b is given by the smaller real solution [28,33].

A straightforward estimate of the maximum wave set-up height can be derived using the concept of gradual wave breaking in the nearshore, or equivalently, assuming that the breaking index $\gamma_b = 0.8$ remains constant in the entire surf zone. In such ideal conditions the maximum wave set-up height is [3]

$$\bar{\eta}_{\max} = \frac{5}{16} \gamma_b H_b = 0.25 H_b. \quad (3)$$

Similarly to [28], we only consider waves that approach the seaward border of the surf zone from the direction of $\pm 15^\circ$ with respect to the normal to the coast as a potential source of high wave set-up.

The largest danger occurs if the maximum wave set-up occurs simultaneously with very high offshore water levels (interpreted here, as mentioned above, as water levels modelled using an ocean circulation model at a distance of a few kilometres from the shoreline). The water level time series (once in 6 h) is extracted for 11 offshore locations (Fig. 1) from the output of Rossby Centre Ocean (RCO, Swedish Meteorological and Hydrological Institute) model. The principles, implementation, and forcing of the RCO model have been comprehensively described in the scientific literature [14–16], and we provide here only a few core features of this model. Its horizontal resolution is 2×2 nautical miles (about 3.7 km). We use the output of the model run for May 1961–May 2005 that was coupled to a sea ice model. The water level of the model is steered using boundary information in the northern Kattegat. The

model is forced with a meteorological data set with a horizontal resolution of 22 km [21] and generally represents both the time series and statistics of water levels well. It reasonably replicates the wind-driven gentle slope in the average water level towards the eastern and northern ends of the Baltic Sea but partially fails to reproduce the largest storm surges in the western Baltic Sea [17].

3. SYNCHRONIZATION OF HIGH WAVE SET-UP AND WATER LEVEL

The all-time highest simulated wave set-up varies from 0.26 to 0.96 m (Fig. 2). Some of the very high wave set-up values characterize areas where this phenomenon apparently does not occur because of the nature of the shore. For example, almost 1 m high wave set-up hindcast for some sections of the Suurupi Peninsula (which are open to very high waves) is unrealistic because of a steep scarp at the waterline [28]. While it is natural that predominant westerly winds may often cause high wave set-up in coastal sections open to the west and north-west [28], northerly and north-easterly winds (which are relatively infrequent in the Gulf of Finland [26]) may create almost the same values of wave set-up in coastal sections of Muuga Bay that are open to the east (Fig. 2).

The total water levels at the shoreline are evaluated by adding the instantaneous values of wave set-up to the offshore water levels simulated using the RCO model. The two time series overlap for the years 1981–2005.

The highest wave set-up almost never occurs simultaneously with very high offshore water levels (Fig. 3). The reason is that large waves that attack the northern coast of Estonia are normally excited by strong northerly winds while high sea levels are produced by persistent westerly winds. This feature is mirrored by the different appearance of the relevant scatter diagrams (Fig. 3) for coastal sections that are open to different directions. The correlation between the instantaneous values of these two components of the total water level is fairly weak at all sites presented in Fig. 3. For locations open to the west or north-west the highest modelled offshore water levels (1.4–1.6 m) occur simultaneously with comparatively large wave set-up values (up to 0.5 m). For locations open to the east the largest offshore water levels are associated with very low wave set-up values (normally a few centimetres; only in one occasion 0.3 m). On the one hand, this feature indicates that the contribution of wave set-up into the total water level at the shoreline is normally negligible in the coastal segments that are open to the easterly directions. On the other hand, wave set-up may substantially contribute to the coastal flooding in all sections that are exposed to the westerly winds.

A similar asymmetry becomes evident in the formation of the total water levels that are comparable with the maximum offshore water level. The shoreline water levels higher than 1.4 m in sections that are open to the east are mostly formed by the relevant offshore water levels and contain only a minor contribution from wave set-up. In such sections almost all very high wave set-up events occur when the offshore water level is modest (Fig. 3).

The situation is considerably different in sections that are open to the west. The overall shape of the 'map' of the frequency of occurrence of different offshore water levels and wave set-up values has an elongated shape and extends from the origin to the water levels of about 1 m and wave set-up values of 0.4 m. High offshore water levels (>1 m) are often accompanied by wave set-up values ≥ 0.3 m.

4. CONTRIBUTION OF WAVE SET-UP INTO EXTREME WATER LEVELS

The total water level at the shoreline was evaluated for each 6-h time interval as the sum of the offshore water level from the RCO model and the highest wave set-up during this interval. The largest resulting values in 1981–2005 varied between 1.6 and 2.3 m along the study area (Fig. 4). The contribution of the offshore water level was in the range of 0.8–1.7 m. This constituent exclusively governed the all-time maxima of the total water level in about half (99 out of 174) of the coastal sections. This means that waves either approached the coast under large angles or propagated towards the open sea during the extreme offshore water level events.

While Fig. 3 reveals that the high offshore water levels were never fully synchronized with extreme wave set-up events, Fig. 4 suggests that these two quantities often exhibit antiphase behaviour in some sections open to the east. Still, wave set-up substantially (up to about 0.5 m) contributes to the total water level in a part of such coastal segments (Fig. 4, Table 1). The largest total water levels only insignificantly exceeded the all-time highest offshore water levels in these sections because during easterly winds (when the approaching waves were high) the offshore water level remained well below the all-time highest values.

The proportion of wave set-up in the relevant annual maxima of the total water level presents another perspective on its contribution to dangerously high water levels (Fig. 5). In coastal sections that are open to the north-west the annual highest total water level systematically exceeds the similar maximum of the offshore water level (Fig. 5a, b) because of a substantial contribution from wave set-up (which is comparable with the annual highest wave set-up). In sections that are open to the west the contribution of wave set-up to

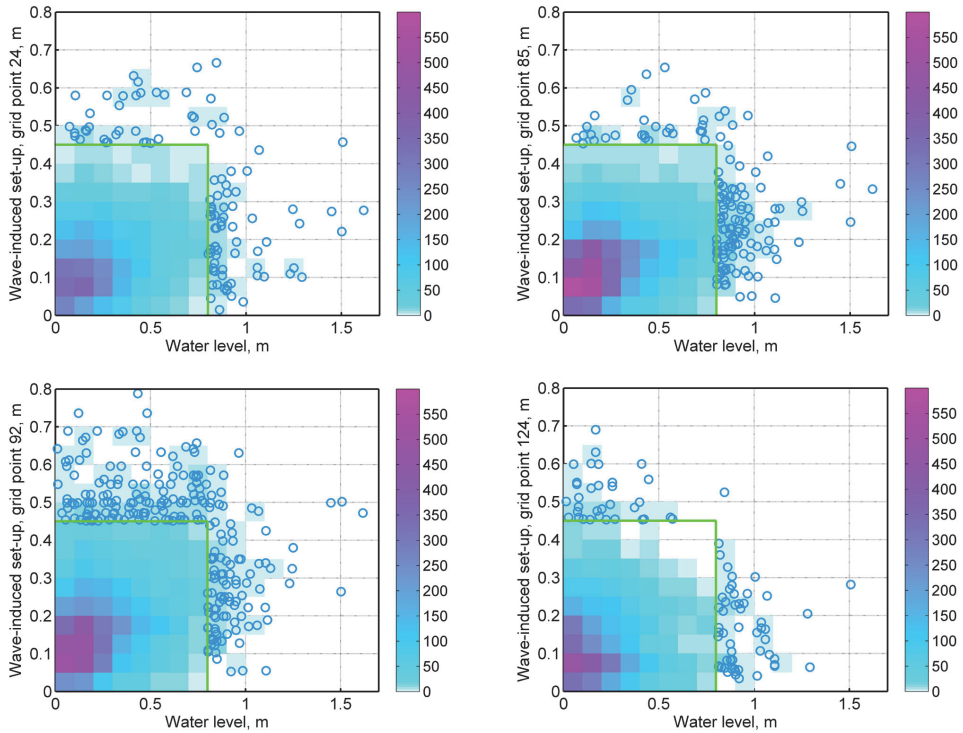


Fig. 3. Scatter diagrams of the occurrence of different offshore water levels and various wave set-up values at four representative sections of the study area: section 24 (Tiskre, a bayhead open to the north-west and partially to the west), section 85 (Pirita Beach, open only to the north-west), section 92 (western coast of the Viimsi Peninsula, open to the west), and section 124 (eastern coast of the Viimsi Peninsula, open to the north-east). The colour code corresponds to ≥ 2 occasions (otherwise the area is left white) with a particular wave set-up (with a step of 0.05 m) and water level (with a step of 0.1 m). Single cases of wave set-up > 0.45 m and water levels > 0.8 m (outside of the rectangle bordered by green lines) are represented as separate circles. The situations with zero wave set-up (waves propagating offshore) and cases with offshore water levels below the long-term average are not shown.

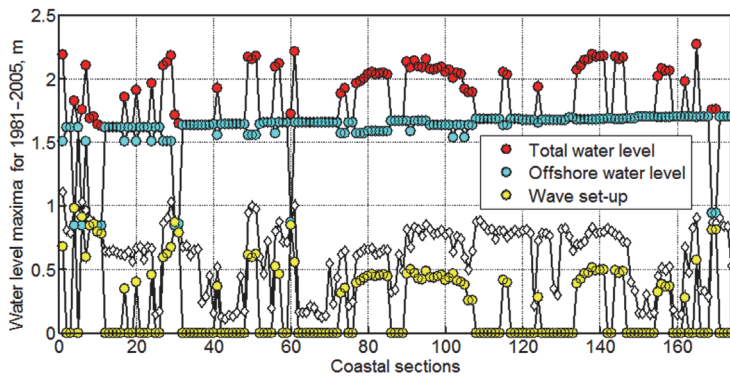


Fig. 4. The contribution of the hindcast instantaneous offshore water level and wave set-up into the all-time highest water level at the shoreline. The modelled all-time offshore water level maximum (not shown) varies insignificantly (from 1.6 m to 1.7 m) along the shore. White diamonds indicate the all-time highest wave set-up values. See Fig. 2 for the numbering of coastal sections.

Table 1. The contribution of the offshore maximum water level from the RCO model and hindcast wave set-up into all-time highest total water levels at the Estonian shoreline of the Gulf of Finland

Location (grid cell No.)	Total maximum at the shoreline, m	Contribution from		Modelled maximum of single components	
		Offshore water level, m	Wave set-up, m	Offshore water level, m	Wave set-up, m
Tiskre (24)	1.96	1.507	0.457	1.617	0.666
Pirita (85)	2.033	1.587	0.446	1.667	0.654
Viimsi (92)	2.139	1.667	0.472	1.667	0.833
Muuga (124)	1.935	1.653	0.282	1.674	0.726

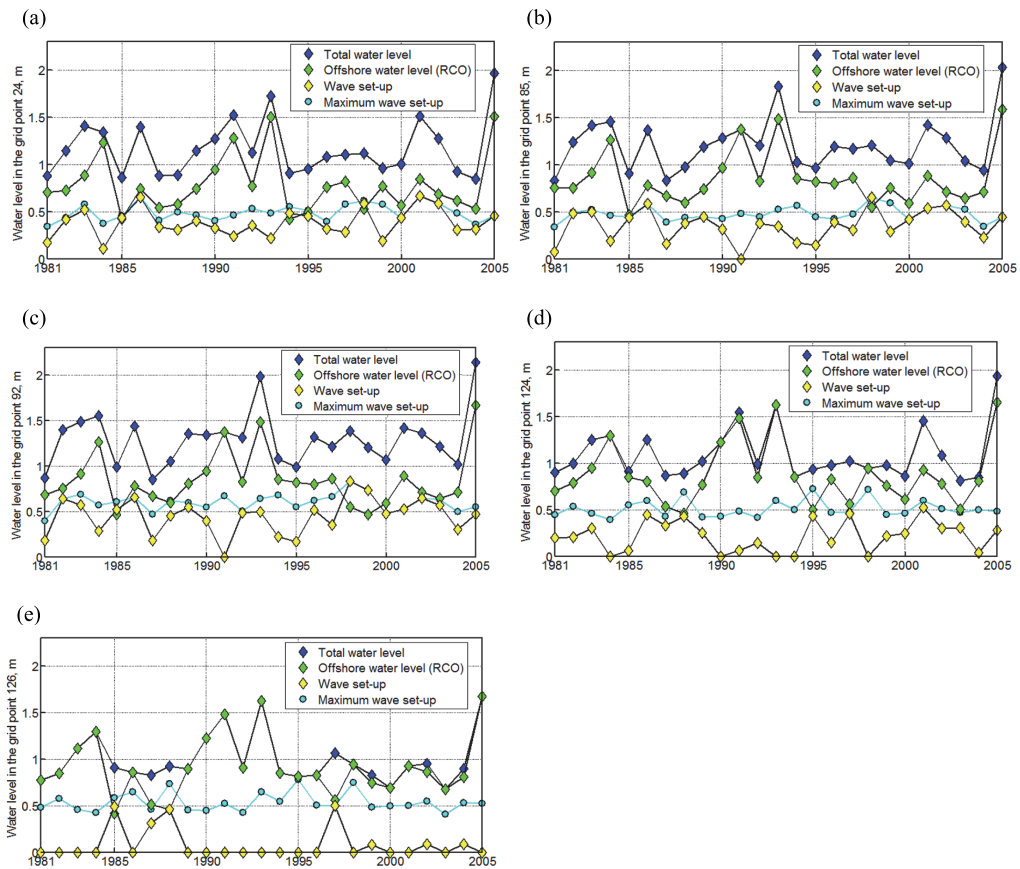


Fig. 5. The proportion of the wave set-up and offshore water level in the formation of annual maxima of the total water level at the shoreline at four representative sections of the study area: (a) Tiskre (section 24), (b) Pirita (85), (c) Viimsi (92), (d) Muuga (124), (e) a location close to Muuga Harbour (126) where wave set-up almost does not contribute. See Fig. 2 for the numbering of coastal sections.

the annual total water level maxima is clearly smaller and does not become evident in some years (Fig. 5c). In coastal segments that are open to the east (Fig. 5d, e)

wave set-up infrequently contributes to the total water level maxima.

5. EVENTS RESPONSIBLE FOR HIGHEST WAVE SET-UP VALUES

In this section storms refer to all events associated with either the all-highest waves or the all-highest wave set-up values for single coastal sections of the study area between January 1981 and February 2014. The all-time highest waves were excited by six storms that all occurred in 1995 or later (Fig. 6a). The situation is completely different for storms that caused the largest wave set-up heights. The contribution of wave set-up to the annual maximum total water level substantially varies in different years. The largest contributions to the water level in sections of Tallinn Bay open to the east occurred at the beginning of the study interval in the 1980s (Fig. 5e). Our simulations confirm that this feature remains true also for the Muuga Bay area (Fig. 6b).

The all-time highest wave set-up events were much more widely distributed over different years (Fig. 6b). In total, 50 storms contributed to these events in January 1981–October 2012. Similarly to [28], a substantial number (15) of such storms occurred at the beginning of the 1980s. The stormy years 1981–1982 were apparently followed by less stormy years in 1983–1989 and then by quite a calm half-decade 1990–1994. These variations qualitatively match the course of various storm indices for Stockholm [20]. The described feature may be interpreted as indicating a rotation in the wind (and wave approach) directions in storms in the Gulf of Finland [28]. This interpretation is consistent with changes in the statistics of wind directions in the Estonian mainland [7]. The changes match quasi-periodic long-term (25–30 y) cycles in many storm-related data sets in the Estonian coastal sea [30] and may mirror the shift of North Atlantic storm tracks [10].

The inclusion of the data from November 2012–February 2014 considerably modifies the pattern of storms responsible for the highest waves and wave set-up values (Fig. 6c). While until October 2012 about a third of all-time highest wave set-up values were created in the 1980s (Fig. 6b), many such values stemming from 1981–1982 were overridden from November 2012 onwards. During this shorter than 1.5-y time interval (that only includes two windy seasons) as many as 24 storms apparently created new all-time (since 1981) highest wave set-up values. The year 2013 contained 18 such storms. The total number of storms responsible for the highest wave set-up increased from 50 during the time interval of January 1981–October 2012 to 58 during the time interval of January 1981–February 2014.

As the extension of sea ice was quite limited in the Gulf of Finland in winters 2012/2013 and 2013/2014, the reconstructed wave properties apparently match well the actual wave fields. The majority of highest wave set-up values now stem from 1995 onwards (Fig. 6c). The described changes in 2012–2014 may be interpreted as

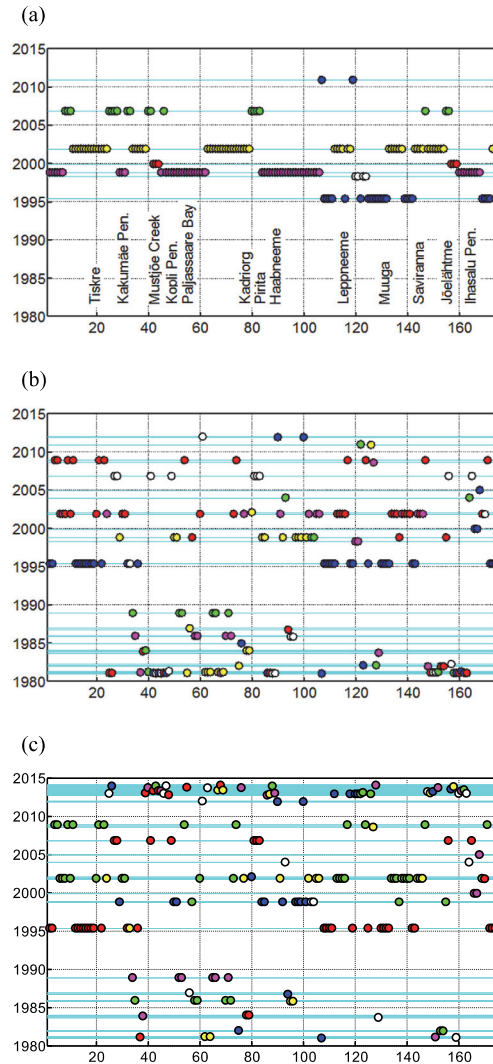


Fig. 6. (a) Six storms that caused the highest waves in different coastal sections of the study area in 1981–2014; (b) 50 storms, and (c) 58 storms that caused the highest wave set-up in these sections in January 1981–October 2012 and in January 1981–February 2014. The horizontal lines indicate single storms that produced the highest wave set-up at least in one section. Each storm is marked with a single colour. The colours vary cyclically. Note that the Kalbädagrund data set does not contain information about the wind speed during the maximum and aftermath of the extreme eastern storm on 29–30 November 2012. Therefore the largest waves approaching from the east may be missing in our reconstructions. See Fig. 2 for the numbering of coastal sections.

an implicit evidence that strong (north-)easterly winds have returned to the Gulf of Finland region. This conjecture is to some extent supported by recent wave measurements. The highest significant wave height in the Gulf of Finland (where the largest waves usually occur during westerly storms) reached for the second time its all-time maximum (5.2 m, first measured in 2001) in an easterly storm in November 2012 [19].

The temporal distribution of storms and associated wind directions during which the all-time highest total water levels were created appears greatly different from the above. Two storms were responsible for all of the overall highest water levels at the shoreline (Fig. 7). Almost all coastal sections had the overall highest water level during an exceptional storm on 8–9 January 2005 [25]. The maximum offshore water levels extracted from the RCO model reached 1.6–1.7 m in the study area. These values slightly exceed the maximum observed water levels (1.52 m [29] and 1.55 m [6]). Although the pattern of storms that were responsible for the highest wave set-up events is remarkably different (Fig. 6), in some coastal segments quite high contribution of wave set-up was apparently present during the two storms. Even if none of the 33-y highest wave set-up events occurred during the January 2005 storm, the contribution of wave set-up into the total water level was substantial (Fig. 4). The distribution of wind directions during the highest total water level occasions (Fig. 7) once more confirms that coastal sections that are open to the west or north-west are the most likely

candidates for exceptional total water levels owing to simultaneous occurrence of the high offshore water level and large waves that propagate almost directly onshore.

6. CONCLUDING REMARKS

The presented results show that wave set-up may act as an important component of marine-induced coastal hazards not only on the open ocean coasts (that are often impacted by high waves) but also on the shores of semi-sheltered relatively small water bodies such as the Baltic Sea. Similarly to the open ocean coasts [2], the extreme values of wave set-up may be over 50% of the maximum offshore water levels. The actual contribution of wave set-up to the total water levels at the shoreline is smaller in areas that are sheltered with respect to waves approaching from predominant wind directions. In these sections the high offshore water levels normally do not occur simultaneously with large wave set-up heights. Owing to such a mismatch the actual contribution of wave set-up generally does not exceed 0.5 m in the study area in the Gulf of Finland. This contribution, however, may represent a substantial hazard to certain coastal sections: the theoretical maxima of the total water level at the shoreline may reach well over 2 m in locations that are favourable for the formation of wave set-up. Wave set-up phenomena normally do not occur if the coast is protected by a seawall or by natural obstacles such as reed, bushes, or stones [2]. Still, it is likely that up to 50% of the study area may be potentially affected by high set-up [28].

The extensive alongshore variation of the wave set-up heights is a reflection of the significant dependence of this phenomenon on the match of the wave propagation direction and the geometry of the coastline. As the return period of unfavourable combinations of wave properties is considerably larger than that of just high waves or water levels, more effort is needed to establish adequate statistics of wave set-up heights. Moreover, every coastal segment seems to have its own ‘perfect storm’ in terms of wave set-up. This feature highlights the particular role of wind direction in the formation of the highest water levels. The most dangerous situations (in which the total water level at the shoreline may substantially exceed the all-time maximum for the offshore water level) are likely to occur during (north-)westerly storms and in coastal sections that are open to the north-west.

The seeming (possibly cyclic) rotation of wind direction in strong storms and especially the return of strong (north-)easterly wave storms in the Gulf of Finland in 2012–2014 may lead to a situation where some other coastal sections will experience very large wave set-up heights. There are, however, obvious

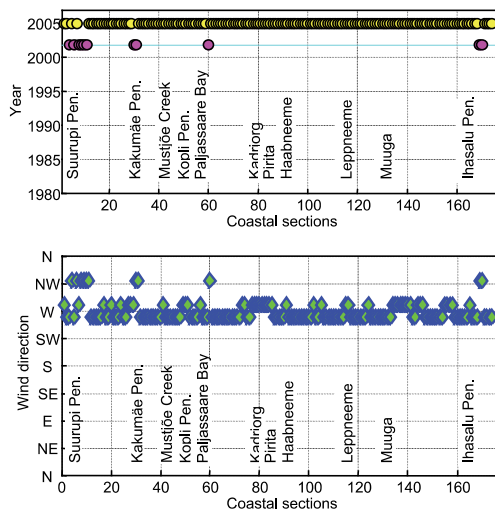


Fig. 7. Storms (above) and wind directions (below) that were responsible for the highest total water levels at the shoreline. See Fig. 2 for the numbering of coastal sections.

limitations for such changes in the study area. Storm tracks that cross Estonia to the south create strong northerly winds (and waves) along the northern coast but do not yield remarkably high sea level events in the Gulf of Finland. Cyclones that pass Estonia to the north yield strong westerly winds. They have a larger potential to raise sea level, but limited fetch for waves along the study area. A better ‘synchronization’ of a high offshore water level and large wave set-up can occur along the western coast of Estonia and along the coasts of Latvia and Lithuania.

Finally, we would like to emphasize that the presented results have been obtained using simplified schemes of the calculation of wave properties, a one-point wind data set with considerable gaps, and partially unrealistic assumptions for the formation of wave set-up on ideal beaches. In particular, no specific validation of the simulated wave properties has been performed. Therefore, the quantitative outcome of this research should be taken with caution.

ACKNOWLEDGEMENTS

The research was supported by institutional financing of the Estonian Ministry of Education and Research (IUT33-3), the Estonian Science Foundation (grant 9125), and through support of the European Regional Development Fund to the Centre of Excellence in Non-linear Studies CENS. The simulated hydrographic data were kindly provided by the Swedish Meteorological and Hydrological Institute in the framework of the BONUS BalticWay cooperation.

REFERENCES

- Alari, V. and Kõuts, T. 2012. Simulating wave–surge interaction in a non-tidal bay during cyclone Gudrun in January 2005. In *Proceedings of the IEEE/OES Baltic 2012 International Symposium “Ocean: Past, Present and Future. Climate Change Research, Ocean Observation & Advanced Technologies for Regional Sustainability,” May 8–11, Klaipėda, Lithuania*. IEEE Conference Publications, doi: 10.1109/BALTIC.2012.6249185
- Dean, R. G. and Bender, C. J. 2006. Static wave set-up with emphasis on damping effects by vegetation and bottom friction. *Coast. Eng.*, **53**, 149–165.
- Dean, R. G. and Dalrymple, R. A. 1991. *Water Wave Mechanics for Engineers and Scientists*. World Scientific.
- Hall, J. W., Dawson, R. J., Barr, S. L., Batty, M., Bristow, A. L., Carney, S. et al. 2010. City-scale integrated assessment of climate impacts, adaptation, and mitigation. In *Energy Efficient Cities: Assessment Tools and Benchmarking Practices* (Bose, R. K., ed.). The World Bank, 63–83.
- Hallegette, S., Green, C., Nicholls, R. J., and Corfee-Morlot, J. 2013. Future flood losses in major coastal cities. *Nat. Clim. Change*, **3**(9), 802–806.
- Hünicke, B., Zorita, E., Soomere, T., Madsen, K. S., Johansson, M., and Suursaar, Ü. 2015. Recent change – sea level and wind waves. In The BACC II Author Team, *Second Assessment of Climate Change for the Baltic Sea Basin*. Regional Climate Studies, Springer, 155–185.
- Jaagus, J. 2009. Long-term changes in frequencies of wind directions on the western coast of Estonia. In *Climate Change Impact on Estonian Coasts* (Kont, A. and Tõnisson, H., eds). Publication 11/2009. Institute of Ecology, Tallinn University, Tallinn, 11–24.
- Keevallik, S. and Soomere, T. 2010. Towards quantifying variations in wind parameters across the Gulf of Finland. *Estonian J. Earth Sci.*, **59**, 288–297.
- Komen, G. J., Cavaleri, L., Donelan, M., Hasselmann, K., Hasselmann, S., and Janssen, P. A. E. M. 1994. *Dynamics and Modelling of Ocean Waves*. Cambridge University Press, Cambridge.
- Lehmann, A., Getzlaff, K., and Harlaß, J. 2011. Detailed assessment of climate variability in the Baltic Sea area for the period 1958 to 2009. *Climate Res.*, **46**, 185–196.
- Leppäranta, M. 2012. Ice season in the Baltic Sea and its climatic variability. In *From the Earth’s Core to Outer Space*. Lecture Notes Earth Sci., **137**, 139–149.
- Leppäranta, M. and Myrberg, K. 2009. *Physical Oceanography of the Baltic Sea*. Springer, Berlin.
- Longuet-Higgins, M. S. and Stewart, R. W. 1964. Radiation stresses in water waves: a physical discussion with applications. *Deep-Sea Res.*, **11**, 529–562.
- Meier, H. E. M. 2001. On the parameterization of mixing in three-dimensional Baltic Sea models. *J. Geophys. Res.–Oceans*, **106**, C30997–C31016.
- Meier, H. E. M. and Höglund, A. 2013. Studying the Baltic Sea circulation with Eulerian tracers. In *Preventive Methods for Coastal Protection* (Soomere, T. and Quak, E., eds). Springer, 101–130.
- Meier, H. E. M., Döscher, R., and Faxén, T. 2003. A multiprocessor coupled ice–ocean model for the Baltic Sea: application to salt inflow. *J. Geophys. Res.–Oceans*, **108**(C8), 32–73.
- Meier, H. E. M., Broman, B., and Kjellström, E. 2004. Simulated sea level in past and future climates of the Baltic Sea. *Climate Res.*, **27**, 59–75.
- Pettersson, H., Kahma, K. K., and Tuomi, L. 2010. Predicting wave directions in a narrow bay. *J. Phys. Oceanogr.*, **40**(1), 155–169.
- Pettersson, H., Lindow, H., and Brüning, T. 2013. Wave climate in the Baltic Sea 2012. HELCOM Baltic Sea Environment Fact Sheets 2012. <http://helcom.fi/baltic-sea-trends/environment-fact-sheets/hydrography/wave-climate-in-the-baltic-sea/> (accessed 28.02.2015).
- Rutgersson, A., Jaagus, J., Schenk, F., and Stendel, M. 2014. Observed changes and variability of atmospheric parameters in the Baltic Sea region during the last 200 years. *Climate Res.*, **61**, 177–190.
- Samuelsson, P., Jones, C. G., Willén, U., Ullerstig, A., Gollovik, S., Hansson, U. et al. 2011. The Rossby Centre Regional Climate Model RCA3: model description and performance. *Tellus A*, **63**, 4–23.

22. Schmager, G., Fröhle, P., Schrader, D., Weisse, R., and Müller-Navarra, S. 2008. Sea state, tides. In *State and Evolution of the Baltic Sea 1952–2005* (Feistel, R., Nausch, G., and Wasmund, N., eds). Wiley, Hoboken, NJ, 143–198.
23. Sooäär, J. and Jaagus, J. 2007. Long-term changes in the sea ice regime in the Baltic Sea near the Estonian coast. *Proc. Estonian Acad. Sci. Eng.*, **13**, 189–200.
24. Soomere, T. 2005. Wind wave statistics in Tallinn Bay. *Boreal Environ. Res.*, **10**, 103–118.
25. Soomere, T., Behrens, A., Tuomi, L., and Nielsen, J.W. 2008. Wave conditions in the Baltic Proper and in the Gulf of Finland during windstorm Gudrun. *Nat. Hazards Earth Syst. Sci.*, **8**, 37–46.
26. Soomere, T., Myrberg, K., Leppäranta, M., and Nekrasov, A. 2008. The progress in knowledge of physical oceanography of the Gulf of Finland: a review for 1997–2007. *Oceanologia*, **50**(3), 287–362.
27. Soomere, T., Viška, M., and Eelsalu, M. 2013. Spatial variations of wave loads and closure depth along the eastern Baltic Sea coast. *Estonian J. Eng.*, **19**, 93–109.
28. Soomere, T., Pindsoo, K., Bishop, S. R., Käär, A., and Valdmann, A. 2013. Mapping wave set-up near a complex geometric urban coastline. *Nat. Hazards Earth Syst. Sci.*, **13**, 3049–3061.
29. Suursaar, Ü., Kullas, K., Otsmann, M., Saaremäe, I., Kuik, J., and Merilain, M. 2006. Cyclone Gudrun in January 2005 and modelling its hydrodynamic consequences in the Estonian coastal waters. *Boreal Environ. Res.*, **11**, 143–159.
30. Suursaar, Ü., Jaagus, J., and Tõnissson, H. 2015. How to quantify long-term changes in coastal sea storminess? *Estuar. Coast. Shelf S.*, **156**, 31–41.
31. Tuomi, L., Kahma, K. K., and Petttersson, H. 2011. Wave hindcast statistics in the seasonally ice-covered Baltic Sea. *Boreal Environ. Res.*, **16**, 451–472.
32. Tuomi, L., Kahma, K. K., and Fortelius, C. 2012. Modelling fetch-limited wave growth from an irregular shoreline. *J. Marine Syst.*, **105**, 96–105.
33. Viška, M. and Soomere, T. 2013. Simulated and observed reversals of wave-driven alongshore sediment transport at the eastern Baltic Sea coast. *Baltica*, **26**(2), 145–156.

Laineaju roll veetaseme kujunemises Tallinna lahe ümbruse randades

Katri Pindsoo ja Tarmo Soomere

Laineaju ehk murdlainetes lisanduv veetõus on mittelineaarne nähtus, mida põhjustab lainete murdumise käigus vabanev impulss ja mille tõttu võib üksikutes rannaosades (kuhu suured lained saabuvad peaaegu risti rannaga) veetase rannajoonel arvestataval määral tõusta. On analüüsitud laineaju osakaalu ekstreemsete veetasemete kujunemisel Tallinna ja Muuga lahe randades. Laineaju maksimaalne kõrgus leitakse aastate 1981–2014 jaoks arvutatud tuulelainetuse parameetrite alusel. Oluline lainekõrgus, lainete tipp-periood ja lainelevi domineeriv suund on leitud lainemudeli WAM kolmeastmelise rakenduse abil. Mudelite hierarhia kasutamine võimaldab leida vajalikud suurused lahutusvõimega ligikaudu 470 m. Veetase avamerel on leitud nn Rossby Centre (RCO, Rootsi meteoroloogia ja hüdroloogia instituut) hüdrodünaamilisest mudelist. On näidatud, et laineaju võib üksikutes rannalõikudes tõsta veetaset 0,7–0,8 m võrra. Kõrgeim mõõdetud avamere veetase uuringualal on 1,52–1,55 m. Kõrgeimad avamere veetasemed ei esine üldjuhul samaaegselt ülikõrgete laineaju situatsioonidega. Laineaju roll kõigi aegade kõrgeimate rannaäärsete veetasemete kujunemisel on siiski märkimisväärne, lisades mõnedes rannaosades kõigi aegade kõrgeimatele avamere veetasemetele kuni 0,5 m. Laineaju osakaal aasta kõrgeima veetaseme kujunemisel varieerub oluliselt. Suurim tähtsus on laineajul üldiselt lääne või loode poole avatud randades ja lääne- ning põhjakaare tormidega.

Paper IV

Soomere T., **Pindsoo K.** 2016. Spatial variability in the trends in extreme storm surges and weekly-scale high water levels in the eastern Baltic Sea. *Continental Shelf Research*, 115, 53–64, doi: 10.1016/j.csr.2015.12.016.



Contents lists available at ScienceDirect

Continental Shelf Research

journal homepage: www.elsevier.com/locate/csr

Research papers

Spatial variability in the trends in extreme storm surges and weekly-scale high water levels in the eastern Baltic Sea

Tarmo Soomere^{a,b,*}, Katri Pindsoo^a^a Institute of Cybernetics at Tallinn University of Technology, Akadeemia tee 21, 12618 Tallinn, Estonia^b Estonian Academy of Sciences, Kohtu 6, Tallinn, Estonia

ARTICLE INFO

Article history:

Received 28 June 2015

Received in revised form

22 December 2015

Accepted 30 December 2015

Available online 31 December 2015

Keywords:

Water level

Trends

Extremes

Storm surge

Baltic Sea

ABSTRACT

We address the possibilities of a separation of the overall increasing trend in maximum water levels of semi-enclosed water bodies into associated trends in the heights of local storm surges and basin-scale components of the water level based on recorded and modelled local water level time series. The test area is the Baltic Sea. Sequences of strong storms may substantially increase its water volume and raise the average sea level by almost 1 m for a few weeks. Such events are singled out from the water level time series using a weekly-scale average. The trends in the annual maxima of the weekly average have an almost constant value along the entire eastern Baltic Sea coast for averaging intervals longer than 4 days. Their slopes are ~ 4 cm/decade for 8-day running average and decrease with an increase of the averaging interval. The trends for maxima of local storm surge heights represent almost the entire spatial variability in the water level maxima. Their slopes vary from almost zero for the open Baltic Proper coast up to 5–7 cm/decade in the eastern Gulf of Finland and Gulf of Riga. This pattern suggests that an increase in wind speed in strong storms is unlikely in this area but storm duration may have increased and wind direction may have rotated.

© 2015 Elsevier Ltd. All rights reserved.

1. Introduction

The risks and damages associated with coastal flooding show a rapid increase (Hallegatte et al., 2013) and are one of the largest concerns of countries with extensive low-lying nearshore areas. Although the course of the local water level, the main agent of the relevant risk, does not follow any simple rule (Weisse et al., 2014), the analysis of its linear trends based on its past behaviour is still a powerful tool to obtain a first approximation of the future projections. The relevant efforts have not only confirmed the overall sea level rise (Cazenave et al., 2014) but also established contribution of this rise to local water level maxima (Mudersbach et al., 2013; Xu and Huang, 2013). These efforts have also highlighted an increase in the magnitude of local storm surges for a number of locations round the globe. These processes occur on the coasts of the open ocean (Sun et al., 2013; Talke et al., 2014), in shelf seas (Weisse et al., 2012) and in semi-enclosed basins (Ullmann et al., 2007; Wiśniewski and Wolski, 2011; Masina and Lamberti, 2013).

It is not always clear beforehand which component of the water

level (or its physical driver) is responsible for an increase in the maxima in question. For example, on the German North Sea coast prior to the mid-1950s and from about 1990 onwards, changes in high sea levels matched mean sea level changes but from the mid-1950s to 1990 were significantly different from those observed in the mean sea level (Mudersbach et al., 2013).

The contributions from different forcing factors to the total water level are often considered as mostly independent. This assertion is equivalent to the linear superposition principle and makes it possible to analyse separately the course and timing of water level variations caused by each driver (e.g., Losada et al., 2013). More importantly, it allows in-depth analysis of changes in the contributions caused by each single driver (e.g., Howard et al., 2014; Weisse et al., 2014).

Analysis of the behaviour of single components is particularly convenient in locations where the water level reacts to contributions that act at greatly different time scales. A separation of the water level into three components driven by fundamentally different mechanisms – the long-term mean and its slow variations, tides and storm surges – is a classic approach for research into water level dynamics (Pugh and Vassie, 1978, 1980; Haigh et al., 2010a). Likewise, it is traditional to analyse separately the periodic and random components of water level (Haigh et al., 2010b). Attempts of this kind have been also made for locations that contain a substantial range of subtidal (time scales from diurnal to

* Corresponding author at: Institute of Cybernetics at Tallinn University of Technology, Akadeemia tee 21, 12618 Tallinn, Estonia.

E-mail addresses: soomere@cs.ioc.ee (T. Soomere), katri.pindsoo@ioc.ee (K. Pindsoo).

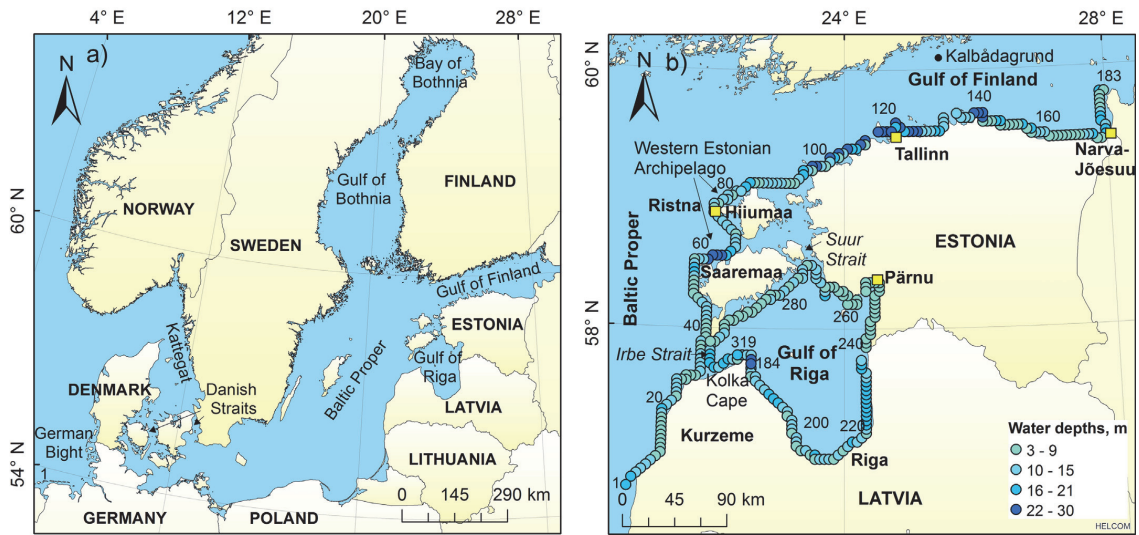


Fig. 1. (a) Scheme of the Baltic Sea and the study area, (b) Water depth at the selected RCO model grid cells in the eastern Baltic Sea (colour scale) and locations of water level gauges (yellow squares at Pärnu, Ristna, Tallinn and Narva-Jõesuu) used in the analysis. The grid cells are numbered consecutively from the western coast of Latvia to eastern Gulf of Finland, and then counterclockwise along the coast of the Gulf of Riga starting from Kolka Cape. (For interpretation of the references to colour in this figure legend, the reader is referred to the web version of this article.)

seasonal) water level variability (Percival and Mofjeld, 1997; Wong and Moses-Hall, 1998; Guannel et al., 2001; Wilson et al., 2014).

The issues of water level are particularly challenging in semi-enclosed water bodies such as the Baltic Sea (Fig. 1a) where the sea-level rise may be faster than in the adjacent regions (Stramska and Chudziak, 2013). The properties of the course of water level depend here on specific factors such as local salinity (Ekman and Mäkinen, 1996) or spatial variations in the tectonic motions (Richter et al., 2012). The latter feature leads to substantial variability in properties of the observed (relative) water levels in different locations of the Baltic Sea (Scotto et al., 2009). The northern part of this basin experiences a rapid postglacial uplift and an associated relative sea level decrease (Johansson et al., 2001). The central part of the sea feels a weak relative sea level rise (Dailidienė et al., 2004, 2006) whereas the southern part is affected by a faster sea level rise owing to a gradual crustal downlift on the order of 0.2 cm/decade (Harff and Meyer, 2011).

These trends are often superposed by variations in the properties of short-term water level fluctuations. These variations appear different in different part of the sea. For example, short-term sea level variability has clearly changed in the northern Baltic Sea (Johansson et al., 2001) whereas no clear trend in the height of storm surges seems to exist for the German Bight (although the frequency and duration of storms have increased in this part of the sea, Gönner, 2003). The pattern of trends is asymmetric: the trends in minima of water levels are much smaller than similar trends in maximum water levels (Barbosa, 2008).

The possibility of extensive variations in the water volume of the entire Baltic Sea substantially complicates the analysis of the future projections of the course of local water level and of its extremes. These fundamentally aperiodic variations are driven by atmospheric impact and usually occur on time scales of a few weeks (Feistel et al., 2008; Leppäranta and Myrberg, 2009). Even moderate winds from certain directions can reverse the typical estuarine circulation in the Baltic Sea with respect to the Atlantic Ocean. In particular, westerly winds over the Danish straits (Fig. 1a) with speeds of only 2–5 m/s can block the outflow of

brackish water from the Baltic Sea (Lehmann et al., 2012). The overall freshwater surplus (Leppäranta and Myrberg, 2009) will then cause an increase in the water volume in the Baltic Sea.

The largest impact to the Baltic Sea water volume arises from sequences of storm cyclones (Post and Kõuts, 2014) that force large amounts of the North Sea water to flow into the Baltic Sea over a few weeks (Stigebrandt and Gustafsson, 2003; Lehmann and Post, 2015). The associated water level increase in the entire sea may reach 1 m (Johansson et al., 2001) similarly to Chesapeake Bay (Bosley and Hess, 2001). For many coastal segments this value is comparable with the all-time maximum storm surge height (Averkiev and Klevanny, 2010). The most devastating surges in this sea are created by strong storms that approach when the overall water volume of the Baltic Sea is unusually large (Johansson et al., 2001). The combination of an increased water level of the entire sea with strong local storms is a probable reason for a few local water level recordings that appear as statistically unpredictable outliers, but are nevertheless caused by storms of reasonable strength (Suursaar and Sooäär, 2007; Suursaar et al., 2015). Another interesting feature of water level maxima along the eastern coast of the Baltic Sea is the massive variation (from about 2 to 9 cm/decade, Suursaar and Sooäär, 2007) in the slopes of their trendlines whereas almost no correlation exists between the changes in the mean and maximum water levels.

These features call for the further analysis of the processes driving water level in the Baltic Sea and similar water bodies. Several efforts have been made to single out the components of water level and to analyse separately their variability and long-term trends. The relevant approaches range from straightforward filtering and averaging techniques up to the use of wavelet methods (Percival and Mofjeld, 1997; Bastos et al., 2013). The state-of-the-art of these approaches is presented in (Johansson, 2014). The analysis in the current paper is motivated by the observation that the weekly-scale average water level in a large section of the eastern Baltic Sea coast represents a quasi-Gaussian process while the residual (the total water level minus the weekly average), interpreted as the local storm surge (Haigh et al., 2010a),

reflects a Poisson process (Soomere et al., 2015a,b). The existence of such a separation of the total water level into clearly distinguishable components with different probability distribution functions makes it possible to more exactly establish the role of each of these components (and their drivers) in the observed changes in the maximum water levels. This separation also sheds some light on the question: Which mechanism primarily drives the sea level extremes and associated coastal floodings (cf. Haigh et al., 2010b; Mudersbach et al., 2013).

In this paper we make an attempt to separate the overall increasing trend in maximum water levels along the eastern Baltic Sea coasts into trends of the two components: local storm surges and basin-scale water level. Although direct observations and measurements of the height and spatial extent of coastal floodings form the corner stone for the understanding these phenomena, their better prediction and the associated risk assessments, the observed data sets normally do not provide enough information about what happens along the entire coastline. The existing network of tidal gauges is not perfect even in the most densely covered areas such as the North Sea (Arns et al., 2015) or the Baltic Sea (Hünicke et al., 2015). Moreover, the records of some gauges may contain extensive distortions (e.g., by local wave set-up, Eelsalu et al., 2014) and do not always provide an adequate quantification of the spatial extent of single surges (Brakenridge et al., 2013). For this reason we largely rely on numerically simulated water levels. Similarly to (Soomere et al., 2015b), numerically modelled time series are used to highlight the pattern of spatial variations in the trends of the two components for the entire study area. A comparison of the outcome with the analysis of observed water levels in single locations indicates that local effects may play substantial role in some of the observed data sets.

The paper is organised as follows. Section 2 presents an insight into the data sets, the approach used for the separation of water level constituents and the concept of block maxima. The study mostly relies on numerically simulated water level time series produced using the Rossby Centre Ocean model run in the Swedish Meteorological and Hydrological Institute. This data set is complemented by water level time series from four observation sites along the Estonian coast. Section 3 provides an analysis of spatial variations in trends of maxima of storm surge heights and weekly average water levels (equivalently, the basin-scale water volume). Section 4 focuses on the interpretation of the established features.

2. Material and method

2.1. Modelled and observed water level data sets

The data sets used in this paper were extracted from the output of the Rossby Centre Ocean Model (RCO), provided in the framework of BONUS BalticWay cooperation (Soomere et al., 2014). As this circulation model has been repeatedly described in the scientific literature, we present here only a few aspects relevant to our research. The reader is referred to (Meier et al., 2003; Meier and Höglund, 2013) for further information about this model.

The horizontal and vertical resolutions of the RCO model are 2×2 nautical miles (about 3.7 km) and 3–12 m, respectively. These values are commonly considered to be acceptable for the reproduction of the large-scale motion patterns and basic statistics of mesoscale motions in the Baltic Sea and its larger sub-basins such as the Gulf of Finland or the Gulf of Riga (Myrberg et al., 2010). The model uses boundary information about water level in the northern Kattegat (Fig. 1a). The model run for May 1961–May 2005, the data from which are used in our analysis, was forced with a meteorological data set with a horizontal resolution of

22 km derived from the ERA-40 re-analysis (Samuelsson et al., 2011) and was coupled to a sea ice model. The output of the model replicates both time series and statistics of water levels generally well. A certain discrepancy between modelled and observed storm surges has been found in the western Baltic Sea (Meier et al., 2004). As the modelled statistics of extremes has very good match with similar statistics of measured water level data for most of the Estonian coast, a possible reason for this mismatch may be the ignoring of wave-induced set-up in the RCO model (Eelsalu et al., 2014).

Our focus is on the spatial patterns of the behaviour of maximum water levels in the nearshore. To study these patterns, the water level time series were extracted for a set of nearshore locations along the eastern Baltic Sea coast. These locations were selected as a continuous belt of the model grid cells along the coasts of Latvia and Estonia (Fig. 1b). To avoid local distortions of the water level (e.g., because of subgrid-scale features caused by small islands and unresolved bathymetric features in the nearshore and in very shallow water), the cells were mostly selected in the range of model water depths 6–30 m (except for the shallow vicinity of Pärnu Bay where the depth in a few locations is 3–5 m).

The link between the modelled and measured or observed water levels is not straightforward in large brackish water basins such as the Baltic Sea (Ekman and Mäkinen, 1996). The RCO model employs the principle of volume conservation. This means that the impact of spatio-temporal variations in salinity and temperature of water masses on water level is neglected. The resulting (thermohaline and halohaline) effects are, however, small in shallow seas such as the Baltic Sea.

The combination of the predominance of south-westerly winds and baroclinic motions due to the horizontal salinity gradient give rise to substantial water level gradient from the Danish straits (Fig. 1a) up to the northern Bay of Bothnia (Meier et al., 2004). The difference between the water level in Kattegat and in the northernmost parts of the sea reaches about 30–35 cm in the Bay of Bothnia (Fig. 1a) and is somewhat smaller in the Gulf of Finland and the Gulf of Riga (Ekman and Mäkinen, 1996). The water level in the model is governed by water level variations in Kattegat (Fig. 1a) that are recorded using the height system NH60 (Meier et al., 2004). The model seabed (and thus the water depths in the model) follows the so-called Warnemünde topography (Seifert et al., 2001) that is compiled using information from various surveys based on different height systems. This steady bathymetry neglects the land uplift in northern parts of the Baltic Sea and downlift in southern parts (Steffen and Wu, 2011). These processes may appreciably change the entire volume of the Baltic Sea for a fixed water level.

We use time series of 64 293 single water level values (sampled once in 6 h for each RCO model grid point in Fig. 1b) during the time interval of 29 May 1961–31 May 2005. Because of relatively low sampling frequency these values basically represent a certain proxy for local storm surge heights, as duration of the water level peak may be considerably shorter. This data set is complemented with observed water levels at Tallinn Harbour in 1945–1995, Narva-Jõesuu in 1950–2010, Ristna in 1950–2012 and Pärnu in 1950–2010 (Figs. 1b, 2). Water level observations in Tallinn Harbour were made once in every 6 hours until April 1950 (no records are available for the year 1946), in Ristna until February 1962 and in Pärnu until September 1951. All later observations or measurements were made hourly. To comply with the modelled data only measurements for the years 1961–2005 (1961–1995 in Tallinn) are considered.

These data sets have been extensively described and analysed from various viewpoints, e.g., the overall course and periodic components of the water level (Raudsepp et al., 1999), projections of extreme water levels and their return periods (Suursaar and

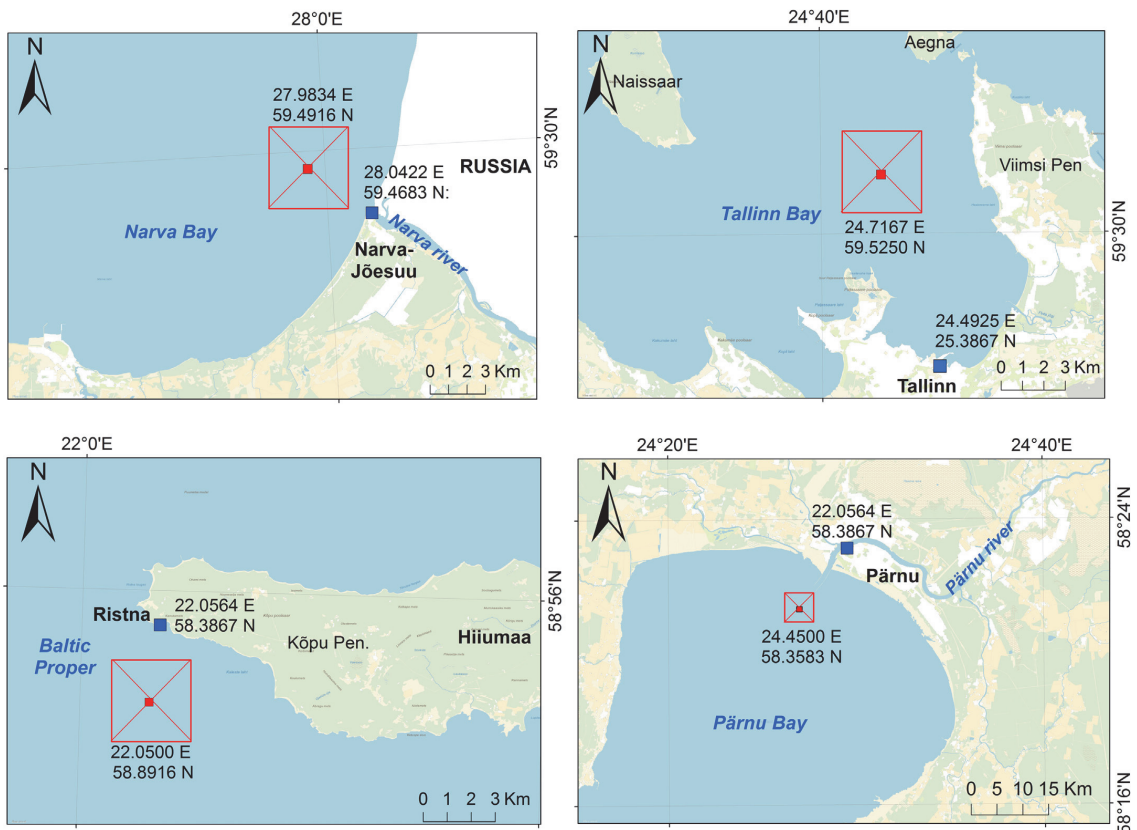


Fig. 2. Location schemes of the RCO model grid cells and coordinates of their centroids in Narva Bay, Tallinn Bay, Baltic Proper close to Hiiumaa and Pärnu Bay, and water level gauges at Tallinn Harbour (until 1995), Pärnu, Narva-Jõesuu and Ristna (Kalana Harbour).

Sooäär, 2007), the feasibility of ensemble approach for projections of water level extremes (Eelsalu et al., 2014) or the separation of the total water level into short-term and weekly-scale components (Soomere et al., 2015b). The gauge at Tallinn Harbour seems to most adequately represent the offshore water level (Eelsalu et al., 2014) and the data from this site is chosen to illustrate our approach.

As we focus on the temporal course of maxima of the water level, possible deviations of the long-term mean modelled water levels from the actual values are immaterial and the modelled water level time series are de-meant for the further analysis.

2.2. Trends in the annual maxima of total water level

The properties of trends in the observed long-term water level have been studied in detail for the eastern Baltic Sea coast. The relevant rates mostly vary in the range of 2–3 cm/decade in Estonian coastal waters (Suursaar and Sooäär, 2007; Suursaar et al., 2015). These values are usually much smaller than the increase in the annual water level maxima that ranges between 3.2 and 9 cm/decade (Jaagus and Suursaar, 2013). As we are specifically interested in spatial patterns of the trends for maxima and the changes in the mean water level are more or less constant for the entire study area, we removed the trend in the mean water level by means of simple de-trending of both the modelled and observed

data sets.

We employ the concept of block maxima (the set of examples of highest water levels over certain periods of time) in our analysis. See, e.g., Haigh et al. (2010a) for the discussion of this approach. The monthly maximum values of any water level characteristic may be strongly correlated as the relaxation time of the entire Baltic Sea water volume is a few weeks (Leppäranta and Myrberg, 2009). The interrelations between monthly maxima are even more complicated in this water body because of frequent time lag between the atmospheric impact and the reaction of water level (Johansson et al., 2014).

It is therefore reasonable to follow the common practice (e.g., Ribeiro et al., 2014) and to use the largest values that occur once in a year (Fig. 3). For 6-h modelled data they are equivalent to the 99.93th percentile of the annual data sets and thus close to the commonly used 99.9th percentiles (Mudersbach et al., 2013). These values for subsequent years may be substantially correlated in the Baltic Sea because of the long relaxation time of the events of its increased water volume. For example, exceptionally large water level maxima in December of one year normally contain a considerable contribution from the overall increase in the Baltic Sea water level. As it takes a few weeks for the water to leave the sea, such events may strongly contribute to the water level in January of the subsequent year.

A natural way to construct an alternative set of block maxima is

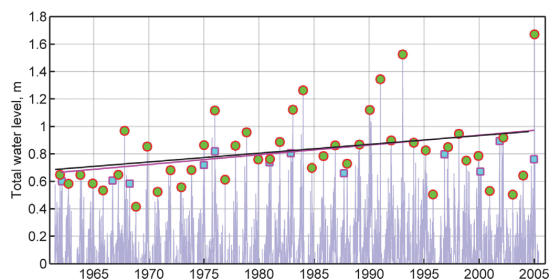


Fig. 3. Trends in stormy-season (green circles, 7.1 cm/decade, red trendline) and annual (cyan squares, visible if different from the stormy-season maxima, 6.4 cm/decade, black trendline) modelled water level maxima near Tallinn (Fig. 2) in 1961–2004. The Sen's slope for both trends is 6.4 cm/decade. The 95% confidence intervals for the Sen's slope of stormy-season maxima and for the annual maxima are [0.9, 11.6] cm/decade and [2.3, 9.8] cm/decade, respectively. (For interpretation of the references to colour in this figure legend, the reader is referred to the web version of this article.)

to pick up the maxima over autumn and winter stormy seasons (August–March). These values (from May of one year to April of the subsequent year, Fig. 3) are clearly separated from each other by calm spring seasons (Johansson et al., 2001; Suursaar et al., 2002; Jaagus and Suursaar, 2013) and are thus uncorrelated.

As both sets of maxima exhibit extensive interannual variability (Fig. 3), we use two methods for the evaluation of their trends. Firstly, the formal linear trend is calculated using the classic method for direct approximation of the annual or stormy-period maxima with a linear function. Alternatively, we employ the Theil–Sen estimator to evaluate whether any of the components had a trend with a nonzero slope. This estimator is less sensitive with respect to outliers than the classic approximation and thus gives more adequate estimate of statistical significance of the nonzero trends.

Both the modelled annual maxima and maxima of over stormy seasons of the total water level exhibit quite a rapid increasing trend about 7 cm/decade near Tallinn (Fig. 3). The increase is statistically significant at a 97% level and almost by a factor of two faster than established from observations for 1948–1995 (Suursaar and Sooäär, 2007). The difference stems from the use of time series of different length and is consistent with an acceleration of the increase in the water level extremes during the latter decades (Suursaar and Sooäär, 2007). Interestingly, even though several single values of the annual and stormy-season maxima are fairly different, the two trendlines almost coincide (Fig. 3).

2.3. Local storm surges and weekly average water levels

The common way to separate processes with different temporal scales from the total time series is based on singling out a certain average and on further specification of a residual (total minus average). The relevant procedures range from the calculation of simple running average or the application of various filtering techniques (e.g., Haigh et al., 2010a,b) through wavelet-type techniques (Percival and Mofjeld, 1997) to spectrogram-type representations that are able to decompose the outcome of one-point measurements of surface elevations into single constituents and that make it possible to quantify both the variations in the time-space domain and the energy content of each component (Torsvik et al., 2015).

Tide-driven water level fluctuations are a few centimetres (Leppäranta and Myrberg, 2009) and more or less periodic (e.g., seasonal) variations form only about 10% of the total range of the water level in the study area (Raudsepp et al., 1999; Medvedev, 2014). The aperiodic signal of the de-trended data sets consists of two major constituents: variations in the water volume of the entire Baltic Sea and local storm surges. Although the impact of wave set-up may play a massive role in some observations sites (notably in Ristna, Eelsalu et al., 2014), we do not consider this phenomenon.

As these aperiodic water level variations are driven by phenomena with fairly different time scales compared to single storms, they can be effectively separated by using a simple average over a certain time interval. Ideally, the resulting average should mirror the course of the entire Baltic Sea water level while the residual should reflect the local storm surges (Fig. 4). A convenient averaging length is about 8 days. For this length the average water level (called weekly average below) follows a quasi-Gaussian distribution whereas the residual (the total water level minus the average, called storm surge height below) reflects a Poisson-type process (Soomere et al., 2015b). The choice of the value of 8.25 days (198 h) simply reflects the temporal resolution (6 h) of the simulated water level data set and the necessity to use an odd number of data points in order to appropriately compare the weekly average and the instantaneous values.

The weekly average water level contains a substantial amount (at times almost half of the maximum surge height) of short-term storm surges (Fig. 4). Therefore, it is not an accurate proxy of the water volume of the entire sea. In particular, it does not adequately describe the calm water level between single storms that push water into the Baltic Sea. Still the maxima of the weekly average water level seem to properly reflect the largest values of the entire Baltic Sea water level after strong storms have passed, e.g., around 01 February, 15–20 March or 9–15 April 1990 (Fig. 4).

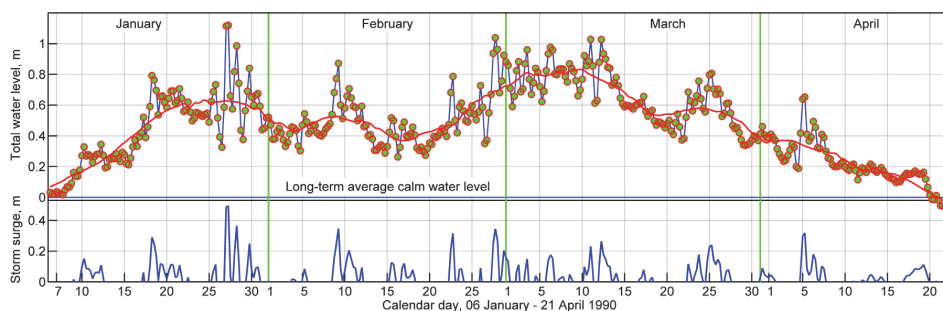


Fig. 4. Numerically simulated total water level (green circles connected with a blue line), its 198-h (8.25-day) average (red) and the positive part of the residual (the total water level minus the 8.25-day average, interpreted as the positive storm surge, blue, lower panel) near Tallinn (Fig. 1). (For interpretation of the references to colour in this figure legend, the reader is referred to the web version of this article.)

As we are specifically interested in the water level maxima, we only consider positive storm surges with respect to the weekly average. The height of a local storm surge is interpreted in this paper as the difference between the total water level and the weekly average (Fig. 4). For the first storm in a sequence of events after a long calm period this value roughly corresponds to the common understanding of a storm surge. Similarly to the weekly average, the storm surge height not always exactly represents the local reaction of the water surface to single storms. The heights of subsequent storm surges may contain a certain impact of the previous ones. When the water level is relaxed after a storm, development of a seiche may lead to a certain water level down compared to the weekly average. Also, if a storm approaches the study area from the north, its first phase may contain strong easterly winds that may cause substantial local negative surges.

The (annual) maximum values of storm surges do not necessarily coincide with similar maxima of the weekly average. Therefore, the introduced separation of the total water level into the two components may be able to more properly characterise the changes in the relevant background processes. To a first approximation, such changes can be to some extent characterised by analysing trends in the annual maxima of these quantities.

3. Results

3.1. Maxima of storm surge heights and weekly average water levels

The overall courses of the weekly average water level and the residual (storm surge height) are qualitatively very similar to the course of the total water level (Fig. 5). They all reveal strong seasonal signal and extensive intra- and interannual variations throughout the entire study area. Not unexpectedly, the standard deviation (std) of the weekly average water level (0.067 m at Tallinn) is only about 25% of the std of the total water level (0.25 m) or the std of the storm surge height (0.23).

The entire range of the annual maxima of the weekly average (from about 0.2 m up to 0.8 m) is almost the same as the similar range of storm surge heights (Fig. 5). The distribution of these maxima is different. The annual and stormy-season maxima of the weekly average water level are mostly concentrated at 0.5–0.6 m and the relevant time series contains a few very small outliers (annual maxima below 0.2 m). The similar maxima for the (positive) storm surges are at the levels of 0.3–0.4 m and their set contains several large outliers reaching the levels of 0.6–0.8 m (Fig. 5). This property is consistent with the observation that the applied separation of the water level components assigns all positive outliers of the water level maxima to the time series of relative storm surge heights (Soomere et al., 2015b). The std of the annual maxima of the total water level is 0.22 m (0.27 m for the stormy season maxima). The relevant std for the maxima of the weekly average and of the storm surge height are roughly equal to about half of these values, 0.13–0.16 m and 0.12–0.14 m, respectively.

For the averaging interval of 8.25 days all the discussed maxima (both weekly-scale average water level and storm surge height; both in terms of annual and stormy-season maxima) exhibit an increase in the entire study area (Fig. 6). This feature partially reflects the fact that each measure incorporates a certain part of the course of the counterpart. The ratio of the slopes of the relevant trendlines, however, varies considerably. The approximate parity of the increase rates (3–4 cm/decade, Fig. 5) of the weekly average and of the storm surge heights is characteristic only for a small region in the central part of the Gulf of Finland and in some sections of the eastern Gulf of Riga. The increase in the maxima of storm surge heights with respect to the weekly average is

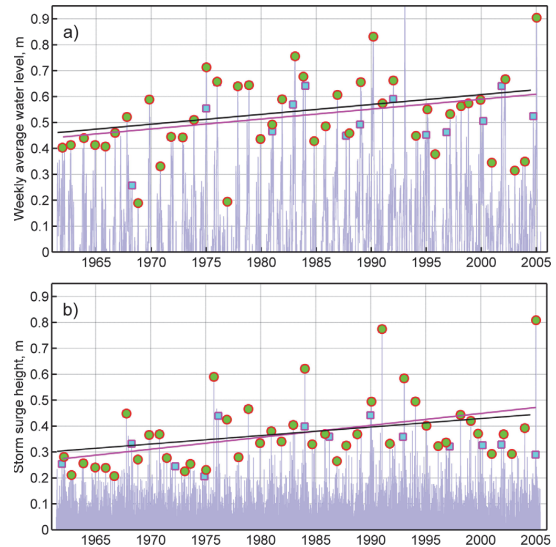


Fig. 5. Trends in the maxima of water level components near Tallinn in 1961–2005. (a) Trends in stormy-season (circles, 3.8 cm/decade, Sen's slope 4.0 cm/decade, 95% confidence interval [0.0, 7.4] cm/decade; red trendline) and annual (squares, visible only if different from the stormy-season maxima, 3.8 cm/decade; Sen's slope 3.5 cm/decade, 95% confidence interval [1.3, 6.8] cm/decade, black trendline) maxima of the weekly average water level; (b) trends in stormy-season maxima (circles, 4.6 cm/decade, Sen's slope 3.7 cm/decade, 95% confidence interval [1.6, 5.8] cm/decade; red trendline) of the (relative) storm surge heights and in similar annual maxima (squares, visible only if different from the stormy-season maxima, 3.3 cm/decade, Sen's slope 2.9 cm/decade, 95% confidence interval [0.7, 5.1] cm/decade; black trendline). (For interpretation of the references to colour in this figure legend, the reader is referred to the web version of this article.)

considerably (by a factor of two) faster in the eastern Gulf of Finland (at Narva-Jõesuu) but much (by several times) slower on the coasts of the Baltic Proper (at Ristna). The slopes of the trends also depend strongly on the averaging interval.

3.2. Spatial distribution of slopes of trends

It is natural that the course of water level in areas with complicated geometry such as the eastern and northern Baltic Sea may contain a substantial local component and may vary considerably in different locations. An analysis of the variations in the trends in various characteristics of the water level maxima may give a flavour of the relative role of single water level components in different parts of the sea.

Consistently with the results of Suursaar and Sooäär (2007), the trend for the total water level maxima (both on the annual basis and for the stormy season) varies in the range of 5–10 cm/decade (Fig. 6). The spatial patterns of trends of these two measures almost coincide. The magnitudes of these trends evaluated for the annual and for stormy-season maxima almost coincide in the eastern Gulf of Finland and along the Baltic Proper coast of Latvia. The largest increase (8–10 cm/decade) occurred in the eastern Gulf of Finland and along the eastern Gulf of Riga coast. The trends are much smaller, mostly in the range of 5–7 cm/decade, along the open coast of the Baltic Proper and at the entrance to the Gulf of Finland. The smallest slopes (about 5 cm/decade) occurred at the south-western coast of Saaremaa in a coastal section that is completely open to the predominant strong south-westerly winds. The slope of this trend almost exactly matches the one for the German North Sea coast (Mudersbach et al., 2013).

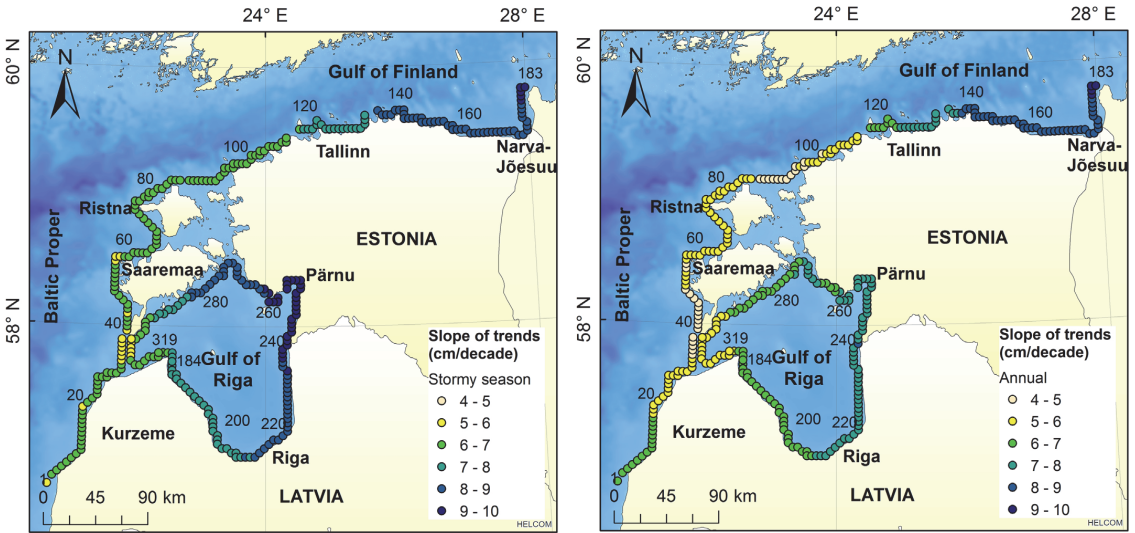


Fig. 6. Slope (cm/decade) of trends in the stormy-season and annual maxima of total water level in 1961–2004.

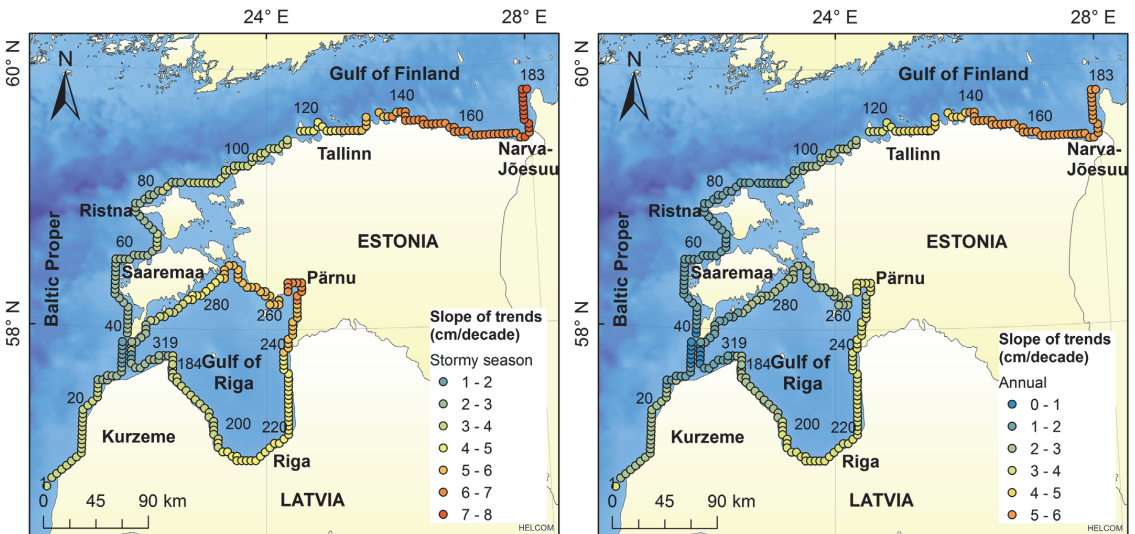


Fig. 7. Slope (cm/decade) of trends in the stormy-season and annual maxima of storm surge heights (total water level minus 8.25-day average) in 1961–2004.

To understand the nature of the variation in the trends of the maxima of storm surge heights and of the weekly average water level, we first consider the spatial pattern of the relevant slopes of these trends in the study area for a fixed averaging interval of 8.25 days used in Soomere et al. (2015b). There is a clear difference (up to 2–3 cm/decade) in the estimates of the slopes for the stormy season and for the calendar year (Figs. 7 and 8) in most of the study area. The trends in annual maxima are about 10–15% slower and exhibit larger spatial variation than those for stormy-season maxima, except for the open Baltic Sea coast of Latvia. As discussed in the Introduction, such difference in the slopes of these trends suggests that the annual maxima are to some extent correlated in some regions of the study area.

The trends in the annual and stormy-season maxima of storm

surge heights contain extensive spatial variability (Fig. 7). They range from almost zero (for annual maxima at the open coast of the Baltic Proper) up to 7.3 cm/decade (for stormy-season maxima in the easternmost Gulf of Finland). The slopes of similar maxima of storm surge heights are relatively large (5–7 cm/decade) in the eastern Gulf of Finland and reach comparable values (> 5 cm/decade) along the eastern coast of the Gulf of Riga, with a clearly defined maximum of almost 7 cm/decade in the interior of Pärnu Bay (Fig. 8). The increase rate has been much lower in the western Gulf of Riga and along the coast of the Western Estonian archipelago. A definite but relatively slow increase (3–4 cm/decade) has occurred along the northwestern coast of Latvia for both annual and stormy season surge maxima.

Interestingly, the maxima of storm surge heights exhibit almost

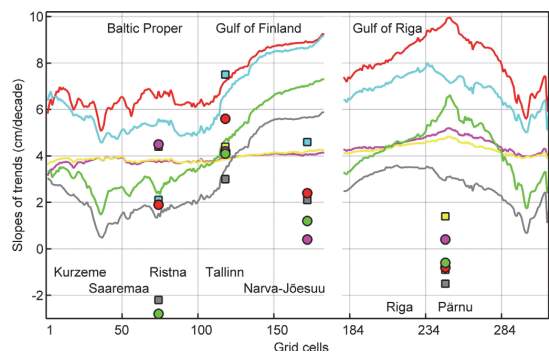


Fig. 8. Alongshore variation in the slopes of trends (cm/decade, evaluated using classic linear approximation) of water level components in 1961–2004. Red and cyan: total water level, stormy seasons and calendar year, respectively; magenta and yellow: 8-day average, stormy seasons and calendar year, respectively; green and grey: storm surge, stormy seasons and calendar year, respectively. For observed data sets the colours are the same, circles indicate trends for stormy-season maxima and squares – for annual maxima. The Sen's slopes almost exactly follow the presented ones whereas the differences in magnitude are mostly less than ± 1.5 cm/decade. The typical width of 95% confidence intervals for various Sen's slopes is from ± 2 to ± 3 cm/decade. The slopes larger than 3 cm/decade are all statistically significant at a 95% level. The numbering of grid cells follows Fig. 1b. (For interpretation of the references to colour in this figure legend, the reader is referred to the web version of this article.)

no trend in several locations of the Western Estonian archipelago (Figs. 7 and 8). The increase in their annual maxima is below 1 cm/decade along the south-western coast of Saaremaa. In such locations the increase in the maxima of total water level is almost completely governed by changes in the weekly average water level. Even though this measure is not a perfect proxy of the entire Baltic Sea water volume, this feature suggests that in this region the water level maxima largely follow the changes in the maximum values of the water volume of the Baltic Sea.

The slopes of trends in the maxima of weekly average water level have a qualitatively similar spatial pattern (Fig. 8). The fastest increase in these maxima have occurred in the eastern Gulf of Finland and in the entire Gulf of Riga. However, all these trends are close to 4 cm/decade. The range of their spatial variations is by an order of magnitude smaller than the above-discussed variations in the total water level and in storm surge heights. The slopes evaluated on the annual basis and for stormy seasons almost coincide. This feature indicates that the correlation between subsequent values in these two data sets is on the same level. As there is effectively no correlation between stormy-season maxima, it is likely that the annual maxima of weekly average water level (water volume of the entire sea) are also almost uncorrelated.

Similar slopes of the trendlines for the observed maxima of total water level and for its components adequately match the numerically evaluated slopes only at Tallinn (Fig. 8). The match is almost perfect for the trends in the weekly average and storm surge heights but less complete for the total water level. The water level gauge in Tallinn was located in relatively deep water (about 10 m) at the entrance to Tallinn Harbour. The entire Tallinn Bay is sheltered for most of predominant strong winds and is only open to the north-northwest. The water level recordings at this site therefore adequately represent the water level at a reasonable distance from the shoreline and contain, if at all, a very small contribution from local effects such as the local wind surge, wave set-down or set-up.

The match of the slopes extracted from modelled data is much less satisfactory for three other water level measurement sites. It is likely that most of the mismatches stem from issues related to the

particular locations of the water level gauges. Although the quality of observed water level data from Ristna is questionable because of likely impact of strong wave set-up (Eelsalu et al., 2014), the match of slopes of trendlines is very good for the weekly average water level. This feature is not unexpected because the locally increased water level owing to wave set-up is rapidly relaxed when the wave height decreases and the “memory” of the Baltic wave fields is relatively short; usually well below 12 h. The slopes of trends in observed maxima of storm surge heights have even a different sign compared to the similar trends for simulated maxima. As a consequence, the slopes for the observed total water level maxima significantly differ from the slopes for the simulated maxima. This property apparently signals that wave-set up plays a decisive role in the formation of observed water level maxima at Ristna.

The match between the slopes in question for the simulated and observed data is very poor at Pärnu and Narva-Jõesuu. The measurement sites at Narva-Jõesuu and Pärnu are located in large river mouths. As the local storm surge in Pärnu is very sensitive with respect to the particular wind direction over this relatively large but shallow (depths 4–6 m) bay (Suursaar et al., 2003), it could be hypothesised that the atmospheric forcing of the RCO model may have problems with replication of wind directions in the strongest storms and thus with the reproduction of the local surge. This assertion, however, does not explain the mismatch of the trends in the modelled and measured weekly averages of the water level. The water level in Narva-Jõesuu may be modified by wave set-up for some wind directions and also by the presence of a sill near the river mouth (Laanearu et al., 2007). However, the described major mismatch calls for further research towards understanding its reasons and suggests that circulation models with much better resolution, possibly coupled with wave models, should be used to adequately evaluate water levels in the vicinity of the measurement sites.

3.3. The role of the averaging interval

The invariance of the slope of the trendlines for the maxima of the weekly average water level with respect to the particular location (Fig. 8) is somewhat surprising. As discussed above, this measure contains a substantial contribution from local storm surges (Fig. 4), and thus should at least partially reflect the large variations in the local water level during strong storms.

To understand how this invariance is formed, let us consider spatial variations in the slope in question for different averaging intervals (Fig. 9). It is natural that for short averaging intervals the average water level largely follows the total water level. Therefore, it is not unexpected that for short averaging intervals the slopes of trendlines of the maxima of the resulting average have a magnitude and spatial variation similar to that of the total water level maxima (Fig. 9). It is also natural that for short averaging intervals the amplitude of residual fluctuations (total water level minus average) is relatively small and that the changes to their maxima are also modest in the entire study area. A straightforward conjecture is that the spatial variations in the slopes of trendlines for the maxima of such residuals for relatively short averaging times (not shown) are both quantitatively and qualitatively similar to the corresponding properties of the trendlines for the total water level maxima.

Similarly to the above-discussed material, the trends in the annual and stormy-season maxima of the average water level are considerably different for short averaging intervals. The likely reason for the difference is a frequent correlation of the subsequent annual maxima. As discussed above, when a strong maximum of the entire Baltic Sea water volume occurs in December, it may considerably impact water level in January of subsequent year. The stormy-season maxima are uncorrelated and

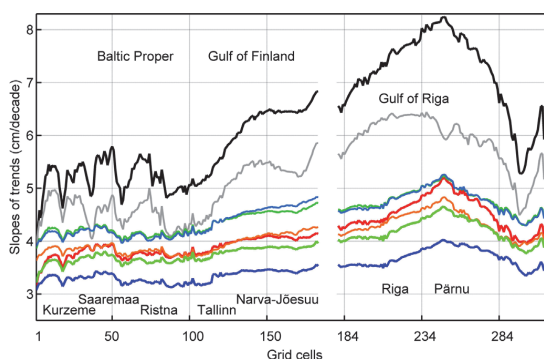


Fig. 9. Spatial variations in the slope of the trendline of the maxima of the average water level for different averaging lengths. Dark and light grey: 18-h average, stormy-season and annual maxima, respectively; red and orange: 8.25-day (198-h) average stormy-season and annual maxima, respectively (equivalent to yellow and pink lines in Fig. 8); light and dark green: 16.25-day (390-h) average stormy-season and annual maxima, respectively; blue and cyan: 24.25-day (582-h) average stormy-season and annual maxima, respectively. The lines representing slopes for stormy-season maxima are wider than their counterparts for annual maxima. The numbering of grid cells follows Fig. 1b. (For interpretation of the references to colour in this figure legend, the reader is referred to the web version of this article.)

thus exhibit a faster increase.

An increase in the length of the averaging interval leads to twofold changes in the appearance of the spatial variations in and interrelations of the quantities in question. Firstly, it leads to the levelling off the spatial variations in the slopes of both trendlines in question (Fig. 9). The slopes of trendlines of stormy-season (annual) maxima vary by almost 3 cm/decade (2 cm/decade) for an averaging length of 18 h. This variation decreases to the level of about 1.5 cm/decade for averaging lengths of 4.25 days and stays around 1 cm/decade for even longer averaging lengths in the entire study area. The spatial variations almost completely vanish for intervals longer than 6 days in the Baltic Proper and the Gulf of Finland, and for about 5 days in the Gulf of Riga. The remaining level of spatial variations in the slopes (about 1 cm/decade) can be interpreted as indicating the level of the contribution of local storm surges into the maxima of average water levels. Its presence once more signals that the (multi-)weekly average evaluated from local water level time series is an acceptable but still not a perfect proxy of the entire Baltic Sea water level.

Secondly, an increase in the length of the averaging interval leads to a complicated pattern of mutual variations in the values of the slopes of the two sets of trendlines (Fig. 9). The above-discussed decrease is monotonic and much faster for the slopes evaluated based on stormy-season maxima. As a result, the slopes evaluated for the annual and stormy-season maxima (about 3.5–4 cm/decade in the Baltic Proper and in the Gulf of Finland, 4–4.7 cm/decade in the Gulf of Riga) almost exactly coincide for averaging intervals of about 6 days for the Baltic Proper and Gulf of Finland area and about 10 days for the Gulf of Riga.

A further increase in the averaging interval to 16–24 days leads to a further decrease in the slopes for stormy-season maxima. This process is an expected feature because longer averaging intervals tend to smooth out all the short-time and weekly-scale maxima. Interestingly, a further increase in the averaging intervals leads to an increase in the slopes of trendlines evaluated for the annual maxima (thinner lines in Fig. 9). The minimum of slopes in question occurs for about 7–8 days for the coast of Kurzeme (Fig. 1b) and eastern Gulf of Riga and for about 10–11 days for the Gulf of Riga. This further increase is apparently caused by the above-discussed side impact of longer averaging intervals that may level off

the maxima of subsequent years towards the larger values. These slopes increase to a level of 4–4.5 cm/decade in the Baltic Proper and in the Gulf of Finland and to a level of 4.5–5 cm/decade in the Gulf of Riga (and up to 5.2 cm/decade in the interior of Pärnu Bay). These values exceed by about 1 cm/decade the similar values for slopes of trendlines for stormy-season maxima. Differently from the slopes for stormy-season maxima, the slopes for annual maxima of water levels almost coincide for averaging intervals longer than about two weeks.

The slopes of the discussed trendlines are systematically (albeit only slightly) larger in the Gulf of Riga than in the rest of the study area. Also, both above-discussed rearrangements in the appearance of the spatial distribution of the two sets of slopes occur in the Gulf of Riga for about 2 days longer averaging intervals (while the spatial variations levelled off for about 1 day shorter averaging intervals). This feature may reflect a characteristic delay time of the formation of water level maxima in this gulf because of the limited flow rates through relatively shallow and narrow straits – Irbe Strait and Suur Strait (Fig. 1b) that connect this gulf with the rest of the Baltic Sea. This property gives rise to the possibility for the water level in the entire Gulf of Riga to reach larger values than in the rest of the Baltic Sea and to stay elevated for some time. It is likely that strong westerly winds push sizeable water volumes from the Baltic Proper into this water body and in this way support long-term elevated water level in the gulf. Such phenomenon is not possible in the Gulf of Finland. As there is no sill between the Gulf of Finland and the northern Baltic Proper, the signal of water level changes propagates into the Gulf of Finland with the shallow-water wave speed and reaches the eastern end of this gulf within 6–7 h.

3.4. Possible changes in the directional structure of forcing

Several presented results suggest that notable changes in the atmospheric forcing may have occurred over the simulation time. The extensive spatial variation in the slopes of the trendlines of maximum water levels (Figs. 6–8) supports the conjecture that wind directions in strong storms may have changed in the northern Baltic Sea (Soomere et al., 2013). Further support to this hypothesis provides a decrease in the observed maxima of storm surge heights at Ristna. As observations at this site seem to incorporate a large contribution of wave set-up (Eelsalu et al., 2014), the mismatch of this decrease with the modelling results may be interpreted as a signal of change in the magnitude of wave set-up in strong storms. As the set-up height substantially depends on the wave approach direction, a turn in the wind directions in strong storms is likely.

There is increasing evidence about changes in the wind, air-flow and wave approach directions in the vicinity of the study area and in the entire Baltic Sea basin. The frequency of south-western winds have considerably increased in some observation sites of Estonia in 1966–2005 (Jaagus, 2009; Jaagus and Kull, 2011). The prevailing wind directions in several meteorological stations at the Estonian coast have rotated by about 20° from the south or south-west towards the west in 1966–2011 (Suursaar, 2013, 2015). The annual average geostrophic air-flow over the southern Baltic Sea has abruptly turned by about 40° at the end of the 1980 s (Soomere et al., 2015a). These changes have become naturally evident in the wave properties. The most frequent observed wave approach direction at Narva-Jõesuu has rotated by > 90° in 1954–2008 (Räämet et al., 2010) and a decrease in hindcast high wave heights has noted at a location about 60 km to the south of Ristna (Suursaar, 2015).

The highest water levels are created by very strong storms. Such events occur irregularly, have extremely different properties and normally affect different sections of the Baltic Sea coast.

However, a flavour of the changes in the atmospheric forcing may be extracted from the analysis of the properties of air-flow. The average air-flow is a vector, the components of which are average wind velocity components (usually zonal or east-west and meridional or north-south) over some time interval. It points to where and how rapidly the air, on average, is moving. The use of this quantity is at best justified for wind fields that exhibit clear prevalence of some directions – which is the case in the Baltic Sea basin. Differently from, e.g., the most frequent wind direction, air-flow incorporates information about wind speed and therefore could be used as an indicator of changes in strong wind directions.

Extreme water levels are first of all a function of wind properties on the open sea. The only long-term wind measurement site in the vicinity of the study area that provides reliable information about offshore wind properties is Kalbådagrund. This is a caisson lighthouse in the central part of the Gulf of Finland (Fig. 1b, 59°59' N, 25°36' E) where the wind field is practically not affected by the presence of mainland. The wind measurements at this site are performed since 1981 at the height of 32 m above the mean sea level. As we are interested in changes in the wind direction, we use the measured data without any height correction. The recordings in 1981 have many gaps and are omitted in the analysis below.

The annual mean wind speed at Kalbådagrund shows a very slow decrease (~ 0.1 m/s/decade, Soomere et al., 2010). The annual average values of the zonal and meridional components of air-flow for 1982–2013 (1.43 m/s and 1.03 m/s; positive to the east and north, respectively) reflect the predominance of south-easterly winds in this region (Fig. 10). The slope of the formal trendline of the zonal component (-3 cm/s/decade) is almost zero, indicating that this component has had no marked changes since the 1980s. The similar trendline for the meridional component (with a slope of -11 cm/s/decade) indicates a decrease in this component from the level of ~ 1.2 m/s to ~ 0.8 m/s in 1982–2013, that is, by about 30%. As the averages of both components exhibit extensive inter-annual variability (Fig. 10), we again use the Theil-Sen estimator (that is insensitive with respect to outliers) to evaluate whether any of the components had a statistically significant nonzero trend. This estimator confirms that the zonal component possesses no definite trend while the Sen's slope for the meridional component is even steeper (-13.5 cm/decade). Even though the latter trend (nonzero Sen's slope) is statistically significant at quite a low level of 80%, it provides a hint of a rotation of wind directions in strong storms in the study area.

4. Concluding remarks

The relative contribution of different drivers of water level into the increase in the water level maxima in 1961–2004 is evaluated using a separation of the water level into weekly-scale average and short-term components. The former mirrors the water volume of

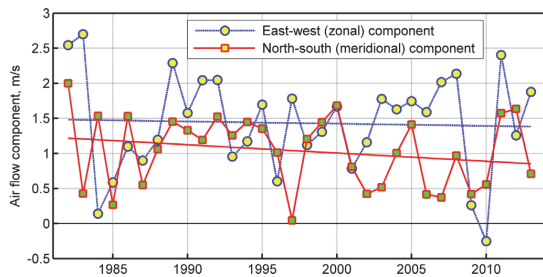


Fig. 10. Annual average zonal and meridional air-flow components and their trendlines for 1982–2013 at Kalbådagrund in the Gulf of Finland.

the entire Baltic Sea (which is impacted by longer sequences of atmospheric events) while the latter reflects the impact of single storms. The properties of maxima extracted from time series produced by the Rossby Centre Ocean model are compared with similar properties found for four observation sites along the Estonian coast. Long-term trends in the mean water level and land uplift are disregarded.

The total maxima of water level increase at a spatially variable rate of 5–10 cm/decade in the eastern Baltic Sea. The increase is relatively rapid in the eastern Gulf of Finland and in most of the Gulf of Riga and slower on the open Baltic Proper coasts.

Almost all spatial variability in the slopes of trends in the total water level maxima is represented in the variations of such slopes evaluated from the heights of surges driven by single storms. The stormy-season maxima of storm surges reveal almost no changes (below 1 cm/decade) on the south-western coast of the Western Estonian archipelago. The changes in the maxima of the total water level in this region are thus almost exclusively governed by similar changes in the water volume of the entire Baltic Sea, equivalently, by the impact of specific sequences of wind events that are mirrored in the average water level (Lehmann and Post, 2015). A natural conjecture is that the wind speed in strong storms (that are responsible for such maxima) has not increased significantly in the Baltic Proper. However, the increase in the maxima of the “proxy” of the water volume of the entire sea signals that either the duration of storms that push water into the Baltic Sea or the length of such series of storms has increased.

The maxima of storm surge heights in the eastern Gulf of Riga and the eastern Gulf of Finland exhibit a substantial increase. This first suggests that most of the changes in the spatial variability in the local water level in the eastern Baltic Sea are driven by changes in single storms. The remarkable spatial variation shown here together with the conjecture about wind speeds, evidence of overall changes in wind directions from the literature and information extracted from the properties of air-flow over the Gulf of Finland suggest that wind directions in strong storms may have rotated over the time interval in question. A similar conjecture has been derived from the analysis of properties of wave-induced setup (Soomere et al., 2013).

An approximation to the basin-scale water level is obtained from the weekly-scale average of water level time series. Not surprisingly, the trends of the maxima of such “proxy” basin-scale water levels are almost constant along long sections of the coast. This feature makes it possible to adequately evaluate the trend in the maxima of the basin-scale component from observed or modelled data at virtually any location.

The slopes of the trends of the maxima of total water level and of weekly-scale average have the same qualitative spatial pattern for shorter averaging intervals (up to 2–3 days). The spatial structure of slopes of weekly-scale averages rapidly levels off with an increase of the averaging interval. The spatial variations reach quite a low value of 1.5 cm/decade for averaging intervals of 4 days and almost completely vanish for intervals longer than 6 days in the Baltic Proper and the Gulf of Finland, and for about 5 days in the Gulf of Riga. Both the values of slopes and their alongshore variations are relatively large in the Gulf of Riga. This difference apparently reflects the delay in the development of large water level variations in the Gulf of Riga, the presence of relatively large basin-wide slopes during strong storms in this basin and possibly also the specific geometry of some parts of this gulf.

The slopes of trendlines for annual maxima of the weekly-scale average water level estimated from calendar years and stormy seasons reveal generally a similar spatial pattern. Their dependence on the averaging interval is different. The slopes evaluated from stormy-season maxima gradually decrease when the averaging interval increases while the slopes estimated based on

annual maxima first decrease but starting from about 8-day averaging length increase again. The values of slopes estimated using the two options have a very good match for the averaging intervals of about 8 days. This time scale seems to be particularly convenient for the separation of different constituents of water level in the eastern Baltic Sea (Soomere et al., 2015b) and its use may provide a new insight into properties of different contributions to the local water level. The described pattern of variations in the magnitudes of slopes apparently reflects the gradual levelling off of single maxima and an increasing correlation between the maxima in subsequent years for longer averaging intervals.

Although the calculation of the average water level largely smooths out short-term variations, the kind of average used in the analysis includes part of storm surges. Still, a natural conjecture is that an increase in the length of the sequence of storms that drive extremely high water levels in the Baltic Sea (Post and Kõuts, 2014) has the largest potential for encountering even higher water levels on the coasts of the Baltic Proper. In contrast, single storms from unfavourable directions apparently provide the highest water levels in semi-enclosed sub-basins of the sea (Suursaar and Sooäär, 2007).

Finally, the performed analysis revealed extensive mismatch between the quantities extracted from numerical simulations and similar characteristics evaluated from water level observations. An almost perfect match exists for Tallinn where the recordings of the water level gauge are not affected by local and/or shallow-water phenomena. The mismatch for other locations is apparently caused by the impact of local effects such as the local wind surge, wave set-down or set-up in the water level recordings. While *in situ* recordings are definitely the best source for the analysis and projections of extreme water levels in the immediate vicinity of observation sites, the established mismatch signals that the use of such data for more remote locations may not be justified and projections based on numerical simulations could be much more adequate for many coastal segments.

Acknowledgements

The research was supported by Institutional block Grant IUT33-3 of the Estonian Ministry of Education and Research, project “BalticCheckpoint” of the call MARE/2014/09 “Sea-basin checkpoints”, Grant 9125 by the Estonian Science Foundation, EEA Grant 2/EEZLV02/14/GS/022 and through support of the ERDF to the Centre of Excellence in Non-linear Studies CENS. The simulated hydrographic data were kindly provided by the Swedish Meteorological and Hydrological Institute in the framework of the BONUS BalticWay cooperation.

References

- Arns, A., Wahl, T., Haigh, I.D., Jensen, J., 2015. Determining return water levels at ungauged coastal sites: a case study for northern Germany. *Ocean. Dyn.* 65, 539–554.
- Averkiev, A.S., Klevanny, K.A., 2010. A case study of the impact of cyclonic trajectories on sea-level extremes in the Gulf of Finland. *Cont. Shelf Res.* 30, 707–714.
- Barbosa, S.M., 2008. Quantile trends in Baltic Sea level. *Geophys. Res. Lett.* 35 (Art. No. L22704), 6.
- Bastos, A., Trigo, R.M., Barbosa, S.M., 2013. Discrete wavelet analysis of the influence of the North Atlantic oscillation on Baltic Sea level. *Tellus A* 65 (Art. No. 20077), 12.
- Bosley, K.T., Hess, K.W., 2001. Comparison of statistical and model-based hindcasts of subtidal water levels in Chesapeake Bay. *J. Geophys. Res.–Oceans* 106 (C8), 16869–16885.
- Brakenridge, G.R., Syvitski, J.P.M., Overeem, I., Higgins, S.A., Kettner, A.J., Stewart-Moore, J.A., Westerhoff, R., 2013. Global mapping of storm surges and the assessment of coastal vulnerability. *Nat. Hazards* 66, 1295–1312.
- Cazenave, A., Dieng, B., Meyssignac, B., von Schuckmann, K., Decharme, B., Berthier, E., 2014. The rate of sea-level rise. *Nat. Clim. Chang.* 4, 358–361.
- Dailidienė, I., Tilickis, B., Stankevičius, A., 2004. General peculiarities of long-term fluctuations of the Baltic Sea and the Kurshiu Marios lagoon water level in the region of Lithuania. *Environ. Res. Eng. Manag. Technol.* 4 (30), 3–10.
- Dailidienė, I., Davulienė, L., Tilickis, B., Stankevičius, A., Myrberg, K., 2006. Sea level variability at the Lithuanian coast of the Baltic Sea. *Boreal Environ. Res.* 11, 109–121.
- Elsalu, M., Soomere, T., Pindsoo, K., Lagema, P., 2014. Ensemble approach for projections of return periods of extreme water levels in Estonian waters. *Cont. Shelf Res.* 91, 201–210.
- Ekman, M., Mäkinen, J., 1996. Mean sea surface topography in the Baltic Sea and its transition area to the North Sea: a geodetic solution and comparisons with oceanographic models. *J. Geophys. Res.–Oceans* 101 (C5), 11993–11999.
- Feistel, R., Nausch, G., Wasmund, N. (Eds.), 2008. State and evolution of the Baltic Sea 1952–2005. Wiley, Hoboken, New Jersey.
- Gönnert, G., 2003. Storm tides and wind surge in the German Bight: Character of height, frequency, duration, rise and fall in the 20th century [Sturmfluten und Windstau in der Deutschen Bucht Charakter, Veränderungen und Maximalwerte im 20. Jahrhundert]. *Küste* 67, 185–366.
- Guannel, G., Tissot, P., Cox, D.T., Michaud, P., 2001. Local and remote forcing of subtidal water level and setup fluctuations in coastal and estuarine environments. In: *Coastal Dynamics 2001: 4th Conference on Coastal Dynamics*; Lund; Sweden; 11–15 June 2001, pp. 443–452.
- Haigh, I.D., Nicholls, R., Wells, N., 2010a. A comparison of the main methods for estimating probabilities of extreme still water levels. *Coast. Eng.* 57, 838–849.
- Haigh, I.D., Nicholls, R., Wells, N., 2010b. Assessing changes in extreme sea levels: application to the English Channel, 1900–2006. *Cont. Shelf Res.* 30, 1042–1055.
- Hallegatte, S., Green, C., Nicholls, R.J., Corfee-Morlot, J., 2013. Future flood losses in major coastal cities. *Nat. Clim. Chang.* 3, 802–806.
- Harff, J., Meyer, M., 2011. Coastlines of the Baltic Sea—zones of competition between geological processes and a changing climate: examples from the Southern Baltic. In: Harff, J., Björck, S., Hoth, P. (Eds.), *The Baltic Sea Basin*. Springer-Verlag, Berlin, Heidelberg, pp. 149–164.
- Howard, T., Pardaens, A.K., Bamber, J.L., Ridley, J., Spada, G.L., Hurkmans, R.T.W., Lowe, J.A., Vaughan, D., 2014. Sources of 21st century regional sea-level rise along the coast of northwest Europe. *Ocean. Sci.* 10, 473–483.
- Hünicke, B., Zorita, E., Soomere, T., Madsen, K.S., Johansson, M., Suursaar, Ü., 2015. Recent Change – Sea Level and Wind Waves. In: *The BACC II Author Team, Second Assessment of Climate Change for the Baltic Sea Basin, Regional Climate Studies*. Springer, pp. 155–185.
- Jaagus, J., 2009. Long-term changes in frequencies of wind directions on the western coast of Estonia. *Publ. Inst. Ecol. Tallinn. Univ.* 11, 11–24 [in Estonian, with English summary].
- Jaagus, J., Kull, A., 2011. Changes in surface wind directions in Estonia during 1966–2008 and their relationships with large-scale atmospheric circulation. *Estonian J. Earth Sci.* 60, 220–231.
- Jaagus, J., Suursaar, Ü., 2013. Long-term storminess and sea level variations on the Estonian coast of the Baltic Sea in relation to large-scale atmospheric circulation. *Estonian J. Earth Sci.* 62, 73–92.
- Johansson, M., 2014. Sea level changes on the Finnish coast and their relationship to atmospheric factors. *Finn. Meteorol. Inst. Contrib.* 109, 132 (PhD thesis, University of Helsinki).
- Johansson, M., Boman, H., Kahma, K., Launiainen, J., 2001. Trends in sea level variability in the Baltic Sea. *Boreal Environ. Res.* 6, 159–179.
- Johansson, M., Pellikka, H., Kahma, K., Ruosteenoja, K., 2014. Global sea level rise scenarios adapted to the Finnish coast. *J. Mar. Syst.* 129, 35–46.
- Laanearu, J., Koppel, T., Soomere, T., Davies, P.A., 2007. Joint influence of river stream, water level and wind waves on the height of sand bar in a river mouth. *Nord. Hydrol.* 38, 287–302.
- Lehmann, A., Post, P., 2015. Variability of atmospheric circulation patterns associated with large volume changes of the Baltic Sea. *Adv. Sci. Res.* 12, 219–225.
- Lehmann, A., Myrberg, K., Höflich, K., 2012. A statistical approach to coastal upwelling in the Baltic Sea based on the analysis of satellite data for 1990–2009. *Oceanologia* 54, 369–393.
- Leppäranta, M., Myrberg, K., 2009. *Physical Oceanography of the Baltic Sea*. Springer, Berlin, p. 378.
- Losada, I.J., Reguero, B.G., Méndez, F.J., Castanedo, S., Abascal, A.J., Mínguez, R., 2013. Long-term changes in sea-level components in Latin America and the Caribbean. *Glob. Planet. Chang.* 104, 34–50.
- Masina, M., Lamberti, A., 2013. A nonstationary analysis for the Northern Adriatic extreme sea levels. *J. Geophys. Res.–Oceans* 118, 3999–4016.
- Medvedev, I.P., 2014. Seasonal fluctuations of the Baltic Sea level. *Russ. Meteorol. Hydrol.* 39, 814–822.
- Meier, H.E.M., Höglund, A., 2013. Studying the Baltic Sea circulation with Eulerian tracers. In: Soomere, T., Quak, E. (Eds.), *Preventive Methods for Coastal Protection*. Springer, Cham, Heidelberg, pp. 101–130.
- Meier, H.E.M., Döschner, R., Faxén, T., 2003. A multiprocessor coupled ice-ocean model for the Baltic Sea: application to salt inflow. *J. Geophys. Res.–Oceans* 108 (C8), 32–73.
- Meier, H.E.M., Broman, B., Kjellström, E., 2004. Simulated sea level in past and future climates of the Baltic Sea. *Clim. Res.* 27, 59–75.
- Mudersbach, C., Wahl, T., Haigh, I.D., Jensen, J., 2013. Trends in high sea levels of German North Sea gauges compared to regional mean sea level changes. *Cont. Shelf Res.* 65, 111–120.
- Myrberg, K., Ryabchenko, V., Isaev, A., Vankevich, R., Andrejev, O., Bendtsen, J., Erichsen, A., Funkquist, L., Inkala, A., Neelov, I., Rasmus, K., Rodriguez Medina, M.,

- Raudsepp, S., Passenko, J., Söderkvist, J., Sokolov, A., Kuosa, H., Anderson, T.R., Lehmann, A., Skogen, M.D., 2010. Validation of three-dimensional hydrodynamic models in the Gulf of Finland based on a statistical analysis of a six-model ensemble. *Boreal Environ. Res.* 15, 453–479.
- Percival, D.B., Mofjeld, H.O., 1997. Analysis of subtidal coastal sea level fluctuations using wavelets. *J. Am. Stat. Assoc.* 92, 868–880.
- Post, P., Kõuts, T., 2014. Characteristics of cyclones causing extreme sea levels in the northern Baltic Sea. *Oceanologia* 56, 241–258.
- Pugh, D., Vassie, J., 1978. Extreme sea-levels from tide and surge probability. In: *Proceedings of the 16th Coastal Engineering Conference (Hamburg)*, vol. 1, ASCE, New York, pp. 911–930.
- Pugh, D., Vassie, J., 1980. Applications of the joint probability method for extreme sea-level computations. *Proc. Inst. Civ. Eng.* 69, 959–975.
- Räämet, A., Soomere, T., Zaitseva-Pärnaste, I., 2010. Variations in extreme wave heights and wave directions in the northeastern Baltic Sea. *Proc. Estonian Acad. Sci.* 59, 182–192.
- Raudsepp, U., Toompuu, A., Kõuts, T., 1999. A stochastic model for the sea level in the Estonian coastal area. *J. Mar. Syst.* 22, 69–87.
- Ribeiro, A., Barbosa, S.M., Scotto, M.G., Donner, R.V., 2014. Changes in extreme sea-levels in the Baltic Sea. *Tellus A* 66 (Art. No. 20921), 10.
- Richter, A., Groh, A., Dietrich, R., 2012. Geodetic observation of sea-level change and crustal deformation in the Baltic Sea region. *Phys. Chem. Earth* 53–54, 43–53.
- Samuelsson, P., Jones, C.G., Willén, U., Ullerstig, A., Gollovik, S., Hansson, U., Jansson, C., Kjellström, E., Nikulin, G., Wyser, K., 2011. The Rossby Centre Regional Climate Model RCA3: Model description and performance. *Tellus A* 63, 4–23.
- Scotto, M.G., Barbosa, S.M., Alonso, A.M., 2009. Model-based clustering of Baltic sea-level. *Appl. Ocean. Res.* 31, 4–11.
- Seifert, T., Tauber, F., Kayser, B., 2001. A high resolution spherical grid topography of the Baltic Sea, revised edition. *Baltic Sea Science Congress, 25–29 November 2001, Stockholm, Post. #147*. (www.iowarnemuende.de/iowtopo_resampling.html).
- Soomere, T., Zaitseva-Pärnaste, I., Räämet, A., Kurennoy, D., 2010. Spatio-temporal variations of wave fields in the Gulf of Finland. *Fund. Appl. Hydrophys.* 4 (10), 90–101.
- Soomere, T., Pindsoo, K., Bishop, S.R., Käär, A., Valdmann, A., 2013. Mapping wave set-up near a complex geometric urban coastline. *Nat. Hazards Earth Syst. Sci.* 13, 3049–3061.
- Soomere, T., Döös, K., Lehmann, A., Meier, H.E.M., Murawski, J., Myrberg, K., Stanev, E., 2014. The potential of current- and wind-driven transport for environmental management of the Baltic Sea. *Ambio* 43, 94–104.
- Soomere, T., Bishop, S.R., Viška, M., Räämet, A., 2015a. An abrupt change in winds that may radically affect the coasts and deep sections of the Baltic Sea. *Clim. Res.* 62, 163–171.
- Soomere, T., Eelsalu, M., Kurkin, A., Rybin, A., 2015b. Separation of the Baltic Sea water level into daily and multi-weekly components. *Cont. Shelf Res.* 103, 23–32.
- Steffen, H., Wu, P., 2011. Glacial isostatic adjustment in Fennoscandia—A review of data and modeling. *J. Geodyn.* 52, 169–204.
- Stigebrandt, A., Gustafsson, B., 2003. Response of the Baltic Sea to climate change – theory and observations. *J. Sea Res.* 49, 243–256.
- Stramska, M., Chudziak, N., 2013. Recent multiyear trends in the Baltic Sea level. *Oceanologia* 55, 319–337.
- Sun, J., Zuo, J., Huang, L., Cai, X., Li, Q., 2013. Characteristics and causes of typhoon and storm surge along coast of East China Sea. *J. Hohai Univ.* 41, 461–465.
- Suursaar, Ü., 2013. Locally calibrated wave hindcasts in the Estonian coastal sea in 1966–2011. *Estonian J. Earth Sci.* 62, 42–56.
- Suursaar, Ü., 2015. Analysis of wave time series in the Estonian coastal sea in 2003–2014. *Proc. Estonian Acad. Sci.* 64, 289–304.
- Suursaar, Ü., Sooäär, J., 2007. Decadal variations in mean and extreme sea level values along the Estonian coast of the Baltic Sea. *Tellus A* 59, 249–260.
- Suursaar, Ü., Kullas, T., Otsmann, M., 2002. A model study of the sea level variations in the Gulf of Riga and the Vainameri Sea. *Cont. Shelf Res.* 22, 2001–2019.
- Suursaar, Ü., Kullas, T., Otsmann, M., Kõuts, T., 2003. Extreme sea level events in the coastal waters of West Estonia. *J. Sea Res.* 49, 295–303.
- Suursaar, Ü., Jaagus, J., Tõnisson, H., 2015. How to quantify long-term changes in coastal sea storminess? *Estuar. Coast. Shelf Sci.* 156, 31–41.
- Talke, S.A., Orton, P., Jay, D.A., 2014. Increasing storm tides in New York Harbor 1844–2013. *Geophys. Res. Lett.* 41, 3149–3155.
- Torsvik, T., Soomere, T., Didenkulova, I., Sheremet, A., 2015. Identification of ship wake structures by a time-frequency method. *J. Fluid Mech.* 765, 229–251.
- Ullmann, A., Pirazzoli, P.A., Tomasin, A., 2007. Sea surges in Camargue: trends over the 20th century. *Cont. Shelf Res.* 27, 922–934.
- Weisse, R., von Storch, H., Niemeyer, H.D., Knaack, H., 2012. Changing North Sea storm surge climate: an increasing hazard? *Ocean Coast. Manag.* 68, 58–68.
- Weisse, R., Bellafiore, D., Menéndez, M., Méndez, F., Nicholls, R.J., Umgieser, G., Willems, P., 2014. Changing extreme sea levels along European coasts. *Coast. Eng.* 87, 4–14.
- Wilson, M., Meyers, S.D., Luther, M.E., 2014. Synoptic volumetric variations and flushing of the Tampa Bay estuary. *Clim. Dyn.* 42, 1587–1594.
- Wiśniewski, B., Wolski, T., 2011. A long-term trend, fluctuations and probability of the sea level at the southern Baltic coast. *J. Coast. Res. Spec.* (64), 255–259.
- Wong, K.-C., Moses-Hall, J.E., 1998. On the relative importance of the remote and local wind effects to the subtidal variability in a coastal plain estuary. *J. Geophys. Res.–Oceans* 103, 18393–18404.
- Xu, S., Huang, W., 2013. Effects of sea level rise on frequency analysis of 1% annual maximum water levels in the coast of Florida. *Ocean. Eng.* 71, 96–102.

**DISSERTATIONS DEFENDED AT
TALLINN UNIVERSITY OF TECHNOLOGY ON
CIVIL ENGINEERING**

1. **Heino Mölder.** Cycle of Investigations to Improve the Efficiency and Reliability of Activated Sludge Process in Sewage Treatment Plants. 1992.
2. **Stellian Grabko.** Structure and Properties of Oil-Shale Portland Cement Concrete. 1993.
3. **Kent Arvidsson.** Analysis of Interacting Systems of Shear Walls, Coupled Shear Walls and Frames in Multi-Storey Buildings. 1996.
4. **Andrus Aavik.** Methodical Basis for the Evaluation of Pavement Structural Strength in Estonian Pavement Management System (EPMS). 2003.
5. **Priit Vilba.** Unstiffened Welded Thin-Walled Metal Girder under Uniform Loading. 2003.
6. **Irene Lill.** Evaluation of Labour Management Strategies in Construction. 2004.
7. **Juhan Idnurm.** Discrete Analysis of Cable-Supported Bridges. 2004.
8. **Arvo Iital.** Monitoring of Surface Water Quality in Small Agricultural Watersheds. Methodology and Optimization of Monitoring Network. 2005.
9. **Liis Sipelgas.** Application of Satellite Data for Monitoring the Marine Environment. 2006.
10. **Ott Koppel.** Infrastruktuuri arvestus vertikaalselt integreeritud raudtee-ettevõtja korral: hinnakujunduse aspekt (Eesti peamise raudtee-ettevõtja näitel). 2006.
11. **Targo Kalamees.** Hygrothermal Criteria for Design and Simulation of Buildings. 2006.
12. **Raido Puust.** Probabilistic Leak Detection in Pipe Networks Using the SCEM-UA Algorithm. 2007.
13. **Sergei Zub.** Combined Treatment of Sulfate-Rich Molasses Wastewater from Yeast Industry. Technology Optimization. 2007.
14. **Alvina Reihan.** Analysis of Long-Term River Runoff Trends and Climate Change Impact on Water Resources in Estonia. 2008.
15. **Ain Valdmann.** On the Coastal Zone Management of the City of Tallinn under Natural and Anthropogenic Pressure. 2008.
16. **Ira Didenkulova.** Long Wave Dynamics in the Coastal Zone. 2008.
17. **Alvar Toode.** DHW Consumption, Consumption Profiles and Their Influence on Dimensioning of a District Heating Network. 2008.
18. **Annely Kuu.** Biological Diversity of Agricultural Soils in Estonia. 2008.

19. **Andres Tolli.** Hiina konteinerveod läbi Eesti Venemaale ja Hiinasse tagasisaadetavate tühjade konteinerite arvu vähendamise võimalused. 2008.
20. **Heiki Onton.** Investigation of the Causes of Deterioration of Old Reinforced Concrete Constructions and Possibilities of Their Restoration. 2008.
21. **Harri Moora.** Life Cycle Assessment as a Decision Support Tool for System optimisation – the Case of Waste Management in Estonia. 2009.
22. **Andres Kask.** Lithohydrodynamic Processes in the Tallinn Bay Area. 2009.
23. **Loreta Kelpšaitė.** Changing Properties of Wind Waves and Vessel Wakes on the Eastern Coast of the Baltic Sea. 2009.
24. **Dmitry Kurennoy.** Analysis of the Properties of Fast Ferry Wakes in the Context of Coastal Management. 2009.
25. **Egon Kivi.** Structural Behavior of Cable-Stayed Suspension Bridge Structure. 2009.
26. **Madis Ratassepp.** Wave Scattering at Discontinuities in Plates and Pipes. 2010.
27. **Tiia Pedusaar.** Management of Lake Ülemiste, a Drinking Water Reservoir. 2010.
28. **Karin Pachel.** Water Resources, Sustainable Use and Integrated Management in Estonia. 2010.
29. **Andrus Räämet.** Spatio-Temporal Variability of the Baltic Sea Wave Fields. 2010.
30. **Alar Just.** Structural Fire Design of Timber Frame Assemblies Insulated by Glass Wool and Covered by Gypsum Plasterboards. 2010.
31. **Toomas Liiv.** Experimental Analysis of Boundary Layer Dynamics in Plunging Breaking Wave. 2011.
32. **Martti Kiisa.** Discrete Analysis of Single-Pylon Suspension Bridges. 2011.
33. **Ivar Annus.** Development of Accelerating Pipe Flow Starting from Rest. 2011.
34. **Emlyn D.Q. Witt.** Risk Transfer and Construction Project Delivery Efficiency – Implications for Public Private Partnerships. 2012.
35. **Oxana Kurkina.** Nonlinear Dynamics of Internal Gravity Waves in Shallow Seas. 2012.
36. **Allan Hani.** Investigation of Energy Efficiency in Buildings and HVAC Systems. 2012.
37. **Tiina Hain.** Characteristics of Portland Cements for Sulfate and Weather Resistant Concrete. 2012.
38. **Dmitri Loginov.** Autonomous Design Systems (ADS) in HVAC Field. Synergetics-Based Approach. 2012.
39. **Kati Kõrbe Kaare.** Performance Measurement for the Road Network: Conceptual Approach and Technologies for Estonia. 2013.

40. **Viktorija Voronova.** Assessment of Environmental Impacts of Landfilling and Alternatives for Management of Municipal Solid Waste. 2013.
41. **Joonas Vaabel.** Hydraulic Power Capacity of Water Supply Systems. 2013.
42. **Inga Zaitseva-Pärnaste.** Wave Climate and its Decadal Changes in the Baltic Sea Derived from Visual Observations. 2013.
43. **Bert Viikmäe.** Optimising Fairways in the Gulf of Finland Using Patterns of Surface Currents. 2014.
44. **Raili Niine.** Population Equivalence Based Discharge Criteria of Wastewater Treatment Plants in Estonia. 2014.
45. **Marika Eik.** Orientation of Short Steel Fibres in Concrete: Measuring and Modelling. 2014.
46. **Maija Viška.** Sediment Transport Patterns Along the Eastern Coasts of the Baltic Sea. 2014.
47. **Jana Pöldnurk.** Integrated Economic and Environmental Impact Assessment and Optimisation of the Municipal Waste Management Model in Rural Area by Case of Harju County Municipalities in Estonia. 2014.
48. **Nicole Delpeche-Ellmann.** Circulation Patterns in the Gulf of Finland Applied to Environmental Management of Marine Protected Areas. 2014.
49. **Andrea Giudici.** Quantification of Spontaneous Current-Induced Patch Formation in the Marine Surface Layer. 2015.
50. **Tiina Nuuter.** Comparison of Housing Market Sustainability in European Countries Based on Multiple Criteria Assessment. 2015.
51. **Erkki Seinre.** Quantification of Environmental and Economic Impacts in Building Sustainability Assessment. 2015.
52. **Artem Rodin.** Propagation and Run-up of Nonlinear Solitary Surface Waves in Shallow Seas and Coastal Areas. 2015.
53. **Kaspar Lasn.** Evaluation of Stiffness and Damage of Laminar Composites. 2015.
54. **Margus Koor.** Water Distribution System Modelling and Pumping Optimization Based on Real Network of Tallinn. 2015.
55. **Mikk Maivel.** Heating System Efficiency Aspects in Low-Energy Residential Buildings. 2015.
56. **Kalle Kuusk.** Integrated Cost-Optimal Renovation of Apartment Buildings toward Nearly Zero-Energy Buildings. 2015.
57. **Endrik Arumägi.** Renovation of Historic Wooden Apartment Buildings. 2015.
58. **Tarvo Niine.** New Approach to Logistics Education with Emphasis to Engineering Competences. 2015.
59. **Martin Thalfeldt.** Total Economy of Energy-Efficient Office Building Facades in a Cold Climate. 2016.

60. **Aare Kuusik.** Intensifying Landfill Waterwaste and Biodegradable Waste Treatment in Estonia. 2016.
61. **Mart Hiob.** The Shifting Paradigm of Spatial Planning in Estonia: The Rise of Neighbourhood Participation and Conservation of Built-up Areas through the Detailed Case Study of Supilinn, a Historic Suburb of Tartu City, Estonia. 2016.
62. **Martin Heinvee.** The Rapid Prediction of Grounding Behavior of Double Bottom Tankers. 2016.
63. **Bharat Maharjan.** Stormwater Quantity and Quality of Large Urban Catchment in Tallinn. 2016.
64. **Nele Nutt.** The Restoration of Nationally Protected Estonian Manor Parks in the Light of the Florence Charter. 2017.
65. **Üllar Alev.** Renovation and Energy Performance Improvement of Estonian Wooden Rural Houses. 2017.
66. **Simo Ilomets.** Renovation Need and Performance of Envelopes of Concrete Apartment Buildings in Estonia. 2017.
67. **Argo Kuusik.** Determining Biogas Yield from Industrial Biodegradable Waste. 2017.